Of Mice and Mucins

Models for studying the role of mucins in the intestine

The study described in this thesis was performed at the Laboratory of Pediatrics, Neonatology of the Erasmus MC / Sophia Children's Hospital, Rotterdam, the Netherlands and at the Groupe regulation transcriptionnelle et signalisation cellulaire, Unité INSERM No560, Lille Cedex, France.

Part of this study was financially supported by the Sophia Foundation for Scientific Research (SSWO; project number 406), Rotterdam, the Netherlands; Netherlands Organization of Scientific Research, Den Haag, the Netherlands; The Foundation "De Drie Lichten", Leiden, the Netherlands; Inserm, Paris, France and the Association François Aupetit, Paris, France.

Financial support by The Section Experimental Gastroenterology (SEG) of the Netherlands Society of Gastroenterology (NVGE); The J.E. Jurriaanse Stichting; Nestlé Nederland B.V.; AstraZeneca BV; Nutricia Nederland B.V.; Numico Research; Tramedico; Zambon Nederland B.V and BD Biosciences, for the publication of this thesis is gratefully acknowledged

ISBN: 90-9021140-3
Layout: L.W. Goedegebure
Cover: L.W. Goedegebure and M. van der Sluis
Printed by: PrintPartners, Ipskamp BV (www.ppi.nl)

Of Mice and Mucins:
Models for studying the role of mucins in the intestine

Muis en mucines:
Modellen om de rol van mucines in de darm te bestuderen

Proefschrift

ter verkrijging van de graad van doctor aan de
Erasmus Universiteit Rotterdam
op gezag van de rector magnificus
Prof.dr. S.W.J. Lamberts
en volgens besluit van het College voor Promoties

De openbare verdediging zal plaatsvinden op
woensdag 29 november 2006 om 15.45 uur

door

Maria van der Sluis
Geboren te Terneuzen

Promotiecommissie

Promotoren:
Prof.dr. H.A. Büller
Prof.dr. J.B. van Goudoever

Overige leden:
Prof.dr. E.J. Kuipers
Dr. I. van Seuningen
Prof.dr. D. Tibboel

Copromotoren:
Dr. A.W.C. Einerhand
Dr. I.B. Renes

To a Mouse

The best laid schemes o'mice an'men
Gang aft a-gley

Robert Burns (1759 – 1796)

Voor een ieder die aan dit proefschrift heeft bijgedragen

Contents

Chapter 1

General Introduction

Partly published as:
Alexandra W.C. Einerhand, Ingrid B. Renes, Mireille K. Makkink, Maria van der Sluis, Hans A. Büller and Jan Dekker. *Role of mucins in inflammatory bowel diseases: important lessons from experimental models.*

European Journal of Gastroenterology & Hepatology, Vol 14 (6); 1-8, 2002.

Abbreviations used in this paper

CD, Crohn's disease; HNF, hepatocyte nuclear factor; IBD, inflammatory bowel disease; IL, interleukin; MUC, Mucin; NF-κB, nuclear factor kappa B; STAT, signal transducers and activators of transcription; Tff3, trefoil factor 3; TNF-α, tumor necrosis factor alpha; TGF-β, transforming growth factor beta; UC, ulcerative colitis; vWF, von-Willebrand-factor

The intestinal tract

The small intestine is the major organ for the absorption of nutrients and also secretes enzymes to complete the digestive processes started in the stomach[1-5]. A 30-50% loss (remaining length, <75 cm in children and <200 cm in adults) often leads to malabsorption, with resultant severe diarrhea, dehydration, electrolyte imbalances, nutrient deficiencies and weight loss[6, 7]. The small intestine from proximal to distal is divided into the duodenum, jejunum, and ileum. The lining of the small intestine is a single-layered epithelium. It covers the surface area of the villi that project into the lumen, and lines the crypts that descend into the underlying connective tissue. Dividing stem cells lie protected in the depth of the crypts. These stem cells generate four types of differentiated progeny: (i) *enterocytes*, with densely packed microvilli on their surfaces to increase their active area, are absorptive in function[2]; (ii) *goblet cells*, secreting the mucin Muc2[8-11] and peptides such as trefoil factor 3 (Tff3)[12], both products which serve protective roles in the gut; (iii) *Paneth cells*, involved in the innate defense system by secreting *cryptdins*, proteins of the defensin family that kill bacteria[13-15], and (iv) *enteroendocrine cells*, producing peptide hormones that act on neurons and other cell types in the gut wall and regulate growth, proliferation and digestive activities of cells of the gut and other tissues[2, 6, 16]. All of these cells stem from undifferentiated multipotent stem cells located near the bottoms of the crypts, above the Paneth cells (Fig. 1A). These multipotent stem cells cannot be conclusively identified as they can produce all cell types within the epithelium. The regulatory mechanism behind lineage specification has not yet been fully elucidated as it is complex and specific markers are lacking[17]. The large intestine, or colon, joins the small intestine at the ileum via a T-shaped junction.

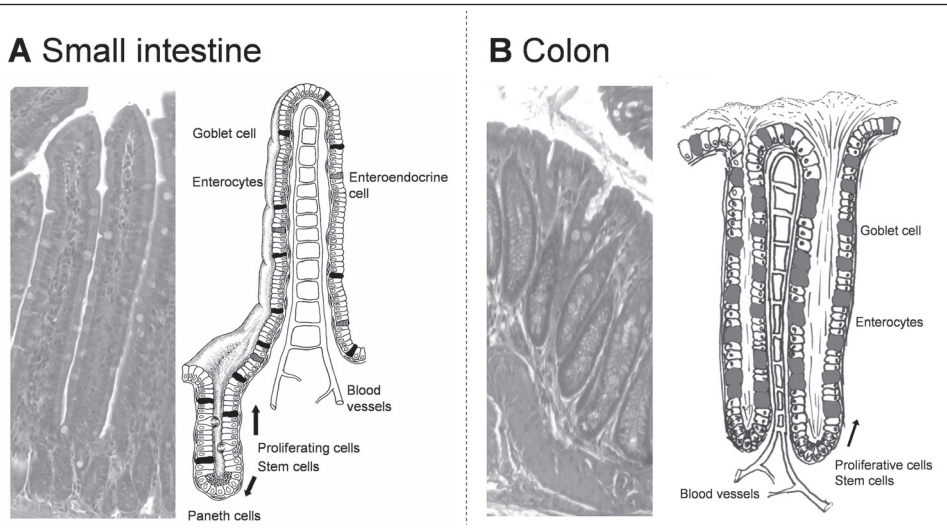

Figure 1. Cell types and structure of the intestine. Haematoxylin and Eosin staining and schematic representation, respectively of (A) the small intestine[3] and (B) colon. The colonic epithelium is organized into crypts and surface cuffs instead of villi and is composed of the same cell types as the small intestine, with the exception of Paneth cells.

One short arm of the T is a blind-ended pouch called the cecum. The colonic epithelium is organized into crypts and surface cuffs instead of villi and is composed of the same cell types as the small intestine, with the exception of Paneth cells (Fig. 1B). Small intestinal enterocytes are specialized in enzymatic digestion, absorption and transportation of dietary nutrients[3-5]. Colonic enterocytes are specialized in electrolyte and water absorption[18-20]. Furthermore, enterocytes of both the small intestine and colon are involved in the epithelial defense through expression of alkaline phosphatase, which acts as an antimicrobial peptide[21, 22]. The epithelium and mucus layer in the intestinal tract form a physical barrier protecting the underlying tissues from potentially toxic and noxious agents. Goblet cells exert a vital protective role by secreting molecules such as mucins and trefoil factors. Mucins are the building blocks of the mucus layer. Previous studies have shown that human, rat and mouse colonic epithelium share the characteristic of expressing mainly one secretory mucin in high amounts, *i.e.* MUC2[8-11]. Stored in bulky apical granules of the goblet cells, Muc2 is crucial to goblet cell morphology[23]. Tff3 is another protein expressed by goblet cells in the intestine and plays an essential role in intestinal mucosa maintenance and repair[12].

Mucins

Many organ systems, including the eyes, gastrointestinal tract, trachea, lungs, bladder, pancreatic duct, gallbladder and the reproductive tracts, protect their epithelium by producing mucins[24]. The mucosal surface throughout the gastrointestinal tract must resist aggressive elements from the external environment present in the diet and encountered during normal function. Mainly composed of secretory gel-forming mucin, more specifically MUC2, mucus in the intestine forms a semi-permeable barrier between the intestinal lumen and the underlying mucosal surface[24].

Functionally, MUC-type mucins can be classified into: i) secretory, gel-forming mucins, ii) membrane-bound mucins, and iii) small soluble mucins.

Ad. i. Secretory, gel-forming mucins are widely acknowledged as important players in gastrointestinal epithelium defense, and are produced in specialized mucous cells of glandular tissues and goblet cells in the gastrointestinal tract[24-27]. These mucins are produced as disulfide-linked oligomers[28], which proves essential for their ability to form viscoelastic mucus-gels. The four members to this group, MUC2, -5AC, -5B, and -6, have been well characterized[29, 30]. In the healthy human intestine, MUC2 is the predominant mucin produced by all goblet cells, and MUC5B is expressed in minor quantities in a subset of goblet cells in the lower colonic crypts [26, 27, 31]. MUC5AC and MUC6 are normally confined to gastric epithelium[32, 33].

Ad. ii. The membrane-bound mucins are involved in epithelial cell-signaling, adhesion, growth, and modulation of the immune system[25, 34-38], and may have a role in cellular behavior – *i.e.* during proliferation and differentiation – as reviewed by Hollingsworth and Swanson[39]. These mucins are made in serous glands or epithelial cells, like enterocytes[37, 40]. MUC1, MUC3A, MUC3B, MUC4 have been extensively studied[41-43]. Membrane-bound mucins can be released from cells in soluble form, when the transmembrane domain has been removed by either proteolysis or alternative

splicing[44-47]. However, they are not exclusively restricted to the cellular membrane. Muc3 and Muc4 are both expressed by the secretory granules of the goblet cells in the intestine[48-50]. Furthermore, Rong *et al*. recently reported that Muc4 in the colon is predominantly expressed by the goblet cells in both rats and humans and that the soluble form of Muc4 prevails[49].

Ad. iii. So far only one small soluble human mucin has been identified (MUC7), which is found in saliva[51].

Many of the known human mucin genes have been grouped into the MUC gene family. So far, seven Muc-type genes have been identified in the mouse (Table I), and these were named after their human orthologues as Muc1, -2, -3, -4, -5ac, -5b and 6[52-59]. Members of the membrane-bound mucins (Muc1, -3, and -4) as well as of the secretory, gel-forming mucins (Muc2, -5ac, -5b and 6, which are clustered on mouse chromosome 7) have been identified, indicating that the mucosal defense and other functions of the mucins are preserved both among man and rodent. Recent research, however, indicates that the current mouse orthologue of the human MUC3 may still go undiscovered. Extensive characterization of the membrane-bound mucin MUC17 has revealed that its carboxyl-terminal sequence resembles both rat and mouse Muc3 more than any other known human protein[60, 61]. Because of the high degree of similarity between the two proteins, and their identical genomic organization, it has been suggested that rodent Muc3 should be referred to as rat/mouse Muc17[61]. Other genes have been assigned to the MUC family (MUC8, -11/12, -13, -16, -18, -19 and -20)[62-69]. Some of these (MUC-11/12, -13, and -16) are expressed in the intestine, but so far their characterization is limited[63, 64, 70].

Table I. Mouse orthologues of human mucins

Mucin	Expression	Mucin class	Chromosome	Reference
Muc1	All epithelia	Membrane-bound	3	55, 137
Muc2	Intestine, goblet cells	secretory	7	54
Muc3	Intestine, enterocytes	Membrane-bound	5	52
Muc4	Virtually all epithelia, and in the goblet cells of the intestine	Membrane-bound, and secretory	16	49, 57
Muc5ac	Stomach, surface epithelium	secretory	7	53
Muc5b	Trachea, submucosal glands Tongue, sublingual glands	secretory	7	56
Muc6	Stomach	secretory	7	58

NOTE Because human MUC17 and mouse Muc3 are almost similar, and their genomic organization is identical, Moiniaux *et al.* suggested that rodent Muc3 should be referred to as rat/mouse Muc17[60].

Peptide structure of mucins

Biochemically, mucins are usually very large, filamentous molecules. Mucin proteins each contain unique variable number of tandem repeats, with regions rich in serine, threonine and proline[71]. Linkage of carbohydrate side chains through *O*-glycosidic bonds to serine and threonine means that these are the major sites of glycosylation in the mucins[24, 40]. The *O*-linked carbohydrates form up to 80% of the molecular weight of the mucins. These very numerous, yet relatively short carbohydrate chains (2-20 monosaccharides), are tightly packed along the polypeptide and are responsible for the overall filamentous structure of mucins. The oligosaccharides make the large central region of the mucin backbone highly resistant to breakdown by proteolyic enzymes[24]. The C- and N- terminal regions of the mucin are much less glycosylated, which renders them susceptible to degradation by proteases. The addition of very large numbers of sulfate and sialic acid residues to the *O*-linked carbohydrates gives the mucins a highly negative surface charge. Figure 2 shows a cartoon representing the most predominant mucin in the colon and colonic mucus layer, MUC2[8-11]. In the secretory mucins Muc2, Muc5ac and Muc5b, the Von Willebrand factor (VWF) domains (C and D types), located in the C- and N-terminus, respectively, are responsible for dimerization and oligomerization[71]. In contrast to the other secretory mucins, Muc6 lacks VWF-type C domains in its C-terminus. A review by Dekker *et al*.[71] gives an elaborate description on mucin sequences, composition and similarities.

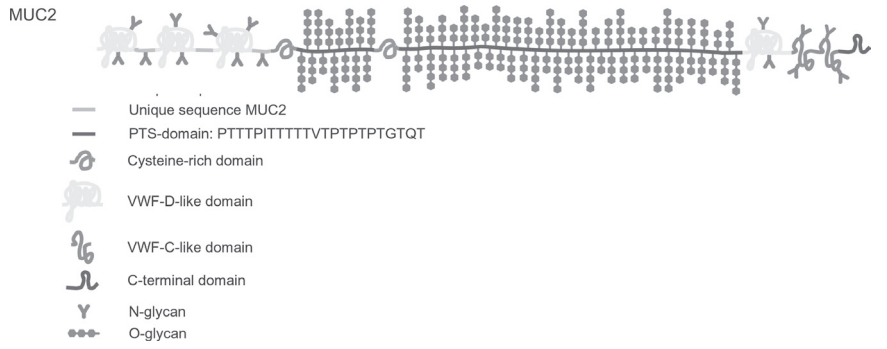

Figure 2. Schematic representation of the mucin MUC2. The schematic representation of MUC2 was already published by Dekker et al[71].

Mucins in disease: Inflammatory bowel disease

The two forms of chronic human inflammatory bowel disease (IBD), Crohn's disease (CD) and ulcerative colitis (UC), are primarily characterized by chronic inflammation of segments of the gastrointestinal tract. Active inflammation will alternate with remission periods. Both are complex diseases believed to result from the interplay of multiple environmental and genetic factors involving: i) the immune system, ii) microbial factors, and iii) the intestinal epithelial barrier.

Mucins, as the primary constituents of extra cellular mucus and the cellular barrier, are intimately associated with each of these three possible etiological factors. Mucins are important epithelial products of the intestine, essential for a proper

epithelial barrier function. Moreover, mucins are crucial in the contacts between many microorganisms and the intestinal mucosa. Therefore a primary defect in mucins could breach the epithelial barrier or lead to altered mucosal-bacterial interactions. Alterations in mucin synthesis, maturation, secretion, and/or degradation are generally thought to be involved in the initiation or perpetuation of IBD symptoms[70, 72, 73]. These quantitative and/or qualitative alterations in mucin synthesis may be related to mutations within mucin genes or to changes in immunological or microbial factors that influence mucin expression or mucus layer maintenance.

In active UC, numbers of goblet cells are reduced and the mucus layer is thinner[74]. In remission periods, numbers of goblet cells return to normal[75, 76]. Furthermore, MUC2 synthesis, secretion and sulfation is decreased in active UC[77-79]. Normally, colonic mucins are highly sulfated, and considered to be more resistant to bacterial degradation in this state. A colonic mucus layer composed of less sulfated mucins is deemed less protective, and was found closely associated with IBD in humans[31, 79-84]. Furthermore, changes in glycosylation of mucins were found in UC[75, 85], and fecal anaerobic bacteria were found able to degrade mucus by producing extracellular glycosidases *in vitro*[86, 87]. Thus, MUC2, as the prominent secretory mucin in the intestine produced by goblet cells, seems to play a key role in maintenance of the mucus layer by protecting the epithelium against bacteria, bacterial products and other luminal substances; in patients with IBD, however, this mucin seems to exert less protective capacities.

Immunological influence on mucins

Several rodent models of colitis were recently developed in which chronic intestinal inflammation occurs as a consequence of alterations in the immune system, leading to failure of normal immuno-regulation in the intestine[88]. These animal models are very suitable for identifying the effects of the immune system on mucin expression. One is the interleukin (IL)-10 deficient ($IL10^{-/-}$) mouse[89-91], which spontaneously develops chronic colitis when maintained in conventional conditions. Colitis severity in these mice depends on both strain background and environmental factors[92, 93]. Upon introduction of normal enteric bacteria, $IL10^{-/-}$ mice rapidly develop symptoms of colitis as evidenced by infiltration of immune cells and induction of pro-inflammatory mediators such as IL12[94].

Mucins and intestinal metabolism

Integrity of the mucus layer depends on the nutritional status of the intestine. For example, malnutrition and starvation will alter the mucus layer by decreasing intestinal mucin synthesis[95, 96]. In addition, the intestine of piglets utilizes between 80-90% of dietary threonine, mainly due to threonine incorporation into mucosal proteins[97]. Interestingly, additional data demonstrated a 60% reduction in whole-body threonine requirements in piglets receiving total parenteral nutrition, compared to orally fed control animals[98]. In this context, the intestinal demand for dietary threonine probably arises from incorporation of threonine into secretory mucins, mainly Muc2, which are rich in threonine residues. Further support for this hypothesis is a study by Faure *et al.*[98] showing that dietary restriction of the essential amino acid threonine impairs intestinal mucin synthesis.

Regulation of mucin expression

Mucin production and secretion by specialized epithelial cells is a common mechanism for mammals to protect and maintain normal cell homeostasis, as reviewed by Van Seuningen *et al.*[99]. The expression of mucin genes is cell- and tissue specific, yet subject to variations during cell differentiation, inflammatory processes and carcinogenesis. In addition, *in vitro* experiments with intestinal cell lines showed that bacteria and bacterial components may influence the expression of mucins[99-103]. Mucin gene transcription is subject to dynamic pathways involving multiple receptors and transcription factors[99]. There are two broad classes of regulatory transcription factors, as reviewed by Brivanlou *et al.*[104]. One of these, the *developmental transcription factors*, are not strictly cell-, tissue-, or region-specific. Arrangement of groups of these factors, in different cell types, helps direct cell determination (choice of cell fate) and differentiation (synthesis of cell-type specific proteins). The second class comprises the *signal dependent transcription factors*. These proteins may be either developmentally restricted in their expression pattern or are present in cells, but are inactive (or minimally active) until cells containing such proteins are exposed to the appropriate intracellular or extracellular signals. These signals can be mediated and influenced by a variety of molecules (*i.e.* hormones, cytokines) and external factors (*i.e.* bacteria).

Developmental transcription factors

Intestinal development proceeds through orchestrated cell growth, differentiation, migration, interactions and apoptosis. Cdx, GATA and hepatocyte nuclear factor (HNF) are all transcription factors from different families, which play a key role in development and cell differentiation in the intestine. They are expressed in embryonic endoderm, the germ layer that gives rise to the digestive system, and in the adult intestine[105-108]. Intestine-specific gene expression, such as intestinal lactase-phlorizin hydrolase and sucrase isomaltase expression, is controlled at the transcriptional level and relies on the activity of multiple tissue-enriched transcription factors like Cdx-1/-2, HNF-1/-3 and GATA-4/-5/-6[109-114]. Interestingly, only Cdx2 has been identified as a regulator of goblet cell-specific Muc2 gene expression[115, 116]. The role of GATA or HNF transcription factors in mucus production, and thus in maintenance of a defense line and protective barrier in intestinal pathophysiology[70], remains to be investigated. Evidence in favor of a regulatory role for these factors on Muc2 gene expression, is that during embryonic development GATA-4/-5/-6, HNF-3α and HNF-3β mRNA are expressed in the primitive intestine in which *Muc2* is also found[106, 107, 117-122]. Moreover, further computer analysis of the murine *Muc2* promoter sequence[123] indicates the presence of several putative HNF binding sites throughout the promoter region.

Signal dependent transcription factors

General homeostasis of cells is determined by a broad spectrum of intracellular or extra cellular signals. Widely diverse factors – for example hormones, cell-cell interactions, bacteria and cytokines – can govern these signaling pathways. To add to the complexity, there is correlation and cross-talk between these individual

factors[99, 104]. Major pathways involve signaling via the nuclear factor kappa B (NF-κB) family, the Smad family and the signal transducers and activators of transcription (STAT) family of transcription factors[104]. Activation of the NF-κB family of transcription factors is influenced by many extracellular factors including tumor necrosis factor alpha (TNF-α), IL-1 and bacterial products. The Smad transcription factors are activated by ligands of the transforming growth factor beta (TGF-β) super family and the STAT signaling pathway is activated by a large number of ligands including cytokines (*i.e.* interferon gamma), growth factors and charged small molecules[104].

There are various direct and indirect indications that synthesis and secretion of secretory mucins can be regulated by immune factors[103, 124-128]. Epithelial cell line studies showed that pro-inflammatory cytokines like TNF-α, IL-1β and IL-13 also induce gene expression of the secretory mucins Muc2 and Muc5ac[126, 129-131]. Likewise, lipopolysaccharide (LPS, a cell wall component of Gram-negative bacteria), which is potentially toxic for cells, and different species of bacteria generally used as probiotic treatment, are also able to up-regulate Muc2 and Muc5ac mucin gene expression in different epithelial cell lines[132-135]. In addition, IL-10 has been shown to induce Muc2 synthesis[136], maybe indirectly by producing IL-13, in addition to facilitating TGF-β production[137]. In diverse epithelial cell lines, TFG-β in turn was found to induce Muc2 transcription via Smad signaling pathways[127]. All this implicates a general mechanism in improvement and maintenance of the protective mucus barrier in intestinal pathophysiology.

Aim and outline of this thesis

If we were to better understand the function and regulation of mucin genes in the intestine, we could identify future potential therapeutic targets in epithelial diseases. Therefore, the major aims of this thesis are:

1. To investigate the influence of changes in mucus production, more specifically Muc2, on the intestinal protective barrier function and elementary intestinal physiology.
2. To gain insight into the complex transcription regulatory mechanisms of the secretory mucins Muc2 and Muc5ac.

Part I Role of mucins in the intestine

The first part of this thesis explores the function of mucins, more specifically Muc2, in the intestine. As mentioned earlier, bacteria can influence mucin expression. In order to elucidate the influence of commensal enteric bacteria on Muc2 synthesis, secretion and sulfation and the role of Muc2 in the pathogenesis of chronic colitis, we first studied how the introduction of specified pathogen free commensal bacteria in germ free IL-10 deficient mice affected Muc2 synthesis (**Chapter 2**). We subsequently addressed the importance of Muc2 in epithelial protection. Thereto, Muc2 deficient mice were characterized, and challenged luminally with dextran sulfate sodium as a means to provide insight into the protective capacities of Muc2 (**Chapter 3**). Thus, considering that the severity of chronic intestinal inflammation may be governed by environmental, immunoregulatory, and epithelial factors, we investigated the protective capacities of Muc2 and IL-10 in the intestine. To this aim

we created Muc2/IL10 double knockout (Muc2/IL10^{DKO}) mice and determined whether combined defects in the immunoregulatory and epithelial factors could exacerbate the pathogenesis of inflammation (**Chapter 4**). These studies indicated that Muc2 has protective capacities in the intestine, which led us to evaluate the role of Muc2 in epithelial protection during serosal challenging conditions (**Chapter 5**). Then, integrity of the mucus layer has been associated with nutritional status. Therefore, we also investigated mucin involvement in intestinal metabolism. As threonine is an essential amino acid we determined threonine utilization by the intestine of Muc2 deficient and wild type mice so as to gain insight into the elementary intestinal physiology (**Chapter 6**).

Part II Regulation of mucin gene expression

As described above, mucin gene expression is subject to complex regulatory mechanisms influenced by developmental and signal dependent transcription factors. Therefore, the second part of thesis focuses on the signal transduction pathways involved in the regulation of intestinal mucin expression. To this aim we assessed the transcriptional regulation of the two secretory mucin genes, Muc2 and Muc5ac. We focused on transcription factors involved in intestinal development, more specifically GATA-4/-5/-6 and HNF-3α/-3β, as these factors are expressed in the primitive intestine in which Muc2 is also found (**Chapter 7** and **Chapter 8**, respectively). Furthermore, mucin gene transcription was shown to be influenced by a broad range of cytokines. Analysis of the Muc5ac promoter showed a high density of binding sites for factors essential for TGF-β signaling. Muc5ac is aberrantly expressed in rectosigmoid villous adenomas and TGF-β was shown to be involved in gastritis and gastric cancer. This led us to study Muc5ac regulation by TGF-β (**Chapter 9**).

This thesis concludes with a summarizing general discussion in which insights obtained from the different studies are combined and future perspectives are discussed (**Chapter 10**).

References

1. Stevens A, Lowe J. Alimentary tract. In: Cook L, ed. Human Histology. Second Edition ed. London: Mosby, 1997:202-206.
2. Madara JL, Trier JS. The Functional Morphology of the Mucosa of the Small Intestine. In: Johnson LR, ed. Physiology of the Gastrointestinal Tract. New York: Raven Press, 1994:1577-1622.
3. Dekker J, Einerhand AWC, Büller HA. Carbohydrate Malabsorption. In: Lifschitz CH, ed. Pediatric Gastroenterology and Nutrition in Clinical Practice. New York: Dekker, M., 2002:339-373.
4. Alpers DH, Bass NM, Engle MJ, DeSchryver-Kecskemeti K. Intestinal fatty acid binding protein may favor differential apical fatty acid binding in the intestine. Biochim Biophys Acta 2000;1483:352-62.
5. Traber PG. Development of Brushborder Enzym Actvity. In: Sanderson IR, Walker WR, eds. Development of the Gastrointestinal Tract. Hamilton: B.C. Decker Inc., 2000:103-122.
6. Martin GR, Beck PL, Sigalet DL. Gut hormones, and short bowel syndrome: The enigmatic role of glucagon-like peptide-2 in the regulation of intestinal adaptation. World J Gastroenterol 2006;12:4117-29.
7. Weale AR, Edwards AG, Bailey M, Lear PA. Intestinal adaptation after massive intestinal resection. Postgrad Med J 2005;81:178-84.
8. Tytgat KM, Büller HA, Opdam FJ, Kim YS, Einerhand AW, Dekker J. Biosynthesis of human colonic mucin: Muc2 is the prominent secretory mucin. Gastroenterology 1994;107:1352-1363.
9. Tytgat KM, Bovelander FJ, Opdam FJ, Einerhand AW, Büller HA, Dekker J. Biosynthesis of rat MUC2 in colon and its analogy with human MUC2. Biochem J 1995;309 (Pt 1):221-9.
10. Herrmann A, Davies JR, Lindell G, Martensson S, Packer NH, Swallow DM, Carlstedt I. Studies on the “insoluble” glycoprotein complex from human colon. Identification of reduction-insensitive MUC2 oligomers and C-terminal cleavage. J Biol Chem 1999;274:15828-36.
11. van Klinken BJ, Einerhand AW, Duits LA, Makkink MK, Tytgat KM, Renes IB, Verburg M, Büller HA, Dekker J. Gastrointestinal expression and partial cDNA cloning of murine Muc2. Am J Physiol 1999;276:115-124.
12. Mashimo H, Wu DC, Podolsky DK, Fishman MC. Impaired defense of intestinal mucosa in mice lacking intestinal trefoil factor. Science 1996;274:262-5.
13. Bevins CL. Paneth cell defensins: key effector molecules of innate immunity. Biochem Soc Trans 2006;34:263-6.
14. Keshav S. Paneth cells: leukocyte-like mediators of innate immunity in the intestine. J Leukoc Biol 2006.
15. Eckmann L. Defence molecules in intestinal innate immunity against bacterial infections. Curr Opin Gastroenterol 2005;21:147-51.
16. Beglinger C, Degen L. Gastrointestinal satiety signals in humans - Physiologic roles for GLP-1 and PYY ? Physiol Behav 2006.
17. Bjerknes M, Cheng H. Gastrointestinal stem cells. II. Intestinal stem cells. Am J Physiol Gastrointest Liver Physiol 2005;289:G381-7.
18. Fleming RE, Parkkila S, Parkkila AK, Rajaniemi H, Waheed A, Sly WS. Carbonic anhydrase IV expression in rat and human gastrointestinal tract regional, cellular, and subcellular localization. J Clin Invest 1995;96:2907-13.
19. Bookstein C, DePaoli AM, Xie Y, Niu P, Musch MW, Rao MC, Chang EB. Na+/H+ exchangers, NHE-1 and NHE-3, of rat intestine. Expression and localization. J Clin Invest 1994;93:106-13.

20. Binder H, Sandle G. Digestion and Absorption: Electrolyte Transport in the Mammalian Colon. In: Johnson LR, ed. Physiology of the Gastrointestinal Tract. New York: Raven Press, 1994:2133-2177.
21. Poelstra K, Bakker WW, Klok PA, Hardonk MJ, Meijer DK. A physiologic function for alkaline phosphatase: endotoxin detoxification. Lab Invest 1997;76:319-27.
22. Poelstra K, Bakker WW, Klok PA, Kamps JA, Hardonk MJ, Meijer DK. Dephosphorylation of endotoxin by alkaline phosphatase in vivo. Am J Pathol 1997;151:1163-9.
23. Velcich A, Yang W, Heyer J, Fragale A, Nicholas C, Viani S, Kucherlapati R, Lipkin M, Yang K, Augenlicht L. Colorectal cancer in mice genetically deficient in the mucin Muc2. Science 2002;295:1726-1729.
24. Strous GJ, Dekker J. Mucin-type glycoproteins. Crit Rev Biochem Mol Biol 1992;27:57-92.
25. Van Klinken BJ, Dekker J, Büller HA, Einerhand AW. Mucin gene structure and expression: protection vs. adhesion. Am J Physiol 1995;269:G613-27.
26. Van Klinken BJ, Dekker J, Büller HA, de Bolos C, Einerhand AW. Biosynthesis of mucins (MUC2-6) along the longitudinal axis of the human gastrointestinal tract. Am J Physiol 1997;273:G296-302.
27. Van Klinken BJ, Dekker J, van Gool SA, van Marle J, Büller HA, Einerhand AW. MUC5B is the prominent mucin in human gallbladder and is also expressed in a subset of colonic goblet cells. Am J Physiol 1998;274:G871-8.
28. Van Klinken BJ, Einerhand AW, Büller HA, Dekker J. The oligomerization of a family of four genetically clustered human gastrointestinal mucins. Glycobiology 1998;8:67-75.
29. Desseyn JL, Aubert JP, Porchet N, Laine A. Evolution of the large secreted gel-forming mucins. Mol Biol Evol 2000;17:1175-84.
30. Moniaux N, Escande F, Porchet N, Aubert JP, Batra SK. Structural organization and classification of the human mucin genes. Front Biosci 2001;6:D1192-206.
31. Tytgat KM, Büller HA, Opdam FJ, Kim YS, Einerhand AW, Dekker J. Biosynthesis of human colonic mucin: Muc2 is the prominent secretory mucin. Gastroenterology 1994;107:1352-63.
32. Van den Brink GR, Tytgat KM, Van der Hulst RW, Van der Loos CM, Einerhand AW, Büller HA, Dekker J. H pylori colocalises with MUC5AC in the human stomach. Gut 2000;46:601-7.
33. Ho SB, Roberton AM, Shekels LL, Lyftogt CT, Niehans GA, Toribara NW. Expression cloning of gastric mucin complementary DNA and localization of mucin gene expression. Gastroenterology 1995;109:735-47.
34. Agrawal B, Gendler SJ, Longenecker BM. The biological role of mucins in cellular interactions and immune regulation: prospects for cancer immunotherapy. Mol Med Today 1998;4:397-403.
35. Wesseling J, van der Valk SW, Vos HL, Sonnenberg A, Hilkens J. Episialin (MUC1) overexpression inhibits integrin-mediated cell adhesion to extracellular matrix components. J Cell Biol 1995;129:255-65.
36. DeSouza MM, Surveyor GA, Price RE, Julian J, Kardon R, Zhou X, Gendler S, Hilkens J, Carson DD. MUC1/episialin: a critical barrier in the female reproductive tract. J Reprod Immunol 1999;45:127-58.
37. Carraway KL, Price-Schiavi SA, Komatsu M, Idris N, Perez A, Li P, Jepson S, Zhu X, Carvajal ME, Carraway CA. Multiple facets of sialomucin complex/MUC4, a membrane mucin and erbb2 ligand, in tumors and tissues (Y2K update). Front Biosci 2000;5:D95-D107.
38. Komatsu M, Jepson S, Arango ME, Carothers Carraway CA, Carraway KL. Muc4/sialomucin complex, an intramembrane modulator of ErbB2/HER2/Neu, potentiates primary tumor growth and suppresses apoptosis in a xenotransplanted tumor. Oncogene 2001;20:461-70.
39. Hollingsworth MA, Swanson BJ. Mucins in cancer: protection and control of the cell surface. Nat Rev Cancer 2004;4:45-60.

40. Gendler SJ, Spicer AP. Epithelial mucin genes. Annu Rev Physiol 1995;57:607-34.
41. Louvet B, Buisine MP, Desreumaux P, Tremaine WJ, Aubert JP, Porchet N, Capron M, Cortot A, Colombel JF, Sandborn WJ. Transdermal nicotine decreases mucosal IL-8 expression but has no effect on mucin gene expression in ulcerative colitis. Inflamm Bowel Dis 1999;5:174-81.
42. Buisine MP, Desreumaux P, Debailleul V, Gambiez L, Geboes K, Ectors N, Delescaut MP, Degand P, Aubert JP, Colombel JF, Porchet N. Abnormalities in mucin gene expression in Crohn's disease. Inflamm Bowel Dis 1999;5:24-32.
43. Buisine MP, Desreumaux P, Leteurtre E, Copin MC, Colombel JF, Porchet N, Aubert JP. Mucin gene expression in intestinal epithelial cells in Crohn's disease. Gut 2001;49:544-51.
44. Baruch A, Hartmann M, Zrihan-Licht S, Greenstein S, Burstein M, Keydar I, Weiss M, Smorodinsky N, Wreschner DH. Preferential expression of novel MUC1 tumor antigen isoforms in human epithelial tumors and their tumor-potentiating function. Int J Cancer 1997;71:741-9.
45. Choudhury A, Moniaux N, Ringel J, King J, Moore E, Aubert JP, Batra SK. Alternate splicing at the 3'-end of the human pancreatic tumor-associated mucin MUC4 cDNA. Teratog Carcinog Mutagen 2001;21:83-96.
46. Choudhury A, Moniaux N, Winpenny JP, Hollingsworth MA, Aubert JP, Batra SK. Human MUC4 mucin cDNA and its variants in pancreatic carcinoma. J Biochem (Tokyo) 2000;128:233-43.
47. Crawley SC, Gum JR, Jr., Hicks JW, Pratt WS, Aubert JP, Swallow DM, Kim YS. Genomic organization and structure of the 3' region of human MUC3: alternative splicing predicts membrane-bound and soluble forms of the mucin. Biochem Biophys Res Commun 1999;263:728-36.
48. Idris N, Carraway KL. Sialomucin complex (Muc4) expression in the rat female reproductive tract. Biol Reprod 1999;61:1431-8.
49. Rong M, Rossi EA, Zhang J, McNeer RR, van den Brande JM, Yasin M, Weed DT, Carothers Carraway CA, Thompson JF, Carraway KL. Expression and localization of Muc4/sialomucin complex (SMC) in the adult and developing rat intestine: implications for Muc4/SMC function. J Cell Physiol 2005;202:275-84.
50. Chang SK, Dohrman AF, Basbaum CB, Ho SB, Tsuda T, Toribara NW, Gum JR, Kim YS. Localization of mucin (MUC2 and MUC3) messenger RNA and peptide expression in human normal intestine and colon cancer. Gastroenterology 1994;107:28-36.
51. Bobek LA, Tsai H, Biesbrock AR, Levine MJ. Molecular cloning, sequence, and specificity of expression of the gene encoding the low molecular weight human salivary mucin (MUC7). J Biol Chem 1993;268:20563-9.
52. Shekels LL, Hunninghake DA, Tisdale AS, Gipson IK, Kieliszewski M, Kozak CA, Ho SB. Cloning and characterization of mouse intestinal MUC3 mucin: 3' sequence contains epidermal-growth-factor-like domains. Biochem J 1998;330:1301-8.
53. Shekels LL, Lyftogt C, Kieliszewski M, Filie JD, Kozak CA, Ho SB. Mouse gastric mucin: cloning and chromosomal localization. Biochem J 1995;311:775-85.
54. Van Klinken BJ, Einerhand AW, Duits LA, Makkink MK, Tytgat KM, Renes IB, Verburg M, Büller HA, Dekker J. Gastrointestinal expression and partial cDNA cloning of murine Muc2. Am J Physiol 1999;276:G115-24.
55. Vos HL, de Vries Y, Hilkens J. The mouse episialin (Muc1) gene and its promoter: rapid evolution of the repetitive domain in the protein. Biochem Biophys Res Commun 1991;181:121-30.
56. Chen Y, Zhao YH, Wu R. In silico cloning of mouse muc5b gene and upregulation of its expression in mouse asthma model. Am J Respir Crit Care Med 2001;164:1059-66.
57. Desseyn JL, Clavereau I, Laine A. Cloning, chromosomal localization and characterization of

the murine mucin gene orthologous to human MUC4. Eur J Biochem 2002;269:3150-9.
58. Desseyn JL, Laine A. Characterization of mouse muc6 and evidence of conservation of the gel-forming mucin gene cluster between human and mouse. Genomics 2003;81:433-6.
59. Escande F, Porchet N, Bernigaud A, Petitprez D, Aubert JP, Buisine MP. The mouse secreted gel-forming mucin gene cluster. Biochim Biophys Acta 2004;1676:240-250.
60. Gum JR, Jr., Crawley SC, Hicks JW, Szymkowski DE, Kim YS. MUC17, a novel membrane-tethered mucin. Biochem Biophys Res Commun 2002;291:466-75.
61. Moniaux N, Junker WM, Singh AP, Jones AM, Batra SK. Characterization of human mucin MUC17: Complete coding sequence and organization. J Biol Chem 2006.
62. Shankar V, Pichan P, Eddy RL, Jr., Tonk V, Nowak N, Sait SN, Shows TB, Schultz RE, Gotway G, Elkins RC, Gilmore MS, Sachdev GP. Chromosomal localization of a human mucin gene (MUC8) and cloning of the cDNA corresponding to the carboxy terminus. Am J Respir Cell Mol Biol 1997;16:232-41.
63. Williams SJ, McGuckin MA, Gotley DC, Eyre HJ, Sutherland GR, Antalis TM. Two novel mucin genes down-regulated in colorectal cancer identified by differential display. Cancer Res 1999;59:4083-9.
64. Williams SJ, Wreschner DH, Tran M, Eyre HJ, Sutherland GR, McGuckin MA. Muc13, a novel human cell surface mucin expressed by epithelial and hemopoietic cells. J Biol Chem 2001;276:18327-36.
65. Yin BW, Lloyd KO. Molecular cloning of the CA125 ovarian cancer antigen: identification as a new mucin, MUC16. J Biol Chem 2001;276:27371-5.
66. Wu GJ, Wu MW, Wang SW, Liu Z, Qu P, Peng Q, Yang H, Varma VA, Sun QC, Petros JA, Lim SD, Amin MB. Isolation and characterization of the major form of human MUC18 cDNA gene and correlation of MUC18 over-expression in prostate cancer cell lines and tissues with malignant progression. Gene 2001;279:17-31.
67. Yang H, Wang S, Liu Z, Wu MH, McAlpine B, Ansel J, Armstrong C, Wu G. Isolation and characterization of mouse MUC18 cDNA gene, and correlation of MUC18 expression in mouse melanoma cell lines with metastatic ability. Gene 2001;265:133-45.
68. Chen Y, Zhao YH, Kalaslavadi TB, Hamati E, Nehrke K, Le AD, Ann DK, Wu R. Genome-wide search and identification of a novel gel-forming mucin MUC19/Muc19 in glandular tissues. Am J Respir Cell Mol Biol 2004;30:155-65.
69. Higuchi T, Orita T, Nakanishi S, Katsuya K, Watanabe H, Yamasaki Y, Waga I, Nanayama T, Yamamoto Y, Munger W, Sun HW, Falk RJ, Jennette JC, Alcorta DA, Li H, Yamamoto T, Saito Y, Nakamura M. Molecular cloning, genomic structure, and expression analysis of MUC20, a novel mucin protein, up-regulated in injured kidney. J Biol Chem 2004;279:1968-79.
70. Corfield AP, Carroll D, Myerscough N, Probert CS. Mucins in the gastrointestinal tract in health and disease. Front Biosci 2001;6:D1321-57.
71. Dekker J, Rossen JW, Büller HA, Einerhand AW. The MUC family: an obituary. Trends Biochem Sci 2002;27:126-31.
72. Corfield AP, Myerscough N, Longman R, Sylvester P, Arul S, Pignatelli M. Mucins and mucosal protection in the gastrointestinal tract: new prospects for mucins in the pathology of gastrointestinal disease. Gut 2000;47:589-94.
73. Shirazi T, Longman RJ, Corfield AP, Probert CS. Mucins and inflammatory bowel disease. Postgrad Med J 2000;76:473-8.
74. Pullan RD, Thomas GA, Rhodes M, Newcombe RG, Williams GT, Allen A, Rhodes J. Thickness of adherent mucus gel on colonic mucosa in humans and its relevance to colitis. Gut 1994;35:353-9.

75. Jacobs LR, Huber PW. Regional distribution and alterations of lectin binding to colorectal mucin in mucosal biopsies from controls and subjects with inflammatory bowel diseases. J Clin Invest 1985;75:112-8.
76. Theodossi A, Spiegelhalter DJ, Jass J, Firth J, Dixon M, Leader M, Levison DA, Lindley R, Filipe I, Price A, et al. Observer variation and discriminatory value of biopsy features in inflammatory bowel disease. Gut 1994;35:961-8.
77. Tytgat KM, Opdam FJ, Einerhand AW, Büller HA, Dekker J. MUC2 is the prominent colonic mucin expressed in ulcerative colitis. Gut 1996;38:554-63.
78. Tytgat KM, van der Wal JW, Einerhand AW, Büller HA, Dekker J. Quantitative analysis of MUC2 synthesis in ulcerative colitis. Biochem Biophys Res Commun 1996;224:397-405.
79. Van Klinken BJ, Van der Wal JW, Einerhand AW, Büller HA, Dekker J. Sulphation and secretion of the predominant secretory human colonic mucin MUC2 in ulcerative colitis. Gut 1999;44:387-93.
80. Raouf AH, Tsai HH, Parker N, Hoffman J, Walker RJ, Rhodes JM. Sulphation of colonic and rectal mucin in inflammatory bowel disease: reduced sulphation of rectal mucus in ulcerative colitis. Clin Sci (Colch) 1992;83:623-6.
81. Nieuw Amerongen AV, Bolscher JG, Bloemena E, Veerman EC. Sulfomucins in the human body. Biol Chem 1998;379:1-18.
82. Corfield AP, Myerscough N, Bradfield N, Corfield C, Gough M, Clamp JR, Durdey P, Warren BF, Bartolo DC, King KR, Williams JM. Colonic mucins in ulcerative colitis: evidence for loss of sulfation. Glycoconj J 1996;13:809-22.
83. Tsai HH, Dwarakanath AD, Hart CA, Milton JD, Rhodes JM. Increased faecal mucin sulphatase activity in ulcerative colitis: a potential target for treatment. Gut 1995;36:570-6.
84. Robertson AM, Wright DP. Bacterial glycosulphatases and sulphomucin degradation. Can J Gastroenterol 1997;11:361-6.
85. Rhodes JM. Unifying hypothesis for inflammatory bowel disease and associated colon cancer: sticking the pieces together with sugar. Lancet 1996;347:40-4.
86. Hoskins LC, Agustines M, McKee WB, Boulding ET, Kriaris M, Niedermeyer G. Mucin degradation in human colon ecosystems. Isolation and properties of fecal strains that degrade ABH blood group antigens and oligosaccharides from mucin glycoproteins. J Clin Invest 1985;75:944-53.
87. Corfield AP, Wagner SA, Clamp JR, Kriaris MS, Hoskins LC. Mucin degradation in the human colon: production of sialidase, sialate O-acetylesterase, N-acetylneuraminate lyase, arylesterase, and glycosulfatase activities by strains of fecal bacteria. Infect Immun 1992;60:3971-8.
88. Fedorak RN, Madsen KL. Naturally occuring and experimental models of inflammatory bowel disease. In: Kirsner JB, ed. Inflammatory bowel disease. 5th ed. Philadelphia: Saunders, 2000:113-143.
89. Elson CO, Sartor RB, Tennyson GS, Riddell RH. Experimental models of inflammatory bowel disease. Gastroenterology 1995;109:1344-67.
90. Kuhn R, Lohler J, Rennick D, Rajewsky K, Muller W. Interleukin-10-deficient mice develop chronic enterocolitis. Cell 1993;75:263-74.
91. Strober W, Fuss IJ, Blumberg RS. The immunology of mucosal models of inflammation. Annu Rev Immunol 2002;20:495-549.
92. Sellon RK, Tonkonogy S, Schultz M, Dieleman LA, Grenther W, Balish E, Rennick DM, Sartor RB. Resident enteric bacteria are necessary for development of spontaneous colitis and immune system activation in interleukin-10-deficient mice. Infect Immun 1998;66:5224-31.
93. Mahler M, Leiter EH. Genetic and environmental context determines the course of colitis developing in IL-10-deficient mice. Inflamm Bowel Dis 2002;8:347-55.

94. Schwerbrock NMJ, Li F, Büller HA, Einerhand AWC, Sartor RB, Dekker J. Altered Muc2 synthesis and sulfation in bacterial induced colitis in IL-10-/- mice. Gastroenterology 2001;120:A696.
95. Smirnov A, Sklan D, Uni Z. Mucin dynamics in the chick small intestine are altered by starvation. J Nutr 2004;134:736-42.
96. Sherman P, Forstner J, Roomi N, Khatri I, Forstner G. Mucin depletion in the intestine of malnourished rats. Am J Physiol 1985;248:G418-23.
97. Schaart MW, Schierbeek H, van der Schoor SR, Stoll B, Burrin DG, Reeds PJ, van Goudoever JB. Threonine utilization is high in the intestine of piglets. J Nutr 2005;135:765-70.
98. Bertolo RF, Chen CZ, Law G, Pencharz PB, Ball RO. Threonine requirement of neonatal piglets receiving total parenteral nutrition is considerably lower than that of piglets receiving an identical diet intragastrically. J Nutr 1998;128:1752-9.
99. Van Seuningen I, Pigny P, Perrais M, Porchet N, Aubert JP. Transcriptional regulation of the 11p15 mucin genes. Towards new biological tools in human therapy, in inflammatory diseases and cancer? Front Biosci 2001;6:D1216-34.
100. Campbell BJ, Rowe GE, Leiper K, Rhodes JM. Increasing the intra-Golgi pH of cultured LS174T goblet-differentiated cells mimics the decreased mucin sulfation and increased Thomsen- Friedenreich antigen (Gal beta1-3GalNac alpha-) expression seen in colon cancer. Glycobiology 2001;11:385-93.
101. Gouyer V, Wiede A, Buisine MP, Dekeyser S, Moreau O, Lesuffleur T, Hoffmann W, Huet G. Specific secretion of gel-forming mucins and TFF peptides in HT-29 cells of mucin-secreting phenotype. Biochim Biophys Acta 2001;1539:71-84.
102. Gratchev A, Siedow A, Bumke-Vogt C, Hummel M, Foss HD, Hanski ML, Kobalz U, Mann B, Lammert H, Stein H, Riecken EO, Hanski C, Mansmann U. Regulation of the intestinal mucin MUC2 gene expression in vivo: evidence for the role of promoter methylation. Cancer Lett 2001;168:71-80.
103. Enss ML, Cornberg M, Wagner S, Gebert A, Henrichs M, Eisenblatter R, Beil W, Kownatzki R, Hedrich HJ. Proinflammatory cytokines trigger MUC gene expression and mucin release in the intestinal cancer cell line LS180. Inflamm Res 2000;49:162-9.
104. Brivanlou AH, Darnell JE, Jr. Signal transduction and the control of gene expression. Science 2002;295:813-8.
105. Molkentin JD. The zinc finger-containing transcription factors GATA-4, -5, and -6. Ubiquitously expressed regulators of tissue-specific gene expression. J Biol Chem 2000;275:38949-52.
106. Sasaki H, Hogan BL. Differential expression of multiple fork head related genes during gastrulation and axial pattern formation in the mouse embryo. Development 1993;118:47-59.
107. Kaestner KH, Hiemisch H, Luckow B, Schutz G. The HNF-3 gene family of transcription factors in mice: gene structure, cDNA sequence, and mRNA distribution. Genomics 1994;20:377-85.
108. Silberg DG, Swain GP, Suh ER, Traber PG. Cdx1 and cdx2 expression during intestinal development. Gastroenterology 2000;119:961-71.
109. Gao X, Sedgwick T, Shi YB, Evans T. Distinct functions are implicated for the GATA-4, -5, and -6 transcription factors in the regulation of intestine epithelial cell differentiation. Mol Cell Biol 1998;18:2901-2911.
110. Van Wering HM, Bosse T, Musters A, De Jong E, De Jong N, Hogen Esch CE, Boudreau F, Swain GP, Dowling LN, Montgomery RK, Grand RJ, Krasinski SD. Complex regulation of the lactase-phlorizin hydrolase promoter by GATA-4. Am J Physiol Gastrointest Liver Physiol 2004;287:G899-G909.

111. Boudreau F, Rings EH, van Wering HM, Kim RK, Swain GP, Krasinski SD, Moffett J, Grand RJ, Suh ER, Traber PG. Hepatocyte nuclear factor-1 alpha, GATA-4, and caudal related homeodomain protein Cdx2 interact functionally to modulate intestinal gene transcription. Implication for the developmental regulation of the sucrase-isomaltase gene. J Biol Chem 2002;277:31909-31917.
112. Bosse T, van Wering HM, Gielen M, Dowling LN, Fialkovich JJ, Piaseckyj CM, Gonzalez FJ, Akiyama TE, Montgomery RK, Grand RJ, Krasinski SD. Hepatocyte nuclear factor-1{alpha} is required for expression but dispensable for histone acetylation of the lactase-phlorizin hydrolase gene in vivo. Am J Physiol Gastrointest Liver Physiol 2006;290:G1016-24.
113. Fang R, Olds LC, Santiago NA, Sibley E. GATA family transcription factors activate lactase gene promoter in intestinal Caco-2 cells. Am J Physiol Gastrointest Liver Physiol 2001;280:G58-67.
114. Krasinski SD, Van Wering HM, Tannemaat MR, Grand RJ. Differential activation of intestinal gene promoters: functional interactions between GATA-5 and HNF-1 alpha. Am J Physiol Gastrointest Liver Physiol 2001;281:G69-84.
115. Yamamoto H, Bai YQ, Yuasa Y. Homeodomain protein CDX2 regulates goblet-specific MUC2 gene expression. Biochem Biophys Res Commun 2003;300:813-8.
116. Mesquita P, Jonckheere N, Almeida R, Ducourouble MP, Serpa J, Silva E, Pigny P, Silva FS, Reis C, Silberg D, Van Seuningen I, David L. Human MUC2 mucin gene is transcriptionally regulated by Cdx homeodomain proteins in gastrointestinal carcinoma cell lines. J Biol Chem 2003;278:51549-56.
117. Morrisey EE, Ip HS, Lu MM, Parmacek MS. GATA-6: a zinc finger transcription factor that is expressed in multiple cell lineages derived from lateral mesoderm. Dev Biol 1996;177:309-322.
118. Morrisey EE, Ip HS, Tang Z, Lu MM, Parmacek MS. GATA-5: a transcriptional activator expressed in a novel temporally and spatially-restricted pattern during embryonic development. Dev Biol 1997;183:21-36.
119. Ang SL, Wierda A, Wong D, Stevens KA, Cascio S, Rossant J, Zaret KS. The formation and maintenance of the definitive endoderm lineage in the mouse: involvement of HNF3/forkhead proteins. Development 1993;119:1301-1315.
120. Zaret K. Developmental competence of the gut endoderm: genetic potentiation by GATA and HNF3/fork head proteins. Dev Biol 1999;209:1-10.
121. Traber PG, Silberg DG. Intestine-specific gene transcription. Annu Rev Physiol 1996;58:275-97.
122. Buisine MP, Devisme L, Savidge TC, Gespach C, Gosselin B, Porchet N, Aubert JP. Mucin gene expression in human embryonic and fetal intestine. Gut 1998;43:519-524.
123. Aslam F, Palumbo L, Augenlicht LH, Velcich A. The Sp family of transcription factors in the regulation of the human and mouse MUC2 gene promoters. Cancer Res 2001;61:570-6.
124. Perrais M, Pigny P, Copin MC, Aubert JP, Van Seuningen I. Induction of MUC2 and MUC5AC mucins by factors of the epidermal growth factor (EGF) family is mediated by EGF receptor/Ras/Raf/extracellular signal-regulated kinase cascade and Sp1. J Biol Chem 2002;277:32258-67.
125. Koo JS, Kim YD, Jetten AM, Belloni P, Nettesheim P. Overexpression of mucin genes induced by interleukin-1 beta, tumor necrosis factor-alpha, lipopolysaccharide, and neutrophil elastase is inhibited by a retinoic acid receptor alpha antagonist. Exp Lung Res 2002;28:315-32.
126. Kim YD, Kwon EJ, Park DW, Song SY, Yoon SK, Baek SH. Interleukin-1beta induces MUC2 and MUC5AC synthesis through cyclooxygenase-2 in NCI-H292 cells. Mol Pharmacol 2002;62:1112-8.
127. Jono H, Shuto T, Xu H, Kai H, Lim DJ, Gum JR, Jr., Kim YS, Yamaoka S, Feng XH, Li JD. Transforming growth factor-beta -Smad signaling pathway cooperates with NF-kappa B to

mediate nontypeable Haemophilus influenzae-induced MUC2 mucin transcription. J Biol Chem 2002;277:45547-57.

128. Dabbagh K, Takeyama K, Lee HM, Ueki IF, Lausier JA, Nadel JA. IL-4 induces mucin gene expression and goblet cell metaplasia in vitro and in vivo. J Immunol 1999;162:6233-7.

129. Kim YD, Jeon JY, Woo HJ, Lee JC, Chung JH, Song SY, Yoon SK, Baek SH. Interleukin-1beta induces MUC2 gene expression and mucin secretion via activation of PKC-MEK/ERK, and PI3K in human airway epithelial cells. J Korean Med Sci 2002;17:765-71.

130. Song KS, Lee WJ, Chung KC, Koo JS, Yang EJ, Choi JY, Yoon JH. Interleukin-1 beta and tumor necrosis factor-alpha induce MUC5AC overexpression through a mechanism involving ERK/p38 mitogen-activated protein kinases-MSK1-CREB activation in human airway epithelial cells. J Biol Chem 2003;278:23243-50.

131. Iwashita J, Sato Y, Sugaya H, Takahashi N, Sasaki H, Abe T. mRNA of MUC2 is stimulated by IL-4, IL-13 or TNF-alpha through a mitogen-activated protein kinase pathway in human colon cancer cells. Immunol Cell Biol 2003;81:275-82.

132. Mack DR, Gaginella TS, Sherman PM. Effect of colonic inflammation on mucin inhibition of Escherichia coli RDEC-1 binding in vitro. Gastroenterology 1992;102:1199-211.

133. Mack DR, Michail S, Wei S, McDougall L, Hollingsworth MA. Probiotics inhibit enteropathogenic E. coli adherence in vitro by inducing intestinal mucin gene expression. Am J Physiol 1999;276:G941-50.

134. Zen Y, Harada K, Sasaki M, Tsuneyama K, Katayanagi K, Yamamoto Y, Nakanuma Y. Lipopolysaccharide induces overexpression of MUC2 and MUC5AC in cultured biliary epithelial cells: possible key phenomenon of hepatolithiasis. Am J Pathol 2002;161:1475-84.

135. Mattar AF, Teitelbaum DH, Drongowski RA, Yongyi F, Harmon CM, Coran AG. Probiotics up-regulate MUC-2 mucin gene expression in a Caco-2 cell-culture model. Pediatr Surg Int 2002;18:586-90.

136. Lee CG, Homer RJ, Cohn L, Link H, Jung S, Craft JE, Graham BS, Johnson TR, Elias JA. Transgenic overexpression of interleukin (IL)-10 in the lung causes mucus metaplasia, tissue inflammation, and airway remodeling via IL-13-dependent and -independent pathways. J Biol Chem 2002;277:35466-74.

137. Fuss IJ, Boirivant M, Lacy B, Strober W. The interrelated roles of TGF-beta and IL-10 in the regulation of experimental colitis. J Immunol 2002;168:900-8.

138. Spicer AP, Parry G, Patton S, Gendler SJ. Molecular cloning and analysis of the mouse homologue of the tumor- associated mucin, MUC1, reveals conservation of potential O-glycosylation sites, transmembrane, and cytoplasmic domains and a loss of minisatellite-like polymorphism. J Biol Chem 1991;266:15099-109.

Part I

Role of Mucins in the Intestine

Chapter 2

Development of Chronic Colitis by Interleukin 10 Deficient Mice

Published as:
Nicole M.J. Schwerbrock, Mireille K. Makkink, Maria van der Sluis, Alexandra W.C. Einerhand, Hans A. Büller, Balfour R. Sartor and Jan Dekker. *Interleukin 10 deficient mice are defective in colonic Muc2 synthesis, both before and after induction of colitis by commensal bacteria.*

Inflammatory Bowel Diseases 10(6): 811-823, 2004

Abstract

Germ-free (GF) interleukin 10 deficient ($IL10^{-/-}$) mice develop chronic colitis after colonization by normal enteric bacteria. Mucin 2 (Muc2) is the major structural component of the protective colonic mucus. Our aim was to determine if primary or induced aberrations in Muc2 synthesis occur in GF $IL10^{-/-}$ mice that develop colitis after bacterial colonization. GF $IL10^{-/-}$ and wild type (WT) mice were colonized with commensal bacteria for various intervals up to 6 weeks. Colitis was quantified by histological score and IL-12 secretion. Muc2 synthesis, total level of Muc2, and Muc2 sulfation were measured quantitatively. GF $IL10^{-/-}$ mice showed 10-fold lower Muc2 synthesis and Muc2 levels compared to GF WT mice, but Muc2 sulfation was not different. When bacteria were introduced, $IL10^{-/-}$ mice developed colitis, whereas WT mice remained healthy. Muc2 synthesis was unchanged in WT, but $IL10^{-/-}$ mice showed a peak increase in Muc2 synthesis 1 week after bacterial introduction, returning to baseline levels after 2 weeks. Total Muc2 levels decreased 2-fold in WT mice, but remained at stable low levels in $IL10^{-/-}$ mice. Upon introducing bacteria, Muc2 sulfation increased 2-fold in WT mice, whereas in $IL10^{-/-}$ mice Muc2 sulfation decreased 10-fold. Conclusions: A primary defect in colonic Muc2 synthesis is present in $IL10^{-/-}$ mice, whereas bacterial colonization and colitis in these mice led to reduced Muc2 sulfation. These quantitative and structural aberrations in Muc2 in $IL10^{-/-}$ mice likely reduce the ability of their mucosa to cope with non-pathogenic commensal bacteria and may contribute to their susceptibility to develop colitis.

Abbreviations used in this paper

GF, germ-free; IBD, inflammatory bowel disease; IL, interleukin; MUC, Mucin; Tff3, trefoil factor 3; SPF, specific pathogen free; WT, wild type

Introduction

Secretory mucins play cytoprotective roles by forming a protective mucus layer covering the underlying epithelium in the gastrointestinal tract[1, 2]. The large intestinal epithelium confronts a particularly hostile environment, containing very large amounts of predominantly anaerobic bacteria of many species. Breaching the protective epithelial barrier can lead to a chronic cycle of inflammation that progressively damages the epithelial barrier function, thereby initiating a self-perpetuating inflammatory process[3]. Many gastrointestinal diseases, particularly the chronic inflammatory bowel diseases (IBD), show escalation of mucosal inflammation due to transient or sustained damage to the epithelium[4-6]. Inflammation may flare despite immunosuppressive therapies. The causes of these exacerbations are generally not understood, and are most likely multifactorial, including genetic and environmental factors. However, accumulating evidence implicates commensal enteric bacteria in playing an important role in the initiation and perpetuation of chronic, immune-mediated intestinal inflammation[3, 7, 8]. The most compelling evidence for a role for bacteria in the pathogenesis of intestinal inflammation comes from rodent models of IBD, in which both the host genetics and the micro-ecology can be precisely manipulated[9, 10].

We have demonstrated previously that the human colonic epithelium expresses one secretory mucin in very high amounts: Mucin2 (MUC2). Importantly, we also have shown that in patients with ulcerative colitis the activity of the mucosal inflammation correlates significantly with a decrease in MUC2 synthesis and MUC2 secretion[11-13]. Adjacent to ileal ulcers in Crohn's disease MUC2 is absent and MUC5AC and MUC6 are induced[14]. Pullan and coworkers demonstrated that the mucus gel of the colon was significantly thinner during active inflammation implying that the thickness of the mucus gel is affected by IBD or perhaps contributes to the pathogenesis of inflammation[15]. Also the mucus layer of IBD patients is more easily penetrated and colonized by enteric bacteria[16, 17]. These results in human colonic tissue suggest that MUC2 plays an important role in colonic cytoprotection, but the limited availability of tissues during early stages of disease and the lack of information on the early, sub-clinical stages of disease hamper further studies. There are however many colitis models in the mouse that are well suited to test the susceptibility of the colonic epithelium to luminal substances[9, 18].

In this study we used a genetically engineered mouse strain deficient for interleukin 10 (IL-10), which constitutes a well-accepted model for human IBD[4, 19, 20]. These mice develop Th1-mediated chronic colitis when housed under specific pathogen free (SPF) conditions, but under germ-free (GF, completely sterile) conditions these mice develop no signs of inflammation [21]. Adult GF IL10$^{-/-}$ mice develop mild colonic inflammation within 1 week after colonization with specific pathogen free enteric bacteria; this colitis progresses to severe intensity by 5 weeks of bacterial colonization[21]. Wild type (WT) mice, which were born and raised under GF conditions, do not develop colitis upon introduction of commensal enteric bacteria under SPF conditions[21]. These, and a wealth of similar data, indicate that the presence of bacteria in the colon is a prerequisite for the development of chronic, immune-mediated colitis in a genetically susceptible host[3, 22-25].

Previously, we established that Muc2 is the dominant colonic secretory mucin in mice[26, 27] similar to humans and rats[28, 29]. To reveal the influence of commensal enteric bacteria on Muc2 synthesis, secretion and sulfation and the possible role of Muc2 in the pathogenesis of chronic colitis, we studied the effects of the introduction of SPF commensal bacteria in GF IL10$^{-/-}$ mice on mucin biosynthesis at different times after bacterial exposure. Following previously established procedures for measuring Muc2 levels in human, rat and murine tissues[12, 13, 26], we quantified Muc2 synthesis, total Muc2, Muc2 sulfation, Muc2 mRNA, and secretion of Muc2 in the colonic tissues of these mice.

First, we documented that no congenital differences existed in the Muc2 levels between 129 SvEv SPF WT mice, the genetic background of the IL10$^{-/-}$ mice, and the BALB/c WT mice. Having established that there were no significant differences between the various parameters of Muc2 synthesis among these two mice strains, we determined the levels of Muc2 in GF IL10$^{-/-}$ and GF WT mice. Thus, we were able to study any differences in Muc2 levels related to the lack of endogenous IL-10 that could pre-dispose to epithelial and/or mucosal damage upon introduction of commensal bacteria. After colonization with SPF enteric bacteria for variable times, we correlated changes in Muc2 in the IL10$^{-/-}$ and WT mice with the development of colonic inflammation. Thus, we were able to detect changes in synthesis or sulfation of Muc2 that were induced by bacterial colonization or by inflammation. We established that aberrant levels in Muc2 occurred in IL10$^{-/-}$ mice during both the GF and SPF states and suggest that these abnormalities may contribute to the development of colitis in IL10$^{-/-}$ mice.

Materials and Methods

Animals

Animals used in this study were 12-16 weeks-old 129 SvEv mice carrying a homozygous null-mutation of the IL-10 gene, formally designated IL10^{tm1Cgn}[19, 20]. The latter mice were indicated as IL10$^{-/-}$ mice throughout this study. Since GF 129 SvEv WT mice were unavailable, 12-13 weeks-old GF BALB/c mice served as WT controls. All GF mice were provided by the Gnotobiotic Rodent Facility of the College of Veterinary Medicine, North Carolina State University, Raleigh, N.C., where the mice were housed under GF conditions in Trexler flexible film isolators with autoclaved food and water ad libitum, as previously described[21]. GF mice were documented to be sterile by aerobic and anaerobic culture of fecal and Gram stain pellets every 2 weeks and at necropsy. For bacterial colonization, GF mice were moved to a SPF mouse facility, where they were initially housed in sterile micro-isolators with sterile food and water. After three days, normal enteric bacteria were introduced by swabbing the mouths of GF mice with a homogenate of feces of SPF mice, and by placing bedding and feces from SPF mice into the cages. Mice were then on the same day placed in clean cages and from then on housed under SPF conditions until analysis. The SPF bacteria that were introduced in these mice were documented to be free of Helicobacter species[21]. For comparison purposes, male 10-12 weeks-old SPF 129 SvEv and BALB/c mice were obtained from Charles River Nederland (Maastricht, the Netherlands). All mice were kept in the same facility

under SPF conditions, and were colonized with the same strains of normal enteric bacteria.

Experimental design

BALB/c mice and IL10$^{-/-}$ mice were born and raised in a GF environment. Groups of GF BALB/c mice and GF IL10$^{-/-}$ mice were sacrificed for study of Muc2 in the absence of bacterial stimulation. In other GF mice, SPF bacteria were introduced and mice were maintained in a strict SPF environment until necropsy for BALB/c mice at 1 (n=6) and 4 weeks (n=4) and for the IL10$^{-/-}$ mice at 1 (n=5), 2 (n=4) and 6 weeks (n=4) after bacterial colonization. We studied three regions of the large intestine in each mouse: cecum, proximal colon, and distal colon. The mice were killed by cervical dislocation and large intestinal tissue explants were prepared immediately. Four explants were taken for metabolic labeling and immediately put in appropriate pre-warmed culture medium, as described below. Sections of the cecum were prepared for fragment cultures, as described below. Additionally, large intestinal segments were fixed in 4% (w/v) paraformaldehyde in PBS, or frozen in liquid nitrogen and stored at minus 80°C for RNA analysis.

Histology and immunohistochemistry of large intestinal sections

Large intestinal segments, fixed in paraformaldehyde, were embedded, sectioned (6-µm thick), and processed for either histochemical staining or immunohistochemical detection of proteins. Histochemical staining was performed with: i. hematoxylin and eosin (HE), ii. alcian blue (AB) at pH 2.5 followed by periodic acid/Schiff's reagent (PAS), or iii. high iron diamine (HID) followed by alcian blue at pH 2.5. A gastrointestinal histological score ranging from 0 to 4 was used in a blinded fashion to evaluate intestinal inflammation, as validated for IL10$^{-/-}$ mice[21]. Expression of Muc2 was detected by immunohistochemistry using a polyclonal anti-murine Muc2 antibody as we described earlier[26, 27].

Measurements of IL-12 secretion

IL-12 secretion by cecal fragments was measured as previously described[21]. Briefly, small sections of cecal tissue were washed with PBS to remove feces, and subsequently gently shaken in RPMI medium containing 1% (w/v) penicillin and 1% (w/v) streptomycin for 30 min. The tissue sections were cut into small fragments and cultured in wells in duplicate in 1000 µl of RPMI 1640 medium (Gibco-BRL, Gaithersburg MD, USA) containing 1% (w/v) of both penicillin and streptomycin, and 5% (v/v) heat-inactivated fetal calf serum, at 37°C for 18 h. Culture supernatants were collected and stored at minus 20°C until analysis. IL-12 secretion in the culture supernatants was measured by enzyme-linked immunosorbent assay (ELISA), using anti-IL-12 antibodies C15.6 and C17.8 (Pharmingen, San Diego, CA, USA) for capture and detection, respectively, of the IL-12p40 subunit[21, 25]. The amount of binding of biotinylated antibodies was detected using horseradish peroxidase-labeled streptavidin (Kirkegaard and Perry Laboratories, Gaithersburg, MD, USA). IL-12p40 concentrations were calculated using a standard curve with recombinant IL-12 p70 (Pharmingen). IL-12 p40 secretion was measured in duplicate culture supernatants in each separate experiment.

Metabolic labeling of large intestinal explants

Of each region of each mouse large intestine, two explants were metabolically labeled *ex vivo* with [^{35}S]methionine/cysteine to label proteins, including Muc2 precursors, and two further explants were metabolically labeled with [^{35}S]sulfate to label glycoproteins, particularly mature mucin. Metabolic labeling was performed as described previously[12, 13, 26, 30]. Briefly, two biopsies were placed separately in 100 µl tissue culture medium devoid of either methionine/cysteine or sulfate and pulse-labeled for 30 min by adding respectively 100 µCi [^{35}S]methionine/cysteine (Translabel, ICN, Costa Mesa CA, USA) or 100 µCi Na[^{35}S]sulfate (ICN). The [^{35}S]methionine/cysteine-labeled explants were homogenized immediately. The two [^{35}S]sulfate-labeled explants were chase-incubated separately for 4 h in 500 µl medium devoid of radiolabel, but containing a standard concentration of non-radiolabeled sulfate. All incubations took place in RPMI 1640 medium (Gibco-BRL) supplemented with antibiotics and glutamine (Sigma, St. Louis, USA) at 37°C under 95% O_2/ 5% CO_2. All explants were homogenized separately at 0°C in 1000 µl homogenization buffer containing Triton X-100 (BDH, Poole, UK) and various protease inhibitors. The media from chase-incubations were mixed with 500 µl of this buffer and thoroughly mixed. The homogenates and media were stored at minus 20°C until further analysis as described in the next paragraphs.

Measurement of protein synthesis

Protein content was measured in the homogenate of each explant, using a bicinchoninic acid protein assay kit and bovine serum albumin as a standard (Pierce, Rockford IL, USA). Total incorporation of radioactivity in proteins was determined using a PhosphorImager with ImageQuant software (Molecular Dynamics, B&L systems, Zoetermeer, the Netherlands) after trichloroacetic acid precipitation, as previously described[12].

Quantitation of radiolabeled Muc2

We described the Muc2 quantitation protocol previously in studies on the quantification of human, rat and mouse Muc2 synthesis in colonic biopsies[12, 13, 26, 30]. In these studies, we showed that after pulse-labeling with [^{35}S]methionine/cysteine for 30 min the Muc2 precursor could be identified on SDS-PAGE, which is detectable as a band at approximately 600 kDa. The [^{35}S]sulfate-labeled mature Muc2 was detected on SDS-PAGE as a 550 kDa band. For the quantitation of [^{35}S]sulfate- and [^{35}S]methionine/cysteine-labeled mature Muc2, equal aliquots of each radiolabeled homogenate were analyzed on reducing SDS-PAGE (3% (w/v) stacking, 4% (w/v) running gel). Gels were fixed in 10% (v/v) methanol/10% (v/v) acetic acid, stained with PAS, dried and then the Muc2 bands were quantified (in arbitrary units, a.u.) by autoradiography using a PhosphorImager and ImageQuant software. In each sample the Muc2 precursor synthesis was corrected for the total protein synthesis, measured by trichloroacetic acid precipitation as described above. To determine [^{35}S]sulfate-incorporation into Muc2, the amount of [^{35}S]sulfate-labeled Muc2 in a tissue homogenate, as determined from the 550 kDa mature Muc2 band on SDS-PAGE, was corrected for the total Muc2 contents in the respective homogenates, determined as described below. For each explant, the [^{35}S]sulfate-incorporation into

Muc2 was also corrected for differences in protein content between the individual homogenates.

Quantitation of total Muc2

We described this quantitation protocol previously for human and murine Muc2[12, 13, 26, 30]. In short, to analyze the total Muc2 (i.e. both radiolabeled and non-radiolabeled Muc2, and Muc2 precursor as well as mature Muc2) Western-type dot blotting was performed, using an antibody that recognizes peptide epitopes of precursor as well as mature murine Muc2 [26, 27]. The linear range of the assay was determined by serial dilution of samples, and subsequently a sample size was chosen that allowed measurement of each sample within the linear range of the assay. Homogenates were diluted and 100 µl of ^{35}S-labeled homogenate containing exactly 1 µg protein as measured using a BCA protein assay kit was dot blotted onto nitro-cellulose (Nitran, Schleier & Schuell, Dassel, Germany). Then the blot was incubated with anti-mouse Muc2 antibodies, washed and incubated for 2 h with ^{125}I-labeled protein A (specific activity 17.0 mCi/µg, Amersham, Buckinghamshire, UK). Binding of ^{125}I-labeled protein A to the polyclonal anti-mouse Muc2 antiserum was detected by autoradiography using a PhosphorImager (expressed in a.u.), after the blot was covered by two sheets of 3MM Whatman filter paper in order to eliminate background radiation of intrinsic ^{35}S-label as present in the homogenates. The percentage of secreted Muc2 was calculated as the amount of Muc2 in the medium divided by the sum of the amount of Muc2 in the tissue and in the medium. This was multiplied by 100 to give the percentage of secreted Muc2.

Quantitation of mRNA

RNA was isolated from the various regions of the murine large intestine, using Trizol reagent (Gibco-BRL) following the manufacturer's protocol. The Northern blot analysis was essentially carried out as previously described[11]. Briefly, 2 µg total RNA derived from each tissue sample was separated on a 0.8% (w/v) agarose gel containing 10 mM HEPES (Sigma) pH 7.5 and 2.2 M formaldehyde (Merck, Darmstadt, Germany). Integrity of RNA was assessed by analysis of the 28 S and 18 S ribosomal RNAs after electrophoresis and staining by ethidium bromide. Spot blotting of the RNA to Hybond N$^+$ membrane (Amersham) was carried out using a vacuum-operated manifold (BioRad, Veenendaal, the Netherlands). The blot was hybridized to either a ^{32}P-labeled 244 bp SalI-EcoRI fragment of the murine Muc2 cDNA, or to a ^{32}P-labeled 438 bp rat trefoil factor family peptide 3 (Tff3) probe, as we described previously[29, 31, 32]. After autoradiography by exposure of the membrane to a PhosphorImager plate, the probe was stripped from the blot. The membrane was re-probed with a ^{32}P-labeled human glyceraldehydephosphate dehydrogenase (GAPDH) probe. The level of hybridization on the spot blots to the murine Muc2 probe and the GAPDH probe were measured through autoradiography using a PhosphorImager and ImageQuant software, as described[26].

Statistical analysis

Statistical significance was assessed by one-way analysis of variance test and Mann-Whitney U-test. Results were considered as statistically significant at $P<.05$.

Results

Wild type mice: Comparison of the Muc2 synthesis in BALB/c and 129 SvEv mice

Since GF 129 SvEv WT mice were unavailable, GF BALB/c mice of the same age served as WT controls. It was however not known if these two strains of mice expressed the same levels of Muc2, or if these strains differed in any of the other parameters relevant to this study. Therefore, SPF mice of both strains, BALB/c (n = 7) and 129 SvEv (i.e. the parental strain of the IL10$^{-/-}$ mice, n = 6) were tested for their ability to synthesize Muc2 in their colonic epithelia. Following the previously established procedures, described in the Material and Methods section, we measured in the colonic tissue of these mice: (i). total protein synthesis, (ii). Muc2 precursor protein synthesis, (iii) total Muc2 levels in colonic mucosa, (iv). sulfation levels of Muc2, (v). Muc2 mRNA levels, (vi) secretion of Muc2, (vii) secretion of sulfated Muc2, and (viii) Tff3 mRNA levels. As documented in Figure 1 and Table I, there were no statistically significant differences in these parameters as measured between these mouse strains. The only remarkable observation, in the comparison between these two WT strains, was that the degree of sulfation of Muc2, as produced by colonic explants of the 129 SvEv mice, was higher in each of the colonic regions than in the BALB/c mice. However, these differences are statistically significant only for the proximal colon. Collectively these data indicate that there are no differences in the parameters that are relevant to this study among these two mouse strains, when born and raised under SPF conditions.

Introduction of normal enteric bacteria

We investigated specific changes in the large intestine during onset and development of colitis in IL10$^{-/-}$ mice after the introduction of SPF bacteria into GF IL10$^{-/-}$ mice, versus BALB/c WT control mice. During these experiments, there were no significant changes in animal behavior, stool consistency or body weight within or between the groups (data not shown). Total protein synthesis in the BALB/c mice was

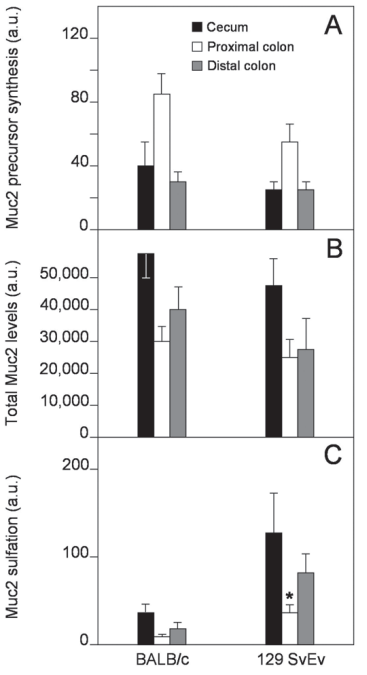

Figure 1. Muc2 synthesis in wild-type BALB/c and 129 SvEv mice. Muc2 precursor synthesis (Panel A), total Muc2 levels (Panel B), and the sulfation of total Muc2 (Panel C) were measured in wild-type BALB/c (n = 7), and 129 SvEv (n = 6) mice in the cecum and the proximal and distal colon. All mice were kept in the same facility under SPF conditions, and were colonized with the same strains of normal enteric bacteria. SEMs are indicated. *Asterisks* denotes a statistically significant difference in sulfation level between Muc2 form the proximal colon of the 129 SvEv and BALB/c mice (P<.05).

increased at day 7 after the introduction of enteric bacteria (Table II). At day 7 after the introduction of SPF bacteria the total protein synthesis was higher in all regions of the large intestine of the BALB/c mice, compared to the comparable region of the large intestine of the IL10$^{-/-}$ mice. At days 28-42 the protein synthesis levels of both strains returned to levels not significantly different from the respective levels on day 0 after introduction of bacteria.

Table I. Protein synthesis, Muc2 and trefoil family factor 3 (Tff3) mRNA levels and secretion of total and $^{35}SO_3$-labeled Muc2 in wild-type BALB/c and 129 SvEv mice.

Region	Strain*	Total protein synthesis (a.u./mg) †	Muc2 mRNA (a.u.)	Tff3 mRNA (a.u.)	Secretion total Muc2 (%)	Secretion $^{35}S0_3$-labeled Muc2 (%)
Cecum	BALB/c	209.1 [50.4] ‡	442.5 [61.7]	342.2 [57.8]	52.8 [5.4]	64.0 [8.6]
	129 SvEv	470.2 [154.1]	405.4 [45.2]	286.0 [53.2]	64.1 [9.4]	52.0 [5.8]
Proximal Colon	BALB/c	413.0 [91.8]	5142.8 [919.9]	479.0 [86.2]	25.9 [5.0]	21.6 [7.0]
	129 SvEv	287.8 [48.5]	5898.3 [836.5]	496.6 [90.3]	34.3 [5.6]	22.5 [5.2]
Distal Colon	BALB/c	328.1 [64.4]	459.9 [37.4]	381.9 [44.7]	44.6 [6.2]	32.1 [4.5]
	129 SvEv	411.9 [114.7]	579.9 [94.1]	333.8 [118.4]	38.8 [8.2]	34.2 [5.8]

NOTE. * Normal SPF BALB/c (n = 7) and 129 SvEv (n = 6) mice were analyzed as indicated in the legends of Figure 1.
† a.u., arbitrary units
‡ SEMs are indicated between brackets.

IL-10 normally plays an important role in the regulation of the immune responses by inhibiting innate immune cell production of the pro-inflammatory cytokine IL-12. We measured IL-12p40 secretion by cecal tissues from each group. IL10$^{-/-}$ and BALB/c mice revealed nearly undetectable levels of IL-12p40 in cecum culture supernatants under GF conditions. Upon introduction of commensal bacteria, the IL10$^{-/-}$ mice housed under SPF conditions for 42 days showed significantly increased levels of cecal IL-12 secretion, whereas BALB/c mice revealed no significant changes in IL-12 levels over the 28-day period of observation (Fig. 2).

Large intestinal morphology

The cecum and proximal and distal colon of IL10$^{-/-}$ and BALB/c mice showed similar histology with no evidence of inflammation under GF conditions (not shown). BALB/c mice revealed no significant morphological alterations by HE staining after the introduction of SPF bacteria in all large intestinal regions, as exemplified for proximal colon in Figure 3A, B. In contrast, the large intestines of the IL10$^{-/-}$ mice displayed major differences in each colonic region after inoculation with commensal bacteria, primarily characterized by epithelial hyperplasia and mononuclear infiltrates

(Fig. 3C, D). The inflammation was quantified in a blinded fashion using a standardized histological score ranging from 0 (no inflammation) to 4 (severe inflammation)[21]. The GF IL10$^{-/-}$ tissue showed only a very low grade of inflammation (inflammation score, 0.58 [SEM, 0.05]). The inflammation scores did not change significantly in the BALB/c mice after the introduction of SPF bacteria. However, after the introduction of commensal bacteria in the IL10$^{-/-}$ mice the histologic inflammatory score increased significantly (P<.05) to 2.50 [SEM, 0.34], 2.56 [SEM, 0.54], and 2.31 [SEM, 0.40], after 7, 14 and 42 days of bacterial exposure, respectively.

Figure 2. Cecal IL-12 secretion in BALB/c and IL10$^{-/-}$ mice. IL-12 secretion was measured from cecum explants, which were cultured in vitro for 24 h (measured as pg IL-12 per 0.025 g tissue protein). Days after inoculation of the germ-free mice (GF) with normal enteric bacteria are indicated, day 0 indicates the GF status. *Asterisks*, indicates a significant increase in IL-12 production in tissue from IL10$^{-/-}$ mice on day 7, relative to BALB/c mice on day 7 (P<.02). [a] Indicates a significant increase in the IL-12 production by explants from the IL10$^{-/-}$ on these respective days, relative to IL10$^{-/-}$ mice on day 0 (P<.02). SEMs are indicated.

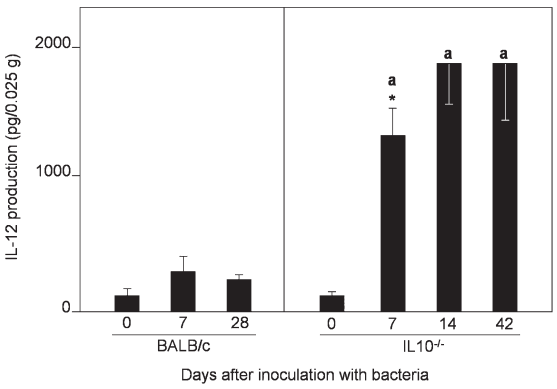

Table II. Total protein synthesis in BALB/c and IL10$^{-/-}$ mice.

Region	Strain*	Day 0	Day 7	Day 14	Day 28	Day 42
Cecum	BALB/c	62.5 [12.7] [§]	237.3 [60.5] [‡]	n.d. [–]	95.3 [34.2]	n.d.
	IL10$^{-/-}$	194.0 [60.5] [†]	171.6 [51.7]	90.5 [30.2]	n.d.	282.0 [32.7]
Proximal colon	BALB/c	80.0 [10.7]	272.0 [66.9] [‡]	n.d.	188.8 [81.4]	n.d.
	IL10$^{-/-}$	189.8 [75.6]	161.4 [74.4]	103.8 [36.3]	n.d.	205.0 [63.0]
Distal colon	BALB/c	129.5 [77.5]	295.5 [70.9] [‡]	n.d.	167.9 [109.4]	n.d.
	IL10$^{-/-}$	237.4 [121.9]	85.6 [28.8]	118.5 [39.1]	n.d.	142.0 [38.3]

NOTE. * On day 0, GF mice from either strain were colonized with normal enteric bacteria under SPF conditions. Days after inoculation with bacteria are indicated, day 0 indicates the GF status. Total protein synthesis was measured as explained in the Methods section, and is expressed as a.u./mg.
[†] The protein synthesis in the cecum of the IL10$^{-/-}$ was significantly higher than in the cecum of GF BALB/c mice (P<.05).
[‡] The protein synthesis in each region of the large intestine of the BALB/c mice was higher on day 7, than in the cognate regions of the IL10$^{-/-}$ mice (P<.05).
[–] n.d., not determined.
[§] SEMs are indicated between brackets.

Goblet cells, the source of secretory mucins like Muc2, were numerous in each large intestinal region of the GF as well as the bacteria-colonized mice of both strains, as detected by AB/PAS and HID/AB staining (Fig. 3E-L). Interestingly, the IL10$^{-/-}$ mice revealed altered PAS and HID staining patterns upon introduction of SPF bacteria. GF IL10$^{-/-}$ mice, like BALB/c mice, displayed PAS- and HID-positive goblet cells in the upper half of the colonic crypts. Remarkably these PAS- and HID-positive cells were absent in crypts of the bacteria-colonized IL10$^{-/-}$ mice, shown in Figure 3H and 3L, respectively. This is indicative of structural changes in the glycosylation of the mucins in these cells of the upper crypts. In particular, the absence of HID-staining indicated that the IL10$^{-/-}$ mice colonized by enteric bacteria have a lower level of sulfation of the mucins within these goblet cells, relative to the GF situation.

Immunohistological staining revealed that the goblet cells in both GF and bacteria-colonized BALB/c mice stained positive for Muc2 (Fig. 3M, N). Also in IL10$^{-/-}$ mice, both in GF status and after colonization with enteric bacteria, all goblet cells were stained for Muc2 (Fig. 3O, P), indicating that Muc2 was still produced by goblet cells after bacterial colonization.

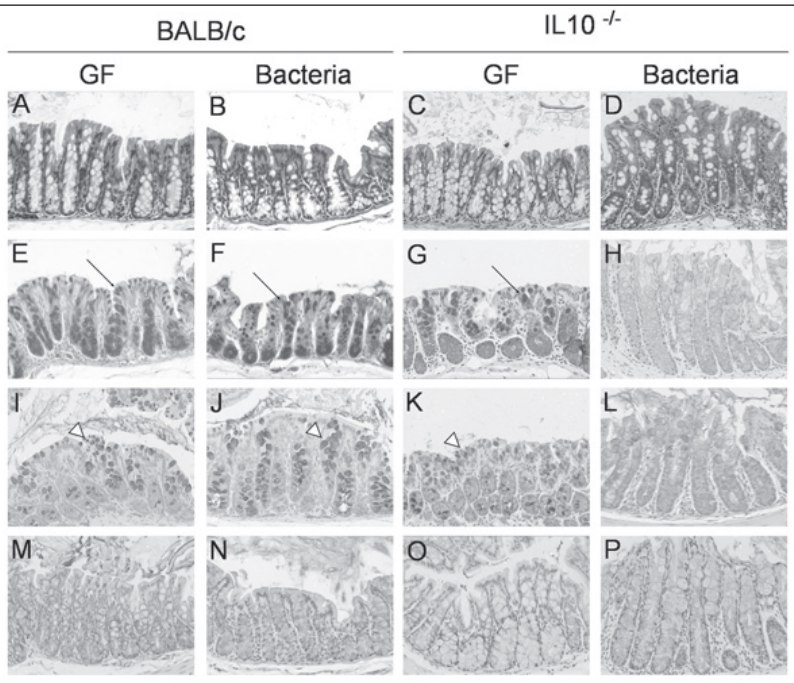

Figure 3. Histochemistry of BALB/c and IL10$^{-/-}$ proximal colon. Tissue sections were prepared from the proximal colon of BALB/c and IL10$^{-/-}$ mice in germ-free (GF) conditions and at 7 days after the introduction of SPF normal enteric bacteria (Bacteria). The tissue sections were stained histochemically with hematoxylin and eosin (Panels A-D), AB/PAS (Panels E-H), or HID/AB (Panels I-L). The arrows in Panels E-G indicate PAS-positive goblet cells in the upper half of the crypts. The arrowheads in Panels I-K indicate HID-positive goblet cells in the upper half of the crypts. Sections were stained immunohistochemically for the presence of Muc2 protein, using a polyclonal anti-murine Muc2 antiserum (Panels M-P). All micrographs were recorded at the identical magnification of 200x. Please also see page 219.

Muc2 levels in BALB/c and IL10$^{-/-}$ mice

Muc2 precursor synthesis was determined as the metabolic incorporation of [^{35}S]methionine/cysteine into this protein in tissue explants. The level of Muc2 precursor synthesis was approximately ten-fold lower in each of the large intestinal regions of GF IL10$^{-/-}$ mice than in the respective regions of the large intestines of GF BALB/c mice (Fig.4). Following colonization with bacteria, the BALB/c mice exhibited no significant differences in precursor biosynthesis. In contrast, IL10$^{-/-}$ mice exposed to SPF bacteria for 7 days showed a 5- to 20-fold increase in Muc2 precursor synthesis, which returned to levels similar to those of GF IL10$^{-/-}$ mice after 14 days of exposure to bacteria (Fig. 4). Thus, early colonization (7 days) with bacteria induced a strong, but transient, increase in Muc2 precursor biosynthesis in IL10$^{-/-}$ mice, which at other time points showed defective Muc2 synthesis.

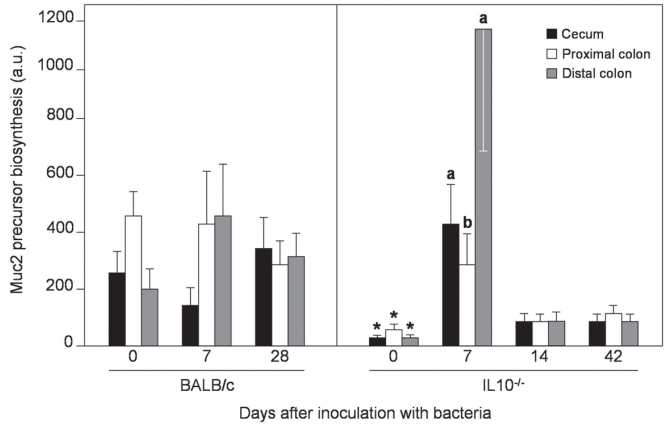

Figure 4. Muc2 precursor synthesis in BALB/c and IL10$^{-/-}$ mice. Muc2 precursor synthesis was measured in tissue explants from the cecum and proximal and distal colon of BALB/c and IL10$^{-/-}$ mice. Days after inoculation with normal enteric bacteria are indicated, day 0 indicates the GF status. The Muc2 precursor synthesis, in each colonic region, was significantly lower in the GF IL10$^{-/-}$ mice, relative to the GF BALB/c mice (*P<.005). The Muc2 precursor biosynthesis increased significantly on day 7, relative to day 0, in the explants of the IL10$^{-/-}$ mice in each of the respective regions of the large intestine (^{a}P<.01, ^{b}P<.05). SEMs are indicated.

The total levels of Muc2 were determined by Western-type spot-blotting that measures the levels of mature Muc2 plus Muc2 precursor (Fig. 5). GF IL10$^{-/-}$ mice showed statistically significant 3- to 10-fold lower levels of total Muc2, compared to GF BALB/c mice. Bacterial colonization induced a statistically significant decrease of total Muc2 levels in BALB/c mice by 7 days after inoculation, and total Muc2 levels remained significantly reduced until at least 28 days after exposure to bacteria. Muc2 levels in the IL10$^{-/-}$ mice hardly changed after the introduction of bacteria and total levels of Muc2 remained much lower in the IL10$^{-/-}$ mice at each time point compared to BALB/c mice (Fig. 5).

The degree of sulfation of the mature Muc2 molecules was measured by labeling large intestinal tissue segments metabolically by [^{35}S]sulfate for 30 min, chase-incubating in fresh medium for 4 h, and homogenizing the tissue. The

incorporation of [^{35}S]sulfate into Muc2 was quantified after SDS-PAGE, and was related to the total amount of Muc2 in the homogenate and medium, respectively, as determined by Western-type spot-blot analysis (Fig. 6). GF IL10$^{-/-}$ mice showed a slightly higher colonic Muc2 sulfation compared to GF BALB/c mice, yet this difference was not statistically significant in any region of the large intestine (Fig. 6 and results not shown). Introduction of bacteria led to progressively increased sulfate incorporation in Muc2 in the colon of BALB/c mice after 7 and 28 days after inoculation with bacteria (Fig. 6). In contrast, IL10$^{-/-}$ mice revealed a progressive decrease in sulfate incorporation into Muc2 upon introduction of bacteria, reaching statistical significance after 42 days of exposure to bacteria (Fig. 6).

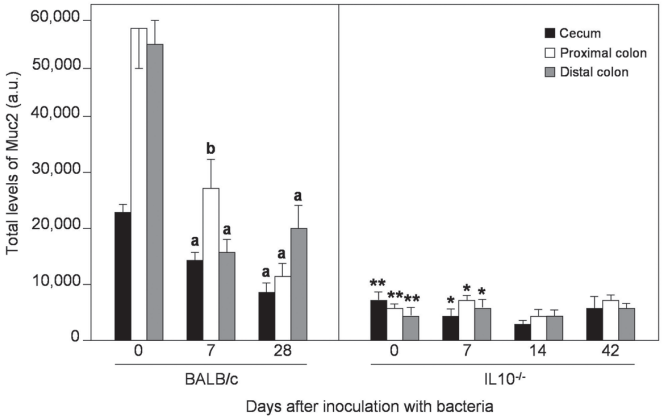

Figure 5. Total Muc2 levels in BALB/c and IL10$^{-/-}$ mice. Total Muc2 levels were measured in tissue explants from the cecum and proximal and distal colon of BALB/c and IL10$^{-/-}$ mice. Days after inoculation with normal enteric bacteria are indicated, day 0 indicates the GF status. The Muc2 level was significantly lower in each of the large intestinal regions of the GF IL10$^{-/-}$ mice, relative to the GF BALB/c mice (**P<.005). Also on day 7, the Muc2 levels were significantly lower in each of the large intestinal regions of the IL10$^{-/-}$ mice, relative to BALB/c mice on day 7 (*P<.05). The Muc2 levels in the large intestinal regions of the BALB/c mice decreased significantly on day 7 and 28 after exposure to bacteria, relative to the Muc2 levels in the respective regions of GF BALB/c mice (^{a}P<.01, ^{b}P<.05). SEMs are indicated.

Muc2 mRNA levels

The Muc2 mRNA levels were measured in the GF BALB/c mice in the cecum (980 a.u. [SEM, 80]), proximal colon (2890 a.u. [SEM, 700]), and in the distal colon (2630 a.u. [SEM, 760]). When these Muc2 mRNA levels were compared with the respective large intestinal regions of bacteria-exposed BALB/c animals, after 7 and 28 days after the introduction of bacteria, no statistically significant differences in Muc2 mRNA levels were identified. Also the Muc2 mRNA levels of the GF IL10$^{-/-}$ mice were measured in the cecum (1180 a.u. [SEM, 600]), proximal colon (2540 a.u. [SEM, 1330]), and in the distal colon (1990 a.u. [SEM, 1000]). After exposure of IL10$^{-/-}$ mice to bacteria, for 7, 14 or 42 days, no statistically significant changes were found in any of the large intestinal segments. Moreover, the Muc2 mRNA levels in the IL10$^{-/-}$ mice did not differ statistically from the levels in the BALB/c mice at any time during the experiment in any given large intestinal segment.

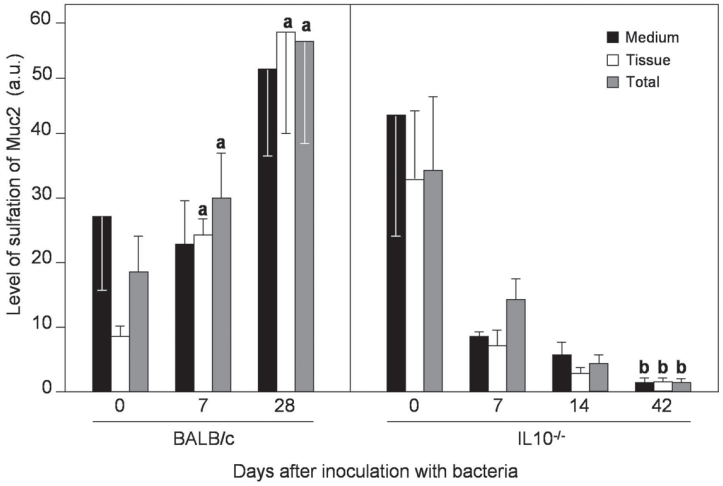

Figure 6. Muc2 sulfation in BALB/c and IL10$^{-/-}$ mice. The levels of Muc2 sulfation were measured, in explants of the proximal colon of BALB/c and IL10$^{-/-}$ mice, of the Muc2 present in the tissue and medium and of the total Muc2. Days after inoculation with normal enteric bacteria are indicated, day 0 indicates the GF status. The sulfation of Muc2 increased gradually and significantly after 7 and 28 days of exposure to bacteria in the proximal colon of the BALB/c mice, relative to GF BALB/c ($^{a}P<.01$). In IL10$^{-/-}$ mice, the level of sulfation of Muc2 decreased to significantly lower levels at day 42, relative to GF IL10$^{-/-}$ ($^{b}P<.05$). SEMs are indicated.

Table III. Secretion of total Muc2 in BALB/c and IL10$^{-/-}$ mice.

Region	Strain*	Day 0	Day 7	Day 14	Day 28	Day 42
Cecum	BALB/c	40.9 [4.2] §	45.9 [5.2]	n.d. ‡	48.7 [1.9]	n.d.
	IL10$^{-/-}$	45.8 [5.7]	27.5 [4.4] †	65.5 [6.1]	n.d.	29.5 [5.3]
Proximal colon	BALB/c	19.7 [3.7]	18.9 [2.0]	n.d.	17.0 [1.5]	n.d.
	IL10$^{-/-}$	24.1 [7.5]	25.6 [10.9]	31.8 [2.5]	n.d.	34.5 [5.5]
Distal colon	BALB/c	24.0 [5.0]	23.6 [3.3]	n.d.	25.7 [8.2]	n.d.
	IL10$^{-/-}$	21.9 [4.2]	22.1 [3.6]	31.8 [2.5]	n.d.	34.0 [3.1]

NOTE. * On day 0, GF mice from either strain were exposed to normal enteric bacteria under SPF conditions. Days after inoculation with bacteria are indicated, day 0 indicates the GF status. Secretion of total Muc2 was measured as explained in the Methods section, and is expressed as percentage of secreted Muc2 during 4 h of tissue culture.
† The secretion of Muc2 from the cecum of IL10$^{-/-}$ mice at day 7 decreased specifically relative to both GF IL10$^{-/-}$ mice and IL10$^{-/-}$ mice at day 14 ($P<.05$).
‡ n.d., not determined.
§ SEMs are indicated between brackets.

Secretion of Muc2 and $^{35}SO_3$-labeled Muc2

Secretion of total Muc2 was quantified by Western-type spot-blotting in tissue explants and cognate media of large intestinal segments that were incubated for 4 h in tissue culture medium (Table III). Upon introduction of bacteria, there were no statistically significant differences between the percentages of secreted Muc2 from colonic tissues of the BALB/c mice in any of the large intestinal regions. As shown in table III, only the cecum of IL10$^{-/-}$ mice showed remarkable changes in Muc2 secretion. Cecal Muc2 secretion decreased in 7 days after exposure to bacteria, then increased after 14 days of exposure, and then returned to basal levels after 42 days. In the proximal and distal colon of IL10$^{-/-}$ mice, secretion of total Muc2 was not significantly altered during the course of the experiment. No statistical significant differences were found between the percentage of secretion of Muc2 from IL10$^{-/-}$ tissue and BALB/c tissue at any time or any large intestinal region.

We also measured the secretion of $^{35}SO_3$-labeled Muc2 from the large intestinal explants within 4 h of incubation in tissue culture medium (Table IV). With one exception there were no significant changes in the secretion of $^{35}SO_3$-labeled Muc2 in the tissues of either the BALB/c mice or the IL10$^{-/-}$ mice. Only the percentage of secretion of $^{35}SO_3$-labeled Muc2 from the distal colon in the IL10$^{-/-}$ mice, 14 days after exposure to bacteria, was significantly decreased relative to GF IL10$^{-/-}$ tissue.

Table IV. Secretion of $^{35}S0_3$-labeled Muc2 in BALB/c and IL10$^{-/-}$ mice.

Region	Strain*	Day 0	Day 7	Day 14	Day 28	Day 42
Cecum	BALB/c	39.3 [8.0] §	38.0 [9.6]	n.d. ‡	45.3 [3.3]	n.d.
	IL10$^{-/-}$	49.2 [8.0]	36.3 [1.6]	50.4 [1.7]	n.d.	42.5 [7.8]
Proximal colon	BALB/c	36.0 [11.6]	36.8 [9.3]	n.d.	21.3 [9.0]	n.d.
	IL10$^{-/-}$	18.4 [3.6]	23.7 [5.8]	18.6 [2.5]	n.d.	25.6 [7.7]
Distal colon	BALB/c	37.1 [15.5]	31.7 [5.9]	n.d.	25.2 [5.8]	n.d.
	IL10$^{-/-}$	26.4 [5.2]	25.0 [4.4]	11.9 [3.0] †	n.d.	10.2 [4.3]

NOTE. * On day 0, GF mice from either strain were exposed to normal enteric bacteria under SPF conditions. Days after inoculation with bacteria are indicated, day 0 indicates the GF status. Secretion of $^{35}S0_3$-labeled Muc2 was measured, and is expressed as percentage of secreted $^{35}S0_3$-labeled Muc2 during 4 h of tissue culture.
† The secretion of $^{35}S0_3$-labeled Muc2 from the distal colon of IL10$^{-/-}$ mice at day 14 decreased, relative to GF IL10$^{-/-}$ mice ($P<.05$).
‡ n.d., not determined.
§ SEMs are indicated between brackets.

Discussion

Muc2 is the most prominent secretory large intestinal mucin in mammals studied so far[27-29, 33, 34]. It is produced in bulk by the specialized goblet cells, and it is seen as the most important compound of the colonic mucus layer. As this mucus is strategically positioned between the lumen and the epithelium, it has long been hypothesized that this mucus layer, and thus Muc2, may protect the animal against the development of colitis. In particular, MUC2 synthesis in humans with IBD was found to be decreased [12, 13], particularly in the epithelium adjacent to ileal ulcers of Crohn's disease[14]. However, it is impossible to determine in these clinical studies whether these observed abnormalities in MUC2 synthesis are primary defects or whether they are induced by the inflammatory response. One of the most important prerequisites for the development of colitis is the presence of bacteria in the colon. It has been convincingly shown that normal enteric bacteria can induce immune-mediated colitis in rodents with genetically-engineered abnormalities in immune regulation[3, 21-25]. Muc2 forms a natural barrier to the contact of bacteria with the underlying colonic epithelium. Thus, any change in quantity or structure of Muc2 could influence the effects of bacteria on the large intestinal mucosa, and be instrumental in the development of colitis.

In this study, we set out to quantify the Muc2 synthesis in IL10$^{-/-}$ and WT mice before and after the introduction of bacteria in the lumen of the intestine. In the GF state IL10$^{-/-}$ mice have no evidence of biochemical or histological inflammation and no activation of innate or acquired immune responses[21]. This provided us with the opportunity to evaluate the possible roles of Muc2 in both the induction as well as the perpetuation of the inflammation, and the ensuing epithelial damage, in experimental colitis. The first question that we addressed was, is there a primary defect in the Muc2 synthesis in GF IL10$^{-/-}$ mice? The second question was, is there a difference in the Muc2 synthesis following the introduction of normal enteric bacteria into IL10$^{-/-}$ mice, and during the early, mid and late phases of colitis and tissue damage? And third and finally, does colonization with commensal enteric bacteria alter Muc2 synthesis in normal mice? The answer to each question is yes. Both the total Muc2 levels and the Muc2 precursor synthesis are dramatically lower in the IL10$^{-/-}$ mice than in the WT controls, even before bacterial colonization and the onset of inflammation. Interestingly, the IL10$^{-/-}$ mice show a sharply increased Muc2 biosynthesis 7 days after introduction of bacteria, which is a transient process that returns to low baseline values by 2 weeks of bacterial colonization. This indicates that there is an induction of Muc2 synthesis in response to the first exposure to enteric bacteria or to the initial development of inflammation in this model. However, this induction is rapidly reversed as the inflammatory process progresses. These results are compatible with the observations of Madsen *et al*[35], who demonstrated a defect in mucosal permeability in young SPF IL10$^{-/-}$ mice prior to the onset of histologic evidence of inflammation. This permeability defect corresponded to the presence of luminal bacteria[36], and could be attenuated by treatment with Lactobacilli[35], but the mechanisms regulating this permeability defect were not delineated.

The consistency of our findings was indicated by the fact that each change in Muc2 synthesis was corroborated by similar results in each of the three large

intestinal regions that were studied. Each tissue fragment of the respective colonic regions was treated and processed independently. Nevertheless, the cecum, and proximal and distal colon showed the same patterns of changes in Muc2 synthesis. Moreover, this was true for all parameters of the Muc2 synthesis that were measured. This indicates that our results are technically sound, as each finding in a particular region of a particular mouse is reproduced by similar findings in another region of the same animal. Furthermore, the changes in the Muc2 synthesis occur throughout the entire large intestine, and were not restricted to a particular region. This implies that the mechanisms that induce the changes in the Muc2 synthesis, either induced by the absence of IL-10 in GF $^{-/-}$ mice or by the introduction of bacteria or inflammation in the IL10$^{-/-}$ SPF mice, operate in the entire large intestine.

There are various direct and indirect indications that synthesis and secretion of secretory mucins are regulated by immune-mediators[37-42]. Likewise the present study suggests that the absence of IL-10 leads to decreased Muc2 synthesis. This could be a direct effect of IL-10, suggesting that IL-10 could induce Muc2 synthesis[43]. Alternatively, IL-10 in the healthy mouse could be responsible for the induction of the stimulatory factors that normally enhance Muc2 production in the colon. For example, IL-10 down-regulates the Th1 response and facilitates TGF-beta production[44]. In turn, TGF-beta can induce MUC2 transcription[39]. Likewise, enteric bacteria, particularly probiotic species, can stimulate mucin gene expression in colonic epithelial cells. Lactobacillus species induce MUC2 and MUC3 expression and secretion in cultured epithelial cell lines[45, 46].

Irrespective of the exact mechanisms of the regulation of Muc2 levels in the murine colon, it appears that the large differences in Muc2 protein synthesis were not a result of decreased colonic Muc2 mRNA levels in IL10$^{-/-}$ mice. This discrepancy between Muc2 mRNA and protein expression was found not only in the differences in Muc2 synthesis between the IL10$^{-/-}$ and the BALB/c mice, but also in the transient upsurge of Muc2 synthesis in the IL10$^{-/-}$ mice 7 days after introduction of enteric bacteria. Technically, we are able to measure Muc2 mRNA quantities in a very large range. Therefore, the similar levels of Muc2 mRNA in both mice strains and during the development of colitis seem genuine and suggest posttranscriptional regulation of colonic Muc2. This lack of correlation between Muc2 mRNA levels and Muc2 precursor synthesis was previously found in the human and mouse colon[12, 26]. This indicates that the efficiency by which the Muc2 mRNA is translated into Muc2 protein may be an important mechanism of the regulation of Muc2 synthesis in the colon.

As colitis progressed from mild to severe in the IL10$^{-/-}$ mice over the 42 days of observation, the colonic Muc2 sulfation decreased progressively. Decreased sulfation was also observed in human ulcerative colitis[13, 47-50], and in the distal colon during experimental colitis[29], suggesting that changes in Muc2 sulfation are associated with colonic inflammation. Sulfation of secretory mucins has two possible roles in their biological function. First, the degree of sulfation affects the gel forming properties of the secretory mucins. Increasing sulfation of mucins yields a gel with a higher viscosity[51], which is predicted to be more resistant to physical erosion. The progressively lowered levels of sulfate on Muc2 may result in a mucus gel with decreasing viscosity and increasing susceptibility to erosion. This may increase the contact of the enteric bacteria with the epithelium or increase the penetration of these bacteria into the

mucosa, thereby promoting and/or perpetuating mucosal inflammation. Mucosally adherent bacteria, especially Bacteroides and Enterobacteriaceae, are dramatically increased in IBD patients[17]. In vitro studies have demonstrated that adherence of pathogenic bacteria to epithelial cells can be inhibited by induction of MUC3 by Lactobacillus species[45, 52], and by serum amyloid A3[53]. In addition, decreased sulfate residues on colonic mucins could enhance its degradation by bacterial enzymes[48], which may further deteriorate the protective mucus gel barrier. Bacteroides vulgatus isolated from IBD patients secrete mucin-degrading enzymes[31]. However, lower levels of sulfate on Muc2 could also be beneficial, since fewer sulfates available for metabolism by sulfate-reducing bacteria could result in less production of toxic sulfides. Increased numbers of sulfate-reducing bacteria have been demonstrated in ulcerative colitis patients[54]. These bacteria are able to use sulfate as energy source and reduce the sulfate to highly toxic sulfides[32, 55, 56].

While this work was in progress, a Muc2 deficient ($Muc2^{-/-}$) mouse strain was developed by genetic engineering that not only developed intestinal carcinoma[57], but also developed colonic inflammation under SPF conditions[58]. Moreover, if challenged under SPF conditions by the cytotoxic agent dextran sulfate sodium, $Muc2^{-/-}$ mice developed more active and earlier onset colitis than WT mice or heterozygous $Muc2^{+/-}$ mice[58, 59]. These results strongly indicate that Muc2 plays an important role in protecting the colonic mucosa against colitis and also against the development of adenocarcinoma of the colonic epithelium. It remains to be demonstrated if bacteria are instrumental in the induction of colitis in $Muc2^{-/-}$ mice.

In conclusion, $IL10^{-/-}$ mice exhibit a primary defect in the level of large intestinal Muc2 synthesis, which may make these mice more susceptible to developing colitis in the presence of normal enteric bacteria. Introduction of enteric bacteria induced colitis in the $IL10^{-/-}$ mice and led to a reduction in Muc2 sulfation. This decreased sulfation may influence the gel-forming properties of Muc2 and contribute to the perpetuation of colitis. These quantitative and structural aberrations in Muc2 in $IL10^{-/-}$ mice likely reduce the ability of the epithelium to cope with non-pathogenic commensal bacteria and may contribute to the sensitivity of these mice to develop colitis.

Acknowledgements

We like to express our gratitude to Daniel K. Podolsky who kindly provided us with the rat Tff3 cDNA. The Sophia Foundation for Scientific Research, Rotterdam, the Netherlands, is gratefully acknowledged for their financial support. Research at the University of North Carolina was supported by NIH grants RO1 DK53347 and P30 DK34987 and the Crohn's and Colitis Foundation of America. We thank Lisa Holt, Fengling Li and Toni Grenther for technical support.

References

1. Van Klinken BJ, Dekker J, Büller HA, Einerhand AW. Mucin gene structure and expression: protection vs. adhesion. Am J Physiol 1995;269:G613-27.
2. Strous GJ, Dekker J. Mucin-type glycoproteins. Crit Rev Biochem Mol Biol 1992;27:57-92.
3. Sartor RB. Microbial influences in inflammatory bowel disease. In: Sartor RB, Sandborn WJ, eds. Kirsner's Inflammatory Bowel Diseases 6th ed. Amsterdam: Elsevier Publishers, 2004:138-162.
4. Berg DJ, Zhang J, Weinstock JV, Ismail HF, Earle KA, Alila H, Pamukcu R, Moore S, Lynch RG. Rapid development of colitis in NSAID-treated IL-10-deficient mice. Gastroenterology 2002;123:1527-42.
5. Bouma G, Strober W. The immunological and genetic basis of inflammatory bowel disease. Nat Rev Immunol 2003;3:521-533.
6. Podolsky DK. Inflammatory bowel disease. N Engl J Med 2002;347:417-29.
7. Campieri M, Gionchetti P. Bacteria as the cause of ulcerative colitis. Gut 2001;48:132-5.
8. Sartor RB. Postoperative recurrence of Crohn's disease: the enemy is within the fecal stream. Gastroenterology 1998;114:398-400.
9. Sartor RB. Animal models of intestinal inflamation. In: Sartor RB, Sandborn WJ, eds. Kirsner's Inflammatory Bowel Diseases 6th ed. Amsterdam: Elsevier Publishers, 2004:120-137.
10. Strober W, Fuss IJ, Blumberg RS. The immunology of mucosal models of inflammation. Annu Rev Immunol 2002;20:495-549.
11. Tytgat KM, Opdam FJ, Einerhand AW, Büller HA, Dekker J. MUC2 is the prominent colonic mucin expressed in ulcerative colitis. Gut 1996;38:554-63.
12. Tytgat KM, van der Wal JW, Einerhand AW, Büller HA, Dekker J. Quantitative analysis of MUC2 synthesis in ulcerative colitis. Biochem Biophys Res Commun 1996;224:397-405.
13. Van Klinken BJ, Van der Wal JW, Einerhand AW, Büller HA, Dekker J. Sulphation and secretion of the predominant secretory human colonic mucin MUC2 in ulcerative colitis. Gut 1999;44:387-93.
14. Buisine MP, Desreumaux P, Leteurtre E, Copin MC, Colombel JF, Porchet N, Aubert JP. Mucin gene expression in intestinal epithelial cells in Crohn's disease. Gut 2001;49:544-51.
15. Pullan RD, Thomas GA, Rhodes M, Newcombe RG, Williams GT, Allen A, Rhodes J. Thickness of adherent mucus gel on colonic mucosa in humans and its relevance to colitis. Gut 1994;35:353-9.
16. Schultsz C, Van Den Berg FM, Ten Kate FW, Tytgat GN, Dankert J. The intestinal mucus layer from patients with inflammatory bowel disease harbors high numbers of bacteria compared with controls. Gastroenterology 1999;117:1089-97.
17. Swidsinski A, Ladhoff A, Pernthaler A, Swidsinski S, Loening-Baucke V, Ortner M, Weber J, Hoffmann U, Schreiber S, Dietel M, Lochs H. Mucosal flora in inflammatory bowel disease. Gastroenterology 2002;122:44-54.
18. Mahler M, Rozell B, Mahler JF. Pathology of the gastrointestinal tract of genetically engineerd and spontaneous mutant mice. In: Ward JM, Mahler JF, Maronpot MM, Sundberg JP, eds. Pathology of Genetically Engineerd Mice. Ames, IA: Iowa State Universitity Press, 2000:267-295.
19. Kuhn R, Lohler J, Rennick D, Rajewsky K, Muller W. Interleukin-10-deficient mice develop chronic enterocolitis. Cell 1993;75:263-74.
20. Berg DJ, Davidson N, Kuhn R, Muller W, Menon S, Holland G, Thompson-Snipes L, Leach MW, Rennick D. Enterocolitis and colon cancer in interleukin-10-deficient mice are associated with aberrant cytokine production and CD4(+) TH1-like responses. J Clin Invest 1996;98:1010-20.
21. Sellon RK, Tonkonogy S, Schultz M, Dieleman LA, Grenther W, Balish E, Rennick DM, Sartor RB. Resident enteric bacteria are necessary for development of spontaneous colitis and

immune system activation in interleukin-10-deficient mice. Infect Immun 1998;66:5224-31.
22. Taurog JD, Richardson JA, Croft JT, Simmons WA, Zhou M, Fernandez-Sueiro JL, Balish E, Hammer RE. The germfree state prevents development of gut and joint inflammatory disease in HLA-B27 transgenic rats. J Exp Med 1994;180:2359-64.
23. Schultz M, Tonkonogy SL, Sellon RK, Veltkamp C, Godfrey VL, Kwon J, Grenther WB, Balish E, Horak I, Sartor RB. IL-2-deficient mice raised under germfree conditions develop delayed mild focal intestinal inflammation. Am J Physiol 1999;276:G1461-72.
24. Dianda L, Hanby AM, Wright NA, Sebesteny A, Hayday AC, Owen MJ. T cell receptor-alpha beta-deficient mice fail to develop colitis in the absence of a microbial environment. Am J Pathol 1997;150:91-7.
25. Veltkamp C, Tonkonogy SL, De Jong YP, Albright C, Grenther WB, Balish E, Terhorst C, Sartor RB. Continuous stimulation by normal luminal bacteria is essential for the development and perpetuation of colitis in Tg(epsilon26) mice. Gastroenterology 2001;120:900-13.
26. Makkink MK, Schwerbrock NM, Mahler M, Boshuizen JA, Renes IB, Cornberg M, Hedrich HJ, Einerhand AW, Büller HA, Wagner S, Enss ML, Dekker J. Fate of goblet cells in experimental colitis. Dig Dis Sci 2002;47:2286-97.
27. Van Klinken BJ, Einerhand AW, Duits LA, Makkink MK, Tytgat KM, Renes IB, Verburg M, Büller HA, Dekker J. Gastrointestinal expression and partial cDNA cloning of murine Muc2. Am J Physiol 1999;276:G115-24.
28. Tytgat KM, Bovelander FJ, Opdam FJ, Einerhand AW, Büller HA, Dekker J. Biosynthesis of rat MUC2 in colon and its analogy with human MUC2. Biochem J 1995;309:221-9.
29. Tytgat KM, Büller HA, Opdam FJ, Kim YS, Einerhand AW, Dekker J. Biosynthesis of human colonic mucin: Muc2 is the prominent secretory mucin. Gastroenterology 1994;107:1352-63.
30. Dekker J, Van Klinken JW, Büller HA, Einerhand AW. Quantitation of biosynthesis and secretion of mucin using metabolic labeling. Methods Mol Biol 2000;125:65-73.
31. Ruseler-van Embden JG, van der Helm R, van Lieshout LM. Degradation of intestinal glycoproteins by Bacteroides vulgatus. FEMS Microbiol Lett 1989;49:37-41.
32. Magee EA, Richardson CJ, Hughes R, Cummings JH. Contribution of dietary protein to sulfide production in the large intestine: an in vitro and a controlled feeding study in humans. Am J Clin Nutr 2000;72:1488-94.
33. Herrmann A, Davies JR, Lindell G, Martensson S, Packer NH, Swallow DM, Carlstedt I. Studies on the “insoluble” glycoprotein complex from human colon. Identification of reduction-insensitive MUC2 oligomers and C-terminal cleavage. J Biol Chem 1999;274:15828-36.
34. Karlsson NG, Herrmann A, Karlsson H, Johansson ME, Carlstedt I, Hansson GC. The glycosylation of rat intestinal Muc2 mucin varies between rat strains and the small and large intestine. A study of O-linked oligosaccharides by a mass spectrometric approach. J Biol Chem 1997;272:27025-34.
35. Madsen KL, Doyle JS, Jewell LD, Tavernini MM, Fedorak RN. Lactobacillus species prevents colitis in interleukin 10 gene-deficient mice. Gastroenterology 1999;116:1107-14.
36. Madsen KL, Malfair D, Gray D, Doyle JS, Jewell LD, Fedorak RN. Interleukin-10 gene-deficient mice develop a primary intestinal permeability defect in response to enteric microflora. Inflamm Bowel Dis 1999;5:262-70.
37. Dabbagh K, Takeyama K, Lee HM, Ueki IF, Lausier JA, Nadel JA. IL-4 induces mucin gene expression and goblet cell metaplasia in vitro and in vivo. J Immunol 1999;162:6233-7.
38. Enss ML, Cornberg M, Wagner S, Gebert A, Henrichs M, Eisenblatter R, Beil W, Kownatzki R, Hedrich HJ. Proinflammatory cytokines trigger MUC gene expression and mucin release in the

intestinal cancer cell line LS180. Inflamm Res 2000;49:162-9.

39. Jono H, Shuto T, Xu H, Kai H, Lim DJ, Gum JR, Jr., Kim YS, Yamaoka S, Feng XH, Li JD. Transforming growth factor-beta -Smad signaling pathway cooperates with NF-kappa B to mediate nontypeable Haemophilus influenzae-induced MUC2 mucin transcription. J Biol Chem 2002;277:45547-57.
40. Kim YD, Kwon EJ, Park DW, Song SY, Yoon SK, Baek SH. Interleukin-1beta induces MUC2 and MUC5AC synthesis through cyclooxygenase-2 in NCI-H292 cells. Mol Pharmacol 2002;62:1112-8.
41. Koo JS, Kim YD, Jetten AM, Belloni P, Nettesheim P. Overexpression of mucin genes induced by interleukin-1 beta, tumor necrosis factor-alpha, lipopolysaccharide, and neutrophil elastase is inhibited by a retinoic acid receptor alpha antagonist. Exp Lung Res 2002;28:315-32.
42. Perrais M, Pigny P, Copin MC, Aubert JP, Van Seuningen I. Induction of MUC2 and MUC5AC mucins by factors of the epidermal growth factor (EGF) family is mediated by EGF receptor/Ras/Raf/extracellular signal-regulated kinase cascade and Sp1. J Biol Chem 2002;277:32258-67.
43. Lee CG, Homer RJ, Cohn L, Link H, Jung S, Craft JE, Graham BS, Johnson TR, Elias JA. Transgenic overexpression of interleukin (IL)-10 in the lung causes mucus metaplasia, tissue inflammation, and airway remodeling via IL-13-dependent and -independent pathways. J Biol Chem 2002;277:35466-74.
44. Fuss IJ, Boirivant M, Lacy B, Strober W. The interrelated roles of TGF-beta and IL-10 in the regulation of experimental colitis. J Immunol 2002;168:900-8.
45. Mack DR, Ahrne S, Hyde L, Wei S, Hollingsworth MA. Extracellular MUC3 mucin secretion follows adherence of Lactobacillus strains to intestinal epithelial cells in vitro. Gut 2003;52:827-33.
46. Mattar AF, Teitelbaum DH, Drongowski RA, Yongyi F, Harmon CM, Coran AG. Probiotics up-regulate MUC-2 mucin gene expression in a Caco-2 cell-culture model. Pediatr Surg Int 2002;18:586-90.
47. Corfield AP, Myerscough N, Bradfield N, Corfield Cdo A, Gough M, Clamp JR, Durdey P, Warren BF, Bartolo DC, King KR, Williams JM. Colonic mucins in ulcerative colitis: evidence for loss of sulfation. Glycoconj J 1996;13:809-22.
48. Nieuw Amerongen AV, Bolscher JG, Bloemena E, Veerman EC. Sulfomucins in the human body. Biol Chem 1998;379:1-18.
49. Robertson AM, Wright DP. Bacterial glycosulphatases and sulphomucin degradation. Can J Gastroenterol 1997;11:361-6.
50. Tsai HH, Dwarakanath AD, Hart CA, Milton JD, Rhodes JM. Increased faecal mucin sulphatase activity in ulcerative colitis: a potential target for treatment. Gut 1995;36:570-6.
51. Sellers LA, Allen A, Morris ER, Ross-Murphy SB. Mucus glycoprotein gels. Role of glycoprotein polymeric structure and carbohydrate side-chains in gel-formation. Carbohydr Res 1988;178:93-110.
52. Mack DR, Michail S, Wei S, McDougall L, Hollingsworth MA. Probiotics inhibit enteropathogenic E. coli adherence in vitro by inducing intestinal mucin gene expression. Am J Physiol 1999;276:G941-50.
53. Larson MA, Wei SH, Weber A, Mack DR, McDonald TL. Human serum amyloid A3 peptide enhances intestinal MUC3 expression and inhibits EPEC adherence. Biochem Biophys Res Commun 2003;300:531-40.
54. Gibson GR, Cummings JH, Macfarlane GT. Growth and activities of sulphate/reducing bacteria in gut contents of heathly subjects and patients with ulcerative colitis. FEMS Microbiol Ecol 1991;86:103-111.
55. Levine J, Ellis CJ, Furne JK, Springfield J, Levitt MD. Fecal hydrogen sulfide production in ulcerative colitis. Am J Gastroenterol 1998;93:83-7.

56. Zinkevich VV, Beech IB. Screening of sulfate-reducing bacteria in colonoscopy samples from healthy and colitic human gut mucosa. FEMS Microbiol Ecol 2000;34:147-155.
57. Velcich A, Yang W, Heyer J, Fragale A, Nicholas C, Viani S, Kucherlapati R, Lipkin M, Yang K, Augenlicht L. Colorectal cancer in mice genetically deficient in the mucin Muc2. Science 2002;295:1726-9.
58. Einerhand AW, Renes IB, Makkink MK, van der Sluis M, Büller HA, Dekker J. Role of mucins in inflammatory bowel disease: important lessons from experimental models. Eur J Gastroenterol Hepatol 2002;14:757-65.
59. Van der Sluis M, Makkink MK, Sutmuller M, Büller HA, Dekker J, Augenlicht LH, Velcich A, Einerhand AWC. Muc2 knockout mice are more susceptible to dextran sulfate sodium- induced colitis. Gastroenterology 2002;122:T946.

Chapter 3

Mucin 2 is Critical for Colonic Protection

Published as:
Maria van der Sluis, Barbara A.E. de Koning, Adrianus C.J.M de Bruijn, Anna Velcich, Jules P.P. Meijerink, Johannes B. van Goudoever, Hans A. Büller, Jan Dekker, Isabelle Van Seuningen, Ingrid. B. Renes and Alexandra W.C. Einerhand. Muc2-deficient mice spontaneously develop colitis, indicating that Muc2 is critical for colonic protection.

Gastroenterology, 131(1):117-129, 2006

Abstract

Expression of mucin MUC2, the structural component of the colonic mucus layer, is lowered in inflammatory bowel disease. Our aim was to obtain insight in the role of Muc2 in epithelial protection. Thereto Muc2 knockout ($Muc2^{-/-}$) and Muc2 heterozygous ($Muc2^{+/-}$) mice were characterized and challenged by a colitis-inducing agent, dextran sulfate sodium (DSS). We monitored clinical symptoms, intestinal morphology and differences in intestine-specific protein and mRNA levels. The $Muc2^{-/-}$ mice showed clinical signs of colitis (as of 5 weeks), aggravating as the mice aged. Microscopic analysis of the colon of $Muc2^{-/-}$ showed mucosal thickening, increased proliferation and superficial erosions. Colonic goblet cells in the $Muc2^{-/-}$ mice were negative for Muc2, but trefoil factor 3 was still detectable. In $Muc2^{-/-}$ mice, transient de novo expression of Muc6 mRNA was observed in the distal colon. On day 2 of DSS treatment, the histological damage was more severe in $Muc2^{+/-}$ versus wild type (WT) mice, but the disease activity index (DAI) was not yet different. By day 7, the DAI and histological score were significantly elevated in $Muc2^{+/-}$ versus WT mice. The DAI of the $Muc2^{-/-}$ mice was higher (versus both WT and $Muc2^{+/-}$ mice) throughout DSS treatment. The histological damage in the DSS-treated $Muc2^{-/-}$ mice was different compared to WT and $Muc2^{+/-}$ mice with many crypt abscesses, instead of mucosal ulcerations. Conclusions: This study shows that Muc2 deficiency leads to inflammation of the colon, and contributes to the onset and perpetuation of experimental colitis.

Abbreviations used in this paper

BrdU, bromodeoxyuridine; DAI, disease activity index; DSS, dextran sulfate sodium; IL, interleukin; IBD, inflammatory bowel disease; Muc, Mucin; $Muc2^{-/-}$, Muc2 deficient; Tff3, trefoil factor 3; TNF, tumor necrosis factor.

Introduction

Ulcerative colitis and Crohn's disease are two of the most important inflammatory bowel diseases (IBD) characterized by chronic inflammation and mucosal tissue damage of parts of the gastrointestinal tract. The etiology of these inflammatory disorders remains unknown, but research so far has shown that these diseases are caused by a combination of genetic, environmental, immunoregulatory, and epithelial factors[1-6].

The epithelium and mucus layer in the intestinal tract form a physical barrier between the potential toxic and noxious agents present in the gut lumen and the underlying tissues. Goblet cells exert a vital role since they secrete molecules, which serve protective roles in the gut, like mucins and trefoil factors. Mucins are the building blocks of the mucus layer and previous studies have shown that human, rat and mouse colonic epithelium expresses mainly one secretory mucin in high amounts, MUC2[7-11]. The secretory mucin MUC2 is stored in bulky apical granules of the goblet cells and is the most important factor determining the goblet cell morphology[12, 13]. Trefoil factor 3 (Tff3) is a protein also expressed by goblet cells in the intestine and has shown to play an essential role in the maintenance and repair of the intestinal mucosa[3]. Damage to the epithelium, in particular those events affecting the protective properties as offered by the secretory products of the goblet cells, is a likely cause of the inflammation.

Histology of ulcerative colitis patients often shows depletion of recognizable goblet cells in the colonic epithelium[14]. Defects in the intestine, such as loss of e-cadherin expression, multi-drug resistant protein or Tff3 deficiency, have been shown to lead to higher susceptibility to chronic inflammation that can progressively deteriorate the epithelial barrier function[3, 4, 6]. Furthermore, it has been shown that in patients with ulcerative colitis the activity of the mucosal inflammation correlates significantly with a decrease in MUC2 synthesis[15], and secretion[16], again implying that the mucosal barrier plays a key role in the course of the disease.

To more specifically address the importance of MUC2 in epithelial protection, Muc2 deficient ($Muc2^{-/-}$) mice were generated, through genetic inactivation of the murine Muc2 gene[12]. In these $Muc2^{-/-}$ mice, the intestinal goblet cells were seemingly absent. Interestingly, mice lacking Muc2 developed adenomas as of six months of age, which progressed to invasive adenocarcinoma in the small intestine as well as rectal tumors at an older age. Therefore, Muc2 seems to play a role in the suppression of intestinal cancer[12], but the exact mechanism whereby Muc2 suppresses tumorigenesis remains unclear.

To obtain insight in the role of Muc2 in epithelial barrier function, and thus its possible role in IBD, we characterized the Muc2 knockout ($Muc2^{-/-}$) and heterozygous ($Muc2^{+/-}$) mouse from birth until 16 weeks of age, prior to the development of adenomas and challenged these mice with the colitis-inducing agent, dextran sulfate sodium (DSS). This animal model is the first to provide the possibility to investigate the physiological function of Muc2 in the intestine of the mouse under unchallenged and luminally challenged conditions.

Materials and Methods

Animals

The previously described Muc2$^{-/-}$ mice on mixed genetic background[12] were backcrossed onto a 129SV (Charles River, Maastricht, the Netherlands) genetic background for nine generations followed by intercrosses to generate mice homozygous for the Muc2 disruption. To obtain experimental groups with a minimal age difference between the different litters, all mice were generated from Muc2$^{+/-}$ breedings. Throughout the backcrossing procedure, the targeted Muc2 gene was monitored via PCR assays performed on genomic DNA isolated from tail clips as described by Velcich et al[12]. All the mice were housed in the same specific pathogen-free environment with free access to standard rodent pellets (Special Diets Services, Witham, Essex, England) and acidified tap water in a 12-h light-dark cycle. All animal care and procedures were conducted according to institutional guidelines (Erasmus MC- Animal Ethics Committee, Rotterdam, the Netherlands).

Experimental set-up

Wild type (WT), Muc2$^{+/-}$ and Muc2$^{-/-}$ littermates were scored weekly until the age of 16 weeks to obtain a Disease Activity Index (DAI) as described by Cooper et al[17] (Table I). Briefly, they were scored for the following: weight, softness of the stool, occult faecal blood[18] and general appearance of the mice. One hour prior to sacrifice, bromodeoxyuridine (BrdU), 30 mg/kg body weight (Sigma, St. Louis, USA), was injected intraperitoneally to be able to study epithelial proliferation[19]. The time

Table I. DAI Score.

Score	% weight loss*	Stool consistency	Blood loss	Appearance
0	None (None)	Normal droppings	None	Lively/ normal
1	0-17 (0-10)	Loose droppings	Hemoccult positive	Hunched
2	18-35 (10-20)	Diarrhea	Gross bleeding	Starey coat
3	>35 (>20)			Lethargic

NOTE. Criteria were obtained by pooling all data and calculating quartiles. For the initial phenotyping experiment, the percentage weight loss was calculated by comparing the weight of the mice with corresponding wild-type littermates. For the experiment in which the animals were treated with DSS, percentage weight loss was calculated by using the initial body weight of the individual animals. The classification of the weight loss in the DAI as applied in the DSS experiment appears in parentheses.

curve was started with 16 mice of each genotype, WT, Muc2$^{+/-}$ and Muc2$^{-/-}$. At the ages 5, 8, 12 and 16 weeks, groups of 4 male mice per genotype were sacrificed. Small intestine and colon were excised immediately and either fixed in 4% (w/v) paraformaldehyde in PBS, stored in RNA later (Qiagen, Venlo, the Netherlands) at minus 20°C, or frozen in liquid nitrogen and stored at minus 80°C.

Histology and histological grading

Tissue fixed in 4% (w/v) paraformaldehyde in PBS was prepared for light microscopy and 5 µm thick sections were stained by haematoxylin and eosin (HE) to study histological changes as described previously[20]. Grading of intestinal inflammation was determined as described by Rath and co-workers[21] with slight modifications (Table II). In particular, the scoring of both the percentage of the total ulcer area per section and the number of crypt abscesses for each section were modified. To detect differences in mucosal and epithelial thickness in the colon, 10 well-oriented crypts or epithelial cells were chosen per intestinal segment and measured using calibrated Leica Image Manager 500 software (Leica Microsystems B.V, Rijswijk, the Netherlands). All scores were obtained in a blinded fashion by two independent investigators.

Table II. Histological score to quantify the degree of gastrointestinal inflammation

Criterion	Score				
	0	1	2	3	4
Goblet cells	-	↓	↓↓	↓↓↓	↓↓↓
Mucosa thickening	-	↑	↑↑	↑↑↑	↑↑↑
Inflammatory cells	-	↑	↑↑	↑↑↑	↑↑↑
Submucosa cell infiltration	-	-	↑	↑↑	↑↑↑
Destruction of architecture	-	-	-	↑	↑↑
Ulcers (epithelial cell surface)	0%	0-25%	25-50%	50-75%	75-100%
Crypt Abscesses	0	1-3	4-6	7-9	>10

NOTE. Grading of intestinal inflammation was determined as described by Rath *et al*[21] and adapted. In particular, the scoring of both the percentage of the total of ulcer area of the section and the number of crypt abscesses for each section was modified.

Immunohistochemistry

Five-micrometer-thick sections were cut and prepared for immunohistochemistry, as described previously[22] using the Vectastain Elite ABC kit (Vector Labs, Burlingame CA, USA) and 3,3'-diaminobenzidine as staining reagent. Expression of Muc2 was detected using an anti-Muc2 antibody H-300, (1:1000 in PBS; SC-15334, Santa Cruz, SanverTech, Heerhugowaard, the Netherlands). To detect goblet cells, anti-trefoil factor 3 (Tff3; 1:3000 in PBS; a generous gift from Prof. Dr. D. K. Podolsky[3])

was used. As a marker for enterocyte differentiation in the colon villin was used which was detected with an anti-villin antibody (1:2000 in PBS, generously given by Dr. S. Robine[23]). To visualize BrdU incorporation, the sections were incubated with anti-BrdU (Boehringer Mannheim, Mannheim, Germany) as described previously[19, 20]. $CD3^+$ cells were detected using an anti-human CD3 (DAKO, Heverlee, Belgium; 1:800 in 1% BSA, 0.1% Triton X100 in PBS). Additionally, non-specific binding was reduced by blocking with TENG-T (10 mM Tris-HCl, 5 mM EDTA, 150 mM NaCl, 0.25% (w/v) gelatin, 0.05% (w/v) Tween-20).

mRNA expression of secretory mucins in the distal colon

Total RNAs from mouse tissues were prepared using the QIAamp RNA midi-kit (Qiagen, Venlo, the Netherlands), following the manufacturer's protocol and treated with DNase (Qiagen). Total RNA (1.5 µg) was used to prepare first-strand cDNA (AdvantageTM RT-for-PCR kit; BD Biosciences, Clontech, Alphen aan den Rijn, the Netherlands). PCR was performed on 5 µl of cDNA using primer pairs specific for Muc5ac 5'-GAGGCCAACAAGGTAGAGCACA-3' and 5'-TGGGACAGCAGCAGTATTCAGT-3'[24],Muc5b5'-GAGGTCAACATCACCTTCTGC-3'and 5'- TCTCATGGTCAGTTGTGCAGG-3', Muc6 5'-TGGTCGAAGTACTCATTCTGG-3' and 5'-GTGGCTTGTGTGGCAACGCC-3'and β-actin5'-TCACGCCATCCTGCGTCTGGACT-3' and 5'- CCGGACTCATCGTACTCCT-3' as an internal standard[25]. PCR products were 295 bp, 319 bp, 569 bp and 582 bp respectively. PCR reactions were carried out in 50 µl final solutions as described previously[26] using Invitrogen TAQ polymerase (Invitrogen, Breda, the Netherlands). A positive control for each mucin PCR (stomach for Muc5ac and Muc6, larynx for Muc5b) and a negative control without cDNA were amplified with each PCR experiment. Annealing temperature was 58°C. PCR products were analyzed on 1.5% ethidium bromide stained agarose gels run in 1×Tris/borate/EDTA buffer. As a marker, a 100 base pair DNA ladder (Invitrogen) was used.

Probe preparation and in situ hybridization

RNA isolation, cDNA preparation and PCR for Muc6 was performed as described above. The resulting 569 bp PCR product was isolated using the Qiagen gel extraction kit (Qiagen), ligated into the pGEM-Teasy vector (Promega, Madison, WI, USA) and verified for sequence integrity using T7; SP6 primers and ABI Prism 310 and software (Applied Biosystems, Nieuwerkerk aan den IJssel, the Netherlands). Subsequently, the Muc6 fragment was subcloned into the pBluescript KS vector (Stratagene, La Jolla, CA, United States of America) using the EcoRI restriction enzyme. The pBluescript KS vector contains T3 and T7 RNA polymerase sites. The digoxigenin-11-UTP-labelled sense (T3) and anti sense Muc-6 (T7) RNA probes were prepared according to the manufacturer's protocol (Roche, Almere, the Netherlands). Non-radioactive in situ hybridization was performed according to the method already described[27], with slight modifications[28, 29].

Quantitative real-time PCR (Taqman technology)

The mRNA expression levels of tumor necrosis factor alpha (TNF-α), interleukin-1beta (IL1-β) and interleukin-6 (IL-6), as well as the endogenous housekeeping gene

β-actin were quantified using real-time PCR analysis (Taqman chemistry) based upon the intercalation of SYBR® Green on an ABI Prism 7700 sequence detection system (PE Applied Biosystems, Nieuwerkerk aan den IJssel, the Netherlands). Primers combinations for β-actin (5´-GGGACCTGACGGACTAC-3´ and 5´-TGCCACAGGATTCCATAC-3´), IL-1β (5´-CCCCAACTGGTACATCA-3´ and 5´-AGAATGTGCCATGGTTTC-3´), IL-6 (5´CCCAACAGACCTGTCTAT-3´ and 5´-GGCAAATTTCCTGATTAT-3´) and TNF-α (5´-TGGCCTCCCTCTCATC-3´ and 5´-GCTGGCACCACTAGTT-3´) were designed using the OLIGO 6.22 software (Molecular Biology Insights, Cascade, CO, USA) and purchased from Invitrogen. All primers had a melting temperature (Tm; nearest neighbor method) between 65-66.5°C. All PCRs performed with comparable efficiencies of 95 percent or higher. The PCR was performed using 1x SYBR® Green Master mix (Bioké, Leiden, the Netherlands), 1x ROX reference dye, 15 pmol forward and reverse primers, and 5 μl 5x diluted cDNA ("RNA isolation and cDNA synthesis", as described above) from each mouse as a template in a total reaction volume of 50 μl in a MicroAmp optical 96-well plate and covered with MicroAmp optical caps (Applied Biosystems). Samples were heated for 10 minutes at 95°C and amplified for 40 cycles of 15 seconds at 95°C and 60 seconds at 60°C. To verify the amplification efficiency within each experiment, a serial dilution of cDNA derived from an RNA-pool of control colon samples in dH_2O was amplified in duplicate on each plate. Since all PCRs performed with equal efficiencies, relative mRNA expression levels of TNF-α and IL-1β for each mouse can directly be normalized for input RNA against the β-actin expression of the mice. For this, the relative mRNA expression levels of these target genes were calculated according to the comparative cycle time (Ct) method[30], following the equation:

$$\text{relative mRNA expression} = 2^{-(\text{Ct target-Ct } \beta\text{-actin})} \times 100\%.$$

DSS treatment

One week prior to DSS administration, eight-week-old, specified pathogen free, male WT, $Muc2^{+/-}$ and $Muc2^{-/-}$ littermates were divided into groups of 6 mice, given free access to autoclaved tap water and were weighed daily in order to adjust to the experimental conditions. During the experiment, daily prepared autoclaved tap water supplemented with 2.5% (w/v) DSS (37-40kD, TdB Consultancy, Uppsala, Sweden) was administered for 5 days, followed by a recovery period during which the DSS was omitted from the drinking water. Scoring of the mice was performed daily, using the DAI as adapted from Cooper *et al*[17] as described above. A group of animals were sacrificed on day 2 (onset of disease), day 8 (severe disease) and a control group at the end of the experiment (no DSS). Tissue segments were obtained, processed, and scored as described above.

Statistical analysis

All data are expressed as mean ± SEM. Statistical significance of the 3 different groups of mice during time was assessed by one-way analysis of variance test and Tukey t test. The Mann–Whitney U test was used to analyze changes in mRNA expression assessed by real-time PCR (Prism, version 4.00; GraphPad software, San Diego, CA, USA). The data were considered statistically significant at $P<.05$.

Results

Clinical symptoms

The Muc2 deficient mouse model[12] was used in this study to explore the in vivo function of Muc2 in the colon. There were no significant differences between the WT and Muc2$^{+/-}$ mice regarding body weight at any time (Fig. 1). Moreover, occult blood loss, gross bleeding and rectal prolapses did not occur in WT and Muc2$^{+/-}$ mice. In contrast, Muc2$^{-/-}$ mice were clearly distinguishable from their Muc2$^{+/-}$ and WT littermates at 5 weeks of age due to significant growth retardation [P<.001 Muc2$^{-/-}$ vs.

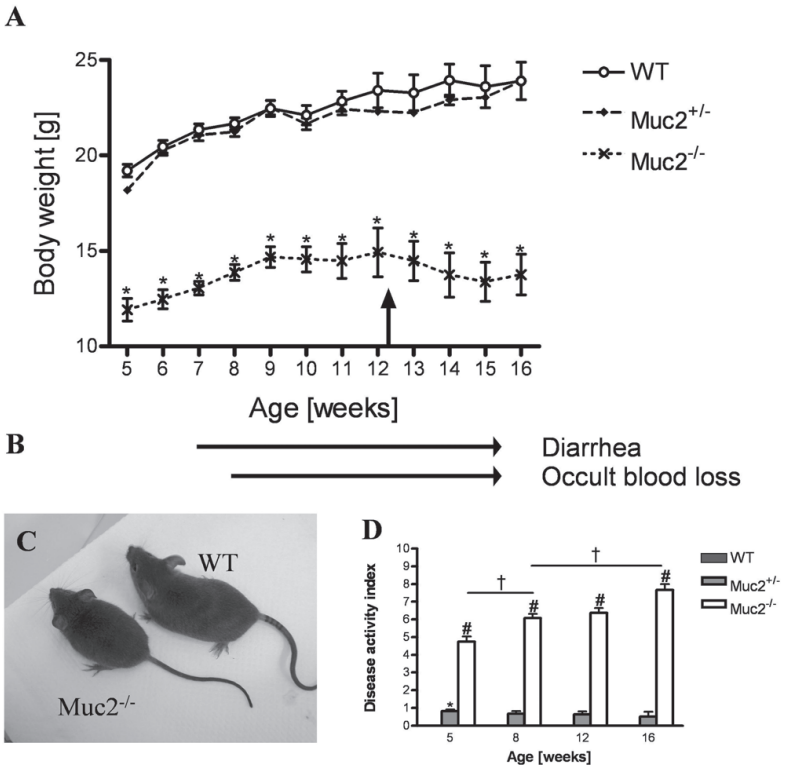

Figure 1. Appearance and clinical symptoms of WT, Muc2$^{+/-}$ and Muc2$^{-/-}$ mice in time. (A) Body weight of the different mice in time. WT and Muc2$^{+/-}$ were indistinguishable, whereas Muc2$^{-/-}$ mice were significantly growth retarded (*WT vs. Muc2$^{-/-}$; P<.001, Muc2$^{+/-}$ vs. Muc2$^{-/-}$; P<.001). The *arrow* in the graph depicts spontaneous death of one Muc2$^{-/-}$ mouse. (B) Clinical symptoms of the Muc2$^{-/-}$ mice, The *arrow* indicates that all Muc2$^{-/-}$ animals showed the described symptoms. These symptoms were not observed in WT and Muc2$^{+/-}$ mice. (C) Photograph of a WT and Muc2$^{-/-}$ mouse at 16 weeks of age. (D) DAI is an accumulative score as adapted from Cooper et al[17]. To be able to calculate percentage weight loss, Muc2$^{+/-}$ and Muc2$^{-/-}$ animals were compared to the average weight of WT littermates of the same age. (#WT and Muc2$^{+/-}$ vs. Muc2$^{-/-}$, P<0.001 at each time point. *WT vs. Muc2$^{+/-}$; P<.05 at 5 weeks of age). DAI of the Muc2$^{-/-}$ mice progressively increased with time (†P<.001 week 5 vs. week 8 and week 8 vs. week 12). The DAI of WT remained zero at each time point investigated. Error bars indicate the SEM.

both WT and Muc2$^{+/-}$, at each time point] (Fig. 1A and C). Over time, the weight difference between the mice increased further as the Muc2$^{-/-}$ mice failed to gain weight. In addition to diarrhea at 7 weeks of age, all Muc2$^{-/-}$ mice showed occult blood loss by week 8. Most Muc2$^{-/-}$ mice developed gross bleeding (9 out of 12) or some mice showed reversible rectal prolapses (3 out of 8, as of 9 weeks of age). Scoring these clinical parameters in conjunction resulted in a DAI as given in Figure 1D. The Muc2$^{-/-}$ mice had a significantly higher DAI score compared to both WT and Muc2$^{+/-}$ mice at each time point investigated [P<.001]. Moreover, the DAI of the Muc2$^{-/-}$ mice progressively increased with time. One of the Muc2$^{-/-}$ mice died at 12.5 weeks of age; therefore, this mouse was excluded from the DAI score. In contrast, none of the WT or Muc2$^{+/-}$ mice died during the time frame studied. With respect to clinical symptoms there was a statistically significant difference between WT and Muc2$^{+/-}$ mice only at 5 weeks of age. Yet, the Muc2$^{+/-}$ mice had a DAI above zero at each time point investigated, whereas the DAI of WT remained zero. The increased disease score in the Muc2$^{+/-}$ mice was attributed to the small, but statistically non-significant, weight difference between WT and Muc2$^{+/-}$ mice, which was seen throughout the experiment (Fig. 1A).

Morphological analysis

In agreement with the clinical observations, there were no morphological differences in the proximal or distal colon between WT and Muc2$^{+/-}$ mice at any of the time points investigated (data not shown). The main characteristic change between Muc2$^{-/-}$ and WT mice was the lack of recognizable goblet cells along the crypt-villus axis of the small intestine as previously reported[12]. Despite this, the small intestine of

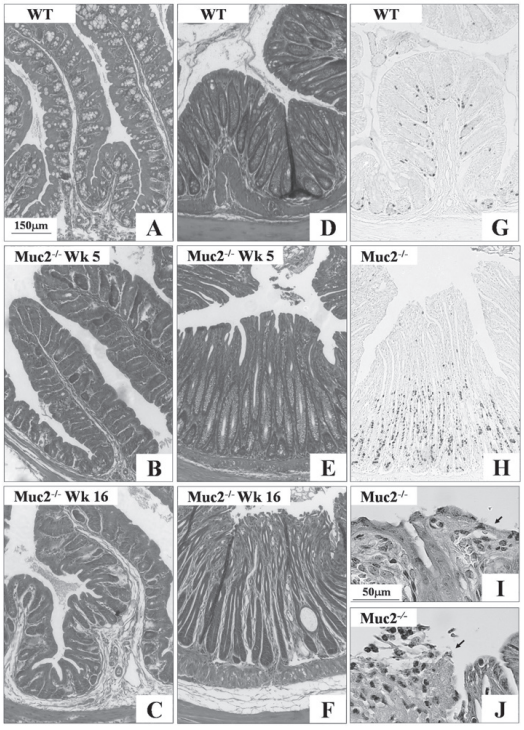

Figure 2. Colonic morphology and proliferation in WT and Muc2$^{-/-}$ mice. Representative sections of WT colon are depicted at 8 weeks of age (A; proximal colon, D; distal colon). (B and C) Proximal colon of the Muc2$^{-/-}$ mice at 5 and 16 weeks of age, respectively. (E and F) Distal colon of the Muc2$^{-/-}$ mice at 5 and 16 weeks of age, respectively. BrdU staining of the distal colon of (G) WT and (H) Muc2$^{-/-}$ both 8 weeks old. Higher magnification of the epithelial cells in Muc2$^{-/-}$ mice at (I) 8 weeks and (J) 16 weeks of age. *Arrows* indicating loss of epithelial cells. The micrographs show representative results of the four mice from each experimental group.

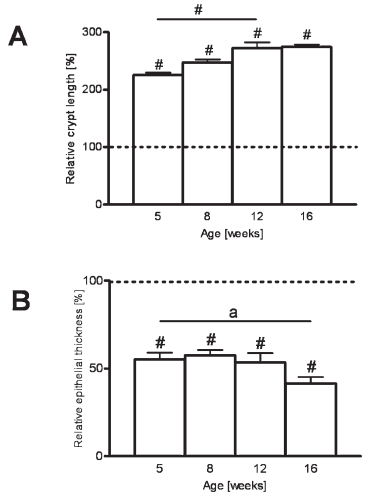

Figure 3. Quantification of the histological changes in the distal colon of Muc2$^{-/-}$ mice. To detect differences in (A) crypt length and (B) height of the epithelial cells in the Muc2$^{-/-}$ mice, 10 well-oriented crypts and epithelial cells in the distal colon were chosen from each individual animal in the experimental groups and measured using calibrated Leica software. At all time points crypt length and cell height were expressed as a percentage of the corresponding values of WT littermates ($^{\#}$P<.001, ^{a}P<.05). Crypt length and of the Muc2$^{-/-}$ mice progressively increased and epithelial height decreased as the mice aged.

Muc2$^{-/-}$ mice showed no changes from WT littermates up to 12 weeks of age. At 16 weeks old, the Muc2$^{-/-}$ mice showed an increase in crypt length compared to the wild type mice (data not shown). However, the colonic morphology of Muc2$^{-/-}$ animals differed considerably from their WT littermates (Fig. 2A-F). In addition to the absence of the characteristic bell shape morphology of the goblet cells in the proximal and distal colon of the Muc2$^{-/-}$ mice, we observed a loss of crypt architecture and of overall structure of the lamina propria in the proximal colon of Muc2$^{-/-}$ animals, 16 weeks of age (Fig. 2C). This was accompanied by a statistically non-significant alteration in crypt length in proximal colon observed from 5- up to 8-week-old Muc2$^{-/-}$ mice. A significant increase in crypt length of the proximal colon in Muc2$^{-/-}$ mice compared to their WT littermates (36%, P<.001) was first detected in 12-week-old mice and remained until 16 weeks of age (data not shown).

Alterations in the distal colon of Muc2$^{-/-}$ mice (Fig 2D-F) were much more severe compared to the proximal colon (Fig. 2A-C). Already at 5 weeks of age, crypt hyperplasia, mild infiltration, flattening of epithelial cells and distortion of the lamina propria were observed. In the distal colon of the Muc2$^{-/-}$ mice, goblet-like cells (Alcian blue positive, data not shown) could be seen deep in the crypts of the distal colon of 5-week-old animals. These Alcian blue-stained cells disappeared as the overall damage of the distal colon increased and were undetectable in tissue sections of 12- to 16-week-old mice. The structure of the epithelial cells in the Muc2$^{-/-}$ mice was distorted and flattened, as depicted in Figure 2F, 2I and 2J. Furthermore, there was severe loss of the architecture of the lamina propria, which was most pronounced in older mice (16 weeks). This coincided with an increase in infiltrating inflammatory cells and the presence of superficial erosions. Figure 3A shows that there was a significant increase of crypt length in the distal colon of the Muc2$^{-/-}$ mice throughout the experiment. As early as 5 weeks of age, the mucosa of Muc2$^{-/-}$ mice showed a thickening of more than 200% [P<.001, Muc2$^{-/-}$ vs. WT, all ages], reaching about 250% increase by 16 weeks [P<.001].

Epithelial proliferation was studied by immunohistochemical staining of incorporated BrdU. No differences were detected between the WT and Muc2$^{-/-}$ mice in distribution or localization of BrdU-positive cells in the proximal colon at all ages (data not shown). In WT mice BrdU-positive cells were localized at the base of the crypts in the distal colon (Fig. 2G, 8 weeks old). In the distal colon of all Muc2$^{-/-}$ mice, however, there was a significant increase in the number of BrdU-positive cells as early as of 5 weeks of age, which remained constant with time, and these cells extended halfway up the crypt (Fig. 2H). There were no differences in number of apoptotic bodies along the crypts, between the Muc2$^{-/-}$ and WT mice (data not shown).

There was significant flattening (P<.001) of colonic epithelial cells of the Muc2$^{-/-}$ animals at 5 weeks of age, resulting in cells of only 40% (P<.001) of the height of the epithelial cells in WT mice at 16 weeks of age (Fig. 3B). Locally, in each of the Muc2$^{-/-}$ mice, there was even complete loss of epithelial cells (Fig. 2I, 2J) resulting into superficial erosions.

Overall, the histology along the proximal-distal axis of the colon in Muc2$^{-/-}$ mice showed an increase in damage mainly characterized by thickening of the intestinal mucosa, flattening and degeneration of the epithelium, superficial erosions and infiltration of inflammatory cells, which aggravated as the mice aged. Moreover, untreated Muc2$^{-/-}$ mice from continuing experiments (our unpublished data; n=34, 8-weeks of age), all show clinical and histological symptoms corresponding to animals of the same age as described above.

Expression of goblet cell and enterocyte markers

Maturation of the intestinal epithelial cells in the Muc2$^{-/-}$ mice was characterized using molecular markers for tissue and cell-type specific differentiation. Two markers for goblet cells, Muc2 and Tff3, were both expressed throughout the whole crypts in the proximal and distal colon of WT and Muc2$^{+/-}$ mice (Fig. 4A and C; showing distal

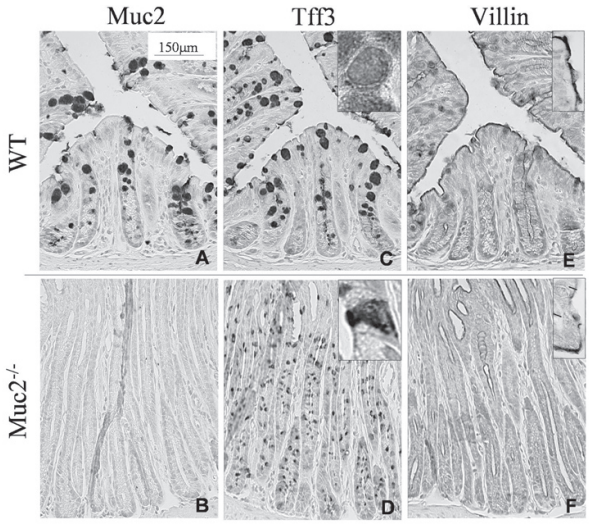

Figure 4. Protein expression in the distal colon. Goblet cells were stained for (A and B) Muc2 and (C and D) Tff3. As an enterocyte marker villin was used (E and F). A, C, and E, are sections representing tissue from the distal colon of WT animals and B, D, and F, represent tissue from the distal colon of Muc2$^{-/-}$ animals, respectively. Inserts in C and D show a close-up of a goblet cell in WT and Muc2$^{-/-}$ mice, respectively. Insert in E shows a close-up of normal villin expression by WT enterocytes. F shows loss and redistribution (*arrow heads*) of villin expression by the epithelial cells of Muc2$^{-/-}$ mice. Please also see page 219.

colon, WT mouse) Goblet cells in the entire colon of the Muc2$^{-/-}$ mice were negative for Muc2 (Fig. 4B), but Tff3 was clearly detectable (Fig. 4D). The goblet cells in the proximal colon as well as distal colon of the Muc2$^{-/-}$ mice showed a distinct change in morphology. Whereas the goblet cells of the WT mice were round and bell shaped (insert of panel 4C; distal colon) the goblet cells of the Muc2$^{-/-}$ mice appeared smaller and more condensed (insert of panel 4D; distal colon).

Villin, a cytoskeletal protein, present in the brush border of enterocytes was used as a marker for this cell type[23]. Villin was uniformly present in the brush border of enterocytes in the proximal and distal colon of both WT mice and Muc2$^{+/-}$ mice (Fig. 4E; showing distal colon, WT mouse). In the distal colon of the Muc2$^{-/-}$ mice, however, a redistribution of villin to the cytoplasm in seemingly unaffected epithelial cells was seen (insert of panel 4F).

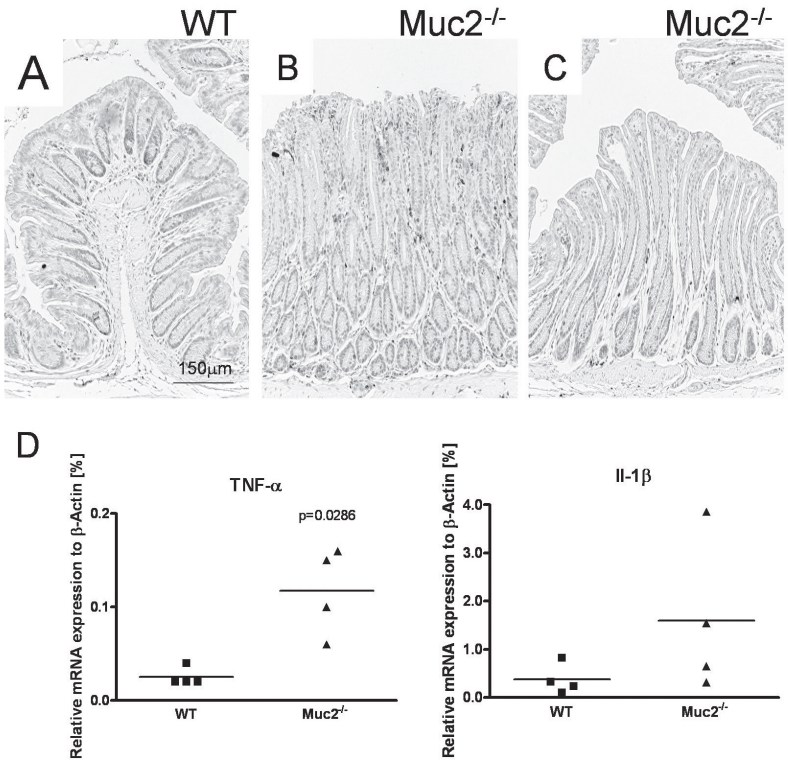

Figure 5. Increased lymphocyte infiltration and expression of inflammatory cytokines. Representative sections presenting lymphocyte infiltration into the colon of (A) WT and (B and C) Muc2$^{-/-}$ animals, detected using an anti-CD3 antibody. In the Muc2$^{-/-}$ mice there was an increase of lymphocyte infiltration, in parts of the colon were there was loss of epithelial cells (B). Parts of the colon that were unaffected (C) were comparable to sections of the WT mice. (D) Real time PCR data of the inflammatory cytokine TNF-α in the colon of Muc2$^{-/-}$ mice was significantly up regulated (P=.03) compared to WT mice. Furthermore, the Muc2$^{-/-}$ mice showed a trend towards up regulation of IL-1β mRNA in the colon.

Increased lymphocyte infiltration and expression of inflammatory cytokines

Lymphocyte infiltration into the colon was evaluated using an anti-CD3 antibody. Representative stained tissue samples are shown in Figure 5A-C. In the Muc2$^{-/-}$ mice there was an increase of lymphocyte infiltration, e.g. CD3 positive cells, in parts of the colon were there was loss of epithelial cells. Parts of the colon that were unaffected were comparable to sections of the WT mice.

In accordance with the histological data, there was a significant increase (5-fold) in expression of mRNA of the inflammatory cytokine TNF-α in the colon of Muc2$^{-/-}$ mice compared to WT mice (P=.03). Furthermore, the Muc2$^{-/-}$ mice showed a trend towards up regulation (4-fold) of IL-1β in the colon (Fig. 5D, showing 8 weeks of age), which was at the brink of significance at 16 weeks of age ((P=.05, n=3), data not shown). However, IL-6 was below detection levels in both types of mice throughout the experiment (data not shown).

mRNA expression and localization of secretory mucins in the distal colon

Apart from Muc2, three other secretory mucins are known to be expressed by the gastrointestinal tract, that structurally resemble Muc2: Muc5ac, Muc5b and Muc6[31]. To evaluate expression of these secretory mucins, we determined the mRNA expression of Muc5ac, Muc5b and Muc6 by RT-PCR. WT, Muc2$^{+/-}$ and Muc2$^{-/-}$ animals showed no expression of Muc5ac and Muc5b mRNA in either the proximal or distal colon (data not shown). In the proximal colon of WT, Muc2$^{+/-}$ and Muc2$^{-/-}$ mice, Muc6 mRNA was detectable throughout the experiment in very low amounts with no differences between the WT and the Muc2$^{-/-}$ mice (data not shown). In the distal colon of the Muc2$^{-/-}$ mice, de novo expression of Muc6 mRNA was observed at 5 weeks of age and the expression declined as the mice aged (Fig. 6A), in contrast to WT mice, which showed no expression of Muc6 at 5 to 12 weeks, but only a low level of expression at 16 weeks.

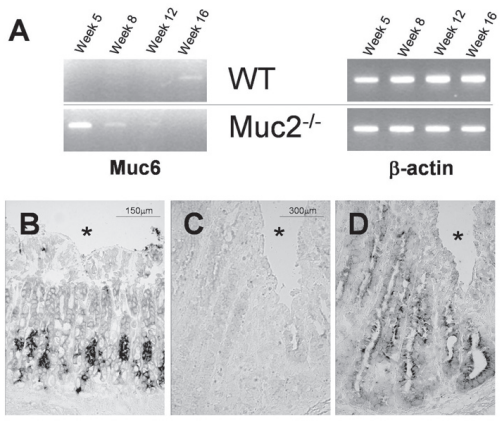

Figure 6. mRNA expression and localization of Muc6 in the distal colon. (A) Endogenous expression of Muc6 mRNA and β-actin in the distal colon of both WT and Muc2$^{-/-}$ animals. The week number above the picture of the PCR product stands for the age of the animals during the experiment. In situ hybridization was used to localize Muc6 mRNA expression in the distal colon of the Muc2$^{-/-}$ mice. (B) Staining of mouse gastric glands with Muc6 digoxigenin-labeled antisense RNA probe as a positive control. (C) Staining of colon mucosa of Muc2$^{-/-}$ mice with Muc6 digoxigenin-labeled sense probe as a negative control. (D) Staining of colon mucosa of Muc2$^{-/-}$ mice with Muc6 digoxigenin-labeled anti-sense probe. *Asterisk* indicates the lumen of the different segments. The tissue samples are representative of 4 mice.

To localize the cells expressing Muc6 mRNA, *in situ* hybridization was performed. As a positive control, and corresponding to previous studies performed in humans[32, 33], Muc6 mRNA was detected only in the mucous neck cells of the stomach, whereas all surface mucous cells were negative (Fig. 6B). The sense probe showed no staining in the stomach (data not shown) and colon, demonstrating that the in situ hybridization is specific for Muc6 (Fig. 6C). As shown in Figure 6D, Muc6 was expressed in the lower parts of the crypts of the distal colon in the $Muc2^{-/-}$ mice at 5 weeks. This correlated in time and location with the presence of Alcian blue-positive cells, seen deep in the crypts of the distal colon of $Muc2^{-/-}$ animals, 5 weeks of age (Fig. 2E). These cells disappeared as the overall damage of the distal colon increased and were undetectable in sections as from 12 to 16 weeks of age (Fig. 2F, 16 weeks).

Effects of DSS treatment

In order to determine the role of Muc2 in epithelial protection, 8-week-old Muc2-deficient and heterozygous mice were challenged with DSS. The susceptibility to DSS-treatment was determined by analyzing the DAI and the histology of the distal colon. During the first days of the DSS-treatment, the WT and $Muc2^{+/-}$ mice showed no striking differences in their response to the DSS (Fig. 7A). The $Muc2^{+/-}$ mice showed a higher DAI in reaction to DSS on day 7 ($P<.04$) and day 8 ($P=.05$), when compared to their WT littermates (Fig. 7A). The $Muc2^{-/-}$ mice had a significantly higher ($P<.001$) DAI from the start of the DSS administration, as described above (Fig. 1D). The rise in DAI score of the $Muc2^{-/-}$ mice during and after DSS-treatment was caused by severe weight loss and the occurrence of severe gross bleeding towards the end of the experiment (DAI of $Muc2^{-/-}$ vs. WT $P<.001$ all time points; DAI of $Muc2^{-/-}$ vs. $Muc2^{+/-}$ $P<.001$ up to day 6, $P<.01$ day 7 and $P<.05$ day 8).

HE-stained sections from paraffin-embedded segments were used to score colonic inflammation (Table 2). The $Muc2^{-/-}$ mice showed a different pathology in reaction to the DSS-treatment compared to the pathology seen in WT and $Muc2^{+/-}$ mice. Before DSS-treatment, the $Muc2^{-/-}$ mice already showed thickening of the intestinal mucosa, change in goblet cell morphology, degeneration of the epithelium and lamina propria, superficial erosions and infiltration of inflammatory cells. On day 2, the reaction of the $Muc2^{-/-}$ was comparable to WT and $Muc2^{+/-}$ mice, with a mild influx of inflammatory cells and overall loss in architecture. However, during severe disease (day 8 after start of DSS-treatment) the $Muc2^{-/-}$ mice displayed substantial crypt abscesses vs. extended ulcerations in the WT and $Muc2^{+/-}$ mice (Fig. 7C).

To further delineate any difference between the WT and $Muc2^{+/-}$ mice, histological damage was scored for mice of both genotypes. No striking differences were seen between WT and $Muc2^{+/-}$ mice (Fig. 7C). Fewer goblet cells were present in the crypts of the $Muc2^{+/-}$ mice, but this did not result in a significantly higher histology score at the start of the DSS-treatment (Fig. 7B). On day 2 (onset of disease) the first changes due to DSS-treatment were detectable. This was characterized by an overall loss in architecture, loss of goblet cells and a mild influx of inflammatory cells (Fig. 7C). During the most severe stage of the disease (day 8), there was a notable difference between the WT and $Muc2^{+/-}$ mice in the percentage epithelial ulcers present in the sections, general loss of architecture, loss of goblet cells and influx of

inflammatory cells (Fig. 7C). When combining the items of the histology score, the Muc2$^{+/-}$ mice had a significantly higher score than the WT mice during DSS treatment (Fig. 7B, day 2 P<.001; day 8 P<.05).

Taking these results together, the DSS-experiment showed that predictably, Muc2$^{-/-}$ mice are more susceptible to colonic damage compared with their WT littermates. Interestingly, the Muc2$^{+/-}$ mice displayed an intermediate sensitivity towards DSS-treatment.

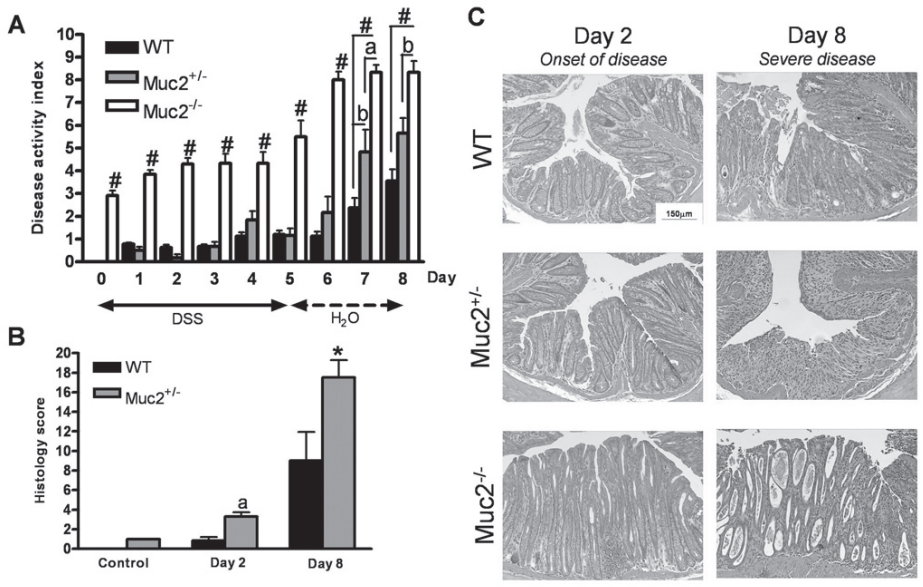

Figure 7. Effects of DSS treatment on disease activity score (DAI) and histology. (A) Relative changes in the DAI of WT (black bars), Muc2$^{+/-}$ (stippled bars) and Muc2$^{-/-}$ (white bars) DSS-treated mice. To be able to calculate percentage weight loss, WT, Muc2$^{+/-}$ and Muc2$^{-/-}$ animals were compared to their individual body weight prior to the DSS-administration. Error bars reflect the SEM of the changes of the DAI score on each day. Days of DSS/water treatment are indicated as *arrows* under the x-axis. (DAI Muc2$^{-/-}$ vs. WT $^{\#}$P<.001 all time points; DAI Muc2$^{-/-}$ vs. Muc2$^{+/-}$ P<.001 up to day 6, ^{a}P<.01 day 7 and ^{b}P<.05 day 8; DAI WT vs. Muc 2$^{+/-}$ day 7 and 8 P<.05) (B) Histology scores as determined according to Rath *el al* [21] determined for WT vs. Muc2$^{+/-}$ mice (^{a}P<.001, *P<.05). Error bars reflect the SEM. (C) Representative sections of the distal colon on day 2 and day 8 after the start of the DSS-administration of WT, Muc2$^{+/-}$ and Muc2$^{-/-}$ mice. Please also see page 220.

Discussion

Muc2 is generally assumed to be essential for epithelial protection. However, this assumption had never been put to the test experimentally. In this study we have addressed this question by characterizing mice deficient in Muc2 from birth until 16 weeks of age and by challenging these mice with an orally administered, noxious agent to determine the protective capacity of the Muc2-deficient, epithelial barrier.

The $Muc2^{-/-}$ animals showed growth retardation and significantly lower body weight at 5 weeks of age, compared to WT and $Muc2^{+/-}$ littermates and these differences in body weight progressed as the mice aged. Growth failure is associated with IBD and is most probably caused by malnutrition[34], a multi-factorial problem. As the mice aged, the $Muc2^{-/-}$ animals showed occult blood loss to gross bleeding and diarrhea. Furthermore, the $Muc2^{-/-}$ mice showed microscopic evidence of colitis as early as 5 weeks of age, which aggravated as the mice aged. Moreover, the rectal prolapses which occasionally developed in $Muc2^{-/-}$ mice, are a characteristic often seen in animal models of IBD such as the IL10-deficient mice[35] Together with weight loss these symptoms are similar to those experienced by patients that suffer from IBD[36], indicating that the $Muc2^{-/-}$ mice constitute a model to study aspects of IBD.

In the proximal colon, there were no distinct changes in epithelial proliferation between WT and $Muc2^{-/-}$ mice in contrast to the distal colon where the proliferation was very much increased and the proliferative zone was much broader in the crypts of the $Muc2^{-/-}$ mice, coinciding with an increase (up to about 250%) in thickness of the colonic mucosa. In germ-free mice, colonic crypts were shown to have a lower mitotic index and labeling index compared to conventional mice[37]. An increase in proliferation in the distal colon of the $Muc2^{-/-}$ mice could thus be explained by an altered bacterial stimulation of the epithelium due to a diminished mucus layer.

A histological hallmark of the $Muc2^{-/-}$ mice was the lack of recognizable goblet cells throughout the entire intestine. These findings correspond with previous studies showing that Muc2, which is stored in apical granules of goblet cells, is the most important factor determining the goblet cell morphology[11-13, 38, 39]. That indeed goblet cells were present in the mucosa of the $Muc2^{-/-}$ was determined by using an antibody against Tff3. Tff3-positive goblet cells were present throughout the entire large intestine. Apparently, goblet cells in absence of Muc2 lose their characteristic goblet-like shape, corroborating the notion that Muc2 is the major phenotypic determinant of goblet cells. This result also supports the hypothesis that Muc2 and Tff3, two markers of the goblet cell phenotype, are not co-coordinately regulated[40].

The inflammation of the distal colon in Muc2 deficient mice, also affects the differentiation of other epithelial colonic cells like the enterocytes as indicated by loss of villin, and the redistribution of villin, from the apical membrane to the cytoplasm. Also other enterocyte-specific protein expression were shown to be down-regulated during intestinal damage[41].

It is well known that pro-inflammatory cytokines play an important role in inflammation of the intestinal mucosa. For instance, TNF-α, IL-1β and IL-6 have shown to play a pivotal role in the pathogenesis of IBD[1, 42, 43]. Analysis of colon tissue samples of the $Muc2^{-/-}$ mice by real time PCR, showed an up-regulation of TNF-α and IL-1β, but not of IL-6. In conjunction these data further support the $Muc2^{-/-}$ mouse as

a unique and new type of colitis model different from previously published models.

By including all regions of the intestine in our study, we have revealed the effect of absence of Muc2 on colonic epithelium throughout the intestine. We determined the expression of other secretory mucin genes, structurally related to Muc2, by RT-PCR. Results of the proximal colon of both WT and Muc2$^{-/-}$ were negative for Muc5ac, Muc5b, and positive for Muc6 mRNA. In the distal colon we were not able to detect Muc5ac or Muc5b in both WT and Muc2$^{-/-}$. These findings are consistent with previous studies in both human and mouse colon[25, 44] and consistent with the previous study on Muc5ac mRNA performed in Muc2$^{-/-}$ mice by Velcich *et al*[12]. Transient *de novo* expression of Muc6 mRNA however, was observed in the distal colon of Muc2$^{-/-}$ mice at 5 weeks of age and declined as the Muc2$^{-/-}$ mice aged. Interestingly, morphological analysis of the distal colon of Muc2$^{-/-}$ mice at 5 weeks of age revealed the presence of goblet-like cells in the lower part of the crypts. Moreover, these goblet-like cells appeared to be Alcian blue-positive and were depleted at 16 weeks, indicating that these goblet-like cells might be expressing Muc6. Indeed, *in situ* hybridization studies demonstrated Muc6 mRNA in the goblet cells deep in the crypts of the Muc2$^{-/-}$ at 5 weeks of age. The induced Muc6 expression in the Muc2$^{-/-}$ mice possibly results from a compensatory protective mechanism within the colonic epithelium. Muc6 was previously shown to be aberrantly expressed in the intestine in pathological situations when mucosal repair is needed and was then associated with trans-differentiation and the development of a gastric cell-like phenotype[45]. The *de novo* expression of Muc6 mRNA in Muc2$^{-/-}$ mice may reflect such a need as a compensatory mechanism.

Our results are partly in contrast to data published from previous studies using the Muc2$^{-/-}$ mouse[12, 13], as we have shown distinct clinical symptoms from an early age, no distinct histology in the small intestine and a pathology in the distal colon. The studies described by Velcich *et al*[12] were performed using a mixed genotypic background (C57/BL6-129SV), while in the current study, the knockout mice had a 129SV background only. It is possible that the differences of phenotype in the Muc2$^{-/-}$ mice can be attributed to differences in strain background as described previously for the IL10 deficient mouse[46].

To investigate the question further, as to whether Muc2 is involved in epithelial protection against luminal factors we induced colitis by giving WT, Muc2$^{+/-}$ and Muc2$^{-/-}$ mice DSS, a cytotoxic agent. DSS induces several clinical symptoms (i.e. diarrhea, bloody stools and weight loss) and histopathological changes (i.e. erosions and crypt loss) in normal rats and mice[17, 20]. Muc2$^{-/-}$ mice showed severe clinical symptoms after receiving DSS in their drinking water, as the disease aggravated, marked by weight loss and gross bleeding. These findings were consistent with a previous pilot conducted in our laboratory[38], and were not surprising as Muc2$^{-/-}$ mice had already had bloody stools and diarrhea before receiving the DSS. Most interestingly however, Muc2$^{+/-}$ mice showed an intermediate clinical response to the DSS-treatment. When investigating the histopathology, Muc2$^{+/-}$ mice showed a significantly more severe reaction to the DSS compared to WT mice, characterized by crypt loss, infiltration and ulcerations. This indicates that (partial) deficiency of Muc2 predisposes the development of colonic inflammation. This is further supported by our earlier studies performed in IL10$^{-/-}$ mice showing that quantitative and structural aberrations

in Muc2, likely reduce the ability of the mucosa to cope with non-pathogenic commensal bacteria and that this may contribute to the susceptibility to develop colitis[39]. The Muc2$^{-/-}$ mice showed a different histopathology compared to both WT and Muc2$^{+/-}$ mice marked by crypt abscesses. DSS has shown to initially cause damage in the intestine by inhibition of proliferation and induction of apoptosis[20]. The different histology displayed by the Muc2$^{-/-}$ mice may be explained by the fact that the Muc2$^{-/-}$ initially had an increased proliferation rate before receiving DSS. This however, needs to be investigated further.

To summarize, loss of Muc2 in the intestine, and therefore breaches in the epithelial barrier, leads to an abnormal morphology marked by an increase in thickness of the gut mucosa, flattening and ulceration of epithelial cells, general loss of architecture, mild increase of inflammatory cells, an increase in proliferation, and decrease of cell differentiation in the colon. Furthermore, we have shown that changes in the mucus composition, caused by Muc2 deficiency, leads to inflammation of the colon and that deficiency of Muc2 contributes to the onset and/or perpetuation of IBD. Moreover, we believe that the Muc2$^{-/-}$ and the Muc2$^{+/-}$ mice are powerful animal-models, enabling us to study the physiological role of the epithelial barrier in many aspects.

Acknowledgements
We would like to thank J. Bouma, D.J. Lindenbergh-Kortleve, M.H.M Melis and I.M.A. Louwers for their excellent technical assistance. The Sophia Foundation for Scientific Research, Rotterdam, The Netherlands Organization for Scientific Research, The Hague, The Foundation “De Drie Lichten”, Leiden, all situated in the Netherlands and The Association François Aupetit, Paris, France are gratefully acknowledged for their financial support.

References

1. Bouma G, Strober W. The immunological and genetic basis of inflammatory bowel disease. Nat Rev Immunol 2003;3:521-533.
2. Einerhand AW, Renes IB, Makkink MK, van der Sluis M, Büller HA, Dekker J. Role of mucins in inflammatory bowel disease: important lessons from experimental models. Eur J Gastroenterol Hepatol 2002;14:757-765.
3. Mashimo H, Wu DC, Podolsky DK, Fishman MC. Impaired defense of intestinal mucosa in mice lacking intestinal trefoil factor. Science 1996;274:262-265.
4. Hermiston ML, Gordon JI. Inflammatory bowel disease and adenomas in mice expressing a dominant negative N-cadherin. Science 1995;270:1203-1207.
5. Van Klinken BJ, Dekker J, Büller HA, Einerhand AW. Mucin gene structure and expression: protection vs. adhesion. Am J Physiol 1995;269:G613-627.
6. Panwala CM, Jones JC, Viney JL. A novel model of inflammatory bowel disease: mice deficient for the multiple drug resistance gene, mdr1a, spontaneously develop colitis. J Immunol 1998;161:5733-5744.
7. Tytgat KM, Büller HA, Opdam FJ, Kim YS, Einerhand AW, Dekker J. Biosynthesis of human colonic mucin: Muc2 is the prominent secretory mucin. Gastroenterology 1994;107:1352-1363.
8. Tytgat KM, Bovelander FJ, Opdam FJ, Einerhand AW, Büller HA, Dekker J. Biosynthesis of rat MUC2 in colon and its analogy with human MUC2. Biochem J 1995;309 (Pt 1):221-9.
9. Herrmann A, Davies JR, Lindell G, Martensson S, Packer NH, Swallow DM, Carlstedt I. Studies on the “insoluble” glycoprotein complex from human colon. Identification of reduction-insensitive MUC2 oligomers and C-terminal cleavage. J Biol Chem 1999;274:15828-36.
10. van Klinken BJ, Einerhand AW, Duits LA, Makkink MK, Tytgat KM, Renes IB, Verburg M, Büller HA, Dekker J. Gastrointestinal expression and partial cDNA cloning of murine Muc2. Am J Physiol 1999;276:115-124.
11. Makkink MK, Schwerbrock NM, Mahler M, Boshuizen JA, Renes IB, Cornberg M, Hedrich HJ, Einerhand AW, Büller HA, Wagner S, Enss ML, Dekker J. Fate of goblet cells in experimental colitis. Dig Dis Sci 2002;47:2286-2297.
12. Velcich A, Yang W, Heyer J, Fragale A, Nicholas C, Viani S, Kucherlapati R, Lipkin M, Yang K, Augenlicht L. Colorectal cancer in mice genetically deficient in the mucin Muc2. Science 2002;295:1726-1729.
13. Yang W, Velcich A, Lozonschi I, Liang J, Nicholas C, Zhuang M, Bancroft L, Augenlicht LH. Inactivation of p21WAF1/cip1 enhances intestinal tumor formation in Muc2-/- mice. Am J Pathol 2005;166:1239-46.
14. Theodossi A, Spiegelhalter DJ, Jass J, Firth J, Dixon M, Leader M, Levison DA, Lindley R, Filipe I, Price A, et al. Observer variation and discriminatory value of biopsy features in inflammatory bowel disease. Gut 1994;35:961-8.
15. Tytgat KM, van der Wal JW, Einerhand AW, Büller HA, Dekker J. Quantitative analysis of MUC2 synthesis in ulcerative colitis. Biochem Biophys Res Commun 1996;224:397-405.
16. Van Klinken BJ, Van der Wal JW, Einerhand AW, Büller HA, Dekker J. Sulphation and secretion of the predominant secretory human colonic mucin MUC2 in ulcerative colitis. Gut 1999;44:387-393.
17. Cooper HS, Murthy SN, Shah RS, Sedergran DJ. Clinicopathologic study of dextran sulfate sodium experimental murine colitis. Lab Invest 1993;69:238-249.
18. Wahba N. An ortho-tolidine hydrochloride test for the detection of occult blood in faeces without dietary restrictions. J Clin Pathol 1965;18:687-688.

19. Boshuizen JA, Reimerink JH, Korteland-van Male AM, van Ham VJ, Koopmans MP, Büller HA, Dekker J, Einerhand AW. Changes in small intestinal homeostasis, morphology, and gene expression during rotavirus infection of infant mice. J Virol 2003;77:13005-13016.
20. Renes IB, Verburg M, Van Nispen DJ, Taminiau JA, Büller HA, Dekker J, Einerhand AW. Epithelial proliferation, cell death, and gene expression in experimental colitis: alterations in carbonic anhydrase I, mucin MUC2, and trefoil factor 3 expression. Int J Colorectal Dis 2002;17:317-326.
21. Rath HC, Herfarth HH, Ikeda JS, Grenther WB, Hamm TE, Jr., Balish E, Taurog JD, Hammer RE, Wilson KH, Sartor RB. Normal luminal bacteria, especially Bacteroides species, mediate chronic colitis, gastritis, and arthritis in HLA-B27/human beta2 microglobulin transgenic rats. J Clin Invest 1996;98:945-953.
22. Verburg M, Renes IB, Meijer HP, Taminiau JA, Büller HA, Einerhand AW, Dekker J. Selective sparing of goblet cells and paneth cells in the intestine of methotrexate-treated rats. Am J Physiol Gastrointest Liver Physiol 2000;279:G1037-1047.
23. Pringault E, Arpin M, Garcia A, Finidori J, Louvard D. A human villin cDNA clone to investigate the differentiation of intestinal and kidney cells in vivo and in culture. Embo J 1986;5:3119-3124.
24. Jonckheere N, Van Der Sluis M, Velghe A, Buisine MP, Sutmuller M, Ducourouble MP, Pigny P, Büller HA, Aubert JP, Einerhand AW, Van Seuningen I. Transcriptional activation of the murine Muc5ac mucin gene in epithelial cancer cells by TGF-beta/Smad4 signalling pathway is potentiated by Sp1. Biochem J 2004;377:797-808.
25. Escande F, Porchet N, Bernigaud A, Petitprez D, Aubert JP, Buisine MP. The mouse secreted gel-forming mucin gene cluster. Biochim Biophys Acta 2004;1676:240-250.
26. Mesquita P, Jonckheere N, Almeida R, Ducourouble MP, Serpa J, Silva E, Pigny P, Silva FS, Reis C, Silberg D, Van Seuningen I, David L. Human MUC2 mucin gene is transcriptionally regulated by Cdx homeodomain proteins in gastrointestinal carcinoma cell lines. J Biol Chem 2003;278:51549-51556.
27. Lindenbergh-Kortleve DJ, Rosato RR, van Neck JW, Nauta J, van Kleffens M, Groffen C, Zwarthoff EC, Drop SL. Gene expression of the insulin-like growth factor system during mouse kidney development. Mol Cell Endocrinol 1997;132:81-91.
28. Renes IB, Verburg M, Bulsing NP, Ferdinandusse S, Büller HA, Dekker J, Einerhand AW. Protection of the Peyer's patch-associated crypt and villus epithelium against methotrexate-induced damage is based on its distinct regulation of proliferation. J Pathol 2002;198:60-68.
29. van der Sluis M, Melis MH, Jonckheere N, Ducourouble MP, Büller HA, Renes I, Einerhand AW, Van Seuningen I. The murine Muc2 mucin gene is transcriptionally regulated by the zinc-finger GATA-4 transcription factor in intestinal cells. Biochem Biophys Res Commun 2004;325:952-60.
30. Meijerink J, Mandigers C, van de Locht L, Tonnissen E, Goodsaid F, Raemaekers J. A novel method to compensate for different amplification efficiencies between patient DNA samples in quantitative real-time PCR. J Mol Diagn 2001;3:55-61.
31. Dekker J, Rossen JW, Büller HA, Einerhand AW. The MUC family: an obituary. Trends Biochem Sci 2002;27:126-131.
32. Ho SB, Roberton AM, Shekels LL, Lyftogt CT, Niehans GA, Toribara NW. Expression cloning of gastric mucin complementary DNA and localization of mucin gene expression. Gastroenterology 1995;109:735-47.
33. Reid CJ, Harris A. Developmental expression of mucin genes in the human gastrointestinal system. Gut 1998;42:220-226.
34. Motil KJ, Grand RJ. Groth failure in children and adolescents with inflammatory bowel disease.

In: Inflammatory Bowel Diseases, Tytgat GNJ, Bartelsman MFWM, van Deventer SJH, eds. Dordrecht: Kluwer Academic Publishers, 1995:588-597.

35. Löhler J, Kühn R, Rennick D, Rajewsky K, Müller W. Interleukin-10-deficient mice: a model of chronic mucosal inflammation. In: Inflammatory Bowel Diseases, Tytgat GNJ, Bartelsman MFWM, van Deventer SJH, eds. Dordrecht: Kluwer Academic Publishers, 1995:410-417.
36. Knigge KL. Inflammatory bowel disease. Clin Cornerstone 2002;4:49-60.
37. Nowacki MR. Cell proliferation in colonic crypts of germ-free and conventional mice--preliminary report. Folia Histochem Cytobiol 1993;31:77-81.
38. Van der Sluis M, Makkink MK, Sutmuller M, Büller HA, Dekker J, Augenlicht LH, Velcich A, Einerhand AWC. Muc2 knockout mice are more susceptible to dextran sulfate sodium- induced colitis. Gastroenterology 2002;122:T946.
39. Schwerbrock NM, Makkink MK, van der Sluis M, Büller HA, Einerhand AW, Sartor RB, Dekker J. Interleukin 10-deficient mice exhibit defective colonic Muc2 synthesis before and after induction of colitis by commensal bacteria. Inflamm Bowel Dis 2004;10:811-23.
40. Matsuoka Y, Pascall JC, Brown KD. Quantitative analysis reveals differential expression of mucin (MUC2) and intestinal trefoil factor mRNAs along the longitudinal axis of rat intestine. Biochim Biophys Acta 1999;1489:336-344.
41. Renes IB, Verburg M, Van Nispen DJ, Büller HA, Dekker J, Einerhand AW. Distinct epithelial responses in experimental colitis: implications for ion uptake and mucosal protection. Am J Physiol Gastrointest Liver Physiol 2002;283:G169-179.
42. Strober W, Fuss IJ, Blumberg RS. The immunology of mucosal models of inflammation. Annu Rev Immunol 2002;20:495-549.
43. Fiocchi C. Inflammatory bowel disease: etiology and pathogenesis. Gastroenterology 1998;115:182-205.
44. Buisine MP, Devisme L, Savidge TC, Gespach C, Gosselin B, Porchet N, Aubert JP. Mucin gene expression in human embryonic and fetal intestine. Gut 1998;43:519-24.
45. Buisine MP, Desreumaux P, Leteurtre E, Copin MC, Colombel JF, Porchet N, Aubert JP. Mucin gene expression in intestinal epithelial cells in Crohn‘s disease. Gut 2001;49:544-551.
46. Mahler M, Leiter EH. Genetic and environmental context determines the course of colitis developing in IL-10-deficient mice. Inflamm Bowel Dis 2002;8:347-55.

Chapter 4

Mucin 2-Interleukin 10 Deficient Mice: Double Trouble

Maria van der Sluis, Janneke Bouma, Audrey Vincent, Anna Velcich, Kermit L. Carraway, Hans A. Büller, Alexandra W.C. Einerhand, Johannes B. van Goudoever, Isabelle Van Seuningen and Ingrid. B. Renes. *Mucin2-Interleukin 10 Deficient Mice: A Lethal Combination.*

Manuscript submitted

Abstract

Expression of the mucin MUC2, the structural component of the colonic mucus layer, is lowered in ulcerative colitis. Furthermore, IL10 knockout ($IL10^{-/-}$) mice develop colitis and have reduced Muc2 levels. Our aim was to obtain insight in the role of Muc2 and IL10 in epithelial protection. Muc2-IL10 double knockout ($Muc2/IL10^{DKO}$) mice were characterized and compared to Muc2 knockout ($Muc2^{-/-}$), $IL10^{-/-}$ and wild type (WT) mice. Clinical symptoms were monitored and intestinal morphology and differences in epithelial-specific protein levels were analyzed. Additionally, levels of the pro-inflammatory cytokines in colonic tissue and serum were determined. $IL10^{-/-}$ mice were indistinguishable from WT mice throughout this experiment and showed no clinical or microscopical signs of colitis. $Muc2/IL10^{DKO}$ mice and Muc2 knockout ($Muc2^{-/-}$) mice showed significant growth retardation and clinical signs of colitis as of 4 and 5 weeks of age, respectively. $Muc2/IL10^{DKO}$ mice had a high mortality rate [50% survival/ 5 weeks] compared to the other types of mice [100% survival]. Microscopic analysis of the colon of $Muc2^{-/-}$ showed mucosal thickening, increased proliferation and superficial erosions, which were even more pronounced in $Muc2/IL10^{DKO}$ mice. Furthermore, pro-inflammatory cytokines were significantly up-regulated, both in tissue (mRNA) and systemically in $Muc2/IL10^{DKO}$ mice. $Muc2/IL10^{DKO}$ mice develop colitis, which is more severe in every aspect compared to $Muc2^{-/-}$ mice. These data indicate that i) in case of Muc2 deficiency, the anti-inflammatory cytokine IL10 can control epithelial damage, though to a limited extent and ii) the mucus layer is most likely a key factor determining colitis.

Abbreviations used in this paper

CD, Crohn's disease; DAI, disease activity index; IBD, inflammatory bowel disease; IL, interleukin; $IL10^{-/-}$, Interleukin-10 knockout mice; Muc, Mucin; $Muc2^{-/-}$, Mucin 2 knockout mouse; WT, wild type mouse; $Muc2/IL10^{DKO}$, Mucin2/IL10 double knockout mouse; Tff3, trefoil factor 3; TNF-α, tumor necrosis factor alpha; UC, Ulcerative colitis

Introduction

Inflammatory bowel diseases (IBD), including ulcerative colitis (UC) and Crohn's disease (CD), are characterized by chronic inflammation and mucosal tissue damage of parts of the gastrointestinal tract. A widely accepted hypothesis suggests that these diseases are caused by a combination of genetic, environmental, immunoregulatory, and epithelial factors[1, 2].

Interleukin(IL)-10 plays a major role in maintenance of intestinal homeostasis by suppressing proinflammatory cytokine production[1, 3, 4]. A well described model mimicking a immunoregulatory defect, is the IL10 deficient ($IL10^{-/-}$) mouse[4-6]. $IL10^{-/-}$ mice spontaneously develop chronic colitis, of which the severity is dependent on both strain background and environmental factors. Relocation of $IL10^{-/-}$ mice from conventional specific pathogen free environments into germ-free isolators eliminates immune system activation and colitis development[7, 8].

The epithelium and mucus layer in the intestinal tract form a physical barrier between the potential noxious agents present in the gut lumen and the underlying tissues. Mucins are the building blocks of the mucus layer and previous studies have shown that human, rat and mouse colonic epithelium expresses mainly one secretory mucin in high amounts, Muc2[9-13]. As we described recently, loss of Muc2 in the intestine, and therefore changes in the protective capacities of the mucus layer, leads to inflammation of the colon and therefore contributes to the onset and/or perpetuation of IBD[14]. In agreement, it has been shown that in patients with UC, the activity of the mucosal inflammation correlates significantly with a decrease in MUC2 synthesis and secretion[15, 16].

Thus, considering that the severity of chronic intestinal inflammation can depend on environmental, immunoregulatory, and epithelial factors, we investigated the protective capacities of Muc2 and IL10 in the intestine, by generating Muc2/IL10 double knockout ($Muc2/IL10^{DKO}$) mice and determining whether the combination of defects in the immunoregulatory and epithelial factors could exacerbate the pathogenesis of inflammation. We therefore characterized $Muc2/IL10^{DKO}$ mice and compared their clinical symptoms and intestinal pathology to $Muc2^{-/-}$ and $IL10^{-/-}$ mice of the same age. This animal model is the first to provide insight into the role that both immunological and epithelial abnormalities, *i.e*. IL10 and Muc2 deficiency, play in the severity of colonic inflammation.

Materials and Methods

Animals

The previously described heterozygous Muc2129SV mice and mice carrying a homozygous null-mutation of the *IL10* gene ($IL10^{-/-}$), formally designated $IL10^{tm1Cgn}$ were bred to generate heterozygous double KO mice[6, 14, 17]. These heterozygous double knockout mice were bred with each other to generate homozygous $Muc2/IL10^{DKO}$ mice.

Throughout the crossing procedure, the targeted Muc2 and IL10 gene were monitored via PCR assays performed on genomic DNA isolated from tail clips as previously described[6, 18]. The mice were housed in the same specific pathogen-

free environment, and all animal care and procedures were conducted according to institutional guidelines (Erasmus MC- Animal Ethics Committee, Rotterdam, the Netherlands).

Experimental set-up

The initial set-up of this experiment was to characterize wild type (WT) (n=24), IL10$^{-/-}$ (n=20) and Muc2/IL10^{DKO} (n=23) littermates from 5 weeks until the age of 16 weeks, consistent with our study on the Muc2$^{-/-}$ mouse[14]. We had to adapt this set-up as the Muc2/IL10^{DKO} had a high mortality rate and Disease Activity Index (DAI) and it was not considered humane to continue this protocol. Therefore Muc2/IL10^{DKO}and corresponding wild type (WT) littermates were sacrificed after 4 (Muc2/IL10^{DKO} n=5, WT n=4), 5 (Muc2/IL10^{DKO} n=7, WT n=4) and 7 (Muc2/IL10^{DKO} n=1) weeks. As a control, IL10$^{-/-}$ and corresponding WT mice were sacrificed at 5, 8, 12, 16 and 34 weeks of age (n=4, each time point) as these mice are known to develop colitis at a later age[7, 19]. Furthermore, all results from Muc2/IL10^{DKO} mice were compared to previously published results on the Muc2$^{-/-}$ mouse[14].

All mice were scored to obtain a DAI as described by Cooper *et al* (Table I)[20]. Briefly, they were scored for the following: weight, softness of the stool, occult faecal blood and general appearance of the mice. Epithelial cell proliferation was determined by *in vivo* DNA labelling with bromodeoxyuridine (BrdU), injected intraperitoneally 30 mg/kg body weight (Sigma, St. Louis, USA) one hour prior to sacrifice[21, 22]. Small intestine and colon were rapidly excised and either fixed in 4% (w/v) paraformaldehyde in PBS, stored in RNA later (Qiagen, Venlo, the Netherlands) at –20°C, or frozen in liquid nitrogen and stored at -80°C.

Table I. Disease Activity Index (DAI) Score.

Score	% weight loss*	Stool consistency	Blood loss	Appearance
0	None	Normal droppings	None	Lively/ normal
1	0-25	Loose droppings	Hemoccult positive	Hunched
2	25-50	Diarrhea	Gross bleeding	Starey coat
3	>50			Lethargic

NOTE. *Criteria were obtained by pooling all data and calculating quartiles. For the percentage weight loss was calculated by comparing the weight of the mice to corresponding WT littermates.

Histology and histological grading

Tissue fixed in 4% (w/v) paraformaldehyde in PBS was prepared for light microscopy and 5 μm thick sections were stained either by 1) haematoxylin and eosin (H&E) or 2) Alcian blue (AB) at pH 2.5 followed by periodic acid/ Schiff's reagent (PAS) as described previously to study histological changes[23]. Intestinal inflammation

was determined by monitoring number of goblet cells, mucosal thickening, presence of inflammatory cells, general destruction of architecture, presence of ulcers and/ or crypt abscesses.

Immunohistochemistry

Five-micrometer-thick sections were cut and prepared for immunohistochemistry, as described previously using the Vectastain Elite ABC kit (Vector Labs, Burlingame CA, USA) and 3,3'-diaminobenzidine as staining reagent[22]. Expression of Muc2 was detected using an anti-Muc2 antibody H-300, (1:1000 in PBS; SC-15334, Santa Cruz, SanverTech, Heerhugowaard, the Netherlands). To detect goblet cells, anti-trefoil factor 3 (Tff3; 1:3000 in PBS; a generous gift from Prof. Dr. D. K. Podolsky) was used [24]. Muc4 was stained using anti-hMUC4 polyclonal antibody (hHA-1) that recognizes a C-terminal peptidic region of MUC4α subunit (1:6000 in 1% BSA, 0.1% Triton X100 in PBS)[25].To visualize BrdU incorporation, the sections were incubated with anti-BrdU (Boehringer Mannheim, Mannheim, Germany) as described previously[26]. $CD3^+$ cells were detected using an anti-human CD3 (DAKO, Heverlee, Belgium; 1:800 in 1% BSA, 0.1% Triton X100 in PBS). Additionally, non-specific binding was reduced by blocking with TENG-T (10 mM Tris-HCl, 5 mM EDTA, 150 mM NaCl, 0.25% (w/v) gelatin, 0.05% (w/v) Tween-20).

Quantitative real-time PCR (Sybergreen)

The mRNA expression levels of the membrane bound mucins Muc1 and -4 as well as the endogenous housekeeping gene β-actin were quantified using real-time PCR analysis (Taqman chemistry) based upon the intercalation of SYBR® Green on an ABI Prism 7700 sequence detection system (PE Applied Biosystems) as previously described[14]. The primers combinations for Muc1 (5´- CTTTCAGAAGACTCCGCCAG -3´, and 5´- GGCCAAGACTGATTCAGAGC -3´) and Muc4 (5''- CCCGCTCATCCACTATC -3´, and 5´- TGGCCTCCATTGTGAC -3´) were designed using the OLIGO 6.22 software (Molecular Biology Insights, Cascade, CO, USA) and purchased from Invitrogen (Breda, the Netherlands). All primers had a melting temperature (Tm; nearest neighbor method) between 65-66.5°C. In addition the mRNA expression levels of tumor necrosis factor alpha (TNF-α), interleukin (IL)-1beta (IL1β) and IL6 as well as the endogenous housekeeping gene β-actin were quantified as previously described[14]. To verify the amplification efficiency within each experiment, a serial dilution of cDNA derived from an RNA-pool of control colon samples in dH_2O was amplified in duplicate on each plate. Since all PCRs were performed with equal efficiencies, relative mRNA expression levels of Muc1, Muc4, TNF-α, IL1β and IL6 for each mouse can directly be normalized for input RNA against the β-actin expression of the mice. For this, the relative mRNA expression levels of these target genes were calculated according to the comparative cycle time (Ct) method[27], following the equation:

$$\text{relative mRNA expression} = 2^{-(\text{Ct target-Ct } \beta\text{-actin})} \times 100\%.$$

Serum cytokine levels

Serum was obtained from coagulated blood collected by heart puncture (15 min at 37°C, then 30 min a 4°C) and stored at –20°C until further analysis. The concentrations of several cytokines (IL12, TNF-α, Interferon gamma (IFN-γ), Monocyte chemoattractant protein-1 (MCP-1), IL10 and IL6) in serum of the mice were determined with a BD Cytometric Bead Array mouse inflammation kit according to manufacturers instructions (BD-Pharmingen, San Diego, USA).

Statistical analysis

All data are expressed as mean ± SEM. Statistical significance of the three different groups of mice during time, was assessed by The One way ANOVA test followed by a Tukey T-test. The Mann-Whitney U-test was used to analyze changes between 2 groups and changes in mRNA expression as assessed by real time PCR (PRISM, version 4.00, Graphpad software, San Diego, CA, USA). The data were considered statistically significant at $P<.05$.

Results

Clinical symptoms

The number of the Muc2/IL10^{DKO} mice was in line with the predicted value from Mendelian genetics, indicating that there was no prenatal selection or death before 4 weeks of age. However, Muc2/IL10^{DKO} mice showed high mortality rates as of 4 weeks of age (Fig.1A). Seven of the 23 mice died between 3 to 4 weeks of age, and 3 additional mice died at the age of 4 to 5 weeks, as shown in Figure 1A. Therefore, we sacrificed two groups of 5 and 7 Muc2/IL10^{DKO} mice at 4 and 5 weeks of age, respectively. These mice did not contribute to the establishment of the survival curve. The only surviving mouse was euthanized at the age of 7 weeks but not considered for further analysis. In contrast, none of the wild type (WT), IL10$^{-/-}$ and Muc2$^{-/-}$ mice died during the time frame studied.

A significant difference (P=.008) in body weight was detected at 4 weeks of age between WT and Muc2/IL10^{DKO} mice. Interestingly WT mice significantly gained weight between the age of 4 and 5 weeks [17.2±1.1 g vs. 22.3±1.4 g, respectively, P=.016], whereas the weight of Muc2/IL10^{DKO} mice remained stable [6.4±0.4 g vs. 6.7±0.3 g, respectively, P=.53]. Similarly, although less severely than Muc2/IL10^{DKO} mice, 5-week-old Muc2$^{-/-}$ mice showed significant growth retardation (Fig.1B). In contrast, there were no significant differences between WT and IL10$^{-/-}$ mice regarding body weight (Fig.1B) at five weeks of age. However, at 8 weeks of age the WT mice were significantly heavier than IL10$^{-/-}$ mice, [25.6±0.2 g vs. 24.2±0.34 g, respectively, P=.005] and this difference was maintained until 34 weeks of age [37.4±1.1 g vs. 32.1±1.0 g, respectively, P=.024].

Furthermore, at 4 weeks of age, all the Muc2/IL10^{DKO} mice showed diarrhea and gross bleeding which persisted until 5 weeks of age whereas none of the other types of mice displayed these clinical symptoms at this age. This resulted in a significantly higher DAI score compared to all the other types of mice (Fig.1C). The DAI score as shown by the WT and the IL10$^{-/-}$ mice is due to weight differences within the groups, and was non significant.

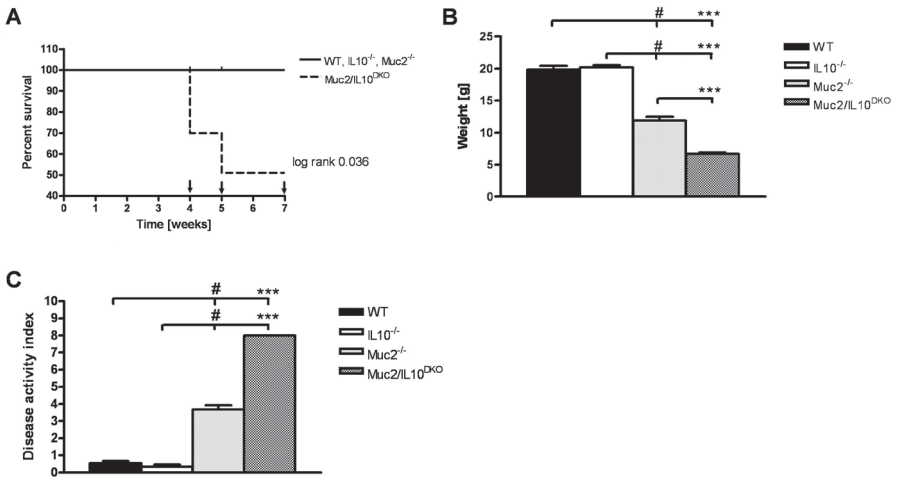

Figure 1. Appearance and clinical symptoms of WT, IL10$^{-/-}$, Muc2$^{-/-}$ and Muc2/IL10^{DKO} mice. (A) Survival of the Muc2/IL10^{DKO} mice during time. Arrows in the graph indicate time points where groups of mice were manually euthanized. N equals the number of mice which survived each time point. None of the WT, IL10$^{-/-}$ and Muc2$^{-/-}$ mice died during the time frame studied. (B) Body weight of the different mice 5 weeks of age. (*P<.0001; #P=.0002) (C) Disease activity index (DAI) is an accumulative score as adapted from Cooper et al.20 (*P<.0001; #P=.0002). Error bars indicate the SEM.

Morphological analysis

In line with the clinical observations, there were no morphological differences in the proximal or distal colon between WT and IL10$^{-/-}$ mice at 5 up to 16 weeks of age. At 34 weeks of age the distal colon of the IL10$^{-/-}$ mice showed mild inflammation characterized by mucosal thickening, influx of inflammatory cells and an overall mild distortion of the architecture (data not shown). The colonic morphology of Muc2/IL10^{DKO} animals differed considerably from their WT littermates (Fig.2A,B proximal colon and Fig.2A,F distal colon). In addition to the absence of the characteristic bell shape morphology of the goblet cells, the Muc2/IL10^{DKO} mice showed crypt hyperplasia, mild infiltration, flattening of epithelial cells and distortion of the lamina propria as of 4 weeks of age in the proximal colon. The overall damage of the colon increased along the proximal-distal axis and in addition to the histopathology described above, severe ulceration and crypt abscesses were observed in the distal colon of the Muc2/Il10^{DKO} mice. These histological characteristics were most pronounced in the older mice (5 weeks).

The presence of goblet cells in the colonic mucosa was determined by an AB/PAS staining, which stains glycoproteins. Goblet cells of the proximal and distal colon were mainly positive for AB at the base of the crypts whereas the PAS positive cells were concentrated higher in the crypts in WT and IL10$^{-/-}$ mice (Fig.2C and G showing WT proximal and distal colon respectively, at 5 weeks of age). This was in contrast to the proximal colon of Muc2/IL10^{DKO} mice in which there were hardly any PAS positive cells (Fig.2D, showing 5 weeks of age). In the distal colon of the Muc2/IL10^{DKO} mice however, there were few small, condensed, PAS positive cells along the crypts and AB positive cells at the base of the crypts (Fig.2H, showing 5 weeks of age).

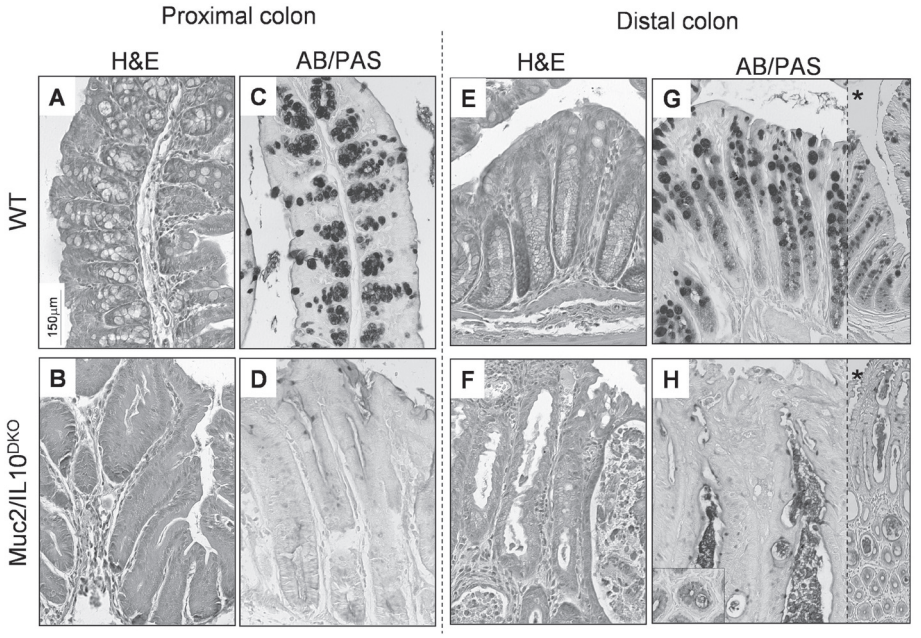

Figure 2. Colonic morphology the WT and Muc2/IL10^{DKO} mice. Representative sections of the colon are depicted at 5 weeks of age (A-C; proximal colon, D-H; distal colon). A-B; E-F represent H&E stainings whereas C-D; G-H represent AB-PAS stainings. A and C, and E and G represent proximal colon and distal colon, respectively of the WT mice. B and D, and F and H represent proximal colon and distal colon, respectively of the WT mice. The insert in H shows a close-up of goblet cells in the crypts of Muc2/IL10^{DKO} mice. The a*sterisks* represents a lower magnification of the distal colon. Please also see page 221.

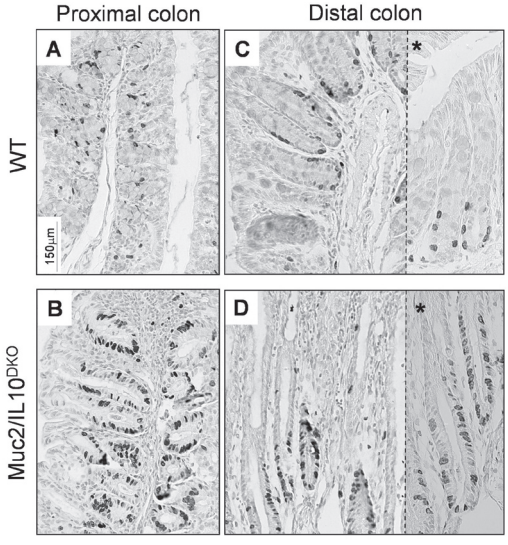

Figure 3. Increased proliferation in the colonic crypts of Muc2/IL10^{DKO} mice. BrdU staining of the proximal (A-B) and distal colon (C-D). In WT mice BrdU-positive cells were localized at the base of the crypts in both proximal and distal colon (A and B, respectively). The Muc2/IL10^{DKO} mice, however, showed a significant increase in the number of BrdU-positive cells in both the proximal and distal colon and these cells extended halfway up the crypt. (C and D, respectively). The a*sterisks* represents a higher magnification of the crypts in the distal colon

Epithelial proliferation was studied by immunohistochemical staining of incorporated BrdU. No differences were detected between the WT and IL10$^{-/-}$ mice in distribution or localization of BrdU-positive cells in the proximal and distal colon at all ages (data not shown). In WT mice BrdU-positive cells were localized at the base, and up to 1/3 of the crypts in the proximal and distal colon (Fig.2A-C, respectively, 5 weeks old). In both the proximal and distal colon of all Muc2/IL10^{DKO} mice, however, there was a significant increase in the number of BrdU-positive cells as early as of 4 weeks of age, which remained constant with time, and these cells extended up, into the crypt (Fig. 3B-D respectively, 5 weeks of age).

Expression of goblet cell markers

The intestinal epithelium of Muc2/IL10^{DKO} mice, as previously shown for the intestine of Muc2ko mice, lack recognizable goblet cells, as determined by AB/PAS staining, however we ascertained the presence and maturation of the goblet cells in the different mouse models by determining the expression of markers for goblet cells, more specifically i) Muc2 and ii) Tff3 a bioactive peptide which is involved in epithelial repair[24]. Muc2 was expressed throughout the crypts of proximal and distal colon of WT and the IL10$^{-/-}$ mice, but could not be detected in both the Muc2$^{-/-}$ and Muc2/IL10^{DKO} mice at any time point (data not shown). Tff3 was expressed by goblet cells, concentrated mainly in the upper portion of the crypts, in both the proximal and distal colon of WT and IL10$^{-/-}$ mice (Fig.4A and C showing WT mice, proximal and distal colon respectively). Goblet cells expressing Tff3 were present in the crypts of proximal and distal colon of the Muc2$^{-/-}$ mice as described previously[14]. However, Tff3-positive goblet cells were hardly detectable in the proximal colon of the Muc2/IL10^{DKO} mice (Fig.4B, showing 5 weeks of age).

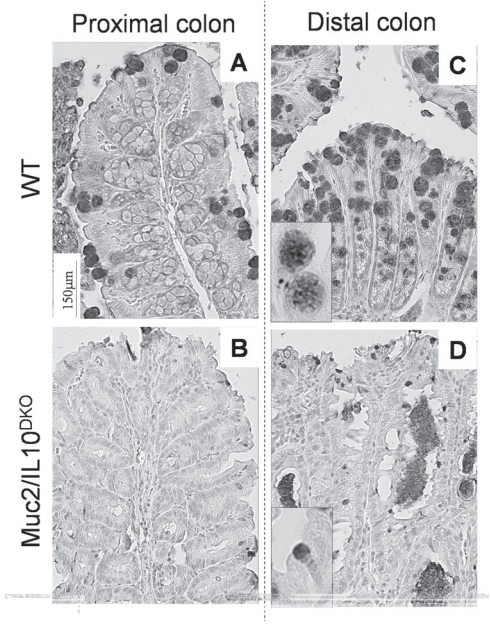

Figure 4. Tff3 expression in colon. Tff3 was expressed by goblet cells in the proximal colon of **(A)** WT mice, but was virtually absent in the proximal colon of **(B)** Muc2/IL10^{DKO} mice. In the distal colon, Tff3 was present in the goblet cells of **(C)** WT mice**,** but in larger numbers compared to the goblet cells of the **(D)** Muc2/IL10^{DKO} mice. Please also see page 221.

Tff3 was detectable in the goblet cells in the distal colon of the Muc2/IL10^{DKO} mice (Fig.4D, showing 5 weeks of age), but in smaller numbers compared to WT mice. Furthermore, the goblet cells in the distal colon of the Muc2/IL10^{DKO} mice showed a distinct change in morphology. Whereas the goblet cells of the WT mice were round and bell shaped (insert of panel 4C; distal colon) the goblet cells of the Muc2/IL10^{DKO} mice appeared smaller and more condensed (insert of panel 4D; distal colon).

Expression of the mucins Muc1 and Muc4

The expression of the membrane bound mucins Muc1 and -4 in the distal colon of each type of mice was quantified by using realtime RT-PCR (Fig.5A). Muc1 expression in the knockout mice did not differ for WT mice. In contrast, Muc4 mRNA was decreased in the distal colon of both Muc2$^{-/-}$ and Muc2/IL10^{DKO} mice. The Muc4 mRNA expression in the distal colon of the Muc2$^{-/-}$ and Muc2/IL10^{DKO} mice correlated to a decreased protein expression in the distal colon as determined by immunohistochemistry (Fig.5B and C showing WT and Muc2/IL10^{DKO} respectively). As Muc4 was expressed by goblet cells in the distal colon, it was also used as a goblet cell marker in the proximal colon of the Muc2/IL10^{DKO} mice. As shown in figure 5D, in WT mice, goblet cells in the surface epithelium of the proximal colon express Muc4. These cells were, however, undetectable in the proximal colon of Muc2/IL10^{DKO} mice (Fig.5E).

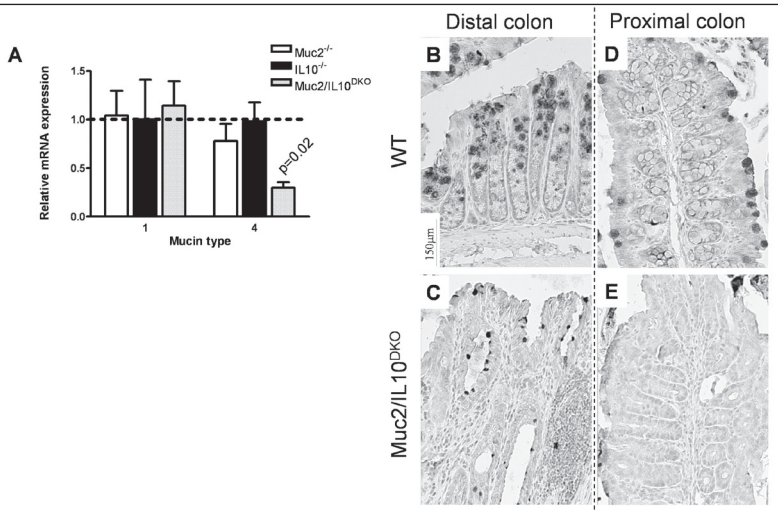

Figure 5. Expression of the mucins Muc1 and Muc4. (A) The mRNA expression of the mucins Muc1 and -4 in the distal colon were quantified. Expressed values (± SEM) are given relative to control values, which were arbitrarily set on 1. (B-E) Muc4 was expressed by goblet cells in both the (B) distal colon of WT and (C) Muc2/IL10^{DKO} mice. (D) Muc4 was expressed by the proximal colon of WT mice, but is hardly detectable in the proximal colon of (E) Muc2/IL10^{DKO} mice.

Increased lymphocyte infiltration and expression of inflammatory cytokines

Lymphocyte infiltration into the colon was evaluated using an anti-CD3 antibody. In both the proximal and distal colon of the WT and IL10$^{-/-}$ mice, single cells

situated in the lamina propria were detected up to 16 weeks of age. In accordance to previously published data there was an increase of lymphocyte infiltration in the Muc2$^{-/-}$ mice in parts of the colon were there was loss of epithelial cells. Parts of the colon that were unaffected were comparable to sections of the Muc2$^{+/+}$ mice[14]. In the Muc2/IL10^{DKO} mice there was an increase of lymphocyte infiltration, e.g. CD3 positive cells in both the proximal and distal colon compared to WT and Muc2$^{-/-}$ mice (Fig. 6A, Muc2/IL10^{DKO} mice, showing distal colon, 5 weeks of age). In addition, there was an increase of lymphocytes along the proximal-distal axis, which coincided, with the increase in histological damage seen in the colon of the Muc2/IL10^{DKO} mice.
Furthermore there was a significant increase in expression of mRNA of the inflammatory cytokines TNF-α, IL1β and IL6 in the distal colon of Muc2/IL10^{DKO} mice compared to WT mice as shown in Figure 6B (5 weeks of age). The mRNA expression levels of these cytokines were not significantly up regulated in IL10$^{-/-}$ and Muc2$^{-/-}$ mice compared to their WT littermates 5 weeks of age (data not shown). As the mRNA expression showed a significant increase of TNF-α, IL1β and IL6 in the distal colon of the Muc2/IL10^{DKO}mice we evaluated the pro inflammatory cytokine levels in the serum of these mice. In accordance with the TAQman data there was an increase in expression of inflammatory cytokines IL-12p70, TNF-α, IFN-γ, MIP-1 and IL6 in the serum of Muc2/IL10^{DKO} mice compared to WT mice as early as 4 weeks of age, which increased as the mice aged (Fig.6C, 5 weeks of age).

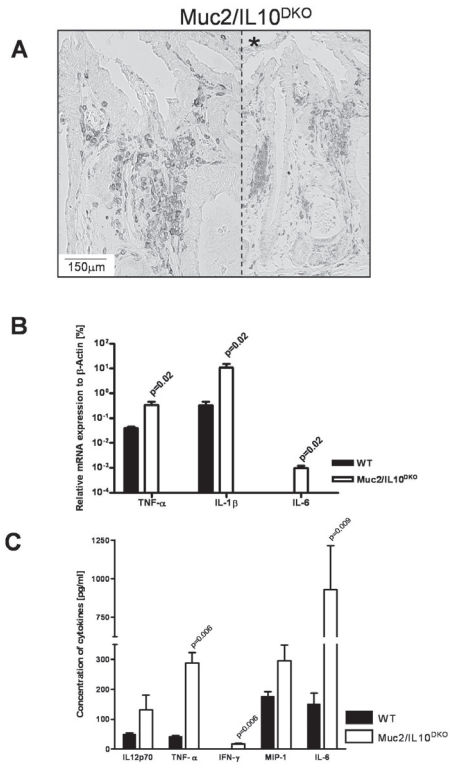

Figure 6. Increased lymphocyte infiltration and expression of inflammatory cytokines in Muc2/IL10^{DKO} mice. (A) Representative sections presenting lymphocyte infiltration into the distal colon of Muc2/IL10^{DKO} mice detected using an anti-CD3 antibody. The a*sterisks* represent a lower magnification of the distal colon. (B) Real time PCR data showed a significant up regulation of the inflammatory cytokines TNF-α, IL-1β and IL6 (P=.02) in the distal colon of Muc2/IL10^{DKO} mice compared to WT mice. (C) Analysis of the serum showed an increase in expression of inflammatory cytokines IL-12p70, TNF-α, IFN-γ, MIP-1 and IL6 in the serum of Muc2/IL10^{DKO} mice compared WT mice. Error bars indicate the SEM.

Discussion

In this study, we addressed the question whether immunological and epithelial deficiencies, more specifically IL10 and Muc2, sensitize the intestine to severe colonic inflammation.

The Muc2/IL10^{DKO} mice showed a high mortality rate compared to Muc2$^{-/-}$, IL10$^{-/-}$ and WT littermates of which none died during the current time frame. Several factors could contribute to the decreased survival rate of Muc2/IL10^{DKO} mice. In fact, these animals showed severe growth retardation, as manifested by lower body weight at 4 weeks of age, compared to WT littermates, which increased as the mice aged. The stunted growth of Muc2/IL10^{DKO} was more severe than that of Muc2$^{-/-}$ mice at 5 weeks of age. Although multiple factors can affect growth in the context of colonic inflammation, the most prominent is the presence and severity of inflammation and inadequate nutritional intake[28], including the levels of pro-inflammatory cytokines (see below)[29, 30]. The body weight of the Muc2$^{-/-}$ and Muc2/IL10^{DKO} mice support this hypotheses, as their weight can be correlated to the severity of inflammation in both types of mice. In addition, Muc2/IL10^{DKO} animals also show occult blood loss to gross bleeding and diarrhea as of 4 weeks of age whereas the WT and IL10$^{-/-}$ mice showed none of these additional symptoms. Interestingly, the Muc2/IL10^{DKO} mouse model seems to recapitulate symptoms that are well established in patients with IBD as growth failure is frequently observed in children with IBD[31]. Further, patients with IBD can suffer from diarrhea, rectal bleeding and weight loss[31].

Histological analysis of the colon of the Muc2/IL10^{DKO} mice additionally confirmed severe inflammation. In addition to the absence of the characteristic bell shape morphology of the goblet cells in the proximal colon the Muc2/IL10^{DKO} mice showed distinct differences displayed as crypt hyperplasia, inflammatory cell infiltration, flattening of epithelial cells and distortion of the lamina propria, which aggravated as the mice aged. This pathology was even more severe and distinct in the distal colon, which in addition to the above characteristics, also showed crypt abscesses. All together these clinical and histological symptoms indicate that the Muc2/IL10^{DKO} mice constitute a model to study aspects of IBD, which has an earlier onset and is more severe compared to both IL10$^{-/-}$ and Muc2$^{-/-}$ mice.

A characteristic difference between Muc2/IL10^{DKO} and WT mice was the lack of recognizable goblet cells throughout the entire intestine. This is in line with previously reported results on the Muc2$^{-/-}$ mice in which goblet cells were seemingly absent[18]. The colonic morphology of Muc2/IL10^{DKO} animals differed considerably from their WT littermates. That indeed goblet cells were present in the mucosa of the Muc2/IL10$^{-/-}$ was determined by using i) an AB/PAS staining ii) an antibody against Tff3 and iii) an antibody against Muc4. Tff3-positive goblet cells were present throughout the entire large intestine in WT, IL10$^{-/-}$ and Muc2$^{-/-}$ mice. This was in contrast to the Muc2/IL10^{DKO} mice, in which Tff3-positive goblet cells were present in the small intestine and distal colon. This coincided with the pattern found for the PAS positive staining of cells in the intestine. The goblet cells in both small and distal colon of the Muc2/IL10$^{-/-}$ mice however, showed loss of their characteristic goblet-like shape, corroborating the notion that Muc2 is the major phenotypic determinant of goblet cells as we described previously for the Muc2$^{-/-}$ mice[14]. The inflammation

of the colon in Muc2/IL10^{DKO} mice apparently affected the differentiation of goblet cells as indicated by a diminished or even loss of AB/PAS, Tff3, and Muc4 staining. This mechanism needs to be further investigated, however loss of differentiation of colonic cells during damage has been described previously as distinct enterocyte-specific proteins were shown to be down-regulated during intestinal damage[14, 32]. Furthermore, the AB positive cells at the base of the crypts in the Muc2/IL10^{DKO} mice could indicate transient expression of other mucins known to be expressed in the intestine or *de novo* expression of Muc6 mRNA as described for the Muc2$^{-/-}$ mice at 5 weeks of age[14]. We can only speculate on the possible function of these mucins in the Muc2/IL10^{DKO} as their functionality in the intestine has not been fully investigated, but as evidenced by the distinct pathology of the colon, these mucins cannot compensate for the absence of Muc2. In addition, in WT and IL10$^{-/-}$ mice BrdU-positive cells were localized at the base of the crypts in the distal colon. Only an increase of proliferation was observed in the distal colon of the Muc2$^{-/-}$ mice, 5 weeks of age[14]. The Muc2/IL10^{DKO} mice, however, a significant increase in proliferation, in both the proximal and distal colon as early as of 4 weeks of age, was observed.

Membrane mucins are usually found at the apical membrane, thereby protecting epithelial cells. However recent studies have also implicated a role for these mucins in signaling, contributing to the modulation of intestinal cell proliferation and differentiation as reviewed by Hollingsworth and Swanson[33]. Proliferation and differentiation are affected in the Muc2$^{-/-}$ and Muc2/IL10^{DKO} mice, as determined by the increased proliferation of the distal colon as well as alteration of markers of the goblet cell lineage. Therefore we investigated the expression of the two best characterized membrane mucins, Muc1 and Muc4, in these knockout mice. Muc1 mRNA was unaffected in all types of knock out mice compared to WT mice. In contrast, Muc4 mRNA, although modestly downregulated in Muc2$^{-/-}$ mice, was significantly downregulated in Muc2/IL10^{DKO} mice. Loss of Muc4 expression in the colon of these mice is in line with a previous study in which Muc4 is associated with highly differentiated, nonproliferating epithelial cells[34].Membrane mucins can be released from cells in soluble form, from which the transmembrane domain has been removed by either proteolysis or alternative splicing. Previous studies demonstrated that Muc4 is associated with epithelial secretion granules of the goblet cells[35, 36]. Furthermore, they showed that in the colon, Muc4 is predominantly expressed by the goblet cells in both rats and humans and that the soluble form of Muc4 predominates. Muc4 was present in fully differentiated goblet cells (present higher in the crypts) through-out the colon of the WT mice. Interestingly loss of differentiation of goblet cells in the colon of Muc2$^{-/-}$ and Muc2/IL10^{DKO} mice was confirmed by diminished Muc4 expression. There was even an almost complete loss of Muc4 protein expression in the goblet cells of the proximal colon in both these types of mice. Furthermore, down regulation of Muc4 and unaltered Muc1 (mRNA) expression indicate that these mucins cannot compensate for the absence of Muc2 in epithelial protection.

An increase in exposure to luminal antigens due to a diminished mucus layer (decrease of Muc2[14] and Muc4, this paper), could initiate inflammation. In the Muc2/IL10^{DKO} mice there was an increase of lymphocyte infiltration, e.g. CD3 positive cells, throughout the colon which was more severe compared to Muc2$^{-/-}$ mice. The increase of infiltration coincided with an up regulation of mRNA for the inflammatory

cytokines TNF-α, IL-1β and IL-6 in the distal colon of Muc2/IL10^{DKO} at 5 weeks of age. In addition, several proinflammatory cytokines, more specifically TNF-α, IFN-γ and IL-6 were significantly up regulated systemically in the Muc2/IL10^{DKO} at 5 weeks of age. It is well known that pro-inflammatory cytokines play an important role in inflammation of the intestinal mucosa. For instance, TNF-α, IL-1β and IL-6 have shown to play a pivotal role in the pathogenesis of IBD[1, 3, 4]. In addition, previous studies demonstrated that IL10 is necessary for the production of TGF-β and that, in agreement, IL10$^{-/-}$ mice lack TGF-β signaling[37, 38]. Lack of both IL10 and TGF-β signaling in the Muc2/IL10^{DKO} further explains the excessive inflammation in these mice compared to Muc2$^{-/-}$ mice. Furthermore, there is increasing evidence in the literature that systemic increase of TNF-α and IL-6 could partly explain the growth retardation in IBD patients and in the current study of the Muc2/IL10^{DKO} mice[29, 30].

To summarize, the Muc2/IL10^{DKO} mouse clearly demonstrates that combined abnormalities in immunoregulatory and epithelial factors greatly accelerate and exacerbate the phenotype of colonic inflammation. In fact, IL10$^{-/-}$ mice show no distinct clinical nor histological signs of colitis at 5 weeks of age indicating that the mucus barrier offers enough protection under unchallenged conditions. Muc2$^{-/-}$ mice however show an abnormal morphology marked by an increase in thickness of the gut mucosa, flattening and ulceration of epithelial cells, general loss of architecture, increase of inflammatory cells, an increase in proliferation, and decrease of cell differentiation in the colon as described previously[14]. This inflammation however is most likely, partly suppressed by IL10 as damage in the Muc2/IL10^{DKO} mice is much more severe, indicating that absence of Muc2 in combination with changes in the immunological regulatory mechanisms *e.g*. lack of IL10, leads to excessive uncontrollable inflammation of the colon, ultimately leading to the animals death. Therefore this study provides evidence that the mucus layer in the intestine, more specifically the mucin Muc2, plays a key role in mucosal protection suggesting that the mucus barrier is one of main factors determining colitis.

Acknowledgements

Sophia Foundation for Scientific Research, Rotterdam, The Netherlands Organization for Scientific Research, The Hague, The Foundation “De Drie Lichten”, Leiden, all situated in the Netherlands, The Association François Aupetit, Paris, France and the National Institutes of Health, Bethesda, United States, are gratefully acknowledged for their financial support. We would like to thank W. Chung, I.M.A. Louwers and L.F. de Ruiter for their excellent technical assistance.

References

1. Bouma G, Strober W. The immunological and genetic basis of inflammatory bowel disease. Nat Rev Immunol 2003;3:521-533.
2. Einerhand AW, Renes IB, Makkink MK, van der Sluis M, Büller HA, Dekker J. Role of mucins in inflammatory bowel disease: important lessons from experimental models. Eur J Gastroenterol Hepatol 2002;14:757-765.
3. Fiocchi C. Inflammatory bowel disease: etiology and pathogenesis. Gastroenterology 1998;115:182-205.
4. Strober W, Fuss IJ, Blumberg RS. The immunology of mucosal models of inflammation. Annu Rev Immunol 2002;20:495-549.
5. Elson CO, Sartor RB, Tennyson GS, Riddell RH. Experimental models of inflammatory bowel disease. Gastroenterology 1995;109:1344-67.
6. Kuhn R, Lohler J, Rennick D, Rajewsky K, Muller W. Interleukin-10-deficient mice develop chronic enterocolitis. Cell 1993;75:263-74.
7. Mahler M, Leiter EH. Genetic and environmental context determines the course of colitis developing in IL-10-deficient mice. Inflamm Bowel Dis 2002;8:347-55.
8. Sellon RK, Tonkonogy S, Schultz M, Dieleman LA, Grenther W, Balish E, Rennick DM, Sartor RB. Resident enteric bacteria are necessary for development of spontaneous colitis and immune system activation in interleukin-10-deficient mice. Infect Immun 1998;66:5224-31.
9. Herrmann A, Lindell G, Nordman H, Carlstedt I. The insoluble glycoprotein complex from human colon contains two MUC2 subunits of different size. Biochem Soc Trans 1995;23:535S.
10. van Klinken BJ, Einerhand AW, Duits LA, Makkink MK, Tytgat KM, Renes IB, Verburg M, Büller HA, Dekker J. Gastrointestinal expression and partial cDNA cloning of murine Muc2. Am J Physiol 1999;276:115-124.
11. Makkink MK, Schwerbrock NM, Mahler M, Boshuizen JA, Renes IB, Cornberg M, Hedrich HJ, Einerhand AW, Büller HA, Wagner S, Enss ML, Dekker J. Fate of goblet cells in experimental colitis. Dig Dis Sci 2002;47:2286-2297.
12. Tytgat KM, Büller HA, Opdam FJ, Kim YS, Einerhand AW, Dekker J. Biosynthesis of human colonic mucin: Muc2 is the prominent secretory mucin. Gastroenterology 1994;107:1352-1363.
13. Tytgat KM, Bovelander FJ, Opdam FJ, Einerhand AW, Büller HA, Dekker J. Biosynthesis of rat MUC2 in colon and its analogy with human MUC2. Biochem J 1995;309 (Pt 1):221-9.
14. van der Sluis M, de Koning BAE, de Bruijn ACJM, Velcich A, Meijerink JPP, van Goudoever JB, Büller HA, Dekker J, van Seuningen I, Renes IB, Einerhand AWC. Muc2-Deficient Mice Spontaneously Develop Colitis, Indicating That MUC2 Is Critical for Colonic Protection. Gastroenterology 2006;131:117-129.
15. Tytgat KM, van der Wal JW, Einerhand AW, Büller HA, Dekker J. Muc2 in ulcerative colitis: a quantitative study. Biochem Soc Trans 1995;23:531S.
16. Van Klinken BJ, Van der Wal JW, Einerhand AW, Büller HA, Dekker J. Sulphation and secretion of the predominant secretory human colonic mucin MUC2 in ulcerative colitis. Gut 1999;44:387-393.
17. Berg DJ, Davidson N, Kuhn R, Muller W, Menon S, Holland G, Thompson-Snipes L, Leach MW, Rennick D. Enterocolitis and colon cancer in interleukin-10-deficient mice are associated with aberrant cytokine production and CD4(+) TH1-like responses. J Clin Invest 1996;98:1010-20.
18. Velcich A, Yang W, Heyer J, Fragale A, Nicholas C, Viani S, Kucherlapati R, Lipkin M, Yang K, Augenlicht L. Colorectal cancer in mice genetically deficient in the mucin Muc2. Science 2002;295:1726-9.

19. Spencer DM, Veldman GM, Banerjee S, Willis J, Levine AD. Distinct inflammatory mechanisms mediate early versus late colitis in mice. Gastroenterology 2002;122:94-105.
20. Cooper HS, Murthy SN, Shah RS, Sedergran DJ. Clinicopathologic study of dextran sulfate sodium experimental murine colitis. Lab Invest 1993;69:238-49.
21. Wahba N. An ortho-tolidine hydrochloride test for the detection of occult blood in faeces without dietary restrictions. J Clin Pathol 1965;18:687-688.
22. Renes IB, Verburg M, Bulsing NP, Ferdinandusse S, Büller HA, Dekker J, Einerhand AW. Protection of the Peyer's patch-associated crypt and villus epithelium against methotrexate-induced damage is based on its distinct regulation of proliferation. J Pathol 2002;198:60-68.
23. Boshuizen JA, Reimerink JH, Korteland-van Male AM, van Ham VJ, Koopmans MP, Büller HA, Dekker J, Einerhand AW. Changes in small intestinal homeostasis, morphology, and gene expression during rotavirus infection of infant mice. J Virol 2003;77:13005-13016.
24. Mashimo H, Wu DC, Podolsky DK, Fishman MC. Impaired defense of intestinal mucosa in mice lacking intestinal trefoil factor. Science 1996;274:262-265.
25. Price-Schiavi SA, Meller D, Jing X, Merritt J, Carvajal ME, Tseng SC, Carraway KL. Sialomucin complex at the rat ocular surface: a new model for ocular surface protection. Biochem J 1998;335 (Pt 2):457-63.
26. Renes IB, Verburg M, Van Nispen DJ, Taminiau JA, Büller HA, Dekker J, Einerhand AW. Epithelial proliferation, cell death, and gene expression in experimental colitis: alterations in carbonic anhydrase I, mucin MUC2, and trefoil factor 3 expression. Int J Colorectal Dis 2002;17:317-326.
27. Meijerink J, Mandigers C, van de Locht L, Tonnissen E, Goodsaid F, Raemaekers J. A novel method to compensate for different amplification efficiencies between patient DNA samples in quantitative real-time PCR. J Mol Diagn 2001;3:55-61.
28. Motil KJ, Grand RJ. Growth failure in children and adolescents with inflammatory bowel disease. In: G.N.J. Tytgat MFWMB, S.J.H. van Deventer, ed. Inflammatory Bowel Diseases: Kluwer Academic Publishers, 1995:588-597.
29. Levine A, Shamir R, Wine E, Weiss B, Karban A, Shaoul RR, Reif SS, Yakir B, Friedlander M, Kaniel Y, Leshinsky-Silver E. TNF promoter polymorphisms and modulation of growth retardation and disease severity in pediatric Crohn's disease. Am J Gastroenterol 2005;100:1598-604.
30. Sawczenko A, Azooz O, Paraszczuk J, Idestrom M, Croft NM, Savage MO, Ballinger AB, Sanderson IR. Intestinal inflammation-induced growth retardation acts through IL-6 in rats and depends on the -174 IL-6 G/C polymorphism in children. Proc Natl Acad Sci U S A 2005;102:13260-13265.
31. Knigge KL. Inflammatory bowel disease. Clin Cornerstone 2002;4:49-60.
32. Renes IB, Verburg M, Van Nispen DJ, Büller HA, Dekker J, Einerhand AW. Distinct epithelial responses in experimental colitis: implications for ion uptake and mucosal protection. Am J Physiol Gastrointest Liver Physiol 2002;283:G169-179.
33. Hollingsworth MA, Swanson BJ. Mucins in cancer: protection and control of the cell surface. Nat Rev Cancer 2004;4:45-60.
34. Idris N, Carraway KL. Sialomucin complex (Muc4) expression in the rat female reproductive tract. Biol Reprod 1999;61:1431-8.
35. Rong M, Rossi EA, Zhang J, McNeer RR, van den Brande JM, Yasin M, Weed DT, Carothers Carraway CA, Thompson JF, Carraway KL. Expression and localization of Muc4/sialomucin complex (SMC) in the adult and developing rat intestine: implications for Muc4/SMC function. J Cell Physiol 2005;202:275-84.

36. Rossi EA, McNeer RR, Price-Schiavi SA, Van den Brande JM, Komatsu M, Thompson JF, Carraway CA, Fregien NL, Carraway KL. Sialomucin complex, a heterodimeric glycoprotein complex. Expression as a soluble, secretable form in lactating mammary gland and colon. J Biol Chem 1996;271:33476-85.
37. Ruiz PA, Shkoda A, Kim SC, Sartor RB, Haller D. IL-10 gene-deficient mice lack TGF-beta/Smad signaling and fail to inhibit proinflammatory gene expression in intestinal epithelial cells after the colonization with colitogenic Enterococcus faecalis. J Immunol 2005;174:2990-9.
38. Fuss IJ, Boirivant M, Lacy B, Strober W. The interrelated roles of TGF-beta and IL-10 in the regulation of experimental colitis. J Immunol 2002;168:900-8.

Chapter 5

The Mucin 2 Deficient Mouse Challenged by Methotrexate

Barbara A.E. de Koning*, Maria van der Sluis*, Dicky J. Lindenbergh-Kortleve, Anna Velcich, Rob Pieters, Hans A. Büller, Alexandra W.C. Einerhand and Ingrid B. Renes.
Methotrexate-induced mucositis in mucin 2 deficient mice.
* Both authors participated equally in this study

Journal of Cellular Physiology, *in press*

Abstract

The mucin Muc2, which is the main structural component of the protective mucus layer, has shown to be up regulated during chemotherapy-induced mucositis. As Muc2 has shown to have protective capacities, up regulation of Muc2 may be a counter reaction of the intestine protecting against mucositis. Therefore, increasing Muc2 protein levels could be a therapeutic target in mucositis prevention or reduction. Our aim was to determine the role of Muc2 in chemotherapy-induced mucositis. Mucositis was induced in Muc2 knockout ($Muc2^{-/-}$) and wild type (WT) mice by injecting methotrexate (MTX). Animals were weighed and sacrificed on days 2-6 after MTX treatment and jejunal segments were analyzed. Before MTX treatment, the small intestine of WT and $Muc2^{-/-}$ mice were similar with respect to epithelial morphology and proliferation. Moreover, sucrase-isomaltase and trefoil factor-3 protein expression levels were comparable between WT and $Muc2^{-/-}$ mice. Up to day 3 after MTX treatment, percentages of weight-loss did not differ. Thereafter, WT mice showed a trend towards regaining weight, whereas $Muc2^{-/-}$ mice continued to lose weight. Surprisingly, MTX-induced intestinal damage of $Muc2^{-/-}$ and WT mice was comparable. Prior to MTX-injection, tumor necrosis factor-α and interleukin-10 mRNAs were upregulated in $Muc2^{-/-}$ mice, probably due to continuous exposure of the intestine to luminal antigens. Conclusion: Muc2 deficiency does not lead to an increase in chemotherapy-induced mucositis. A possible explanation is the mechanism by which Muc2 deficiency may trigger the immune system to release interleukin-10, an anti-inflammatory cytokine before MTX-treatment.

Abbreviations used in this paper

IELs, Intraepithelial Lymphocytes; IL-10, Interleukin-10; Muc2, Mucin 2; MTX, methotrexate; $Muc2^{-/-}$, Mucin 2 knockout mice; WT, Mucin 2 wild type mice; Tff3, trefoil factor 3; TNF-α, Tumor Necrosis Factor-alpha; SI, Sucrase-Isomaltase.

Introduction

Mucositis is one of the most frequent and severest side effects of anti-cancer chemotherapy, for which there is still no definitive prophylaxis. Around 500,000 patients world-wide suffer from mucositis annually[1]. The disorder causes considerable oral and abdominal pain, diarrhea and weight-loss. Moreover, patients suffering from mucositis are predisposed to life-threatening infections[2-4]. All together, this could lead to forced reduction of chemotherapy intensity, thereby potentially reducing the efficacy of anti-cancer treatment[2, 5].

The intestinal mucus layer plays an important role in epithelial defense against mechanical stress, luminal pathogens, enzymes and toxins[6-8]. Goblet cells secrete molecules, such as mucins and trefoil factors that serve protective roles in the gut. Mucins are the most important structural component of mucus layer covering the epithelial cells. The intestine abundantly expresses the secretory mucin, Mucin 2 (Muc2)[9,10]. Abnormalities of secreted products of goblet cells could affect the physical barrier function of the mucus layer in the intestine.

Recent research, supporting the hypothesis that Muc2 might contribute to epithelial defense against chemotherapy-induced damage, showed a halving of the number of goblet cells on days 1-2 after treatment with methotrexate (MTX)[11,12]. Remarkably, Muc2 protein expression was significantly increased during all phases of MTX-induced damage[11, 12].

The role of Muc2 in the protection against mucositis is still unclear, but if its protective capacities could be demonstrated, increasing Muc2 protein levels could be a therapeutic target in mucositis prevention or reduction. We used an experimental Muc2 deficient ($Muc2^{-/-}$) mouse model[13,14] to analyze the role of Muc2 in epithelial protection against MTX-induced intestinal damage.

Materials and Methods

Animals

The previously described $Muc2^{-/-}$ mice of mixed genetic background, were backcrossed onto a 129SV (Charles River, Maastricht, the Netherlands) genetic background for nine generations followed by intercrosses to generate mice homozygous for the Muc2 disruption. Throughout the backcrossing procedure, the targeted Muc2 gene was monitored as previously described[13].

All mice were housed in micro-isolator cages under specific pathogen-free conditions with free access to standard rodent pellets (Special Diets Services, Witham, Essex, UK) and acidified tap water. Animal experiments were performed with permission of the Erasmus MC Animal Ethics Committee (Rotterdam, the Netherlands).

Clinical symptoms

Groups of wild type (WT) and $Muc2^{-/-}$ mice were monitored from 5 until 12 weeks of age. Weekly, weight and clinical signs such as softness of the stool and appearance of fecal occult blood[15] were assessed. At ages 5, 8, and 12 weeks, four mice per group were sacrificed.

MTX-induced mucositis

Mice, (n=16, each group) 8 weeks of age, were injected intraperitoneally with MTX (Emthrexate (PF); Pharmacie B.V., Haarlem, the Netherlands) using dosages of 50 and 25 mg/kg body-weight respectively on day –1 and 0. The concentration of MTX required to induce severe mucositis, was based on a dose-response-curve experiment we previously performed using 129SV WT mice (B.A.E. de Koning, unpublished observations). The induced mucositis in pilot experiment was characterized by villus atrophy, crypt loss and morphological regeneration within six days. Controls (n=4, both groups) were given equivalent volumes of 0.9% NaCl. Mice were weighed daily and groups of four were sacrificed on respective days 2, 3, 4 and 6 after the final MTX injection.

Tissue collection

One hour before sacrifice, the mice were injected with 120 µl 10 mg/ml 5-Bromo 2'deoxyUridine (BrdU; Sigma-Aldrich, Zwijndrecht, the Netherlands), to locate proliferating cells. Segments of the duodenum, mid-jejunum, ileum, proximal and distal colon were collected and processed for histological analyses, stored in RNA Later (Qiagen, Venlo, the Netherlands) at –20°C, or snap-frozen in liquid nitrogen for storage at -80°C and subsequent protein isolation.

(Immuno)histochemistry

Segments of mid-jejunum were fixed in 4% paraformaldehyde in phosphate-buffered saline (PBS), dehydrated and embedded in Paraplast Plus (Sherwood Medical, Den Bosch, The Netherlands). Sections were stained with hematoxylin (Vector Laboratories, Burlingame, CA) and eosin (Sigma-Aldrich) (HE) to study morphological alterations of the crypts and villi. Immunohistochemistry was performed as previously described [14, 16]. To detect incorporated BrdU, anti-BrdU (1:250 in PBS; Roche Applied Sciences, Indianapolis, IN, USA) was used. Expression of Muc2 was detected using a goat polyclonal anti-human Muc2 antibody (H-300; 1:1000 in PBS, SC-15334, Santa Cruz, SanverTech, Heerhugowaard, the Netherlands). As a marker for goblet cell-specific protein expression, a rabbit polyclonal anti-rat trefoil factor family (Tff3; 1:3000 in PBS, kindly provided by Prof. Dr. D.K. Podolsky[17]) was used, and to determine enterocyte-specific protein expression a rabbit polyclonal anti-rat sucrase-isomaltase (SI; 1:9000 in PBS, kindly provided by Dr. K.Y. Yeh[18]) was used. An anti-human CD3 antibody (DAKO, Heverlee, Belgium; 1:800 in 1% BSA, 0.1% Triton X100 in PBS) was used to detect $CD3^+$ T-cells. Additionally, non-specific binding was reduced by blocking with TENG-T (10 mM Tris-HCl, 5 mM EDTA, 150 mM NaCl, 0.25% (w/v) gelatin, 0.05% (w/v) Tween-20). Appropriate positive and negative controls were included in each immunohistochemical assay.

Morphological analysis

The following intestinal histological parameters were studied: morphology of the epithelium, degree of inflammation, villus atrophy, crypt loss, crypt abscess, and mucosal bleedings. All scores were obtained in a blinded fashion by two independent investigators.

Crypt and –villus length

Lengths of ten well-orientated crypts and villi of each individual animal were measured with the use of a Nikon Eclipse E800 microscope and Leica Image Manager 500 software (Leica Microsystems B.V, Rijswijk, the Netherlands). However, in cases of severe disease crypts could not be measured in all slides, due to extensive crypt loss; then, several slides within the jejunal region were combined in order to measure ten whole crypts and villi.

Intraepithelial lymphocytes

Numbers of intraepithelial lymphocytes (IELs) in the villi of the small intestine were determined by counting the number of CD3 positive cells per ten villi of each individual animal. This was done by two independent investigators in a blinded fashion.

Protein dot blotting

The expression of epithelial markers was detected and quantified as previously described[11]. Blots were incubated with anti-SI (1:1000) or anti-Tff3 (1:1500). Bound antibodies were detected using HRP conjugated goat anti-rabbit secondary antibodies (1:1000 in PBS) and SuperSignal® West Femto Luminol Enhancer kit (Pierce, Rockford, IL, USA). The signal was detected and quantified by the ChemiGenius gel documentation system (Syngene, Cambridge, UK).

Western-blot analysis

The same protein homogenate was used as described for protein dot blot analysis. Twenty µg of protein was loaded per lane and run on a 12.5% SDS-PAGE. The separated proteins were transferred to nitrocellulose membranes (Protran BA83, 0.2 µm) which were subsequently blocked[11]. Blots were incubated overnight at 4°C with mouse monoclonal anti-human proliferative cell nuclear antigen (PCNA); clone PC10 (1:250 in blocking buffer; Novo Castra Laboratories, Newcastle upon Tyne, UK). After washing with PBS-0.2% Tween-20, bound antibodies were revealed using HRP conjugated goat anti-mouse secondary antibodies (1:1000 in PBS) and detected and quantified as described above.

Quantitative real-time PCR (Sybergreen technology)

Total RNAs from mouse small intestine were prepared using the QIAamp RNA midi-kit (Qiagen), following the manufacturer's protocol, and treated with DNase (Qiagen). Total RNA (1.5 µg) was used to prepare first-strand cDNA (AdvantageTM RT-for-PCR kit; BD Biosciences, Clontech, Alphen aan den Rijn, the Netherlands). The mRNA expression levels of tumor necrosis factor alpha (TNF-α) and interleukin-10 (IL10) as well as the endogenous housekeeping gene β-actin were quantified using real-time PCR analysis (Sybergreen chemistry) based upon the intercalation of SYBR® Green on an ABI Prism 7700 sequence detection system (PE Applied Biosystems, Nieuwerkerk aan de IJsel, the Netherlands) as described previously[14]. Primer combinations for β-actin (5´-GGGACCTGACGGACTAC-3´ and 5´-TGCCACAGGATTCCATAC-3´), IL-10 (5´-CAAGCCTTATCGGAAATG-3´ and 5´-CATGGCCTTGTAGACACC-3´), and TNF-α (5´-TGGCCTCCCTCTCATC-3´ and

5´-GGCTGGCACCACTAGTT-3´) were designed using the OLIGO 6.22 software (Molecular Biology Insights, Cascade, CO, USA) and purchased from Invitrogen (Breda, the Netherlands).

Statistical analysis

The Mann-Whitney U-test was used to analyze changes in protein and mRNA expression levels. Results were considered statistically significant at P<.05. Data are presented as the mean +/- standard error of the mean (SEM).

Results

Clinical symptoms

To characterize the phenotype of Muc2$^{-/-}$ mice we monitored their weight in relation to WT littermates (Fig. 1). From the start, at week 5 of age, Muc2$^{-/-}$ mice had significantly lower body-weight (P<.0001) and showed growth retardation compared to WT littermates. At 6 weeks of age, Muc2$^{-/-}$ mice exhibited diarrhea and occult blood loss, which occasionally progressed to gross bleeding as of 8 weeks of age.

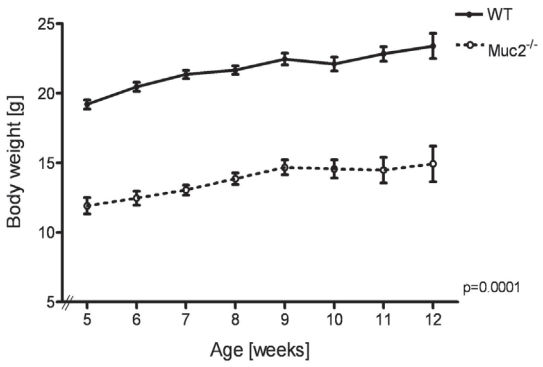

Figure 1. Body-weight of WT and Muc2$^{-/-}$ mice between 5 and 12 weeks of age. As from the start at week 5, Muc2$^{-/-}$ mice weighed significantly less and showed growth retardation compared to their WT littermates. Groups follow similar growth curves, but at a different level. Weight per group is expressed as Mean ± SEM.

Morphological analyses

In order to study morphological changes in the small intestine, HE stained slides of the duodenum, jejunum and ileum of Muc2$^{-/-}$ and WT mice were compared (Fig. 2A, B jejunum; duodenum and ileum are not shown). The main characteristic difference was the lack of recognizable goblet cells along the crypt-villus axis in the Muc2$^{-/-}$ mice throughout the small intestine. There were no further pronounced differences in epithelial morphology up to 12 weeks of age. There were no differences in number of apoptotic bodies along the crypt-villus axis between the Muc2$^{-/-}$ and WT mice. Similarly, there were no significant differences in villus and crypt lengths between Muc2$^{-/-}$ and WT mice at any time investigated (Fig. 2G and H, week 8, jejunum).

Two markers for goblet cells were analyzed: Muc2, which is stored in apical granules of the goblet cells determining the goblet cell morphology [10, 13, 14] and Tff3, a bioactive peptide which is involved in epithelial protection and repair [17, 19, 20]. In the small intestine of WT mice, Muc2 was expressed in goblet cells from the crypt bottom to the tips of the villi (Fig. 2C). Tff3 was also expressed in goblet cells located in the crypts, but was more predominant in goblet cells located on the villi (Fig. 2E). Goblet cells in the small intestine of the Muc2$^{-/-}$ mice were negative for Muc2 (Fig. 2D), but remained positive for Tff3 (Fig. 2F) with an expression pattern similar to that seen in the small intestine of WT mice. The goblet cells of the Muc2$^{-/-}$ mice showed distinctly altered morphology as previously described[13, 14]. Specifically, the goblet cells of the WT mice were round and bell shaped, whereas those of the Muc2$^{-/-}$ mice were smaller, flatter and more condensed.

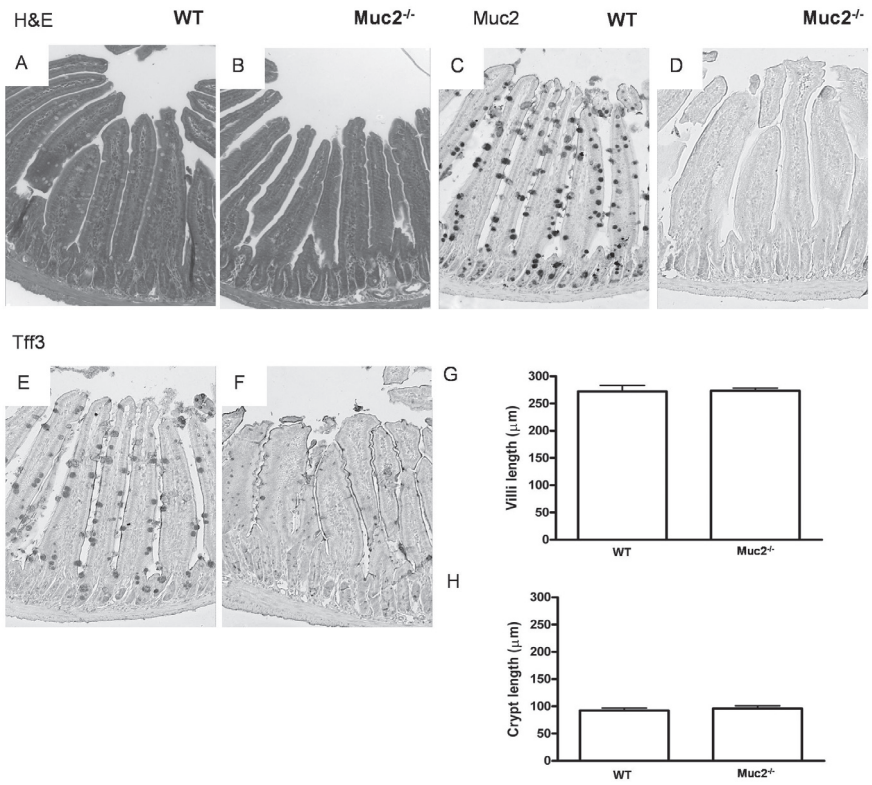

Figure 2. Absence of Muc2 does not affect small intestinal morphology. Representative sections of a hematoxilin eosin (A-B), Muc2 (C-D), and Tff3 (E-F) staining of the small intestine of WT (A,C,E) and Muc2$^{-/-}$ (B,D,F) mice at 8 weeks of age. The most characteristic difference between the Muc2$^{-/-}$ and WT mice was the lack of recognizable goblet cells along the crypt-villus axis of the small intestine in the Muc2$^{-/-}$ mice (B,D). The goblet cells in the small intestine of Muc2$^{-/-}$ mice showed the same expression pattern for Tff3, concentrating on the villi, similar as seen in the small intestine of the WT (E), but showed a distinct change in morphology of the goblet cells (**F**). Villi and crypt length (G,H) of WT and Muc2$^{-/-}$ littermates 8 weeks of age. Villi and crypt lengths per group are expressed as Mean ± SEM.

Methotrexate-induced mucositis model

MTX-treated WT mice showed significant weight-loss compared to the WT controls on days 1, 2, 3 and 5 (P=.003, P=.002, P=.004, P=.045 respectively). After day 3, the treated WT mice started to regain weight, almost equalizing control weights by day 6 (Fig 3A). A significant weight-loss was also seen in MTX-treated Muc2$^{-/-}$ compared to Muc2$^{-/-}$ controls, on day 1 and 3 after treatment (Fig 3B) (P=.008, P=.021, respectively). In addition, weight-loss on day 2 almost reached significance (P=.052). In contrast to WT mice, Muc2$^{-/-}$ mice continued to lose weight during MTX-treatment. Between day 5 and day 6, three of four MTX-treated Muc2$^{-/-}$ mice died, whereas all treated WT mice survived. The three non-surviving mice had suffered severe weight-loss (25%) prior to death. On account of the elapsed time after death, morphological evaluation could not be performed. The clinical symptoms displayed by Muc2$^{-/-}$ mice before MTX treatment, *i.e.* diarrhea and occult blood, did not aggravate after MTX-treatment.

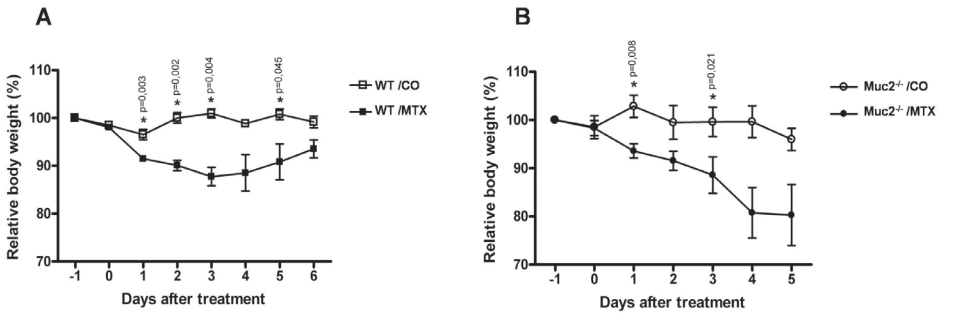

Figure 3. Weight-loss of MTX-treated WT and Muc2$^{-/-}$ mice. Weight of the mice on day –1, before start of the experiment, was set at 100%. A significant decrease in weight versus the saline-treated (i.e. control) mice was seen on days 1, 2, 3 and 5 for the MTX-treated **(**A**)** WT mice and on days 1 and 3 for the MTX-treated **(**B**)** Muc2$^{-/-}$ mice. Weight of the MTX-treated Muc2$^{-/-}$ mice differed at the brink of significance versus that of the control mice on day 2. Weight per group is expressed as Mean ± SEM

The effect of MTX-treatment on intestinal morphology

MTX-induced changes in small intestinal morphology of WT and Muc2$^{-/-}$ mice were examined on days 2, 3, and 4 after treatment (Fig. 4 A-F). On day 2, both MTX-treated WT and Muc2$^{-/-}$ mice showed affected intestinal morphology (Fig. 4A, B). The degree of intestinal damage increased with time, indicated by severe villus atrophy, epithelial flattening and extensive crypt loss in both WT and Muc2$^{-/-}$ mice by day 3 (Fig. 4C, D). Although the mucosa was still severely damaged on day 4, both groups showed the presence of newly formed crypts (Fig 4E, F). On day 6, the intestinal morphology of the WT mice had started to regenerate as evidenced by higher numbers of well-formed crypts and villi (Fig 4G), and regeneration corresponded with improvement in body-weight. The one surviving Muc2$^{-/-}$ mice by day 6 was not considered representative of the whole group and was therefore excluded from further analyses.

To exclude death by intestinal failure we analyzed the proximal and distal colon segments of both the MTX-treated WT and Muc2$^{-/-}$ mice. Apart from lack of recognizable goblet cells in the crypts of the Muc2$^{-/-}$ mice, the proximal segment showed no distinct changes in morphology (data not shown). In contrast, microscopic analysis of the distal colon of untreated Muc2$^{-/-}$ mice, showed mucosal thickening, increased proliferation and superficial erosions in addition to lack of recognizable goblet cells[14], compared to WT mice (Fig 5 A-B). MTX-treatment did not affect colonic morphology in the WT mice, and the pathology of the Muc2$^{-/-}$ mice did not deteriorate (Fig. 5 C and D, respectively).

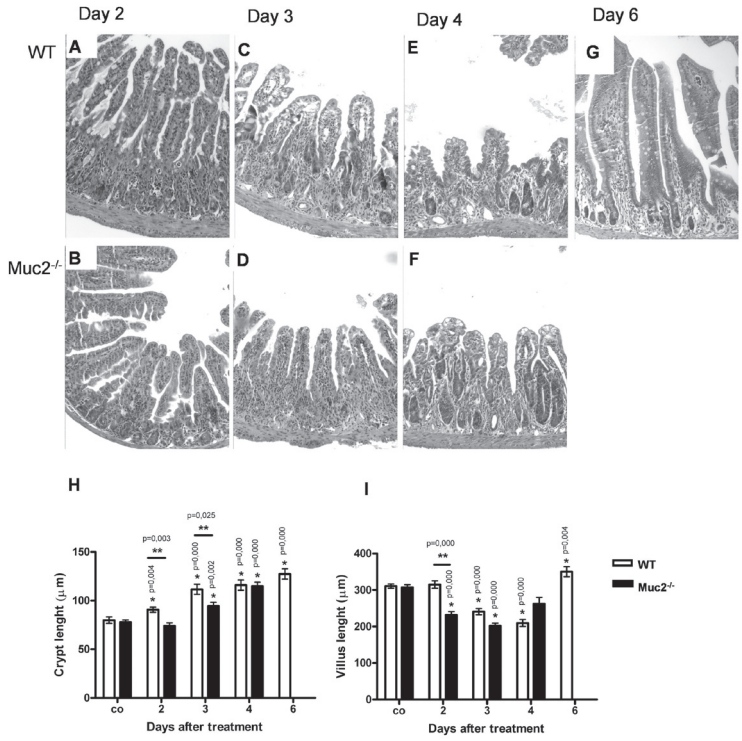

Figure 4. MTX-induced changes in the small intestine in WT and Muc2$^{-/-}$ mice. Morphology of the jejunum of WT (**A,C,E,G**) and Muc2$^{-/-}$ (**B,D,F**) mice on days 2 (**A-B**), 3 (C-D), 4 (E-F) and 6 (G) after MTX-treatment. On day 2, morphology of WT and Muc2$^{-/-}$ mice was mildly affected and characterized by mild crypt loss and epithelial flattening. On days 3 and 4, intestinal damage was more severe, showing increased crypt loss on day 3 and epithelial flattening and villus atrophy on days 3 and 4. Crypt regeneration was seen on day 4, but was more pronounced in the Muc2$^{-/-}$ mice compared to WT mice. On day 6, the intestinal morphology of the WT mice had started to regenerate as evidenced by higher numbers of well-formed crypts and villi. (**H**)Crypt and (**I**) villus lengths of WT and Muc2$^{-/-}$ littermates before and after MTX-treatment. Both groups showed significant villus atrophy and crypt elongation after MTX-treatment. Significant differences were seen on day 2; Muc2$^{-/-}$ mice showed more villus atrophy, but less elongation of crypt length compared to WT mice. On day 3, villus atrophy was comparable in both groups, but still minimal differences were seen in crypt length. In the regenerative phase, day 6, WT mice showed an increase in villus and crypt length compared to control littermates. Bars are expressed in Mean ± SEM. Please also see page 222.

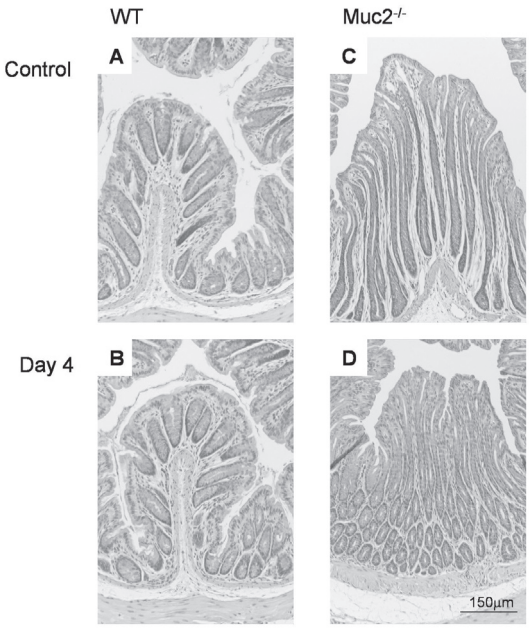

Figure 5. Morphology of the distal colon before and after MTX-treatment. Morphology of the distal colon of (A-B) WT mice and (**C-D**) Muc2$^{-/-}$ mice, untreated (A , C) and day 4 after MTX-treatment (B, D). Untreated Muc2$^{-/-}$ mice showed mucosal thickening and superficial erosions in addition to lack of recognizable goblet cells, compared to WTmice. MTX-treatment did not affect the colonic morphology in the WT mice, and the pathology of the Muc2$^{-/-}$ mice did not deteriorate as determined by the parameters described above.

Crypt and villus length after MTX-treatment

After MTX-treatment crypt length in both WT and Muc2$^{-/-}$ mice progressively increased with time (Fig. 4H). On day 2, WT mice showed a significant increase in crypt length compared to control mice (P=.004). Muc2$^{-/-}$ mice responded similarly one day later. On days 2 and 3, a significant difference (P=.003 and P=.025 respectively) in crypt length was observed between the WT and Muc2$^{-/-}$ mice, with crypts of WT mice longer than those of Muc2$^{-/-}$ mice. However, on day 4, the increase in crypt length was similar in both groups of mice.

In addition, after MTX-treatment a significant villus shortening was observed both in WT mice and in Muc2$^{-/-}$ mice (Fig. 4I). A significant decrease in villus length was seen in Muc2$^{-/-}$ mice on days 2 and 3, and in WT mice on days 3 and 4. Subsequent regeneration of villus length was seen in the Muc2$^{-/-}$ mice on day 4, but in the WT mice not until day 6. MTX-induced changes in villus length between the two types of mice were significantly different on day 2 only (P=.0001).

Effect of MTX-treatment on epithelial proliferation

In WT and Muc2$^{-/-}$ saline-treated (control) mice BrdU-positive cells were seen from the bottom of the crypt up to three quarters of the crypt height, showing no distinct differences in location or number of BrdU positive cells (Fig. 6A, B). On day 2, the proliferative zone in WT mice moved progressively upwards in the crypts towards the crypt-villus junction (Fig. 6 C). At the same time, the proliferative zone in the Muc2$^{-/-}$ mice was only mildly affected, showing a slight shift upwards within the crypts (Fig. 6D). On days 3 and 4, the proliferative zone in both groups had broadened and moved upwards along the crypt-villus axis (Fig. 6E, F showing day 3). Subsequently,

proliferation was quantified by Western blot analysis, using a monoclonal antibody specific for PCNA, a marker for proliferation[21, 22] (Fig. 6G). PCNA expression in the small intestine of the WT mice decreased significantly (P=.01) on day 2 compared to their controls, while the Muc2$^{-/-}$ animals only showed a non-significant decrease. During severe intestinal damage, on days 3 and 4, PCNA expression in both WT and Muc2$^{-/-}$ mice had returned to control levels. On day 6, PCNA expression in the intestine of the WT mice was similar to control level. Overall, PCNA expression levels did not significantly differ between WT and Muc2$^{-/-}$ mice at any time.

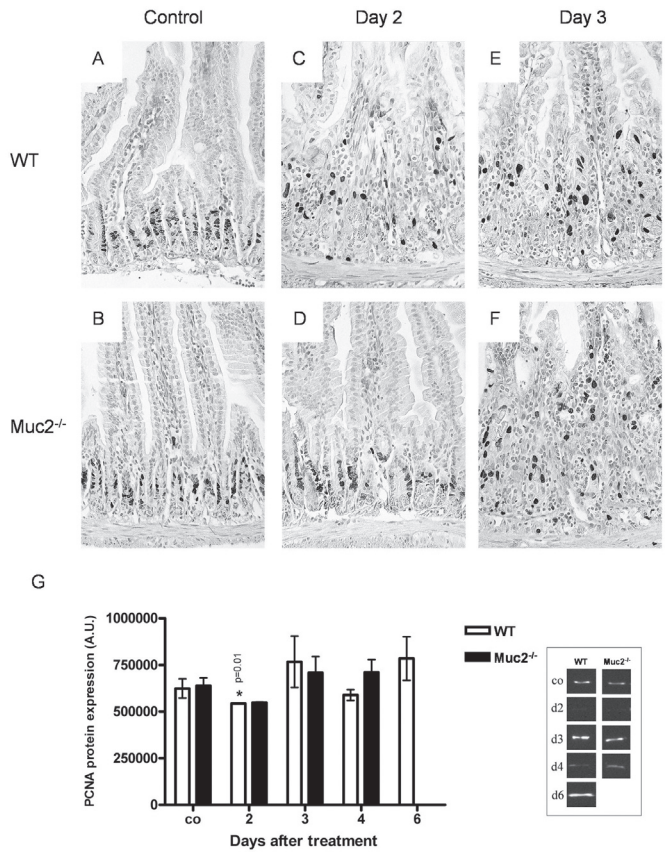

Figure 6. Effect of MTX-treatment on epithelial proliferation . BrdU staining of the jejunum of saline-treated (i.e. control) (A) WT and (B) Muc2$^{-/-}$ mice on day 2 (C-D) and 3 (E-F) after MTX-treatment (BrdU was injected one hour before sacrificing the mice). On day 2, the BrdU positive cells in the Muc2$^{-/-}$ mice were located higher in the crypt. The BrdU positive cells in the WT mice were seen along the entire length of the crypts. A similar pattern was seen in both groups on day 3; BrdU positive cells were not restricted to the crypts and showed a scattered pattern along the entire length of the crypts. (G) Western blot analysis, using a monoclonal antibody specific for PCNA. Representative western blots for each day are shown. The expression of PCNA protein decreased significantly on day 2 in the WT mice. PCNA expression on days 3 and 4 showed mild, non-significant changes in MTX-treated WT and Muc2$^{-/-}$ mice vs. control mice. Bars are expressed in Mean ± SEM.

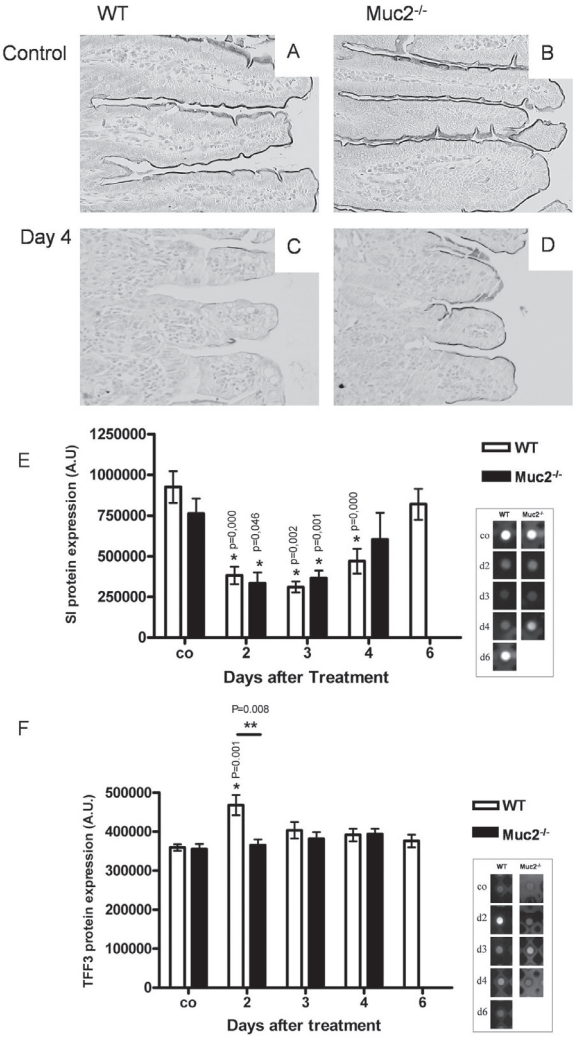

Figure 7. Effect of MTX-treatment on the SI and TFF3 protein expression in the small intestine
Representative sections of SI staining of the small intestine after MTX treatment (A-D). saline-treated (i.e. control) (A) WT and (B) Muc2$^{-/-}$ mice showed a clear SI staining at the brush border along the entire villi. (C) On day 4, SI expression in the WT mice was virtually absent in contrast to (D) the Muc2$^{-/-}$ mice, in which SI expression was partly regenerated and expressed at the tips of the villi. Dot-blot analysis was performed to quantify (E) SI and (F) Tff3 in the small intestine during MTX-treatment. Representative spot blots for each antibody are shown. There was no significant difference in SI and Tff3 expression levels between the Muc2$^{-/-}$ mice and WT controls. SI expression in the MTX-treated WT mice was significantly decreased on days 2, 3 and 4, and returned to control levels on day 6. In contrast, SI expression in Muc2$^{-/-}$ mice was significantly decreased on days 2 and 3 only and showed regeneration on day 4. On day 2, Tff3 expression of the WT mice significantly increased compared to TFF3 expression of the Muc2$^{-/-}$ mice, which maintained at control level. On days 3 and 4, no significant changes were seen in either of the MTX-treated groups. Bars are expressed in Mean + SEM.

Effects of MTX-treatment on enterocyte- and goblet cell-specific protein expression

To gain insight in the functional capacity of the intestinal epithelium after MTX-treatment, we analyzed the expression pattern of SI (Fig. 7A-D). SI is considered a marker for intestinal epithelial differentiation[18,23]. Control Muc2$^{-/-}$ and WT mice showed a clear SI staining at the brush border along the entire villi (Fig. 7A, B). On day 3, during severe mucositis, SI expression was undetectable in the intestine of both WT and Muc2$^{-/-}$ mice (data not shown). However, on day 4, SI expression in Muc2$^{-/-}$ mice had partly regenerated and was detected at the villus tips, in contrast to WT mice (Fig. 7C, D) in which expression of SI was still virtually absent.

SI dot-blot analysis revealed no significant difference in SI expression levels between Muc2$^{-/-}$ and WT control mice (Fig. 7E). SI expression in the MTX-treated WT mice was significantly decreased on days 2, 3 and 4, (P=.0001, P=.002 and P=.0001 respectively) and returned to control levels by day 6, corresponding to the results described for immunohistochemical detection of SI. SI expression in Muc2$^{-/-}$ mice had significantly decreased on days 2 and 3 (P=.046, P=.001 respectively) and was re-established by day 4, in line with the immunohistochemical data.

To quantify Tff3 expression levels, protein dot-blot analyses were performed using a Tff3-specific antibody (Fig. 7F). Interestingly, even though the goblet cells of the Muc2$^{-/-}$ mice showed a distinct change in morphology as detected by the immunohistochemical staining of Tff3 (Fig. 2F), there were no significant differences in Tff3 expression levels between WT and Muc2$^{-/-}$ control mice. On day 2, Tff3 expression increased significantly in MTX-treated WT mice only, compared to WT control mice (P=.001) and MTX-treated Muc2$^{-/-}$ mice (P=.008) and returned to control levels by day 3. In MTX-treated Muc2$^{-/-}$ mice, Tff3 expression levels remained stable at control level throughout the entire experiment.

Release of IL-10 and TNF-α in Muc2$^{-/-}$ intestine prior to MTX-treatment

So far, these data in conjunction suggest Muc2$^{-/-}$ and WT mice have similar intestinal sensitivity to MTX, or even that Muc2$^{-/-}$ mice are less sensitive to MTX-treatment, up to day 4. Absence of Muc2 in Muc2$^{-/-}$ mice may lead to a continuous exposure to luminal antigens, which might have resulted in disbalance in cytokine production prior to MTX-treatment. IELs are one of the first immune cells to encounter antigens that have entered the body via the epithelial surface[24]. Therefore, IELs play an in important in mediating local immune responses in the intestine[24-26]. In order to evaluate two major cytokines involved in anti-inflammatory (IL-10) and pro-inflammatory (TNF-α) responses, we performed quantative real time PCR. Prior to MTX-treatment, Muc2$^{-/-}$ mice showed a non-significant increase in mRNA expression of TNF-α (Fig 8A), but a significant increase (P=.003) in mRNA expression of the anti-inflammatory cytokine IL-10 compared to WT mice (Fig. 8B). The presence of IELs was determined by staining with anti-CD3, which detects both CD4$^+$ and CD8$^+$ T cells. There was an increase of IELs in the Muc2$^{-/-}$ mice before MTX-treatment compared to WT mice (Fig.8C), with a difference at the brink of significance (P=.0571).

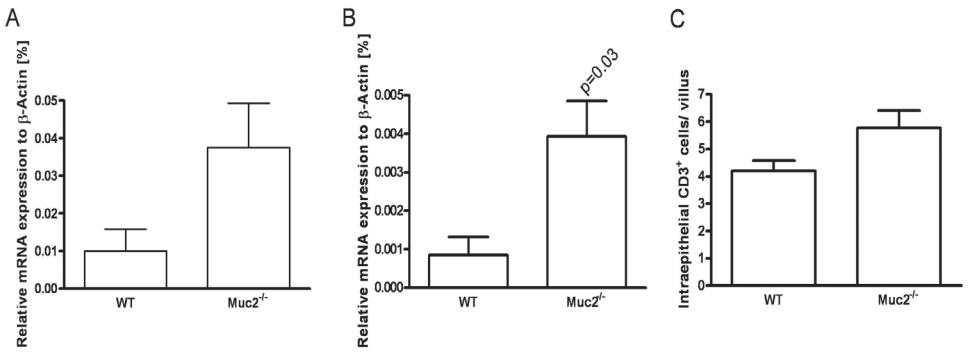

Figure 8. Increased release of IL-10 and TNF-α mRNA in the small intesine of Muc2$^{-/-}$ mice, prior to MTX- treatment. Real time PCR data of (A) TNF-α and (B) IL-10 on RNA isolated from the small intestine of WT and Muc2$^{-/-}$ control, untreated mice. The results were normalized for the housekeeping gene β-actin. The Muc2$^{-/-}$ mice showed a non-significant increase in mRNA expression of TNF-α, but a significant increase in mRNA expression of the anti-inflammatory cytokine IL-10 compared to WT. (C) Quantification of CD3^{+} IELs in the villi of both types of mice Control, untreated Muc2$^{-/-}$ mice showed an increase in IELs compared to WT mice, which was at the brink of significance (p=0.0571) Bars are expressed in Mean + SEM.

Discussion

We addressed the question whether Muc2 is involved in epithelial protection against chemotherapy-induced mucositis in the small intestine by challenging Muc2 deficient mice with the cytostatic drug MTX. As chemotherapy increases the permeability of the intestinal epithelium, we hypothesized that the deficiency of Muc2, and resultant major changes of the mucus layer, would sensitize the intestine to chemotherapy-induced damage.

The Muc2$^{-/-}$ mice weighed significantly less than the WT mice and showed growth retardation. In addition, they showed diarrhea, occult blood loss and even occasional gross bleeding, caused by a distinct pathology in the distal colon[14]. We cannot explain the significant difference in weight at an early age, especially as there was no difference in birth-weight (our unpublished data). There is no indication that the small intestine contributes to any of the described symptoms above, as histological analysis showed no distinct pathology. The only telling difference between the WT and the Muc2$^{-/-}$ mice was the lack of recognizable goblet cells in the Muc2$^{-/-}$ mice, in line with findings from previous studies[13, 14, 27]. Quantification of Tff3 and SI, important markers of the functionality of goblet cells and enterocytes, respectively, showed no difference in expression levels in the small intestine between WT and Muc2$^{-/-}$ mice. Neither did crypt and villus lengths differ between the Muc2$^{-/-}$ and WT mice. Taken together, these data suggest that under unchallenged conditions, Muc2 is not essential for normal epithelial morphology and function in the small intestine. However, this hypothesis is undermined by the fact that the Muc2$^{-/-}$ mice showed significant growth retardation.

Mucositis was induced in WT and Muc2$^{-/-}$ animals by injecting MTX. Up to day 3 there were no differences in percentage of weight-loss compared to initial body-

weights between WT and Muc2$^{-/-}$ mice. Thereafter, however, WT mice showed a trend towards regaining their initial body-weights, whereas Muc2$^{-/-}$ mice continued to lose weight, which may have led to the death of three of four mice on day 5. The intestine of the Muc2$^{-/-}$ mice already had started to regenerate on day 4, as indicated by an earlier regeneration of crypts, restoration of villus length (on day 4) and restoration of enterocyte-specific SI levels in Muc2$^{-/-}$ mice compared to WT mice. Furthermore, the proliferative zone in the Muc2$^{-/-}$ mice seemed to be less affected by MTX-treatment compared to that in WT mice. These results are contradictive to our hypothesis, and do not explain why the mice died during the experiment. We therefore have no indication that death of the Muc2$^{-/-}$ animals could be caused by intestinal failure. This is supported by data showing that the pathology of the distal colon of the Muc2$^{-/-}$ mice did not deteriorate during MTX-treatment, and by the fact that clinical symptoms such as diarrhea and occult blood loss did not aggravate. Since the Muc2$^{-/-}$ mice were significantly lighter than the WT mice before MTX treatment, the same percentage of weight-loss after MTX could have had a bigger impact on the Muc2$^{-/-}$ mice and resulting in the sudden death of these mice. We have now learned, from continuing experiments, that lighter WT mice are also predisposed to death during MTX treatment compared to heavier littermates (B.A.E. de Koning, unpublished observations).

Mucositis is the result of a dynamic cascade of events, in which the release of pro-inflammatory cytokines, activated by transcription-factors and invading bacteria, plays an important role[28]. Mucositis toxicity is correlated with the release of the pro-inflammatory cytokine TNF-α, which is involved in intestinal damage induction[28-31]. Furthermore, TNF-α was shown to play a pivotal role in the pathogenesis of inflammatory bowel disease[32,33]. In contrast, the anti-inflammatory cytokine IL-10, has protective capacities in the intestine, and studies have shown that IL-10$^{-/-}$ mice are predisposed to develop chronic mucosal inflammation[34-36]. As described previously, local expression of (anti-)inflammatory cytokines might to be able to modulate local immune responses[25]. Local immune responses are mediated by e.g. the IELs[24]. IELs are instrumental in mediating tolerance and driving immune regulation and could be activated in the Muc2$^{-/-}$ mice by an increased stimulation caused by the absence of Muc2, the structural component of the mucus layer. Our data reveal a trend towards increased numbers of IELs present in the villi of the Muc2$^{-/-}$ mice before MTX-treatment. Apart from IELs, we also investigated IL-10 and TNF-α production in the intestine of Muc2$^{-/-}$ mice prior to MTX-treatment. Untreated Muc2$^{-/-}$ mice showed a non-significant increase in TNF-α mRNA levels, but a significant increase in IL10 mRNA levels compared to WT mice. These data suggest an opposite TNF-α release in which IL-10 restricts the damage-inducing capacity of TNF-α under unchallenged condition (i.e. not treated with MTX) in the small intestine of Muc2$^{-/-}$ mice. Further support for this hypothesis is the observation that IL-10$^{-/-}$ mice develop more severe mucositis after MTX-treatment than their IL-10$^{+/+}$ littermates and that IELs from IL-10$^{-/-}$ mice were unable to control Th1-induced gut inflammation[24, 37]. Thus, Muc2 deficiency may have led to an altered immune-response prior to MTX challenge. This might explain why the MTX-induced damage was similar, or even less severe in the Muc2$^{-/-}$ mice. This mechanism however, needs further investigation.

In conclusion, our data do not provide evidence that Muc2 deficiency leads

to an increase in chemotherapy-induced mucositis. A possible explanation is the mechanism by which Muc2 deficiency triggers the immune system to release IL-10, an anti-inflammatory cytokine, prior to MTX-treatment.

Acknowledgements
Numico Research BV, Wageningen, the Sophia Foundation for Scientific Research, Rotterdam, The Foundation "De Drie Lichten", Leiden and The Netherlands Organization for Scientific Research, The Hague, all situated in the Netherlands are gratefully acknowledged for their financial support. We would like to thank A.C.J.M de Bruijn for his excellent technical assistance. Y. Simons-Oosterhuis is gratefully acknowledged for the careful design and validation of the IL-10 primers. We thank J. Hagoort for an excellent review of this manuscript. The current address of A.W.C. Einerhand is Lipid Nutrition, Loders Croklaan, Wormerveer, the Netherlands.

References

1. Duncan M, Grant G. Oral and intestinal mucositis - causes and possible treatments. Aliment Pharmacol Ther 2003;18:853-74.
2. Elting LS, Cooksley C, Chambers M, Cantor SB, Manzullo E, Rubenstein EB. The burdens of cancer therapy. Clinical and economic outcomes of chemotherapy-induced mucositis. Cancer 2003;98:1531-9.
3. Ruescher TJ, Sodeifi A, Scrivani SJ, Kaban LB, Sonis ST. The impact of mucositis on alpha-hemolytic streptococcal infection in patients undergoing autologous bone marrow transplantation for hematologic malignancies. Cancer 1998;82:2275-81.
4. McGuire DB. Mucosal tissue injury in cancer therapy. More than muscositis and mouthwash. Cancer Pract 2002;10:179-91.
5. Sonis ST, Elting LS, Keefe D, Peterson DE, Schubert M, Hauer-Jensen M, Bekele BN, Raber-Durlacher J, Donnelly JP, Rubenstein EB. Perspectives on cancer therapy-induced mucosal injury: pathogenesis, measurement, epidemiology, and consequences for patients. Cancer 2004;100:1995-2025.
6. Forstner JF, GG. gastrointestinal mucus. Raven, 1994.
7. Hecht G. Innate mechanisms of epithelial host defense: spotlight on intestine. Am J Physiol 1999;277:C351-8.
8. Strous GJ, Dekker J. Mucin-type glycoproteins. Crit Rev Biochem Mol Biol 1992;27:57-92.
9. Van Klinken BJ, Dekker J, Büller HA, de Bolos C, Einerhand AW. Biosynthesis of mucins (MUC2-6) along the longitudinal axis of the human gastrointestinal tract. Am J Physiol 1997;273:G296-302.
10. Tytgat KM, Büller HA, Opdam FJ, Kim YS, Einerhand AW, Dekker J. Biosynthesis of human colonic mucin: Muc2 is the prominent secretory mucin. Gastroenterology 1994;107:1352-63.
11. Verburg M, Renes IB, Van Nispen DJ, Ferdinandusse S, Jorritsma M, Büller HA, Einerhand AW, Dekker J. Specific responses in rat small intestinal epithelial mRNA expression and protein levels during chemotherapeutic damage and regeneration. J Histochem Cytochem 2002;50:1525-36.
12. Verburg M, Renes IB, Meijer HP, Taminiau JA, Büller HA, Einerhand AW, Dekker J. Selective sparing of goblet cells and paneth cells in the intestine of methotrexate-treated rats. Am J Physiol Gastrointest Liver Physiol 2000;279:G1037-47.
13. Velcich A, Yang W, Heyer J, Fragale A, Nicholas C, Viani S, Kucherlapati R, Lipkin M, Yang K, Augenlicht L. Colorectal cancer in mice genetically deficient in the mucin Muc2. Science 2002;295:1726-1729.
14. van der Sluis M, de Koning BAE, de Bruijn ACJM, Velcich A, Meijerink JPP, van Goudoever JB, Büller HA, Dekker J, van Seuningen I, Renes IB, Einerhand AWC. Muc2-deficient mice spontaneously develop colitis, indicating that Muc2 is critical for colonic protection. Gastroenterology 2006;131:117-129.
15. Wahba N. An ortho-tolidine hydrochloride test for the detection of occult blood in faeces without dietary restrictions. J Clin Pathol 1965;18:687-688.
16. Renes IB, Verburg M, Van Nispen DJ, Taminiau JA, Büller HA, Dekker J, Einerhand AW. Epithelial proliferation, cell death, and gene expression in experimental colitis: alterations in carbonic anhydrase I, mucin MUC2, and trefoil factor 3 expression. Int J Colorectal Dis 2002;17:317-26.
17. Mashimo H, Wu DC, Podolsky DK, Fishman MC. Impaired defense of intestinal mucosa in mice lacking intestinal trefoil factor. Science 1996;274:262-265.

18. Yeh KY, Yeh M, Montgomery RK, Grand RJ, Holt PR. Cortisone and thyroxine modulate intestinal lactase and sucrase mRNA levels and activities in the suckling rat. Biochem Biophys Res Commun 1991;180:174-80.
19. Dignass A, Lynch-Devaney K, Kindon H, Thim L, Podolsky DK. Trefoil peptides promote epithelial migration through a transforming growth factor beta-independent pathway. J Clin Invest 1994;94:376-83.
20. Mashimo H, Wu DC, Podolsky DK, Fishman MC. Impaired defense of intestinal mucosa in mice lacking intestinal trefoil factor. Science 1996;274:262-5.
21. Theon AP, Metzger L, Griffey S. In situ analysis of cellular proliferation in canine, feline and equine tumors by immunohistochemistry: a comparison of bromodeoxyuridine, proliferating cell nuclear antigen, and interchromatin-associated antigen immunostaining techniques. J Vet Diagn Invest 1994;6:453-7.
22. Bromley M, Rew D, Becciolini A, Balzi M, Chadwick C, Hewitt D, Li YQ, Potten CS. A comparison of proliferation markers (BrdUrd, Ki-67, PCNA) determined at each cell position in the crypts of normal human colonic mucosa. Eur J Histochem 1996;40:89-100.
23. Van Beers EH, Büller HA, Grand RJ, Einerhand AW, Dekker J. Intestinal brush border glycohydrolases: structure, function, and development. Crit Rev Biochem Mol Biol 1995;30:197-262.
24. Cheroutre H. IELs: enforcing law and order in the court of the intestinal epithelium. Immunol Rev 2005;206:114-31.
25. De Winter H, Elewaut D, Turovskaya O, Huflejt M, Shimeld C, Hagenbaugh A, Binder S, Takahashi I, Kronenberg M, Cheroutre H. Regulation of mucosal immune responses by recombinant interleukin 10 produced by intestinal epithelial cells in mice. Gastroenterology 2002;122:1829-41.
26. Chen Y, Chou K, Fuchs E, Havran WL, Boismenu R. Protection of the intestinal mucosa by intraepithelial gamma delta T cells. Proc Natl Acad Sci U S A 2002;99:14338-43.
27. Yang W, Velcich A, Lozonschi I, Liang J, Nicholas C, Zhuang M, Bancroft L, Augenlicht LH. Inactivation of p21WAF1/cip1 enhances intestinal tumor formation in Muc2-/- mice. Am J Pathol 2005;166:1239-46.
28. Sonis ST. The pathobiology of mucositis. Nat Rev Cancer 2004;4:277-84.
29. Hall PD, Benko H, Hogan KR, Stuart RK. The influence of serum tumor necrosis factor-alpha and interleukin-6 concentrations on nonhematologic toxicity and hematologic recovery in patients with acute myelogenous leukemia. Exp Hematol 1995;23:1256-60.
30. Abreu-Martin MT, Vidrich A, Lynch DH, Targan SR. Divergent induction of apoptosis and IL-8 secretion in HT-29 cells in response to TNF-alpha and ligation of Fas antigen. J Immunol 1995;155:4147-54.
31. Guy-Grand D, DiSanto JP, Henchoz P, Malassis-Seris M, Vassalli P. Small bowel enteropathy: role of intraepithelial lymphocytes and of cytokines (IL-12, IFN-gamma, TNF) in the induction of epithelial cell death and renewal. Eur J Immunol 1998;28:730-44.
32. Bouma G, Strober W. The immunological and genetic basis of inflammatory bowel disease. Nat Rev Immunol 2003;3:521-533.
33. Strober W, Fuss IJ, Blumberg RS. The immunology of mucosal models of inflammation. Annu Rev Immunol 2002;20:495-549.
34. Kuhn R, Lohler J, Rennick D, Rajewsky K, Muller W. Interleukin-10-deficient mice develop chronic enterocolitis. Cell 1993;75:263-74.
35. Sellon RK, Tonkonogy S, Schultz M, Dieleman LA, Grenther W, Balish E, Rennick DM, Sartor RB. Resident enteric bacteria are necessary for development of spontaneous colitis and

immune system activation in interleukin-10-deficient mice. Infect Immun 1998;66:5224-31.

36. Löhler J, Kühn R, Rennick D, Rajewsky K, Müller W. Interleukin-10-deficient mice: a model of chronic mucosal inflammation. In: Tytgat GNJ, Bartelsman MFWM, van Deventer SJH, eds. Inflammatory Bowel Diseases. Dordrecht: Kluwer Academic Publishers, 1995:410-417.

37. de Koning BA, van Dieren JM, Lindenbergh-Kortleve DJ, van der Sluis M, Matsumoto T, Yamaguchi K, Einerhand AW, Samsom JN, Pieters R, Nieuwenhuis EE. Contributions of mucosal immune cells to methotrexate-induced mucositis. Int Immunol 2006;18:941-9.

Chapter 6

Threonine Metabolism in the Intestine of Mice

Maaike.W. Schaart*, Maria van der Sluis*, Barbara .A.E. de Koning, Henk Schierbeek, Anna Velcich[2], Ingrid B. Renes and Johannes B. van Goudoever. *Dietary threonine metabolism in the intestine of wild type and mucin 2 deficient mice.*
* Both authors participated equally in this study

Manuscript submitted

Abstract

Mucin 2 (Muc2) is the major secretory mucin of the mucus layer that lines the intestinal epithelium. Muc2 is characterized by tandem repeats rich in threonine-proline-serine. Since, previous studies in piglets showed that the intestine utilizes 60-90% of dietary threonine intake, we compared threonine utilization in the intestines of Muc2 knockout ($Muc2^{-/-}$) and wild type (WT) mice to investigate whether dietary threonine is mainly used for intestinal Muc2 synthesis. Concentrations and isotopic enrichment of threonine were measured by GC-(IR)MS in the small intestine, colon and colonic content of mice given a [U-^{13}C]threonine bolus enterally. In the intestinal tract, 40.1% of dietary [^{13}C]threonine was recovered after 6 hours in WT mice – i.e. 32.4% as [^{13}C]threonine and 8.3% as [^{13}C]glycine vs. 43.6% in $Muc2^{-/-}$ mice – i.e. 33.1% [^{13}C] as threonine and 9.5% as [^{13}C]glycine. Most of the dietary [^{13}C]threonine recovered from the intestinal tract was derived from the colonic content in both types of mice. Interestingly, 27.4% of the recovered [^{13}C]threonine in the colonic content of WT mice was incorporated into Muc2. Overall, $Muc2^{-/-}$ mice showed higher amounts of incorporated [^{13}C]threonine into mucosal proteins. Furthermore the entire intestine of $Muc2^{-/-}$ mice showed a significantly higher oxidation rate compared to WT mice. Conclusions: This is the first study demonstrating threonine utilization in mice. In absence of Muc2, dietary threonine is used for constitutive protein synthesis or is metabolically oxidized as shown in $Muc2^{-/-}$ mice. However, one of the pivotal metabolic fates of dietary threonine utilized by the intestine is incorporation into Muc2

Abbreviations used in this paper

h, hour(s); MPE, Mole percent excess; Muc2, Mucin 2; $Muc2^{-/-}$, Mucin 2 knockout mice; WT, wild-type mice; NS, non significant; TDG, threonine dehydrogenase; TDH, threonine dehydratase; PCA, perchloric acid

Introduction

The gastrointestinal tract is lined by a mucus layer – a protective barrier between the epithelium and environment. Mucus production, and thus the mucus layer, is alerted by intestinal stress, *i.e.* inflammatory bowel disease[1] and its integrity has been associated with nutritional state[2-5]. Mucins represent the principal protein constituent of mucus, and Muc2 is the predominant gastrointestinal mucin[6, 7]. Mucins have a central backbone rich in threonine, proline and serine residues that account for 20-55% of total amino acid composition[8]. A characteristic feature is the high density of oligosaccharides *O*-linked to threonine and/or serine residues in the central protein backbone resulting in a high resistance to proteolysis[9].

Animal studies have indicated substantial amino acid metabolism in the intestine[10]. Amino acids are quantitatively important nutrients for growth and development, essential in protein synthesis and obligatory for maintaining intestinal mass and integrity. Studies in piglets showed high intestinal utilization of essential amino acids in first pass. For example, first pass metabolism of lysine and leucine accounts for approximately one-third of total dietary intake[11-15]. The human intestine retains between 20-50% of the dietary intake of specific essential amino acids including threonine, one of the indispensable amino acids[16-19]. Recently we demonstrated that in piglets between 80-90% of dietary threonine is utilized by the intestine[20]. Interestingly, additional data demonstrated a 60% reduction in whole-body threonine requirements in piglets receiving total parenteral nutrition, compared to orally fed control animals[21]. In this context, intestinal demand for dietary threonine probably results from its incorporation into secretory mucins rich in threonine residues. Further support for this hypothesis is a study showing that specific restriction of dietary threonine impaired intestinal mucin synthesis[22]. We therefore hypothesized that the major metabolic fate of dietary threonine is incorporation into intestinal mucins, specifically Muc2. To directly investigate whether dietary threonine is utilized in Muc2 synthesis, we compared [^{13}C]threonine enrichment in the small intestine, colon and faecal proteins of Muc2 deficient mice (Muc2$^{-/-}$), which do not synthesize the Muc2 mucin[23, 24] to that of wild type (WT) mice. Threonine enrichment was also measured in stomach content and in serum to evaluate the whole gastrointestinal tract and systemic availability of dietary threonine.

Once taken up by the mucosal cells, threonine may have different metabolic fates, including oxidation. Threonine is catabolized either by threonine dehydratase (TDH) to NH_4^+ and 2-ketobutyrate, which is irreversibly converted to CO_2, or by threonine dehydrogenase (TDG) to form 2-amino-3-ketobutyrate, which is mainly converted to glycine and acetyl-CoA[25]. In piglets and rats, the TDG pathway accounts for 80% of threonine oxidation[25,26]. If absorbed dietary threonine is not used for intestinal protein synthesis, its metabolic fate might be oxidation. Second, we additionally measured intestinal [^{13}C]glycine amounts in WT and Muc2$^{-/-}$ mice.
Thus, by studying threonine metabolism in Muc2$^{-/-}$ mice and WT mice, we gained insight into intestinal threonine metabolism, and specifically into the role of dietary threonine in intestinal Muc2 synthesis.

Materials and Methods

Animals

8-week-old, female, previously described Muc2$^{-/-}$ mice[24] and corresponding WT littermates were housed in the same specific pathogen-free environment; animal care and procedures were in compliance with Erasmus MC - Animal Ethics Committee guidelines.

Experimental setup

Mice (n=17, for both groups) were weighed and fasted 2 hours (h) prior to receiving a threonine gavage, but had free access to drinking water. They received 2.1 μmol [U-^{13}C]threonine/g body weight (Sigma, St. Louis, USA) orally, based on i) average normal daily food intake (3 g/d) for female inbred strains[27], ii) threonine composition of mouse chow (0.69% (w/w) threonine; 0.50% was used to calculate the definitive threonine amount, as not to overload the gastrointestinal tract) provided by Special Diets Services (Witham, Essex, UK) and iii) corrected for the total 6h time span of the experiment[28]. Similarly, control mice (n=2, for both Muc2$^{-/-}$ and WT mice) received an oral gavage of PBS. After the threonine gavage the mice had free access to standard rodent pellets (Special Diets Services). However, the experiment was initiated in the early morning to simulate normal feeding routine (normal daily intake during the night, and little to no food intake during the day as to minimize dilution of the [U-^{13}C]threonine). The mice were sacrificed by CO_2 inhalation 1, 3 or 6 h (n=5, per genotype, at each time point) after threonine administration. Blood was collected via heart puncture. Plasma was separated from whole blood by centrifugation (3000*g* for 5 min) and kept at -80°C until further analysis. Subsequently, the stomach, small intestine and colon were rapidly removed. The small intestine was halved into duodenum-jejunum and jejunum-ileum segments, referred to as proximal small intestine and distal small intestine, respectively. Both segments were opened longitudinally, thoroughly washed in PBS, weighed, snap frozen in liquid nitrogen and stored at -80°C until protein concentration and tracer enrichment analysis. Both the colon and stomach were opened longitudinally, the contents were removed, weighed, and snap frozen in liquid nitrogen and stored at -80°C.

The same procedure as described for the small intestine was applied to the colon.

Mass spectrometry

Tissue sample preparation

Intestinal tissue samples were homogenized in water (100 mg/ml) and the faecal samples were homogenized by adding water, ratio 2:1. Total protein concentrations were measured using the Bicinchoninic Acid Protein Assay Reagent (Pierce, Rockford, IL, USA). The protein fraction was precipitated by adding 0.5 ml of 2.0 mol/l perchloric acid (PCA) to an aliquot (500μl) of homogenized tissue sample and subsequent centrifugation at 2500g and 4ºC for 20 min. The supernatant was collected for each individual sample. Pellets were washed three times by adding 4 ml of 0.2 mol/l PCA followed by centrifugation. The washing fluids from each sample

were collected and combined with the corresponding supernatant. Excess PCA was neutralized by adding KOH (4 mol/l), followed by brief centrifugation. To be able to determine the concentrations of either free [^{13}C]threonine and [^{13}C]glycine, 20 µl of internal standard (1 mg/ml Norvaline) was added to each sample. Also a standard sample of Norvaline and a known amount of threonine/ or glycine was used to determine the response factor for threonine or glycine, respectively. Subsequently, this factor was used for determination of threonine and glycine concentrations in the samples. These samples were then dried under a nitrogen stream and stored. Twenty microlitre internal standard (1 mg/ml Norvaline) was added to each washed pellet to be able to determine the concentrations of incorporated [^{13}C]threonine and [^{13}C]glycine. Subsequently the pellets were hydrolyzed by adding 0.5 ml of 6 mol/l HCl and incubating at 110°C in sealed tubes for 24h. The protein hydrolyzates were dried under nitrogen at 55°C and the residue was dissolved in 0.5 ml water. Amino acids were isolated from protein hydrolyzates and supernatant by cation exchange separation as described previously[20]. Amino acids were eluted with 3 ml 6M NH_4OH and dried under nitrogen at 30°C[20]. Samples were derivatized with ethyl chloroformiate and threonine was converted to its *N*-ethoxycarbonylethylester derivative by a method described in our previous work[20].

Analysis of tissue samples, stomach and colonic content

[^{13}C]Threonine and [^{13}C]glycine enrichments in the different organs were measured by a Thermo Electron Delta-XP isotope ratio MS (Bremen, Germany) coupled online with a trace GC (Thermo Electron, Breda, the Netherlands) and a combustion interface type 3 (Thermo Electron) which was used for [^{13}C/^{12}C]ratio measurement of both threonine and glycine. Aliquots of 1 µl of the chloroform suspension containing the amino acid derivatives were introduced into the GC system by a CTC PAL autosampler (CTC Switzerland). Chromatographic conditions were as described previously. After separation using capillary GC, amino acids were combusted online at 940°C and introduced as CO_2 into the isotope ratio MS, where the [^{13}C/^{12}C]ratio was measured for both threonine and glycine. The atom percent enrichment was converted to mole percent threonine or glycine enrichment, after accounting for the 2.75-fold or 3.5-fold dilution of carbon in the derivative, respectively, and the measured [^{13}C]abundance (98%) of the threonine tracer**.** The enrichment was expressed as mole percent excess (MPE).

Preparation and analysis of blood samples

Small aliquots of plasma (20 µl) were prepared to determine threonine enrichment and concentration by gas chromatography-mass spectrometry (GC-MS). Briefly, 20µl of internal standard (1 mg/ml Norvaline) was added to 20 µl plasma and deproteinized with sulfocalisylicacid 6%. After centrifugation for 10 min at 4°C and 1000g, the amino acids in the supernatant were isolated by cation exchange separation as described above. The eluate was dried overnight at 30ºC under nitrogen. Residues were resuspended by adding 200 µl dichloromethane, and subsequently dried under nitrogen for 1h at 35ºC. Finally t-butyldimethylsilyl derivates were formed by adding 25 µl of dimethyl-formamide and 25 µl of N-methyl-N-(tert-butyldimethylsilyl)-trifluoroacetamide to the dried residue and heating at 60°C for 1h.

Standard curves were prepared by mixing aqueous solutions of natural and labelled threonine for both enrichment and concentration determination. GC-MS analyses were performed on a Carlo Erba GC8000 gas chromatograph coupled to a Fisons MD-800 mass spectrometer (Interscience BV, Breda, the Netherlands). One microliter of the derivative was analyzed in split mode (1:20) on a DB-17, 30m x 0.25mm capillary column (Agilent, Amstelveen, the Netherlands). Selective ion monitoring was carried out at m/z 404.3, 405.3 and 408.3. The enrichment was MPE.

Calculations

Basal [^{13}C]threonine and [^{13}C]glycine enrichments were determined in each tissue of the control (PBS) mice. These enrichments were subtracted from the [^{13}C]enrichments measured in the experimental animals.
Total [^{13}C]threonine amount in each tissue (µmol) was calculated as follows:

(Threonine enrichment (MPE)/100) * Conc. Threonine $_{tissue}$ (µmol/g) * (weight) $_{tissue}$

Subsequently, for each individual mouse threonine amount was expressed as percentage of total threonine administered enterally. An equivalent calculation was used to determine total [^{13}C]glycine in each tissue sample.

Statistics

Data are presented as mean plus the inter-animal standard error of the mean (SEM). Differences in [^{13}C]threonine (free and incorporated into proteins) for each animal group over time were assessed using ANOVA. Differences in protein levels and [^{13}C]threonine and [^{13}C]glycine (free and incorporated) between the Muc2$^{-/-}$ and WT mice at each time point were evaluated using the Mann-Whitney test (two-tailed). $P<.05$ was considered to indicate statistical significance.

Results

Dietary [^{13}C]threonine distribution

The total [^{13}C]amount recovered consisting of [^{13}C]threonine and [^{13}C]glycine was expressed as percentage of total dietary [^{13}C]threonine intake. The total [^{13}C]amount recovered in the gastrointestinal organs and serum increased with time after threonine administration in both mice types (Fig. 1A). Figure 1B shows that total amounts of free [^{13}C]threonine recovered increased significantly from 4.7% at 1h to 10.1% at 6h after administration in Muc2$^{-/-}$ mice, but not in WT mice. Total amounts of recovered bound [^{13}C]threonine significantly increased in both mice types. Figure 1C shows the distribution of dietary [^{13}C]threonine 6h after [^{13}C]threonine administration. The free amounts of [^{13}C]threonine in the stomach content could not be included in our analysis since they exceeded the maximum measurable amount (41% MPE).

Stomach content

Incorporated [^{13}C]threonine levels in the stomach content decreased with time in both mice types ((WT: 13.9% at 1h vs. 3.6% at 6h, not significant (NS) and (Muc2$^{-/-}$: 6.4% at 1h vs. 2.3% at 6h, NS)). Threonine incorporation did not differ between mice types.

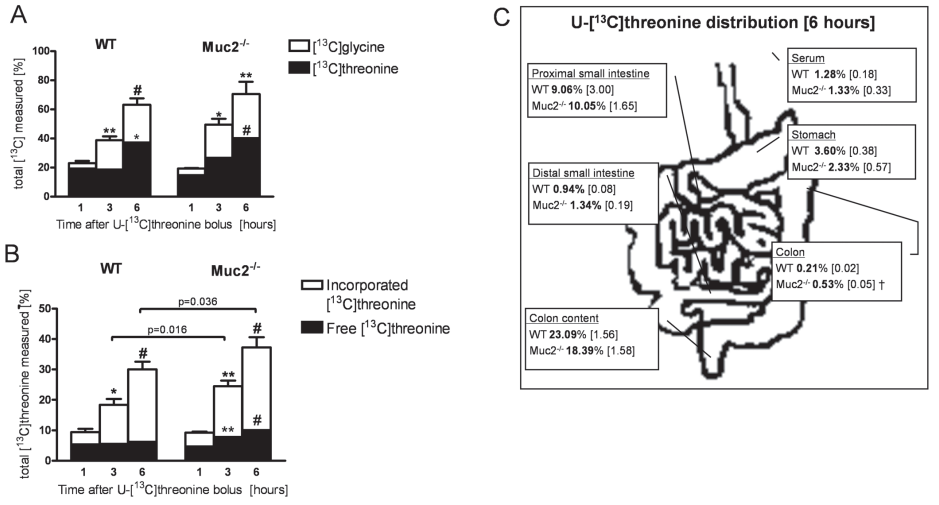

Figure 1. Dietary threonine distribution and recovery. (A) Total [^{13}C] (threonine+glycine) recovered in the tissues sampled *(free and incorporated threonine and glycine in serum, proximal and distal small intestine, colon and colonic content and incorporated threonine and glycine in the stomach)* expressed as percentage of threonine administered during time (hatched bars) [^{13}C]Glycine; (stippled bars) [^{13}C]Threonine; (B) The total amount of free and incorporated [^{13}C]threonine in the tissues sampled. The amounts of free [^{13}C]threonine recovered, increased significantly at 1 h to 6 h after administration in the Muc2$^{-/-}$ mice and was significantly higher at 3 and 6 h compared to the WT mice. The total amount of recovered bound [^{13}C]threonine, significantly increased in both types of mice. (C) The distribution of dietary threonine at 6 hours expressed as percentage of threonine administered. The values represent the sum of free and incorporated threonine in the tissues samples, with exception of the stomach (free [^{13}C] dietary threonine not determinable). Error bars indicate the standard error of mean. All significancies 1 h vs. 3 or 6 hours (* P<.05; †P=.016; **P<.01; # P=.001).

Small intestine

Total protein amounts in the distal small intestine significantly exceeded those in the proximal small intestine (P<.001, Muc2$^{-/-}$ and WT mice, Fig. 2A,D), and did not differ between mice types.

Free [^{13}C]threonine in the proximal small intestine decreased significantly between 1 and 6h after threonine gavage in WT mice, but not in Muc2$^{-/-}$ mice, which showed only a transient decrease of free [^{13}C]threonine at 3h post threonine delivery (Fig. 2B). Incorporated [^{13}C]threonine in the proximal small intestine significantly increased with time in both mice types, but did not significantly differ between types at any time point analyzed (Fig. 2E).

At all time points, free [^{13}C]threonine percentage in the distal small intestine was significantly lower (P<.03) than that in the proximal small intestine in both mice types. In contrast to the proximal part (Fig. 2C), a lower amount of [^{13}C]threonine was incorporated into proteins of the distal small intestine (Fig. 2F). However, threonine incorporation into intestinal proteins significantly increased after the threonine gavage. One hour after enteral threonine, the Muc2$^{-/-}$ mice showed significantly higher threonine incorporation into intestinal proteins compared to WT mice. This difference leveled off at later time points.

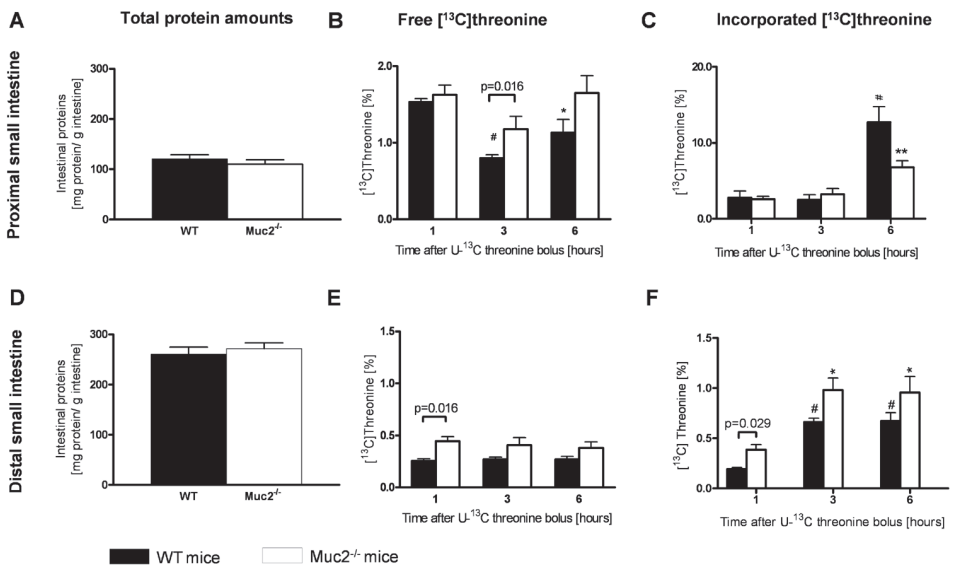

Figure 2. The protein content and threonine metabolism in the small intestine. (A, D) total protein amounts in the proximal and distal small intestine in WT and Muc2$^{-/-}$ mice. (B, E) The free [^{13}C]threonine in the proximal small intestine decreased during time in the WT mice and remained stable in the Muc2$^{-/-}$ and was significantly higher 3 hours after the threonine gavage. The free [^{13}C]threonine in the distal small intestine remained stable during the experimental period and was significantly higher in the Muc2$^{-/-}$ mice at 1 hour after threonine administration [P=.016 1h, Muc2$^{-/-}$ mice vs WT]. (C, F) The incorporated [^{13}C]threonine in proximal small intestine increased during time. The incorporated [^{13}C]threonine in the distal small intestine also increased during time. The Muc2$^{-/-}$ mice showed a trend towards higher [^{13}C]threonine incorporation which was significantly higher after 1h of threonine administration compared to the WT mice. Error bars indicate the standard error of mean. All significancies 1 h vs. 3 or 6 hours *P<.05; **P<.01, #P<.001.

Colon

Total protein concentration in the colon of Muc2$^{-/-}$ mice was modestly but consistently higher than in WT mice (Fig. 3A). The pool of free [^{13}C]threonine in colonic tissue was significantly higher in Muc2$^{-/-}$ mice throughout the experiment and its levels significantly declined over time in both mice types. However, kinetics in WT mice were faster compared to Muc2$^{-/-}$ mice. Incorporated [^{13}C]threonine levels in the colon increased significantly over time and were significantly lower in WT mice at all time points.

Colonic content

WT mice faeces had a significantly higher protein content than those of Muc2$^{-/-}$ mice (WT: 59.2 mg/g and Muc2$^{-/-}$: 50.8 mg/g, P=.022), as shown in Figure 3D.
Free [^{13}C]threonine in colonic content increased with time in both mice types without significant differences between types. Furthermore, levels of incorporated [^{13}C]threonine into the proteins of the colonic content increased significantly over time in both mice types. [^{13}C]threonine incorporation in proteins of colonic content of WT mice at 6h was consistently higher, yet these differences were not statistically

significant. Interestingly, taking into consideration that Muc2 is the principal constituent of the intestinal mucus, we suggest that the difference (27.4%) in [^{13}C]threonine incorporated in proteins of the colonic content of WT and Muc2$^{-/-}$ mice is attributable to the presence of Muc2 mucin in the faeces of WT mice at 6h after threonine intake.

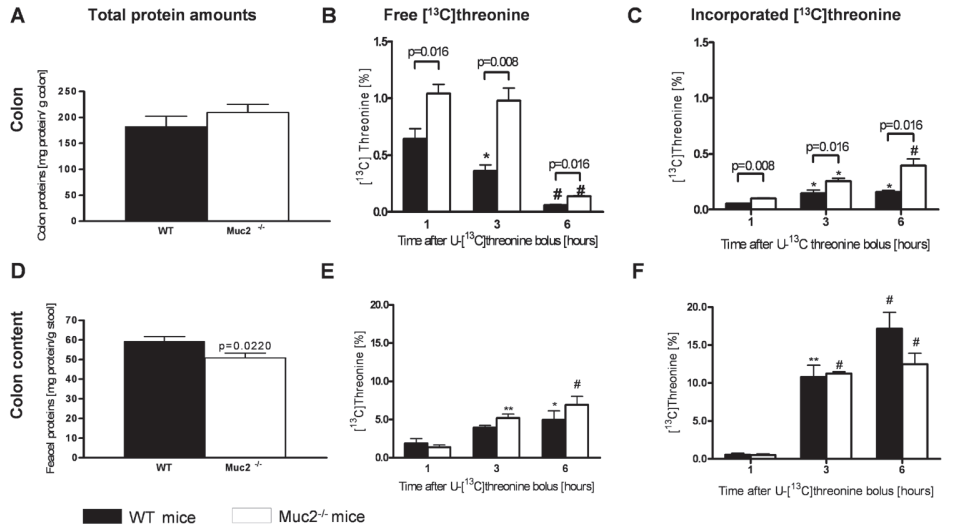

Figure 3. The protein content and threonine metabolism in the colon. (A, D) total protein amounts in the colon and colonic content in WT and Muc2$^{-/-}$ mice. (B, E) The free [^{13}C]threonine in the colon declined during the experimental period in contrast to the colonic content in which the free [^{13}C]threonine increased during the experiment (1 h vs. 3 and 6 h, *P<.05; **P<.01; $^{\#}$P<.001 Muc2$^{-/-}$ mice, WT mice, NS all time points). (C, F) The incorporated [^{13}C]threonine in the colon increased during time. The incorporated [^{13}C]threonine in the colonic content also increased during time. The WT mice showed a trend towards higher [^{13}C]threonine incorporation at 6 h. Error bars indicate the standard error of mean. All significancies 1 h vs. 3 or 6 hours *P<.05; **P<.01, $^{\#}$P<.001.

Serum

Free [^{13}C]threonine levels in serum significantly decreased over time ((WT: 0.7% at 1h vs. 0.02% at 6h, P<.001) and (Muc2$^{-/-}$: 0.4% at 1h. vs. 0.02% at 6h, P<.001)). Levels of incorporated [^{13}C]threonine into proteins in serum increased over time in both groups (0.3% at 1h vs. 1.3% at 6h, P<.01) .

Intestinal and whole body threonine oxidation

Total [^{13}C]glycine levels reflected metabolic oxidation of threonine in the small intestine of both mice types; Figure 4A shows that the initial peak of total glycine accumulation at 3h reverted to basal levels in both mice types by 6h post threonine gavage. However, Muc2$^{-/-}$ mice had persistently higher oxidation rate of dietary threonine, a difference more pronounced in the colon where total [^{13}C]glycine amounts also increased over time in both mice types (Fig. 4B).

Total [^{13}C]glycine amounts in the colonic content of both mice types significantly increased over time without any appreciable difference between types

(Fig. 4C). In serum total [^{13}C]glycine amounts in both mice types also significantly increased over time, without significant differences between types (Fig. 4D).

In summary, WT mice showed 40.1% dietary [^{13}C]threonine recovered in the intestinal tract after 6h vs. 43.6% in Muc2$^{-/-}$ mice. In the whole intestine, 26.2% of administered [^{13}C]threonine in WT mice and 24.1% in Muc2$^{-/-}$ mice, respectively, was incorporated into proteins. Most dietary [^{13}C]threonine recovered from the intestinal tract was detected in the colonic content in both mice types. In all other tissues and blood, except gastric content, [^{13}C]threonine recovered was two to tenfold lower than in colonic content. Interestingly, 27.4% of recovered [^{13}C]threonine in the colonic content of WT mice was incorporated into Muc2. Finally, the entire intestine of the Muc2$^{-/-}$ mice showed a significantly higher oxidation rate compared to WT mice.

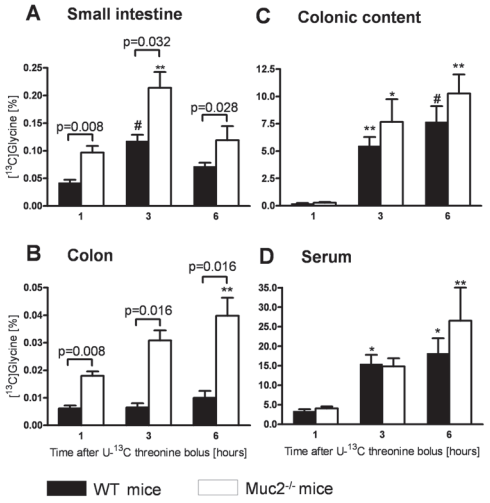

Figure 4. Intestinal and whole body threonine oxidation. (A) The total [^{13}C]glycine amounts inthe small intestine and colon (B) of WT and Muc2$^{-/-}$ mice increased during time. Overall, the Muc2$^{-/-}$ mice showed a higher oxidation of dietary threonine compared to WT mice, which was significantly higher in the small intestine and colon at each time point. (C) The total [^{13}C]glycine amounts in the colonic content and serum (D) of WT and Muc2$^{-/-}$ mice significantly increased during time. There were no significant differences in [^{13}C]glycine levels in the serum between the Muc2$^{-/-}$ and WT mice throughout the experiment. Error bars indicate the standard error of mean. All significancies 1 h vs. 3 or 6 hours *P<.05; **P<.01, #P<.001

Discussion

Previous studies showed that there is substantial amino acid metabolism in the intestine[10]. Specifically, the essential amino acid threonine is thought to be of utmost importance for intestinal Muc2 synthesis[12, 20, 21]. In the current study we aimed to gain more insight into intestinal threonine metabolism, and more specifically the role of dietary threonine in intestinal Muc2 synthesis, by studying threonine utilization in Muc2$^{-/-}$ and WT mice.

In line with previous studies, we found that the murine gastrointestinal tract takes up dietary threonine[11, 20, 21]. We retrieved 40.1% and 43.7% of dietary threonine in WT and Muc2$^{-/-}$ mice, respectively, either as free or incorporated threonine (Fig. 1B). Interestingly, we detected threonine incorporated into proteins of the stomach content after 1h. To our knowledge these results are the first to indicate absorption of dietary nutrients from the lumen of the stomach. As previous studies demonstrated that the stomach wall secretes Muc5ac and Muc6[29], threonine might be incorporated into these proteins in the stomach. However, this remains to be investigated. In the

present study, threonine distribution in the gastrointestinal tract and in serum was similar for both mice types studied. Muc2 deficiency therefore seems to have no initial impact on the intestinal threonine absorption capacity and the systemic availability of dietary threonine. However, [^{13}C]threonine was given as dietary free threonine. The molecular form of ingested threonine (free, peptide bound or protein bound) offered to the epithelium of the gastrointestinal tract might affect whole-body threonine kinetics. This phenomenon was earlier described by Daenzer *et al.,* demonstrating that protein-bound leucine was used more efficiently for liver protein synthesis than dietary free leucine[30]. More specifically, in the gastrointestinal tract we recovered 41.5% of dietary [^{13}C]threonine after 6h in WT mice vs. 44.8% in Muc2$^{-/-}$ mice, either as free or incorporated threonine or glycine. Thus, while dietary threonine utilization seems similar between Muc2$^{-/-}$ and WT mice, the primary metabolic fate, such as protein synthesis or oxidation, may differ. For this reason we investigated threonine metabolism in different intestinal segments.

Overall, the pool of free threonine in the total small intestine remained constant in concentration and amount during the 6h experiment with no significant differences between mice types. In contrast, free threonine in colonic tissue decreased over time in both groups. Remarkably, Muc2$^{-/-}$ mice showed significantly higher amounts of free threonine in colonic tissue, suggesting a dietary threonine excess due to Muc2 deficiency. In contrast to the tissue samples, the colonic content showed a similar increase of free threonine over time in both mice types. This might be due to breakdown of *de novo* synthesized proteins other than Muc2. Our results are supported by findings from previous studies showing that the Muc2 central peptide backbone is highly resistant to proteolytic breakdown by bacteria and enzymes[9]. Additionally, the increase of free [^{13}C]threonine in the colonic content might be caused by saturation of the small intestinal absorption capacity due to excess of [^{13}C]threonine given by gavage.

Incorporation of dietary threonine into intestinal proteins was found to be higher in the proximal small intestine compared to other further distal intestinal segments. The proximal small intestine therefore seems to play a major role in the utilization of dietary threonine, in line with other studies suggesting that most of dietary proteins and amino acids are absorbed by the proximal jejunum[31]. Incorporation of dietary threonine increased in each intestinal segment sampled for both mice types. The higher amounts of [^{13}C]threonine incorporated into proteins of the proximal small intestine – as compared to the distal small intestine and colon – can be explained by i) higher availability of [^{13}C]threonine in the proximal small intestine or ii) higher turnover of secreted proteins along the intestinal proximal-distal axis. The latter hypothesis is supported by a previous study showing that total protein synthesis, and more specifically Muc2 secretion, is higher in the distal colon compared to the proximal colon[32] and is hardly detectable in the small intestine (our unpublished data). In agreement, Atuma *et al.* showed that mucus thickness increases over the intestinal proximal-distal axis[33]. Moreover, in our study total protein amount in colonic content was higher in WT mice, demonstrating that Muc2 is mainly secreted by the colon. Furthermore, most dietary [^{13}C]threonine recovered from the intestinal tract was derived from the colonic content, 27.4% of which was incorporated into the protein Muc2 in WT mice. In addition, a previous study in Muc2$^{-/-}$ mice showed no evidence

of up-regulation of other known secretory mucins of the intestinal tract to compensate for the lack of Muc2[24]. Assuming that this does occur however, 27.4% incorporation of threonine into Muc2 in the WT mice would be an underestimation. Altogether, these data strengthen our hypothesis that dietary threonine is incorporated into the secretory mucin Muc2, with increased secretion rate along the intestinal proximal-distal axis. Furthermore, our data in Muc2$^{-/-}$ mice demonstrate that dietary threonine is also used for intestinal constitutive protein synthesis and secretion.

Regarding the issue of intestinal and whole body threonine oxidation, our data suggest that a large proportion of absorbed threonine is incorporated into Muc2, although not in Muc2 deficient mice. This is why a larger proportion of dietary threonine may have been oxidized. However, there are no data on the presence of catabolic enzymes in murine intestinal mucosa. Previous studies reported absence or only negligible activity of threonine catabolic enzymes in piglet intestinal mucosa[34]. However, in the present study [^{13}C]glycine was detectable in the intestine of both mice types, strongly suggesting that the catabolic enzyme TDG is present and active in murine intestinal mucosa. Overall, Muc2$^{-/-}$ mice oxidized more dietary threonine than WT mice, indicating that Muc2 deficiency results in more inefficient utilization of dietary threonine.

In summary, to our knowledge this is the first study demonstrating threonine utilization in mice. One of the pivotal metabolic fates of dietary threonine utilized by the intestine is its incorporation into Muc2. In the absence of Muc2, dietary threonine is mainly used for constitutive protein synthesis or becomes a substrate for metabolic oxidation.

Acknowledgments

Dedicated to the memory of Peter J Reeds, who died August 13, 2002. Peter J Reeds was Hans van Goudoever's mentor and source of inspiration. The authors thank W. Chung, I.M.A. Louwers and M. van der Reijnst for technical assistance and J. Hagoort for reviewing this manuscript. The Dutch Digestive Foundation, Nieuwegein; Numico Research BV, Wageningen; Sophia Foundation for Scientific Research, Rotterdam and Netherlands Organization for Scientific Research, Den Haag, all based in the Netherlands, are gratefully acknowledged for their financial support.

References

1. Corfield AP, Myerscough N, Longman R, Sylvester P, Arul S, Pignatelli M. Mucins and mucosal protection in the gastrointestinal tract: new prospects for mucins in the pathology of gastrointestinal disease. Gut 2000;47:589-94.
2. Smirnov A, Sklan D, Uni Z. Mucin dynamics in the chick small intestine are altered by starvation. J Nutr 2004;134:736-42.
3. Sherman P, Forstner J, Roomi N, Khatri I, Forstner G. Mucin depletion in the intestine of malnourished rats. Am J Physiol 1985;248:G418-23.
4. Iiboshi Y, Nezu R, Kennedy M, Fujii M, Wasa M, Fukuzawa M, Kamata S, Takagi Y, Okada A. Total parenteral nutrition decreases luminal mucous gel and increases permeability of small intestine. JPEN J Parenter Enteral Nutr 1994;18:346-50.
5. Sakamoto K, Hirose H, Onizuka A, Hayashi M, Futamura N, Kawamura Y, Ezaki T. Quantitative study of changes in intestinal morphology and mucus gel on total parenteral nutrition in rats. J Surg Res 2000;94:99-106.
6. Forstner JF, Forstner GG. Gastrointestinal mucus. In: Johnson LR, ed. Physiology of the Gastrointestinal Tract. 3 ed. New York: Raven Press, 1994:1255-1280.
7. Tytgat KM, Büller HA, Opdam FJ, Kim YS, Einerhand AW, Dekker J. Biosynthesis of human colonic mucin: Muc2 is the prominent secretory mucin. Gastroenterology 1994;107:1352-63.
8. Van Klinken BJ, Dekker J, Büller HA, Einerhand AW. Mucin gene structure and expression: protection vs. adhesion. Am J Physiol 1995;269:G613-27.
9. Strous GJ, Dekker J. Mucin-type glycoproteins. Crit Rev Biochem Mol Biol 1992;27:57-92.
10. Baracos VE. Animal models of amino acid metabolism: a focus on the intestine. J Nutr 2004;134:1656S-1659S; discussion 1664S-1666S, 1667S-1672S.
11. Stoll B, Burrin DG, Henry J, Yu H, Jahoor F, Reeds PJ. Substrate oxidation by the portal drained viscera of fed piglets. Am J Physiol 1999;277:E168-75.
12. Stoll B, Henry J, Reeds PJ, Yu H, Jahoor F, Burrin DG. Catabolism Dominates the First-Pass Intestinal Metabolism of Dietary Essential Amino Acids in Milk Protein-Fed Piglets. J. Nutr. 1998;128:606-614.
13. Yu YM, Wagner DA, Tredget EE, Walaszewski JA, Burke JF, Young VR. Quantitative role of splanchnic region in leucine metabolism: L-[1-13C,15N]leucine and substrate balance studies. Am J Physiol 1990;259:E36-51.
14. van Goudoever JB, Stoll B, Henry JF, Burrin DG, Reeds PJ. Adaptive regulation of intestinal lysine metabolism. Proc Natl Acad Sci U S A 2000;97:11620-5.
15. Stoll B, Burrin DG, Henry J, Yu H, Jahoor F, Reeds PJ. Dietary Amino Acids Are the Preferential Source of Hepatic Protein Synthesis in Piglets. J. Nutr. 1998;128:1517-1524.
16. Matthews DE, Marano MA, Campbell RG. Splanchnic bed utilization of leucine and phenylalanine in humans. Am J Physiol 1993;264:E109-18.
17. Hoerr RA, Matthews DE, Bier DM, Young VR. Leucine kinetics from [2H3]- and [13C]leucine infused simultaneously by gut and vein. Am J Physiol 1991;260:E111-7.
18. Biolo G, Tessari P, Inchiostro S, Bruttomesso D, Fongher C, Sabadin L, Fratton MG, Valerio A, Tiengo A. Leucine and phenylalanine kinetics during mixed meal ingestion: a multiple tracer approach. Am J Physiol 1992;262:E455-63.
19. van der Schoor SR, Reeds PJ, Stellaard F, Wattimena JD, Sauer PJ, Büller HA, van Goudoever JB. Lysine kinetics in preterm infants: the importance of enteral feeding. Gut 2004;53:38-43.
20. Schaart MW, Schierbeek H, van der Schoor SR, Stoll B, Burrin DG, Reeds PJ, van Goudoever

JB. Threonine utilization is high in the intestine of piglets. J Nutr 2005;135:765-70.
21. Bertolo RF, Chen CZ, Law G, Pencharz PB, Ball RO. Threonine requirement of neonatal piglets receiving total parenteral nutrition is considerably lower than that of piglets receiving an identical diet intragastrically. J Nutr 1998;128:1752-9.
22. Faure M, Moennoz D, Montigon F, Mettraux C, Breuille D, Ballevre O. Dietary threonine restriction specifically reduces intestinal mucin synthesis in rats. J Nutr 2005;135:486-91.
23. Velcich A, Yang W, Heyer J, Fragale A, Nicholas C, Viani S, Kucherlapati R, Lipkin M, Yang K, Augenlicht L. Colorectal cancer in mice genetically deficient in the mucin Muc2. Science 2002;295:1726-1729.
24. Van der Sluis M, De Koning BAE, De Bruijn ACJM, Velcich A, Meijerink JPP, Van Goudoever JB, Büller HA, Dekker J, Van Seuningen I, Renes IB, Einerhand AWC. Muc2-deficient mice spontaneously develop colitis, indicating that Muc2 is critical for colonic protection. Gastroenterology 2006;*in press*.
25. Ballevre O, Cadenhead A, Calder AG, Rees WD, Lobley GE, Fuller MF, Garlick PJ. Quantitative partition of threonine oxidation in pigs: effect of dietary threonine. Am J Physiol 1990;259:E483-91.
26. Bird MI, Nunn PB. Metabolic homoeostasis of L-threonine in the normally-fed rat. Importance of liver threonine dehydrogenase activity. Biochem J 1983;214:687-694.
27. Claasen V. Neglected factors in pharmacology and neuroscience research. Elsevier, 1994.
28. Osinski MA, Seifert TR, Cox BF, Gintant GA. An improved method of evaluation of drug-evoked changes in gastric emptying in mice. J Pharmacol Toxicol Methods 2002;47:115-20.
29. Ho SB, Takamura K, Anway R, Shekels LL, Toribara NW, Ota H. The adherent gastric mucous layer is composed of alternating layers of MUC5AC and MUC6 mucin proteins. Dig Dis Sci 2004;49:1598-606.
30. Daenzer M, Petzke KJ, Bequette BJ, Metges CC. Whole-body nitrogen and splanchnic amino acid metabolism differ in rats fed mixed diets containing casein or its corresponding amino acid mixture. J Nutr 2001;131:1965-72.
31. Gausseres N, Mahe S, Benamouzig R, Luengo C, Drouet H, Rautureau J, Tome D. The gastro-ileal digestion of 15N-labelled pea nitrogen in adult humans. Br J Nutr 1996;76:75-85.
32. Renes IB, Boshuizen JA, Van Nispen DJ, Bulsing NP, Büller HA, Dekker J, Einerhand AW. Alterations in Muc2 biosynthesis and secretion during dextran sulfate sodium-induced colitis. Am J Physiol Gastrointest Liver Physiol 2002;282:G382-9.
33. Atuma C, Strugala V, Allen A, Holm L. The adherent gastrointestinal mucus gel layer: thickness and physical state in vivo. Am J Physiol Gastrointest Liver Physiol 2001;280:G922-9.
34. Le Floc'h N, Thibault JN, Seve B. Tissue localization of threonine oxidation in pigs. Br J Nutr 1997;77:593-603.

Part II

Regulation of Mucin Gene Expression

Chapter 7

Regulation of Mouse Mucin 2 by GATA Factors

Partly published as:
Maria van der Sluis, Monique H.M. Melis, Nicolas Jonckheere, Marie-Paule Ducourouble, Hans A. Büller, Ingrid B. Renes, Alexandra W.C. Einerhand, and Isabelle Van Seuningen. *The murine Muc2 mucin gene is transcriptionally regulated by the zinc-finger GATA-4 transcription factor in intestinal cells.*

Biochemical & Biophysical Research Communications, Vol 325(3);952-960, 2004

Abstract
Mucin 2 (MUC2), the major mucin in the intestine, is expressed early during development and shows an altered expression pattern in intestinal bowel diseases. However the mechanisms responsible for MUC2 expression in the intestine during these events are largely unknown. Having found putative GATA binding sites in the murine Muc2 promoter and that GATA-4 is expressed in Muc2-expressing goblet cells of the mouse small intestine, we undertook to study its regulation by GATA factors. A panel of deletion mutants made in pGL3 vector and covering 2.2 kb of the promoter were used to transfect the murine CMT-93 colorectal cancer cell line. The role of the GATA factors on the Muc2 gene regulation was investigated by RT-PCR and co-transfections in the presence of expression vectors encoding either wild type or mutated GATA factors or by mutating the GATA site identified within Muc2 promoter. Four GATA-4 cis-elements were identified in the promoter by EMSA and Muc2 promoter was efficiently activated when GATA-4 was overexpressed in the cells with a loss of transactivation when those sites were either mutated or a mutated form of GATA-4 was used. Overexpression of GATA-5 and GATA-6 also induced activity of Muc2 promoter. Conclusions: Altogether these results point out an important role for GATA factors as potent activators of Muc2 expression in the intestine.

Abbreviations used in this paper
EMSA , Electrophoretic Mobility Shift Assay; LPH, Lactase Phlorizin Hydrolase; Muc, Mucin; SI , Sucrase Isomaltase, WT, wild type

Introduction

The mucus layer in the lumen of the gut forms a physical barrier against micro-organisms and insoluble material[1]. Goblet cells are a hallmark of the intestinal epithelium, and are known to secrete mucins that participate in mucus formation to protect the underlying mucosa. The secretory mucin Muc2, a very large *O*-glycoprotein, is particularly relevant for the study of goblet cell biology as it is exclusively and abundantly expressed by intestinal goblet cells[2, 3]. It is produced throughout the gastro-intestinal tract increasing from small intestine to colon.

Muc2 is expressed early during embryonic development of the intestine[4], which suggests that Muc*2* transcription is under the influence of transcription factors responsible for intestinal development and cell differentiation. The early expression of mucin before mucus cell differentiation or during the process of differentiation indicates that they may be the targets of transcription factors responsible for those programs [5]. This hypothesis has been recently confirmed in a previous study where we showed that the human MUC2 mucin gene is regulated by Cdx1 and Cdx2 transcription factors[6], which are both involved in intestinal cell differentiation[7].

GATA transcription factors belong to another family of transcription factors involved in development and cell differentiation. GATA factors can be grouped into two subfamilies based on structural features and expression patterns. GATA-1, GATA-2 and GATA-3 are involved in haematopoiesis and neurogenesis whereas GATA-4, GATA-5 and GATA-6 possess overlapping patterns in the developing cardiovascular system and in endoderm-derived tissues including the liver, lungs, pancreas, stomach and intestine[8].

During embryonic development GATA-4, GATA-5 and GATA-6 mRNA are expressed in the primitive intestine[9, 10] in which Muc*2* is also found[4]. Their expression in the intestine is sustained during adulthood with a distinct expression pattern along the crypt-villus axis, which strongly correlates with the status of differentiation of the cells. GATA-6 is highly expressed in the proliferating and less differentiated area in the crypts fading in the differentiated cells in the villi whereas GATA-4 and GATA-5 show an opposite pattern with highest expression on the tips of the villi fading towards the crypt[11]. Moreover, GATA factors are known to regulate other intestine-specific genes, which are considered as markers of enterocytes, such as fatty acid binding binding protein[11], intestinal lactase-phlorizin hydrolase (LPH)[11, 12] and sucrase isomaltase (SI)[13].

Characterization of the 5'-regulatory regions of numerous genes has demonstrated that GATA-4, GATA-5 and GATA-6 factors interact with a DNA sequence element containing the core GATA motif (A/T)GATA(A/G)[8]. Computer analysis of the murine *Muc2* promoter sequence[14] revealed the presence of several putative GATA binding sites throughout the promoter region.

Altogether these data are in favour of a role for GATA factors in regulating *Muc2* gene expression. Having found binding sites for these factors in the promoter of *Muc2*, and because of the spatio-temporal restricted pattern of expression of MUC2 and GATA factors along the crypt-villus axis in the intestine, we undertook to study the regulation of the promoter of mouse *Muc2* by GATA-4/-5/-6 factors in a murine colorectal cancer cell line. Implications for MUC2 expression during intestine development and cell differentiation are discussed.

Materials and Methods

Animals

Adult specified pathogen-free Balb/c mice, obtained from Harlan (Zoetermeer, the Netherlands), were killed by cervical dislocation. The intestine was removed and fixed in 4% paraformaldehyde in PBS and subsequently processed for light microscopy as described previously[15]. The animal experiments were performed with the approval of the Animal Studies Ethics Committee of the Erasmus MC (Rotterdam, the Netherlands).

Immunohistochemistry

Five µm thick paraffin sections were cut and deparaffinized through a graded series of xylol-ethanol. Endogenous peroxidase activity was inactivated by 1.5% (v/v) hydrogen peroxide in PBS for 30 min, followed by antigen retrieval in 0.01 M citrate buffer for 10 min at 100°C. Thereafter, sections were incubated with TENG-T (10 mM Tris-HCl, 5 mM EDTA, 150 mM NaCl, 0.25% (w/v) gelatin, 0.05% (w/v) Tween-20) for 30 min to reduce non-specific binding. This was followed by overnight incubation with a 1:2500 dilution of goat anti-GATA-4 antibody (sc-1237X, Santa Cruz Biotechnology, USA) in PBS containing 1% (w/v) bovine serum albumin and 0.1% (v/v) Triton X-100. Then, the sections were incubated for 1h with biotinylated horse anti-goat IgG (diluted 1:2000, Vector Laboratories, England) followed by a 1h incubation with ABC/PO complex (Vectastain Elite Kit, Vector Laboratories) diluted 1:400. Binding was visualized after incubation in 0.5 mg/ml 3,3'-diaminobenzidine (DAB), 0.02% (v/v) H_2O_2 in 30 mM imidazole, 1 mM EDTA (pH 7.0). To visualize goblet cells, sections were stained with Alcian Blue 8GX (BDH, Brunschwig Chemie, Amsterdam, the Netherlands). Finally, sections were dehydrated and mounted.

Muc2-pGL3 deletion mutant constructs

The *Muc2*-pGL3 deletion mutants that cover 2.2 kb of the promoter (Genbank accession number AF221746) were constructed into promoterless pGL3 Basic vector (Promega, Madison, WI, USA) using a PCR-based method as described previously[16, 17]. Briefly, PCR reactions were carried out on mouse genomic DNA using the primers depicted in Table I. PCR products were then subcloned into pCR2.1 vector (Invitrogen, Breda, the Netherlands) before subcloning into *Bgl*II–*Mlu*I sites of the pGL3 Basic vector previously linearized with the same restriction enzymes. All clones were sequenced on both strands on an automatic LICOR sequencer using infrared-labeled RV3 and GL2 primers (Promega). Plasmids used for transfection studies were prepared using the Endofree plasmid Mega kit (Qiagen, Venlo, the Netherlands).

Cell culture

Murine rectal cancer cell line CMT-93 was a kind gift of Dr D. Podolsky (Massachusetts General Hospital, Boston, MA, U.S.A.). The CMT-93 cells were cultured in Dulbecco's modified essential medium containing 10% fetal bovine serum (Roche, Molecular Biochemicals, Meylan, France), 4 mM L-glutamine, penicillin (100 units/ml) and streptomycin (100 µg/ml) as previously discribed[18]. IEC-6 cells

were purchased from the ECACC (European Collection of Animal Cell Cultures). This cell line was established from rat small intestine crypt cells and was cultured in Dulbecco's modified essential medium containing 5% fetal bovine serum, 2 mM L-glutamine, 10 µg/ml insulin, 50 units/ml penicillin and 50 µg/ ml streptomycin. All cells were cultured at 37°C in a humidified 5% CO_2 water-jacketed incubator. All reagents were from Invitrogen unless otherwise indicated.

Table I. Sequences of the pairs of primers used in PCR to produce deletion mutants covering the *Muc2* promoter.

Position in the promoter	Oligonucleotide sequence (5'→ 3')	Orientation
-221/+29	CGC**ACGCGT**TTGGGGCTATGACATCCTGA	Sense
	CGC**AGATCT**GGTGGCTCACGAGGGTGGCAC	Antisense
-563/+29	CGC**ACGCGT**ATGGGGTCAGACACCCGT	Sense
	CGC**AGATCT**GGTGGCTCACGAGGGTGGCAC	Antisense
-729/+29	CGC**ACGCGT**GAGGGCTGCCCAAGTTTTAA	Sense
	CGC**AGATCT**GGTGGCTCACGAGGGTGGCAC	Antisense
-1001/+29	CGC**ACGCGT**GGCAAGCCCAGGGACTGAAG	Sense
	CGC**AGATCT**GGTGGCTCACGAGGGTGGCAC	Antisense
-1568/+29	CGC**ACGCGT**GAGGTGGGAGGACTGGCTTC	Sense
	CGC**AGATCT**GGTGGCTCACGAGGGTGGCAC	Antisense
-2213/+29	CGC**ACGCGT**TCTTGGTCCTCAACCAAAGTT	Sense
	CGC**AGATCT**GGTGGCTCACGAGGGTGGCAC	Antisense

NOTE. *Bgl*II (AGATCT) and *Mlu*I (ACGCGT) sites (bold) were added at the end of the primers to direct subcloning into the pGL3 basic vector.

Transfections

Transfections and co-transfections experiments were performed using Effectene® reagent (Qiagen) as described previously[17] using 1 µg of Muc2-pGL3 deletion mutants. Total cell extracts were prepared after a 48 h incubation at 37°C using 1×Reagent Lysis Buffer (Promega) as described in the manufacturer's instruction manual. Luciferase activity (20 µl) was measured on a TD 20/20 luminometer (Turner Design, Promega). Total protein content in the extract (4 µl) was measured using the bicinchoninic acid method in 96-well plates as described in the manufacturer's instruction manual (Pierce, Bezons, France). In co-transfection experiments, 1 µg of the deletion mutant of interest was transfected with 0.25 µg of the expression plasmid encoding the transcription factor of interest (pMT2-GATA-4

(Dr. S. Cereghini, INSERM, Hôpital Necker, Paris, France), pSG5-GATA-5, pSG5-GATA-6 (Dr. J. K. Divine, Washington University, St-Louis, USA), wild type (WT) pcDNA GATA-4 and mutated forms pcDNA-(-Act) GATA-4, and pcDNA-(C290S) GATA-4, Dr. S. D. Krasinski (Harvard Medical School, Boston, MA, USA). Results were expressed as fold activation of luciferase activity in samples co-transfected with the transcription factor of interest compared with the control co-transfected with the corresponding empty vector. To study the effect on endogenous Muc2 expression, cells (0.5 x 10^6) were transfected with 4 µg of the expression vector of interest, and cultured for 48h before being lysed and processed for total RNA preparation.

RT-PCR

Total RNA from CMT-93 cells was prepared using the RNeasy mini-kit from Qiagen. 1.5 µg of total RNA was used to prepare cDNA (Advantage™ RT-for-PCR kit, Clontech, Ozym, Saint Quentin Fallavier, France). PCR was performed on 5 µl of cDNA using a specific pair of primers (MWG-Biotech, Ebersberg, Germany) for mouse Muc2 mucin gene: forward primer: 5'-TGTGGCCTGTGTGGGAACTTT-3', reverse primer: 5'-CATAGAGGGCCTGTCCTCAGG-3'. Mouse β-actin (forward primer: 5'-TCACGCCATCCTGCGTCTGGACT-3'; reverse primer: 5'-CCGGACTCATCGTACTCCT-3') was used as the internal control. PCR reactions were carried out in 50 µl final solutions as previously described[6]. Annealing temperature was 62°C and 59°C, respectively. PCR products were analyzed on a 1.5% agarose gel run in 1X Tris-borate-EDTA buffer. A 100 basepair DNA ladder was purchased from Amersham Biosciences (GE Healthcare Bio-Sciences, Orsay, France). Expected size for Muc2 and β-actin PCR products are 558 and 582 basepairs, respectively. RT-PCRs were carried out on cDNAs from three different sets of experiments.

Nuclear extract preparation

Nuclear extracts from CMT-93 cells were prepared as described by Van Seuningen *et al*.[19], and kept at –80°C until use. Protein content (2 µl of cell extracts) was measured using the bicinchoninic acid method as described above.

Oligonucleotides and DNA probes

Oligonucleotides used as probes and competitors in EMSAs are shown in Table II. They were synthesized by MWG-Biotech (Ebersberg, Germany). Equimolar amounts of single-stranded oligonucleotides were annealed and radiolabelled using T4 polynucleotide kinase (Promega) and [γ-32P] dATP. Radiolabelled probes were purified by chromatography on a Bio-Gel P-6 column (Bio-Rad, Ivry-sur-Seine, France).

EMSA (electrophoretic mobility shift assay)

The sequence of Muc2 promoter was analyzed with MatInspector V2.2 and Alibaba2 softwares based on the genomatix and gene-regulation databases, respectively, to determine the location of putative transcription factor binding sites[20]. EMSAs were performed as described previously by Mesquita *et al.*[6]. Supershift analyses were carried out using 1 µl of the anti-GATA-4 antibody (sc-1237X,

SantaCruz). Reactions were stopped by adding 2 µl of loading buffer. Samples were loaded on to a 4% non-denaturing polyacrylamide gel and electrophoresis conditions were as described previously[17]. Gels were vacuum-dried and autoradiographed overnight at –80°C.

Site-directed mutagenesis

QuickChange site-directed mutagenesis kit (Stratagene, Amsterdam, the Netherlands) was used to generate site specific mutations in the two proximal GATA sites found in the Muc2 promoter at -168/-165 and -158/-155, respectively. The oligonucleotide containing the double mutation was designed according to the manufacturer's instructions and its sequence is depicted in Table II.

Table II. Sequences of the sense oligonucleotides used for EMSAs and for site-directed mutagenesis.

Oligonucleotides used for EMSA	Sequence (5'→3')
Wild type T216 (-99/-96)	CACAGC*TGTTT*TCCT***GATA***ACTTGGCA
Mutated T216	CACAGC*TGTTT*TCCT**CT**TAACTTGGCA
Wild type T168	TCATATAAA***GATA***AACTCA***GATA***ACCTG
(-168/-165, -158/-155)	
Mutated T168	TCATATAAA**CT**TAAACTCA**CT**TAACCTG
Wild type T225 (-401/-398)	TCCTTATTC***TATC***TAGGCTGGGCT
Wild type T169 (-1521/-1518)	TTGATCATTTT***TATC***TCTGATGTCTTT
Mutated T169	TTGATCATTTT***TA*****AG**TCTGATGTCTTT
Oligonucleotide used for site–directed mutagenesis	
Double mutant (-168/-165;-158/-155)	CCAGGGAGTCATATAAA**CT**TAAACTCA**CT**TAACCTGAATCA

NOTE. Positions of the GATA binding sites, within the probe, relative to the *Muc2* transcription start site are indicated in parenthesis. Putative GATA binding sites in the sequence are bold and in italics. Putative HNF binding site in T216 at -108/-104 is in italics. Mutated nucleotides are bold and underlined. Antisense oligonucleotides were also synthesized and annealed to the sense oligonucleotides to produce double-stranded DNA.

Results and Discussion

The GATA-4, GATA-5 and GATA-6 transcriptions factors are expressed simultaneously in mouse embryonic intestinal tissue as early as ED 9.5[8]. Their importance in regulating several promoters of enterocyte-specific genes, has been previously described[11-13]. The MUC2 mucin is a marker of another intestinal cell type, the goblet cell, and possesses a spatio-temporal pattern of expression in embryonic, fetal and adult intestine[4, 21]. However, regulation of MUC2 mucin expression during development is largely unknown and is mandatory to better understand intestine differentiation and cell lineage establishment[22]. In this work we studied the transcriptional regulation of murine *Muc2* by GATA factors and mapped the cognate cis-elements within the promoter. We focused on the role of GATA-4 factor since it is known to play an important role in directing cell lineage-specific gene expression during development of the vertebrate gut.

GATA-4 is expressed in goblet cells of the mouse small intestine

Muc2 is the main mucin expressed by intestinal goblet cells[2]. Alcian blue staining of the mouse small intestine indicates the presence and location of these goblet cells (Fig. 1). Alcian blue-positive goblet cells are present both along the villi and in the crypts. Immunohistochemical staining of the same section with a GATA-4 specific antibody showed staining of nuclei of all the cells along the crypt-villus axis, including goblet cells (Fig. 1). We can thus conclude that GATA-4 transcription factor is expressed in Muc2-expressing goblet cells in the small intestine. The fact that GATA-4 has been shown to play an important role in the regulation of genes

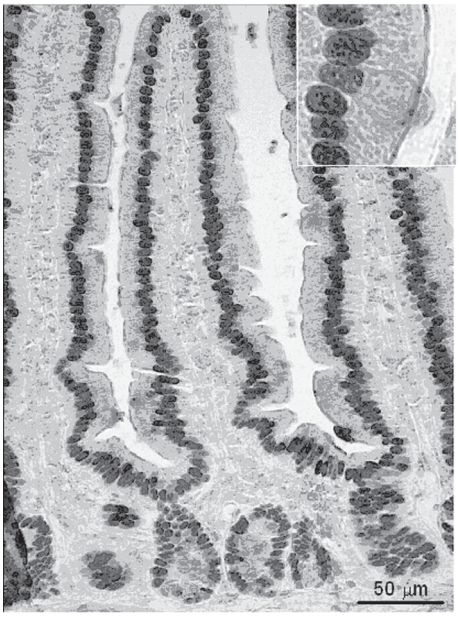

Figure 1. Expression of GATA-4 transcription factor in mouse small intestine by immunohistochemistry. Alcian blue staining was performed as described in the material and methods section. GATA-4 immunostaining was carried out on the same section of mid jejunum of an adult mice using a specific antibody for GATA-4. Sections were counterstained with haematoxylin. Inset : close-up of one GATA-4 expressing goblet cell. Please also see page 223.

expressed in the intestine[11-13] and its co-localization with Muc2 in the goblet cells suggests an important role for GATA-4 in the regulation of *Muc2* gene. In order to confirm this hypothesis we first identified GATA-4 responsive regions within *Muc2* promoter by co-transfection experiments in the presence of WT or mutated forms of either *Muc2* promoter or GATA-4 factor and then identified GATA-4 cis-elements by gel-shift assays.

Muc2 *promoter activity in murine and rat intestinal cells*

To define essential regions that drive *Muc2* transcription, six deletion mutants covering 2.2 kb of the promoter were constructed in the promoterless pGL3 Basic vector (Fig. 2A). Numbering refers to the transcription start site designated as +1 that was previously described[23]. These constructs were then transfected into two different cell lines, a goblet-like cell line CMT-93[24] and a crypt-like cell line IEC-6[25], that both express *Muc2* mRNA. The luciferase diagram shown in Figure 2B, indicates that *Muc2* promoter activity is the strongest in the CMT-93 cell line (black bars). In both cell lines, the highest luciferase activity was obtained with fragment -729/+29. Since the activity increased from the fragment -563/+29 to -729/+29, it indicates that the -729/-564 region possesses essential positive regulatory elements that confer maximal activity to the promoter. In both cell lines, a decreased activity was seen with fragment -1568/+29 when compared with fragments -1001/+29 and -2213/+29. This indicates that there are inhibitory elements present within the -1568/-1002 region of the promoter. In conclusion, despite being active in both cell lines, *Muc2* promoter appears more active in goblet-like CMT-93 cells than in crypt-like IEC-6 cells.

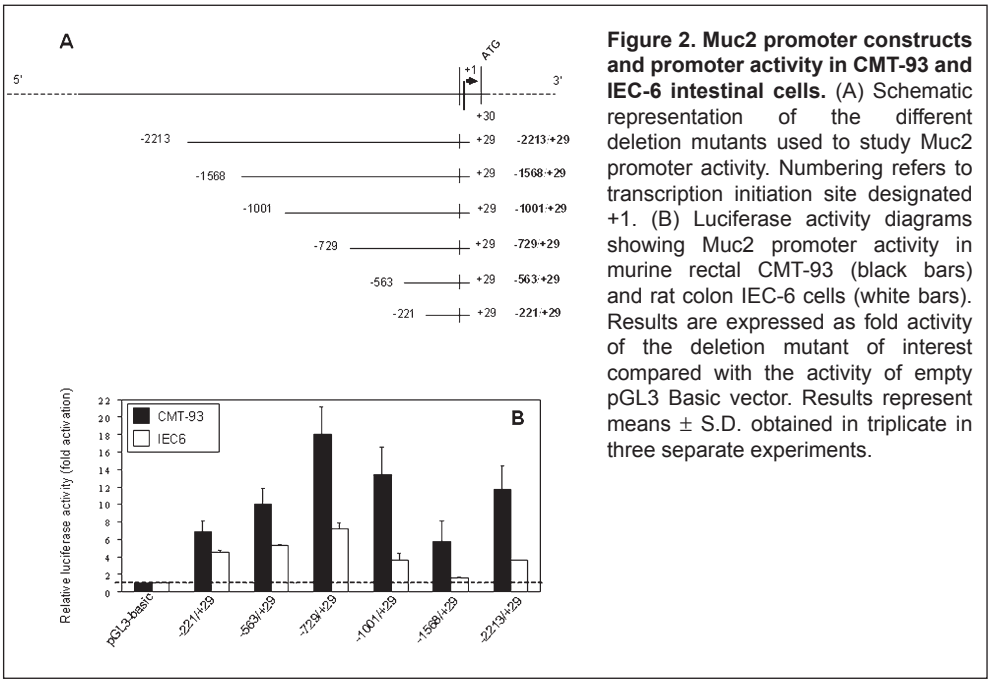

Figure 2. Muc2 promoter constructs and promoter activity in CMT-93 and IEC-6 intestinal cells. (A) Schematic representation of the different deletion mutants used to study Muc2 promoter activity. Numbering refers to transcription initiation site designated +1. (B) Luciferase activity diagrams showing Muc2 promoter activity in murine rectal CMT-93 (black bars) and rat colon IEC-6 cells (white bars). Results are expressed as fold activity of the deletion mutant of interest compared with the activity of empty pGL3 Basic vector. Results represent means ± S.D. obtained in triplicate in three separate experiments.

GATA-4 regulates Muc2 *expression at the transcriptional level*

Effect of GATA-4 overexpression on *Muc2* endogenous expression in CMT-93 cells was studied by RT-PCR (Fig. 3A). The result indicates that *Muc2* mRNA level is substantially increased when GATA-4 is overexpressed in the cells (lane 2) when compared with cells transfected with the empty vector (lane 1). In order to identify GATA-4 responsive regions within *Muc2* promoter, co-transfection experiments were then carried out in the presence of pGL3-*Muc2* deletion mutant -221/+29 and GATA-4 expression vector (Fig. 3B, black bars). The luciferase diagram indicates that overexpression of GATA-4 resulted in a 10-fold increase of luciferase activity of the -221/+29 construct. When a mutated form of the -221/+29 construct was used, in which the GATA sites at -168/-165 and -158/-155 were mutated (GATA to *CT*TA, Table II), 30% of the transactivating activity was lost (white bars). The fact that the luciferase activity did not return to basal levels suggests that either other GATA sites are present with the –221/+29 region and contribute to the GATA-4-mediated transactivating activity or that GATA-4 acts indirectly on the promoter via interactions with co-factors. In order to investigate the latter hypothesis, we co-transfected cells in the presence of the -221/+29 deletion construct with either WT GATA-4 vector or mutated forms (-Act and C290S) (Fig. 3C). The –Act GATA-4 vector encodes a mutated form of GATA-4 in which the activation domains were deleted whereas C290S mutant encodes a GATA-4 form bearing a point mutation at amino acid position 290 (cysteine to serine) in the COOH-terminal zinc finger[26]. Both forms are not able

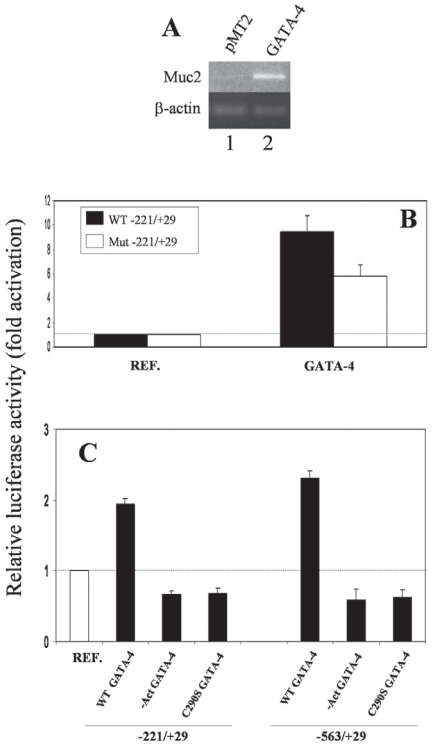

Figure 3. Activation of *Muc2* mRNA level and promoter activity by GATA-4 in CMT-93 cells by RT-PCR and transfection assays, respectively. (A) Endogenous expression of *Muc2* mRNA after co-transfection with GATA-4 expression vector (lane 2) or corresponding empty vector (lane 1). 10 µl (*Muc2*) and 2 µl (β-*actin*) of the PCR products were loaded on a 1.5 % agarose gel and electrophoresed in a 1X Tris-borate buffer in the presence of ethidium bromide. (B) Luciferase diagram showing the effects of overexpression of GATA-4 on WT deletion construct –221/+29 (black bars) or deletion construct –221/+29 with two mutated GATA-4 sites at -168/-165;-158/-155 (white bars). (C) Luciferase diagram showing the effects of co-transfection of WT –221/+29 or -563/+29 pGL3-*Muc2* deletion mutants with WT GATA-4 or mutated GATA-4 expression vectors (-Act GATA-4 and C290S GATA-4). Results are expressed as fold activation of luciferase activity in samples co-transfected with the transcription factor of interest compared with the control co-transfected with the corresponding empty vector (REF.). Results represent means ± S.D. obtained in triplicate in three separate experiments.

to bind DNA cognate element. Co-transfections with the WT vector (WT GATA-4) led to a two-fold activation of both fragments tested (-221/+29 and –563/+29). When the same experiment was performed with the mutated GATA-4 vectors (-Act and C290S), the luciferase activity decreased and returned to basal levels. This implicates that the transcription activation of the *Muc2* promoter by GATA-4 is mediated by a direct interaction of GATA-4 with the DNA sequence.

In conclusion, these experiments demonstrate that (i) GATA-4 induces *Muc2* transcription, (ii) responsive elements are present within the –221/+29 region of the promoter and (iii) GATA-4 binds directly to the promoter to transactivate *Muc2* promoter.

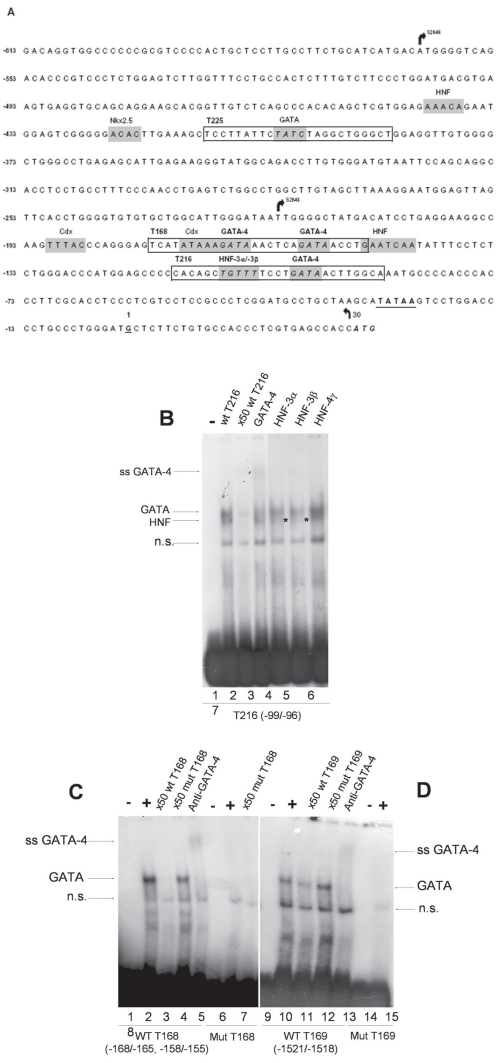

Figure 4. Sequence of the proximal part of *Muc2* promoter and identification of GATA-4 *cis*-elements by EMSA. (A) The transcription site +1 (bold and underlined) is located 29 nucleotides downstream of the TATA box. Gray boxes indicate putative binding sites for transcription factors and boxed sequences indicate the sequences of oligonucleotides used in gel-shift assays. Arrows delineate the sequence of the deletion mutants used in this study. (B) Nuclear extracts were incubated with radiolabeled probe T216 (lanes 1-7). Probe alone (lane 1), radiolabeled T216 with nuclear extract (lane 2), cold competition with 50x excess of wt T216 probe (lane 3). Super shift analysis was performed by preincubating the nuclear extract with 1 µl of anti-GATA-4 (lane 4), anti-HNF-3α (lane 5), anti-HNF-3β (lane 6), or antiHNF-4γ (lane 7) antiβodies, respectively. (C) Nuclear extracts were incubated with wild-type (lanes 1-5) and mutated (lanes 6-8) radiolabeled T168 probe, respectively. Probe alone (lanes 1 and 6), radiolabeled probes with nuclear extract (lanes 2 and 7), cold competition with 50x excess of wt T168 probe (lane 3), cold competition with 50x excess of mutated T168 probe (lanes 4 and 8). Supershift analysis with 1 µl of anti-GATA-4 antibody (lane 5). (D) Nuclear extracts were incubated with WT (lanes 9-13) and mutated (lanes 14 and15) radiolabeled T169 probe, respectively. Probe alone (lanes 9 and 14), radiolabeled probes with nuclear extract (lanes 10 and 15), cold competition with 50x excess of wt T169 probe (lane 11), cold competition with 50x excess of mutated T169 probe (lane 12). Supershift analysis with 1 µl of anti-GATA-4 antibody (lane 13).

Identification of GATA-4 cis-elements within Muc2 promoter

Analysis of the proximal part of Muc2 promoter sequence with MatInspector V2.2 and Alibaba2 softwares indicated the presence of four several putative GATA binding sites at -99/-96, -168/-165, -158/-155 and -401/-398, respectively (Fig. 4A). They all contain the conserved consensus sequence required for GATA binding. To confirm the binding of GATA-4 to these sites, EMSAs were carried out in the presence of nuclear extracts prepared from CMT-93 cells. As shown in Figures 4B and 4C three GATA-4 binding sites were identified in the T216 (one GATA site at –99/-96) and T168 (two GATA sites at -168/-165 and -158/-155) probes, respectively. When radiolabeled probes were incubated with nuclear extracts, two specific shifted bands were visualized with T216 probe (Fig. 4B, lane 2) whereas only one was seen with T168 probe (Fig. 4C, lane 2). Specificity of the protein-DNA complexes were confirmed by the loss of the bands when cold competitions were performed with a 50x excess of the cold probes (Figs. 4B and 4C, lanes 3). As expected, cold competition with a 50x excess of a cold T168 mutated probe (Fig. 4C, lane 4) did not modify the pattern of the shift. Moreover, when the mutated T168 probe was radiolabeled and incubated with nuclear extracts, no shift corresponding to the GATA binding was visualized (Fig. 4C, lane 7). The same result was obtained with radiolabeled mutated T216 (not shown). Finally, implication of GATA-4 in the binding to the T216 and T168 probes was proven by the supershifts (ssGATA-4) obtained when nuclear extracts and radiolabeled probes were incubated with an anti-GATA-4 antibody (Fig. 4B, lane 4 and Fig. 4C, lane 5, respectively). The identification of another GATA-4 cis-element at -99/-96 may thus explain the result shown in Figure 3B in which GATA-4 transactivation was not completely lost when GATA sites at -168/-165 and -158/-155 were mutated. That third proximal GATA-4 cis-element is therefore most likely involved in the regulation of proximal Muc2 promoter by GATA-4. Of interest, this element (-99/-96) is conserved in the promoter of human MUC2 [23, 27], which makes it central in the regulation of MUC2 by GATA-4 between species. When EMSA was performed with radiolabeled probe T225 containing the fourth putative GATA binding site at -401/-398, no binding was observed, indicating that no GATA factor is binding to that site (not shown).

Having found that GATA-4 transactivates the 2.2 kb fragment of Muc2 promoter (not shown) and that a putative GATA binding site was present at -1521/-1518, we undertook to study whether GATA-4 was binding to that site. The result is shown in Figure 4D. As for T168, when radiolabeled T169 was incubated with CMT-93 nuclear extracts one specific retarded band was visualized (GATA, lane 10). The binding was lost when cold competition was carried out in the presence of a 50x excess of the cold T169 probe (lane 11) whereas nothing happened when cold mutated probe was used in the competition (lane 12). Involvement of the GATA consensus sequence in the binding was confirmed by absence of complex formation when the mutated probe was radiolabeled and incubated with nuclear extracts (lane 15). Finally, binding of GATA-4 on that element was confirmed when supershift analysis was performed in the presence of an anti-GATA-4 antibody in the reaction mixture and resulted in a complete supershifting of the protein-DNA complex (ssGATA-4, lane 13).

Of interest, we noticed that when the radioactive probe T216 was incubated with nuclear extracts (Fig. 4B, lane 2) two specific shifted bands were visualized. As

described above, the low mobility complex corresponds to a GATA-4 cis-element. Analysis of the sequence showed that the T216 probe also contained a putative HNF-3 binding site (Fig. 4A), that may be responsible for the second shifted band. To confirm implication of HNF-3 factors in the binding, we performed supershift analysis with specific anti-HNF-3α and anti-HNF-3β antibodies and one irrelevant anti-HNF-4γ antibody, respectively. As can be seen in Figure 4B, incubation with anti-HNF-3α (lane 5) and anti-HNF-3β (lane 6) resulted in the disappearance of the high mobility complex (HNF), indicated by an asterisk, whereas nothing happened with anti-HNF-4γ (lane 7) antibody. This result indicates that HNF-3α and HNF-3β factors bind to their cognate element at -108/-104, located next to the GATA-4 cis-element at -99/-96 within Muc2 proximal promoter. Previous studies have shown that transcription factors from HNF and GATA families are able to act synergistically to transactivate target genes[28-30]. These mechanisms imply either direct binding to DNA or physical interactions between HNF and GATA factors. It is of importance as HNF3 factors are also involved in the formation of mammalian gut endoderm, early lineage specification and intestinal cell differentiation[28-30]. Preliminary results indicate that HNF-3β is also expressed in Muc2-expressing goblet cells in the murine small intestine (I. Renes, unpublished data), which makes it an important factor to consider in Muc2 regulation as well. Cooperation between factors of the HNF and GATA families has already been described and either implied interaction between GATA-5 and HNF-1α[12, 13] or between GATA-4 and HNF-1α[31]. Our results suggest that such a cooperation may exist between GATA-4 and HNF-3α or HNF-3β to regulate Muc2.

In conclusion the binding studies allowed us to identify three GATA-4 cis-elements within the proximal part of Muc2 promoter at -99/-96, -168/-165, and -158/-155, respectively, and one in its distal part at -1521/-1518. Moreover, a HNF-3α/3β cis-element was identified at-108/-104.

GATA-5 and GATA-6 regulate the activity of the promoter of Muc2

GATA factors bind to the same DNA consensus sequence[8]. Since GATA-5 and GATA-6 are also expressed in the small intestine and have been shown to regulate intestine-specific genes[11-13], we undertook to study whether they were also capable of regulating Muc2 at the transcriptional level. To this aim, CMT-93 cells were co-transfected with WT (black bars) or the mutated form (white bars) of pGL3 deletion mutant -221/+29 and GATA-5 or GATA-6 expression vectors, respectively. As shown in Figure 5A, co transfection of the deletion mutant -221/+29 with either GATA-5 or GATA-6 resulted in a very strong induction of luciferase activity (250 fold activation for both factors, black bars). When mutating the -168/-165 and -158/-155 sites in that fragment, the transactivating effect was completely lost (white bars). This shows that GATA-5 and GATA-6 are also able to transactivate the proximal part of Muc2 promoter. When the same experiments were performed using the longer deletion mutant -563/+29 similar effects were obtained (Fig. 5B), with a 12 fold activation of that region of the promoter by both factors. When using the mutated form of that deletion mutant, GATA-5 transactivating effect was only partially lost (30% reduction, white bars). On the other hand, co-transfection of that mutant with GATA-6 resulted in a total loss of GATA-6 transactivating effect, suggesting that the mutated nucleotides are directly involved in the Muc2 transactivation. Since GATA-5 transactivation was

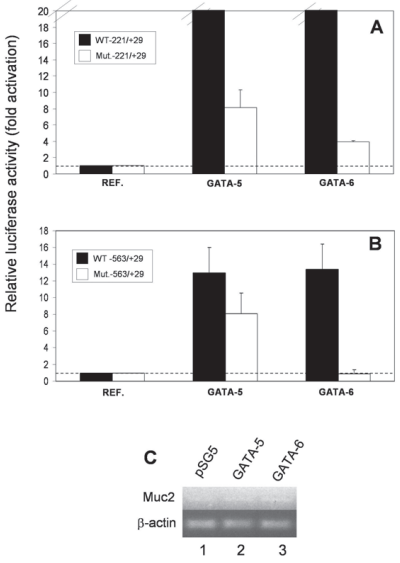

Figure 5. Regulation of *Muc2* mRNA level and promoter activity by GATA-5 and GATA-6 in CMT-93 cells by RT-PCR and transfection assays, respectively. (A) Luciferase diagram showing the effects of overexpression of GATA-5 and GATA-6 on WT deletion construct -221/+29 (black bars) or deletion construct -221/+29 with two mutated GATA-4 sites at -168/-165;-158/-155 (white bars). (B) Luciferase diagram showing the effects of overexpression of GATA-5 and GATA-6 on WT -563/+29 deletion mutant (black bars) or deletion construct -563/+29 with two mutated GATA-4 sites at -168/-165;-158/-155 (white bars). Results are expressed as fold activation of luciferase activity in samples co-transfected with the transcription factor of interest compared with the control co-transfected with the corresponding empty vector (REF.). Results represent means ± S.D. obtained in triplicate in three separate experiments. (C) Endogenous expression of *Muc2* mRNA after cell transfection with either GATA-5 (lane 2) or GATA-6 (lane 3) expression vector or the corresponding empty vector (lane 1).

not completely abolished when using the mutated form of the longest Muc2 deletion mutant (-563/+27), it suggests that Muc2 activation by GATA-5 occurs via indirect mechanisms, most likely involving interactions with co-factors, which bind to the -563/-222 region of the promoter.

We then studied regulation of Muc2 by GATA-5 and GATA-6 in vivo by overexpressing GATA-5 and GATA-6 in the cells followed by the measurement of the level of Muc2 mRNA. When GATA-5 and GATA-6 were overexpressed in CMT-93 cells, only a slight increase of endogenous Muc2 mRNA level was visualized (Fig. 5C, compare lanes 2 and 3 to lane 1). This is in sharp contrast with the strong transactivation at the promoter level and suggests that GATA-5 and GATA-6 need cell-specific co-factors to substantially increase Muc2 endogenous expression in CMT-93 cells. However, it is in agreement with previous data that had established that GATA-5 and GATA-6, which are expressed in numerous tissues, cooperate with cell-specific transcription factors to activate their target genes and confer them a cell-specific pattern of expression[8-11]. For example, GATA-5 was shown to upregulate Muc2 mRNA expression in kidney 293T epithelial cells[32], LPH promoter is efficiently activated when GATA-5 cooperates with HNF-1α and in this case HNF-1α first binds to DNA and then recruits co-factors such as GATA-5, which allows cooperative activation of LPH[13, 33]. Further studies will now be needed to demonstrate whether such a mechanism is also used to upregulate Muc2 expression.

In conclusion, we have shown that GATA-4, which co-localizes with Muc2 in intestinal goblet cells, is a strong transactivator of Muc2 gene expression. GATA-4 induces Muc2 transcription by directly binding to its cognate cis-elements within the promoter. We also showed that GATA-5 and GATA-6, two other members of that family, transactivate Muc2 promoter and that HNF-3α and HNF-3β bind to a

cis-element within the proximal promoter. All these data are in favor of an important role for GATA-4 factor in Muc2 spatio-temporal expression pattern observed in embryonic, fetal and adult small intestine and identifies for the first time Muc2, a gene that is a marker of goblet cells, as a direct target of transcription factors involved in intestinal development and cell differentiation. The identification of GATA-4 as a main regulator of Muc2 is not only important for intestine differentiation but also in other tissues where both GATA-4 and MUC2 are co-expressed. The gastric epithelium in which GATA-4 is also expressed[34] is a good example, especially in gastric cancers associated with development of intestinal metaplasia which are characterized by the ectopic expression of Muc2 [35]. Thus GATA-4 appears as an important general regulator of Muc2 expression and identifies Muc2 as a target of GATA-4 in differentiated intestinal mucosa and metaplastic stomach. Further work is now required to confirm the implication of the other factors, GATA-5, GATA-6 and HNF-3α /3β in the regulation of Muc2 in the intestine and to identify co-factors necessary to activate Muc2 expression *in vivo*.

Acknowledgements

We wish to thank Dr. S. Cereghini (INSERM U423, Hôpital Necker, Paris) for the kind gift of the pMT2-GATA-4 expression vector. We thank Dr. J. K. Divine (Washington University, St-Louis, MO, USA) for the kind gift of the pSG5-GATA-5 and pSG5-GATA-6 expression vectors and Dr. S. D. Krasinski (Harvard Medical School, Boston, MA, USA) for the gift of pcDNA(WT)-GATA-4 vector and its mutated forms pcDNA(-Act)-GATA-4, and pcDNA(C290S)-GATA-4. We are grateful to Dr D. Podolsky (Massachusetts General Hospital, Boston, MA, USA) for providing us with the murine rectal cancer cell line CMT-93.

This work was supported by grants from the Sophia Foundation for Medical Research (MVDS and AWCE), from INSERM/ZonMw

(IVS and AWCE), from l'Association de Recherche sur le Cancer (N°5785, IVS), from la Ligue Régionale du Pas de Calais Contre le Cancer (IVS), from l'Association Francois Aupetit (IVS), and from the European Regional Development Fund. N. Jonckheere is the recipient of a Conseil Régional Nord-Pas de Calais and Centre Hospitalier & Universitaire de Lille PhD fellowship.

References

1. Corfield AP, Carroll D, Myerscough N, Probert CS. Mucins in the gastrointestinal tract in health and disease. Front Biosci 2001;6:D1321-57.
2. Tytgat KM, Büller HA, Opdam FJ, Kim YS, Einerhand AW, Dekker J. Biosynthesis of human colonic mucin: Muc2 is the prominent secretory mucin. Gastroenterology 1994;107:1352-1363.
3. van Klinken BJ, Einerhand AW, Duits LA, Makkink MK, Tytgat KM, Renes IB, Verburg M, Büller HA, Dekker J. Gastrointestinal expression and partial cDNA cloning of murine Muc2. Am J Physiol 1999;276:G115-124.
4. Buisine MP, Devisme L, Savidge TC, Gespach C, Gosselin B, Porchet N, Aubert JP. Mucin gene expression in human embryonic and fetal intestine. Gut 1998;43:519-524.
5. Van Seuningen I, Pigny P, Perrais M, Porchet N, Aubert JP. Transcriptional regulation of the 11p15 mucin genes. Towards new biological tools in human therapy, in inflammatory diseases and cancer? Front Biosci 2001;6:D1216-1234.
6. Mesquita P, Jonckheere N, Almeida R, Ducourouble MP, Serpa J, Silva E, Pigny P, Silva FS, Reis C, Silberg D, Van Seuningen I, David L. Human MUC2 mucin gene is transcriptionally regulated by Cdx homeodomain proteins in gastrointestinal carcinoma cell lines. J Biol Chem 2003;278:51549-51556.
7. Silberg DG, Swain GP, Suh ER, Traber PG. Cdx1 and cdx2 expression during intestinal development. Gastroenterology 2000;119:961-971.
8. Molkentin JD. The zinc finger-containing transcription factors GATA-4, -5, and -6. Ubiquitously expressed regulators of tissue-specific gene expression. J Biol Chem 2000;275:38949-52.
9. Morrisey EE, Ip HS, Lu MM, Parmacek MS. GATA-6: a zinc finger transcription factor that is expressed in multiple cell lineages derived from lateral mesoderm. Dev Biol 1996;177:309-322.
10. Morrisey EE, Ip HS, Tang Z, Lu MM, Parmacek MS. GATA-5: a transcriptional activator expressed in a novel temporally and spatially-restricted pattern during embryonic development. Dev Biol 1997;183:21-36.
11. Gao X, Sedgwick T, Shi YB, Evans T. Distinct functions are implicated for the GATA-4, -5, and -6 transcription factors in the regulation of intestine epithelial cell differentiation. Mol Cell Biol 1998;18:2901-2911.
12. Fang R, Olds LC, Santiago NA, Sibley E. GATA family transcription factors activate lactase gene promoter in intestinal Caco-2 cells. Am J Physiol Gastrointest Liver Physiol 2001;280:G58-67.
13. Krasinski SD, Van Wering HM, Tannemaat MR, Grand RJ. Differential activation of intestinal gene promoters: functional interactions between GATA-5 and HNF-1 alpha. Am J Physiol Gastrointest Liver Physiol 2001;281:G69-84.
14. Aslam F, Palumbo L, Augenlicht LH, Velcich A. The Sp family of transcription factors in the regulation of the human and mouse MUC2 gene promoters. Cancer Res 2001;61:570-6.
15. Renes IB, Boshuizen JA, Van Nispen DJ, Bulsing NP, Büller HA, Dekker J, Einerhand AW. Alterations in Muc2 biosynthesis and secretion during dextran sulfate sodium-induced colitis. Am J Physiol Gastrointest Liver Physiol 2002;282:G382-389.
16. Van Seuningen I, Perrais M, Pigny P, Porchet N, Aubert JP. Sequence of the 5'-flanking region and promoter activity of the human mucin gene MUC5B in different phenotypes of colon cancer cells. Biochem J 2000;348 Pt 3:675-686.
17. Perrais M, Pigny P, Copin MC, Aubert JP, Van Seuningen I. Induction of MUC2 and MUC5AC mucins by factors of the epidermal growth factor (EGF) family is mediated by EGF receptor/Ras/Raf/extracellular signal-regulated kinase cascade and Sp1. J Biol Chem 2002;277:32258-32267.

18. Jonckheere N, Van Der Sluis M, Velghe A, Buisine MP, Sutmuller M, Ducourouble MP, Pigny P, Büller HA, Aubert JP, Einerhand AW, Van Seuningen I. Transcriptional activation of the murine Muc5ac mucin gene in epithelial cancer cells by TGF-beta/Smad4 signalling pathway is potentiated by Sp1. Biochem J 2004;377:797-808.
19. Van Seuningen I, Ostrowski J, Bustelo XR, Sleath PR, Bomsztyk K. The K protein domain that recruits the interleukin 1-responsive K protein kinase lies adjacent to a cluster of c-Src and Vav SH3-binding sites. Implications that K protein acts as a docking platform. J Biol Chem 1995;270:26976-26985.
20. Quandt K, Frech K, Karas H, Wingender E, Werner T. MatInd and MatInspector: new fast and versatile tools for detection of consensus matches in nucleotide sequence data. Nucleic Acids Res 1995;23:4878-4884.
21. Audie JP, Janin A, Porchet N, Copin MC, Gosselin B, Aubert JP. Expression of human mucin genes in respiratory, digestive, and reproductive tracts ascertained by in situ hybridization. J Histochem Cytochem 1993;41:1479-1485.
22. Traber PG. Epithelial cell growth and differentiation. V. Transcriptional regulation, development, and neoplasia of the intestinal epithelium. Am J Physiol 1997;273:G979-981.
23. Velcich A, Palumbo L, Selleri L, Evans G, Augenlicht L. Organization and regulatory aspects of the human intestinal mucin gene (MUC2) locus. J Biol Chem 1997;272:7968-7976.
24. Franks LM, Hemmings VJ. A cell line from an induced carcinoma of mouse rectum. J Pathol 1978;124:35-38.
25. Quaroni A, Wands J, Trelstad RL, Isselbacher KJ. Epithelioid cell cultures from rat small intestine. Characterization by morphologic and immunologic criteria. J Cell Biol 1979;80:248-265.
26. Van Wering HM, Bosse T, Musters A, De Jong E, De Jong N, Hogen Esch CE, Boudreau F, Swain GP, Dowling LN, Montgomery RK, Grand RJ, Krasinski SD. Complex regulation of the lactase-phlorizin hydrolase promoter by GATA-4. Am J Physiol Gastrointest Liver Physiol 2004;287:G899-G909.
27. Gum JR, Hicks JW, Kim YS. Identification and characterization of the MUC2 (human intestinal mucin) gene 5'-flanking region: promoter activity in cultured cells. Biochem J 1997;325 (Pt 1):259-67.
28. Zaret K. Developmental competence of the gut endoderm: genetic potentiation by GATA and HNF3/fork head proteins. Dev Biol 1999;209:1-10.
29. Traber PG, Silberg DG. Intestine-specific gene transcription. Annu Rev Physiol 1996;58:275-97.
30. Ang SL, Wierda A, Wong D, Stevens KA, Cascio S, Rossant J, Zaret KS. The formation and maintenance of the definitive endoderm lineage in the mouse: involvement of HNF3/forkhead proteins. Development 1993;119:1301-1315.
31. Boudreau F, Rings EH, van Wering HM, Kim RK, Swain GP, Krasinski SD, Moffett J, Grand RJ, Suh ER, Traber PG. Hepatocyte nuclear factor-1 alpha, GATA-4, and caudal related homeodomain protein Cdx2 interact functionally to modulate intestinal gene transcription. Implication for the developmental regulation of the sucrase-isomaltase gene. J Biol Chem 2002;277:31909-31917.
32. Ren CY, Akiyama Y, Miyake S, Yuasa Y. Transcription factor GATA-5 selectively up-regulates mucin gene expression. J Cancer Res Clin Oncol 2004.
33. van Wering HM, Huibregtse IL, van der Zwan SM, de Bie MS, Dowling LN, Boudreau F, Rings EH, Grand RJ, Krasinski SD. Physical interaction between GATA-5 and hepatocyte nuclear factor-1alpha results in synergistic activation of the human lactase-phlorizin hydrolase promoter. J Biol Chem 2002;277:27659-27667.

34. Tamura S, Wang XH, Maeda M, Futai M. Gastric DNA-binding proteins recognize upstream sequence motifs of parietal cell-specific genes. Proc Natl Acad Sci U S A 1993;90:10876-10880.
35. Yuasa Y. Control of gut differentiation and intestinal-type gastric carcinogenesis. Nat Rev Cancer 2003;3:592-600.

Chapter 8

Regulation of Mouse Mucin 2 by Hepatocyte Nuclear Factor -3 Factors

Maria van der Sluis*, Audrey Vincent*, Janneke Bouma, Anita Korteland-Van Male, Johannes B. van Goudoever, Ingrid B. Renes and Isabelle Van Seuningen.
Hepatocyte Nuclear Factor 3alpha and -3beta are two important transcriptional regulators of the mucin Muc2 gene in intestinal goblet cells.
* Both authors participated equally in this study

Manuscript in preparation

Abstract

The secretory mucin Muc2, a goblet cell marker, is the major structural component of intestinal mucus and thus plays an important role in maintaining intestinal homeostasis. This mucin has a spatio-temporal pattern of expression during intestinal development and goblet cell differentiation. However, the molecular mechanisms governing its expression during these biological processes are still poorly understood. We previously identified a cis-element for the hepatocyte nuclear factor-3alpha (HNF-3α) and -3beta (HNF-3β) transcription factors next to an important GATA-4 regulatory element. Since HNF-3α and HNF-3β participate in transcriptional programs governing intestinal cell differentiation, we undertook to study their role in Muc2 regulation. Immunohistochemical studies in the mouse small intestine showed co-localisation of HNF-3α and HNF-3β in Muc2-expressing goblet cells. Those two factors were also expressed in the murine CMT-93 colorectal cancer cell line that was used for our transcriptional studies. Gene targeting using RNA interference approach demonstrated that both transcription factors regulate Muc2 transcription. In vivo binding of HNF-3α and HNF-3β to the Muc2 promoter was assessed by chromatin immunoprecipitation assay. Co-transfections experiments with wild-type and mutated forms (for the four HNF3 elements) of the proximal promoter of Muc2 indicated that these four HNF3 elements are necessary to convey Muc2 transcriptional activation. We did not find synergistic activity between GATA-4 and HNF-3α/3β in the proximal promoter. Altogether these results identify *Muc2* as a new target of HNF-3α and HNF-3β and point out an important role for these transcription factors in Muc2 expression in the intestine during development and goblet cell differentiation.

Abbreviations used in this paper

ChIP, Chromatin Immunoprecipitation; E, embryonic day; EMSA, Electrophoretic Mobility Shift Assay; HNF, Hepatocyte nuclear Factor; LPH, Lactase Phlorizin Hydrolase; P, Postnatal days; SI, Sucrase Isomaltase

Introduction

Mucins are complex glycoproteins that represent the major structural proteins of the mucus gel covering the digestive tract surface[1]. The secretory mucin Muc2 is particularly relevant for the study of goblet cell biology as it is exclusively and abundantly expressed by intestinal goblet cells[2, 3].

Muc2 is expressed early during embryonic development of the intestine in a specific spatio-temporal pattern of expression[4]. Moreover, it has been recently identified as a marker of goblet cell since its expression has been associated with differentiation of this type of intestinal cells[5]. Altogether, these data suggest that *Muc2* transcription is under the influence of transcription factors responsible for endoderm-derived cell types during intestinal development and goblet cell differentiation. The early expression of mucins before mucus cell differentiation or during the process of differentiation indicates that their genes may be the targets of transcription factors responsible for those programs[6]. This hypothesis has been recently confirmed in previous studies where we showed that the MUC2 gene is regulated by Cdx1, Cdx2 and GATA-4 transcription factors, which are all involved in intestinal cell differentiation[7-9]. Hepatocyte nuclear factor-3 (HNF-3) HNF-3α and HNF-3β belong to the winged helix/forkhead class of DNA binding proteins also known as Foxa1 and Foxa2, respectively (Fox refers to the Forkhead box)[10]. We will refer to HNF genes in the current manuscript. During embryonic development HNF-3α and HNF-3β mRNA are expressed in the primitive intestine in which Muc2 is also found[4, 11-15]. Intestine-specific enterocyte markers, such as intestinal lactase-phlorizin hydrolase (LPH) and sucrase isomaltase (SI), are controlled at the transcriptional level and relies on the activity of multiple tissue-enriched transcription factors such as Cdx-1/-2, HNF-1/-3/-4 and GATA-4/-5/-6[15 16-19]. HNF3 factors bind the DNA consensus sequence 5'-GATTATTGACTT-3' as monomers[20, 21]. The MUC2 gene is also regulated at the transcriptional level by Cdx[7] and GATA[8] factors however nothing is known regarding its regulation by HNF factors. In a previous study in which we identified GATA-4 as an important regulator of the murine Muc2 gene, we also found a HNF-3α and -3β binding site within the proximal region of the promoter[8]. Moreover, further computer analysis of the murine *Muc2* promoter sequence[22] indicated the presence of several putative HNF binding sites throughout the promoter region. Our previous work suggested a complex regulation of Muc2 in the intestine and more particularly in goblet cells. In order to demonstrate whether HNF3α and HNF3β transcription factors could be part of that complex transcriptional machinery, we undertook to investigate Muc2 regulation by these two factors. Our data demonstrate that both factors bind the promoter *in vivo* and are essential to the basal promoter activity and as such represent important regulators of Muc2 expression in the intestine.

Materials and Methods

Animals

Pregnant female Balb/c mice (Charles River, Maastricht, the Netherlands) were housed at constant temperature and humidity on a 12-h light-dark cycle. The mice had free access to a standard pelleted diet (Special Diets Services, Witham, Essex,

England) and tap water. Pregnant females were sacrificed by cervical dislocation, embryos were isolated and the intestine was excised at E15.5, E17.5, E18.5, postnatal day (P) 1.5 and adults. The small intestine was fixed in 4% paraformaldehyde in PBS and prepared for light microscopy. All the experiments were performed with the approval of the Animal Studies Ethics Committee of our institution (Erasmus MC, Animal Ethics Committee, Rotterdam, the Netherlands).

Immunohistochemistry

Five µm thick paraffin sections were cut and deparaffinized through a graded series of xylol-ethanol. Endogenous peroxidase activity was inactivated by 1.5% (vol/vol) hydrogen peroxide in PBS for 30 min, followed by antigen retrieval in 0.01 M citrate buffer for 10 min at 100°C. Thereafter, sections were incubated with TENG-T (10 mM Tris-HCl, 5 mM EDTA, 150 mM NaCl, 0.25% (w/v) gelatin, 0.05% (w/v) Tween-20) for 30 min to reduce non-specific binding. This was followed by overnight incubation with a 1:1000 dilution of goat anti- HNF-3α (sc-6553X) and HNF-3β (sc-9187X) antibodies (Santa Cruz laboratories, Tebu-Bio, Le Perray en Yvelines, France) in PBS containing 1% (w/v) bovine serum albumin and 0.1% (v/v) Triton X-100. Then, the sections were incubated for 1h with biotinylated horse anti-goat IgG (diluted 1:2000, Vector Laboratories, Peterborough, England) followed by a 1h incubation with ABC/PO complex (Vectastain Elite Kit, Vector Laboratories) diluted 1:400. Binding was visualized after incubation in 0.5 mg/ml 3,3'-diaminobenzidine (DAB), 0.02% (v/v) H_2O_2 in 30 mM imidazole, 1 mM EDTA (pH 7.0). To visualize goblet cells, sections were stained with Alcian Blue 8GX (BDH, Brunschwig Chemie, Amsterdam, the Netherlands). Finally, sections were dehydrated and mounted.

Cell culture

The murine rectal cancer cell line CMT-93 was a kind gift of Dr D. Podolsky (Massachusetts General Hospital, Boston, MA, U.S.A.). The CMT-93 cells were cultured as described in van der Sluis *et al.* [8].

Nuclear extract preparation

Nuclear extracts from CMT-93 cells were prepared as described by Van Seuningen *et al*.[23], and kept at –80°C until use. Protein content (2 µl of cell extracts) was measured using the bicinchoninic acid method as described above.

Western Blotting

The nuclear proteins (20 µg) were separated by electrophoresis using 10% SDS-polyacrylamide gels, followed by electotransfer on a 0.45 *µ*m PVDF membrane (Millipore). Immunostaining was performed as described previously[24]. Briefly, the membrane was washed with Tris-buffered saline-0.2% Tween20 (TBST) containing 20 % non-fat dry milk (w/v), incubated for 1 h at room temperature with the antibodies specific for HNF-3α and HNF-3β (1:1000 dilution, Santa Cruz Laboratories) and then subsequently washed again three times with phosphate-buffered saline containing 0.1% (v/v) Tween-20 before being probed with alkaline phosphatase-conjugated IgGs (Promega). For detection, blots were incubated with Nitro Blue Tetrazolium Chloride and 5-bromo-4-chloro-3-indolyl phosphate substrate (Life Technologies,

Cergy-Pontoise, France). The enzymatic reaction was stopped by soaking the membrane in distilled water.

Cell transfection and luciferase activity assays

The *Muc2*-pGL3 deletion mutants that cover 2.2 kb of the murine Muc2 promoter (Genbank accession number AF221746) were described previously[8]. All plasmids used for transfection were prepared using the Endofree plasmid Mega kit (Qiagen).

Transfections and co-transfections experiments were performed using Effectene® reagent (Qiagen, Courtaboeuf, France) as described previously[25] using 1 μg of Muc2-pGL3 deletion mutants. Total cell extracts were prepared after 48 h incubation at 37°C using 1×Reagent Lysis Buffer (Promega, Charbonnières, France) as described in the manufacturer's instruction manual. Luciferase activity (20 μl) was measured on a TD 20/20 luminometer (Turner Design, Promega). Total protein content in the extract (4 μl) was measured using the bicinchoninic acid method in 96-well plates as described in the manufacturer's instruction manual (Pierce, Bezons, France). In co-transfection experiments, 1 μg of the deletion mutant was transfected with 0.25 μg of the expression plasmid encoding the transcription factor of interest (pMT2-GATA-4 (Dr. S. Cereghini, INSERM, Hôpital Necker, Paris, France), pHD-HNF-3α and pHD-HNF-3β (Dr. J. K. Divine, Washington University, St-Louis, USA). Results were expressed as fold activation of luciferase activity in samples co-transfected with the transcription factor of interest compared with the control co-transfected with the corresponding empty vector.

Site-directed mutagenesis

QuickChange site-directed mutagenesis kit (Stratagene) was used to generate site specific mutations in the four HNF3 binding sites found in the proximal part of *Muc2* promoter. The oligonucleotides containing the mutation were designed according to the manufacturer's instructions and their sequences are depicted in Table I. All mutations were confirmed by DNA sequencing.

RNA interference

CMT-93 cells were seeded 24h before transfection in 24-well tissue culture plates at a density of 23 x 10^3 cells/well in antibiotic free medium. Cells were transfected with 100 nM of either mouse HNF-3α SMARTpool® or mouse HNF-3β SMARTpool® small interfering RNA (siRNA), using 0.5 μl of DharmaFECT™2 transfection reagent according to the manufacturer's instructions. Cells transfected with either siCONTROL™ GAPD siRNA or siCONTROL™ Non-Targeting siRNA Pool#2 and mock-transfected cells were included as controls. DharmaFECT™2 transfection reagent and siRNAs were diluted in serum free medium and incubated for 5 min at room temperature before being mixed and incubated at room temperature for another 20 min. Complete medium (400 μl) was then added to the transfection mix and transferred to the cells. Total RNA was isolated 96h after transfection using the Nucleospin RNA II kit (Macherey-Nagel, Hoerdt, France). Total RNA (1μg) was used to prepare cDNA using oligod(T) (1μl) and recombinant reverse transcriptase M-MLV (1μl) from Promega. PCR was performed on 5 μl of cDNA using a specific

pair of primers (MWG-Biotech, Berlin, Germany) for mouse *Muc2* mucin gene (5'-TGTGGCCTGTGTGGGAACTTT-3', and 5'-CATAGAGGGCCTGTCCTCAGG-3'. Mouse *GAPDH* (forward primer: 5'-TGAAGGGCGACAATCTTCCTC-3'; reverse primer: 5'-CATGTGGGCCATGAGGTCCACCAC-3') was used as the internal control. PCR reactions were carried out in 50 μl final solutions as previously described[7]. Annealing temperatures were 62°C and 59°C, respectively. PCR products were analyzed on a 1.5% agarose gel run in 1X Tris-borate-EDTA buffer. A 100 basepair DNA ladder was purchased from Amersham Biosciences. Expected size for *Muc2* and *GAPDH* PCR products are 558 and 980 basepairs, respectively. All reagents were from Dharmacon (Brebières, France), unless otherwise indicated.

Table I. Sequences of the oligonucleotides used for site-directed mutagenesis.

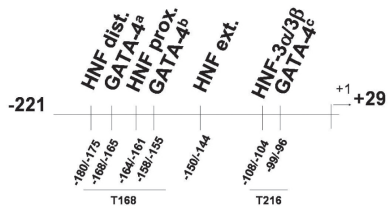

Oligonucleotides used for site-directed mutagenesis		
Mutations	**Sequence 5' γ 3'**	**Position**
WT T216	**CACAGCTGTTTTCCTGATAACTTGGCA**	**-113/-87**
Mut T216 GATA[c]	CCCACAGCTGTTTTCCT*CTTA*ACTTGGCAAATGCCC	-116/-81
Mut T216 HNF-3_/3_	GGAGCCCCCACAGC*TGCGT*TCCTGATAACTTGG	-122/-90
WT T168	**TCATATAAAGATAAACTCAGATAACCT**	**-177/-150**
T168 HNF dist.	CCCAGGGAGTCA*CATGCA*GATAAACTCAG	-186/-158
T168 HNF prox.	CCCAGGGAGTCATATAAAGATA*CGCC*CAGATAAACC	-186/-152
T168 GATA[a+b]	CCAGGGAGTCATATAAA*CT*TAAACTCA*CT*TAACCTGAATCA	-185/-145
T168 HNF dist.+GATA[a+b]	CCCAGGGAGTCA*CATGCACT*TAAACTCA*C*	-186/-159
T168 HNF prox. + GATA[a+b]	CCCAGGGAGTCATATAAA*C*ATA*CGCCCACTT*AACC	-186/-152
T168 HNF ext. +GATA[a+b]	CTCA*CTTA*ACCTG*GATCGG*TATTTCCTCTCCTGGG	-162/-129
WT HNF ext.	**TAACCTGAATCAATATTTCCT**	**-156/-136**
HNF ext.	CTCAGATAACCT*GGATCGG*TATTTCCTCTCTGGG	-162/-129

NOTE. Positions relative to the transcription start site are indicated. Mutated nucleotides are indicated in italics and underlined. Antisense oligonucleotides were also synthesized and used in the reaction mixture for site-directed mutagenesis as described in materials and methods. Muc2 deletion construct -221/+29 is schematically represented with the putative binding sites indicated. The GATA-4 *cis*-elements within the T168 and T216 region and the HNF-3α/3β within the T216 region were identified previously[8].

Chromatin Immunoprecipitation Assay

Soluble chromatin was prepared from 1.0×10^8 CMT-93 cells. Cells were fixed for 10 min at room temperature in 1% (v/v) formaldehyde diluted in the culture medium. Crosslinks were quenched for 5 min with 1x Dulbecco's-PBS (Gibco™, Courbevoie, France) supplemented with 0.125 M Glycine. Thereafter cells were washed consecutively with D-PBS and D-PBS containing 0.5 mM PMSF, 10 μg/ml aprotinin (Sigma, St. Louis, MO, USA), 10 μg/ml leupeptin (Sigma) and 0.2 mM

EDTA. Cells were scraped and collected by centrifugation at 685 x *g* at 4°C for 5 min. Cells were then lysed for 10 min on ice in 2ml of 10mM HEPES buffer pH 7.9 containing 10mM KCl, 1.5 mM $MgCl_2$, 0.1% (v/v) NP-40, 0.2 mM EDTA, 0.5 mM PMSF, 10 μg/ml aprotinin and 10 μg/ml leupeptin. Chromatin was sonicated using Bioruptor™ apparatus (Diagenode, Liège, Belgium) for 10 cycles of 30 sec "on" and 30 sec "off" at 200 W. Debris were cleared by centrifugation at 10,000 x *g* for 10 min at 4°C. The supernatant was pre-cleared by incubating with 50% (v/v) sonicated salmon sperm DNA/protein G agarose gel slurry (Upstate, Mundolsheim, France), to which was added 20 μg/ml BSA and 10 μg/ml sonicated salmon sperm DNA, for 1h at 4°C on a rotating platform. After centrifugation at 1500 x *g* for 1 min at 4°C, an aliquot of the total supernatant was removed as a control (input) and the rest was divided into fractions to be precipitated with either 4 μg of specific antibodies (anti-HNF-3α (sc-6553X), anti-HNF-3β (sc-9187X), anti-GATA4 (sc-1237X), SantaCruz Biotechnology) or with normal rabbit IgGs (Upstate) as the negative control. Immunoprecipitation was performed overnight on a rotating platform at 4°C. Protein G-agarose gel slurry was then added and the incubation was continued for 2 h. Agarose beads were collected and washed sequentially for 4 min in Low Salt Immune Complex Wash Buffer, High Salt buffer, LiCl buffer (Upstate) and twice with TE buffer (pH 8.0). The complexes were eluted with 2 x 0.25 ml of 1% SDS-0.1 M $NaHCO_3$ after a 15 min incubation at room temperature. The eluted immunoprecipitates and the input fraction were incubated overnight in 0.3M NaCl at 65°C followed by a digestion with Qiagen Protease for 1h at 50°C. The DNA was recovered using the Wizard® DNA Clean Up System (Promega) and eluted in 30 μl of 1× TE pH8.0. Three microliters of DNA solution was used as a template for PCR. The primers used for PCR were 5'-AAAGGAATGGAGTTAGTTCAC-3' and 5'-CTTAGCAGGCATCCGAGG-3', covering the -209/-31 region of Muc2 promoter. PCR was performed in a 30 μl final volume consisting of 1x PCR buffer II, 2.5 mM $MgCl_2$, 1.5U AmpliTaq Gold polymerase (Applied Biosystems, Courtaboeuf, France) and 5 pmoles of each primer. The temperature-cycling protocol consisted of 12 min of preheating at 94°C followed by 35 cycles of 45 sec of denaturation at 94°C, 1 min of primer annealing at 50°C, and 1 min of primer extension at 72°C followed by a 10 min final extension at 72°C. Fifteen microliters of the PCR products (239 bp) were loaded and separated on a 2 % agarose gel containing ethidium bromide.

Results

HNF-3α and HNF-3β are expressed in goblet cells of the mouse small intestine

At E15.5, HNF-3α was uniformly expressed by all cells in the developing gut, whereas HNF-3β expression was restricted to the pseudostratified epithelium (Fig1A, showing HNF-3β). HNF3α was expressed by all epithelial and goblet cells in developing crypts and villi, with a slight decrease in intensity of the staining towards the top of the villi (Fig 1C, E, G showing E 18.5, P1.5 and adult respectively). From E17.5 until adulthood the expression of HNF-3β showed a spatio-temporal pattern. More specifically, HNF-3β was observed in the nuclei of the intervillus region (from E 17.5 till P 1.5, Fig. 1D, F and H), in the crypts (adult mice, Fig. 1H) and in goblet cells along the villi (Fig. 1F and H). Alcian blue staining of the mouse small intestine

indicates the location of the goblet cells. Furthermore, immunohistochemical studies performed in developing mouse intestine showed that as from E17.5, the goblet cell markers Muc2 and Tff3 markers were detectable (data not shown).

We can thus conclude that both HNF-3α and HNF-3β transcription factors are expressed in Muc2-expressing goblet cells in the small intestine.

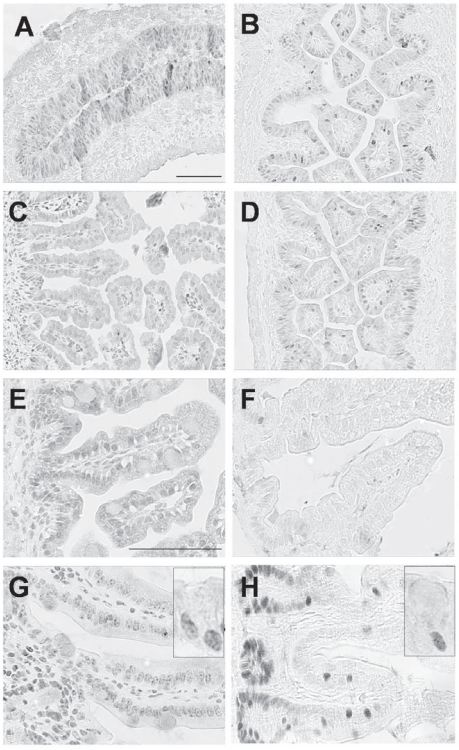

Figure 1. Spatio-temporal expression of HNF-3α and HNF-3β in the mouse small intestine. HNF-3β expression was observed in (A) the pseudostratified epithelium at E15.5, and in the intervillus cells and goblet cells along the villi at (B) E17.5. HNF-3α and -3β staining, respectively of (C-D) E18.5 (E-F) P1.5 and (G-H) adult small intestine. Inserts of G and H show a close-up of a goblet cell stained with HNF-3α and -3β, respectively and counterstained with Alcian Blue. Magnification in A-D and E-H are equal, respectively, bar representing 75μm. Please also see page 223.

Transcriptional regulation of Muc2 by HNF-3α and HNF-3β in murine CMT-93 cells

To study Muc2 transcriptional regulation by HNF-3α and HNF-3β we used the murine colorectal cancer cell line CMT-93. These cells expressed *Muc2* mRNA as shown by RT-PCR (Fig. 2A). Furthermore, these cells expressed HNF-3α and HNF-3β proteins (Fig. 2A) as determined by western blot. In order to identify HNF-3 responsive regions within *Muc2* promoter, co-transfection experiments were then carried out in the presence of pGL3-*Muc2* deletion mutant -221/+29 and HNF-3α or HNF-3β expression vectors (Fig. 2B, black bars and gray bars, respectively). The luciferase diagram indicates that overexpression of both the HNF3 factors resulted in an increase (4-6 fold) of luciferase activity of the -221/+29 construct. When mutated forms of the -221/+29 construct were used, in which the four putative HNF sites were mutated as indicated, transactivation by HNF-3α and -3β was completely lost except for the construct bearing a mutation in the most distal HNF site at -180/-175 (20-30% luciferase activity remaining). This indicates that each of these sites are essential for

efficient transactivation of the proximal promoter of Muc2 both by HNF3α and HNF3β. *In vivo* gene silencing of HNF3α and HNF3β using siRNA approach, confirmed the fact that these two transcription factors regulate Muc2 transcription. Transfection of CMT-93 cells with siRNA specific for HNF3α or HNF3β respectively resulted in a 40%-60% decrease of the amount of Muc2 mRNA in the cells as determined by RT-PCR (Fig. 3).

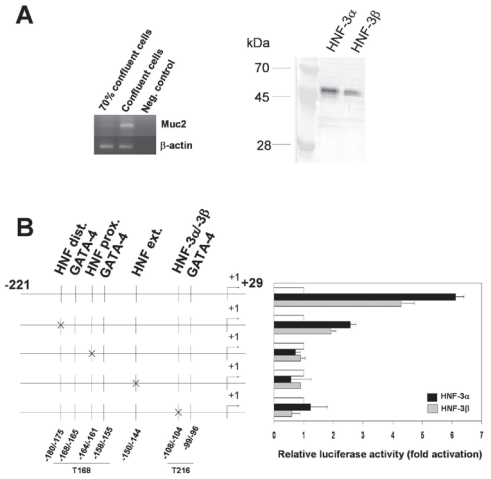

Figure 2. Regulation of Muc2 by HNF-3α and HNF-3β in CMT-93 cells. (A) Endogenous Muc2 mRNA and HNF-3α or HNF-3β protein expression in confluent CMT-93 cells as determined by RT-PCR and western blot, respectively. (B) Luciferase diagram showing the effects of overexpression of HNF-3α (black bars) or HNF-3β (gray bars) on wild-type Muc2 deletion construct –221/+29 or different deletion constructs as schematically represented. Results are expressed as fold activation of luciferase activity in samples co-transfected with the transcription factor of interest compared with the control co-transfected with the corresponding empty vector (REF.). Results represent means ± S.D. obtained in triplicate in three separate experiments.

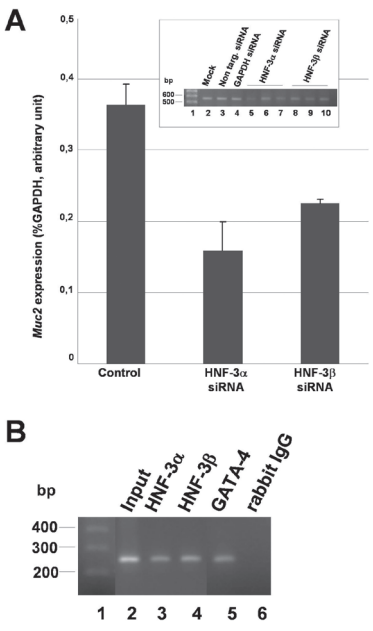

Figure 3. Effect of HNF-3α and HNF-3β in vivo silencing on Muc2 expression in CMT-93 cells and in vivo binding to Muc2 promoter. (A) CMT-93 cells were transfected with siRNA specific for HNF-3α and HNF-3β as described in the Material and Methods. The graph represents densitometric values of the RT-PCR results. A representative example of the RT-PCR results is shown. (B) Protein-DNA complexes from CMT-93 cells were formaldehyde-cross-linked in vivo. Chromatin fragments from these cells were subjected to immunoprecipitation with antibodies against HNF-3α (lane 3), HNF-3β (lane 4), GATA-4 (lane 5) and normal rabbit IgGs (lane 6). After cross-link reversal, the co-immunoprecipitated DNA was amplified by PCR using the indicated primers, and resolved in 2% agarose gel.

In vivo binding of HNF-3α and HNF-3β to the Muc2 promoter in CMT-93 cells

To examine whether HNF-3α and HNF-3β bind to the Muc2 promoter *in vivo*, chromatin from confluent CMT-93 cells was fixed and used for ChIP assays. A specific PCR primer set was used to produce a 239 bp DNA fragment of the –269/–31 *Muc2* promoter region. This region included the four putative HNF3 binding sites determined using MatInspector V2.2[26] and Alibaba2 softwares as well as the GATA-4 *cis*-element previously identified[8]. The 239 bp PCR product was obtained from immunoprecipitates with anti-HNF-3α, anti-HNF-3β and anti-GATA-4 antibodies (Fig. 4A, lanes 3-5). No amplified PCR product was observed when ChIP was carried out with normal rabbit IgGs as the negative control (Fig. 4A, lane 6). These results show that the transcription factors HNF-3α, HNF-3β and GATA-4 bind to the -269/-1 region of Muc2 promoter *in vivo*.

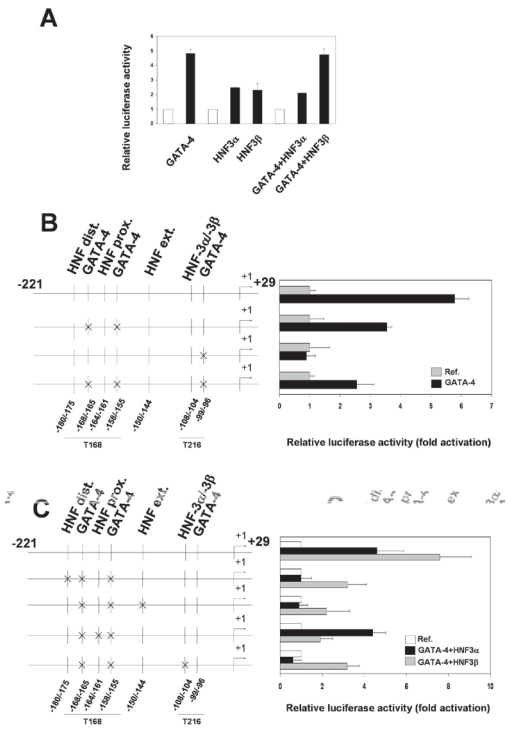

Figure 4. GATA-4 and HNF3 transcription factors do not synergize to activate Muc2 promoter. (A) Luciferase diagram showing the effects of overexpression of GATA-4, HNF-3α or HNF-3β on wild-type deletion construct 221/+29 (black bars). (B) Luciferase diagram showing the effects of co-transfection of wild-type 221/+29 pGL3-Muc2 deletion construct or different mutated 221/+29 pGL3-Muc2 deletion constructs as represented schematically with the wild-type GATA-4 expression vector. (C) Luciferase diagram showing the effects of co-transfection of wild-type 221/+29 pGL3-Muc2 deletion construct or different mutated 221/+29 pGL3-Muc2 deletion constructs as represented schematically with wild-type GATA-4 and HNF-3α (black bars) or HNF3β (gray bars) expression vectors. Results are expressed as fold activation of luciferase activity in samples co-transfected with the transcription factor of interest compared with the control co-transfected with the corresponding empty vector(s) (REF; white bars). Results represent means ± SD obtained in triplicate in three separate experiments.

GATA-4 and HNF3 transcription factors do not synergize to activate Muc2 promoter

Transcription factors from the HNF and GATA families have been shown to be able to act synergistically in transactivating target genes[14, 15, 17]. The luciferase diagram (Fig. 5A) shows that overexpression of GATA-4 and both the HNF3 factors resulted in an increased luciferase activity of the -221/+29 construct corresponding with our previous experiments. However there was no synergistic effect when co-transfecting GATA-4 and HNF-3α or HNF-3β with the -221/+29 deletion construct. When mutating the different GATA sites in the -221/+29 deletion construct there

was loss of transactivation with different efficiencies. Mutation of the two GATA sites within the T168 probe at -168/-165 and -158/-155 resulted into a diminished luciferase activity corresponding to previously published results[8]. This indicates that the more proximal GATA-4 site (at -99/-96) was also active. Indeed when mutating only this site the transactivating effect of GATA-4 on the -221/+29 deletion construct was completely lost, suggesting that this GATA-4 site was the most important to convey Muc2 proximal promoter transactivation. Surprisingly, when mutating all three the GATA sites within the -221/+29 deletion construct, luciferase activity was partly restored.

Co-transfections with GATA-4 and either HNF-3α or -3β and different mutated deletion constructs bearing double GATA/HNF mutations were also performed to identify which site is playing critical role in regulating Muc2 transcription. As expected, co-transfections with wild type (WT) GATA-4 and either HNF-3α or -3β resulted into activation of the wild type -221/+29 deletion construct (Fig. 5C). When mutating the most proximal HNF site (HNF prox., -164/-161) within the T168 region, no loss of transactivation was observed in the presence of HNF-3_ (black bar) whereas 75% was lost in the presence of HNF-3β_(grey bar). When mutating the most distal HNF site (HNF dist.; -180/-175) within the T168 region, 100% and 60% of the transactivation was lost in the presence of HNF-3α or HNF-3β, respectively. However, as the HNF ext. site at -150/-144, proximal to the T216 region and the GATA-4 sites within T216 region were still active (as shown in Figures 2- and 5B), the resulting transactivity with HNF-3β might be caused by these sites. When mutating the HNF ext. site at -150/-144, in addition to the two GATA-4 sites in the T168 region, transactivation by GATA-4/HNF-3α was lost whereas 25% of the activity remained in the presence of HNF-3β. When mutating the two GATA-4 sites in the T168 region (at -168/-165 and -158/-155) and the HNF-3α/3β site at -108/-104 in the T216 region, transactivation by GATA-4 and HNF-3α was completely abolished whereas transactivation by GATA-4 and HNF-3β was reduced by half. Overall, HNF mutations at -180/-175, -150/-144 and -108/-104 completely abolished effects mediated by HNF-3α and mutations at -150/-144 and -164/-161 were the most efficient in inhibiting HNF-3β-mediated effects.

Discussion

Muc2 is expressed early during embryonic development of the intestine[4], which suggests that Muc2 transcription is under the influence of transcription factors responsible for intestinal development and cell differentiation. The early expression of mucin before mucus cell differentiation or during the process of differentiation indicates that they may be the targets of transcription factors responsible for those programs[6]. This hypothesis has been recently confirmed in previous studies on human and mouse Muc2 promoters, in which we showed that the mucin 2 gene is regulated by Cdx1, Cdx2 and GATA-4 transcription factors[7, 8]. Cdx1, Cdx2 and GATA-4 are transcription factors which are also involved in intestinal cell differentiation[9]. During embryonic development HNF-3α and HNF-3β transcription factors are also expressed in the primitive intestine[4, 11-15]. Computer analysis of the murine Muc2 promoter sequence[22] revealed the presence of several putative HNF binding

sites throughout the promoter region. This added to previous results in which we identified a HNF-3α and -3β cis-element within the proximal region of the murine Muc2 promoter[8], suggests that HNF3 transcription factors play an important role in the regulation of Muc2 gene.

In this report we demonstrate that HNF3α and HNF3β transcription factors (i) are co-expressed with Muc2 in colonic goblet cells of the mouse and (ii) that these two transcription factors bind to Muc2 promoter and regulate its transcription *in vivo*. Immunohistochemistry showed that HNF3α was expressed by all epithelial and goblet cells in the crypt and villi, with a slight decrease in intensity of the staining towards the tips of the villi which is in agreement with previous work showing the same pattern of HNF-3α expression along the crypt-villus axis[27]. Localization of HNF-3α in the intestine could imply that this transcription factor is involved in maintaining the differentiation potential of intestinal cells. Further support for this hypothesis are results from previous studies in which they showed that HNF-3α was a critical factor for maintaining the differentiation potential in cell line[13, 28].

Immunohistochemical analysis revealed that HNF-3β was expressed in the region were intestinal stem cells and proliferating cells reside, namely in the intervillus/crypt region, thus suggesting involvement of HNF-3β in maintaining the epithelial cells in an undifferentiated state probably to stimulate epithelial proliferation. This hypothesis is supported by results from a previous study, in which the authors showed that isoforms of the winged helix transcription factors, more specifically, HNF-3/fork head homolog 11A and -11B, induced proliferative signals[20]. Localization of HNF-3β in the crypts our study corresponds to results as previously described by Besnard *et al*.[27]. However, in the current study HNF-3β expression was also observed in differentiated goblet cells along the villi (as of E17.5). This suggests that HNF-3β is required for goblet cell differentiation during development and/or goblet cell-specific gene expression.

Our study shows that HNF-3α and HNF-3β each have the individual capacity of activating *Muc2* both *in vivo* and *in vitro*. HNF-3α has been described as a poor activator compared to HNF3β strong as they would interact with the same DNA binding sequence[29]. However, transfection assays and specific siRNA of these factors showed no distinct differences in potential activation of Muc2, implying that both these factors play a major role in activating Muc2 transcription. Co-transfection assays with GATA-4 and HNF-3α or HNF-3β showed no distinct synergistic effects. Interestingly, as the transcriptions factors are located close to each other on the -221/+29 deletion construct of the Muc2 promoter there may be competition between the transcription factors for the binding. This suggests that the amount of each transcription factor in the cell will be critical and will determine which will be controlling Muc2 transcription. Moreover, preliminary data on a larger fragment of the Muc2 promoter (-1568/+29) indicated that synergistic effects between HNF-3 and GATA-4 occur (unpublished data). This suggests as it has already been described for other intestine-specific genes that synergy between GATA and HNF transcription factors may also control Muc2 transcription[17, 19, 30]. These more remote binding sites within the Muc2 promoter will have to be identified in future experiments. There is increasing evidence that expression levels of intestinal specific target genes (*e.g.* Muc2/ SI) may be a result of gradients and combination of factors during development and differentiation[7, 16, 17, 19,

[30, 31]. Distinct spatio-temporal patterns for several family members of developmental transcription factors (GATA-4/-4/-6, Cdx-2 and HNF-1α/-1β) have been determined in relation to SI and LPH[32], however the expression pattern of these factors in relation to Muc2 in addition to the expression pattern of HNF-3α and -3β and remains to be investigated.

To determine the *in vivo* role of HNF-3α and -3β on Muc2 expression in the intestine of both HNF-3α and -3β deficient mice would be interesting. However, to our knowledge Muc2 expression in these mice has not been determined. HNF-3β deficient mice embryos die because of defect in neural tube and HNF-3α deficient mice develop hypoglycemia and die parentally[13, 29]. Our data however, imply that both HNF-3α and –β could modulate Muc2 expression during development.

In summary, we were able to identify HNF-3α and -3β as major regulators Muc2 gene expression, and showed that HNF-3α and -3β i) are both expressed in Muc2-expressing goblet cells in the small intestine, ii) are both potent activators of the Muc2 promoter activity, iii) mediate Muc2 regulation by directly interacting with their cognate elements within Muc2 proximal promoter, and iv) are both required for endogenous expression of Muc2. Our results identify Muc2, a goblet cell marker, as a new target gene of HNF-3α and HNF-3β and point out an important role for these factors in Muc2 expression in the intestine.

Acknowledgements

We would like to thank C. Chauvin and M.H.M. Melis for their excellent technical assistance. We wish to thank Dr. J. K. Divine (Washington University, St-Louis, USA) for the kind gift of pHD-HNF-3α and pHD-HNF-3β expression vectors and Dr. S. Cereghini for the kind gift of pMT2-GATA-4 vector (INSERM, Hôpital Necker, Paris, France). We are grateful to Dr D. Podolsky (Massachusetts General Hospital, Boston, MA, USA) for providing us with the murine rectal cancer cell line CMT-93.

A. Vincent is the recipient of a Conseil Régional Nord-Pas de Calais and the Institut National de la Santé et de la Recherche Médicale PhD fellowship. This work was supported by grants from the Sophia Foundation for Medical Research (MVDS), from INSERM/ZonMw-NWO (IVS, IBR) and from l'Association Francois Aupetit (IVS).

References

1. Corfield AP, Carroll D, Myerscough N, Probert CS. Mucins in the gastrointestinal tract in health and disease. Front Biosci 2001;6:D1321-57.
2. Tytgat KM, Büller HA, Opdam FJ, Kim YS, Einerhand AW, Dekker J. Biosynthesis of human colonic mucin: Muc2 is the prominent secretory mucin. Gastroenterology 1994;107:1352-1363.
3. van Klinken BJ, Einerhand AW, Duits LA, Makkink MK, Tytgat KM, Renes IB, Verburg M, Büller HA, Dekker J. Gastrointestinal expression and partial cDNA cloning of murine Muc2. Am J Physiol 1999;276:G115-124.
4. Buisine MP, Devisme L, Savidge TC, Gespach C, Gosselin B, Porchet N, Aubert JP. Mucin gene expression in human embryonic and fetal intestine. Gut 1998;43:519-524.
5. van der Sluis M, de Koning BAE, de Bruijn ACJM, Velcich A, Meijerink JPP, van Goudoever JB, Büller HA, Dekker J, van Seuningen I, Renes IB, Einerhand AWC. Muc2-Deficient Mice Spontaneously Develop Colitis, Indicating That MUC2 Is Critical for Colonic Protection. Gastroenterology 2006;131:117-129.
6. Van Seuningen I, Pigny P, Perrais M, Porchet N, Aubert JP. Transcriptional regulation of the 11p15 mucin genes. Towards new biological tools in human therapy, in inflammatory diseases and cancer? Front Biosci 2001;6:D1216-1234.
7. Mesquita P, Jonckheere N, Almeida R, Ducourouble MP, Serpa J, Silva E, Pigny P, Silva FS, Reis C, Silberg D, Van Seuningen I, David L. Human MUC2 mucin gene is transcriptionally regulated by Cdx homeodomain proteins in gastrointestinal carcinoma cell lines. J Biol Chem 2003;278:51549-51556.
8. van der Sluis M, Melis MH, Jonckheere N, Ducourouble MP, Büller HA, Renes I, Einerhand AW, Van Seuningen I. The murine Muc2 mucin gene is transcriptionally regulated by the zinc-finger GATA-4 transcription factor in intestinal cells. Biochem Biophys Res Commun 2004;325:952-60.
9. Silberg DG, Swain GP, Suh ER, Traber PG. Cdx1 and cdx2 expression during intestinal development. Gastroenterology 2000;119:961-971.
10. Kaestner KH, Knochel W, Martinez DE. Unified nomenclature for the winged helix/forkhead transcription factors. Genes Dev 2000;14:142-6.
11. Kaestner KH, Hiemisch H, Luckow B, Schutz G. The HNF-3 gene family of transcription factors in mice: gene structure, cDNA sequence, and mRNA distribution. Genomics 1994;20:377-85.
12. Sasaki H, Hogan BL. Differential expression of multiple fork head related genes during gastrulation and axial pattern formation in the mouse embryo. Development 1993;118:47-59.
13. Ang SL, Wierda A, Wong D, Stevens KA, Cascio S, Rossant J, Zaret KS. The formation and maintenance of the definitive endoderm lineage in the mouse: involvement of HNF3/forkhead proteins. Development 1993;119:1301-1315.
14. Zaret K. Developmental competence of the gut endoderm: genetic potentiation by GATA and HNF3/fork head proteins. Dev Biol 1999;209:1-10.
15. Traber PG, Silberg DG. Intestine-specific gene transcription. Annu Rev Physiol 1996;58:275-97.
16. Van Wering HM, Bosse T, Musters A, De Jong E, De Jong N, Hogen Esch CE, Boudreau F, Swain GP, Dowling LN, Montgomery RK, Grand RJ, Krasinski SD. Complex regulation of the lactase-phlorizin hydrolase promoter by GATA-4. Am J Physiol Gastrointest Liver Physiol 2004;287:G899-G909.
17. Boudreau F, Rings EH, van Wering HM, Kim RK, Swain GP, Krasinski SD, Moffett J, Grand RJ, Suh ER, Traber PG. Hepatocyte nuclear factor-1 alpha, GATA-4, and caudal related homeodomain protein Cdx2 interact functionally to modulate intestinal gene transcription.

Implication for the developmental regulation of the sucrase-isomaltase gene. J Biol Chem 2002;277:31909-31917.

18. Bosse T, van Wering HM, Gielen M, Dowling LN, Fialkovich JJ, Piaseckyj CM, Gonzalez FJ, Akiyama TE, Montgomery RK, Grand RJ, Krasinski SD. Hepatocyte nuclear factor-1{alpha} is required for expression but dispensable for histone acetylation of the lactase-phlorizin hydrolase gene in vivo. Am J Physiol Gastrointest Liver Physiol 2006;290:G1016-24.
19. Fang R, Olds LC, Santiago NA, Sibley E. GATA family transcription factors activate lactase gene promoter in intestinal Caco-2 cells. Am J Physiol Gastrointest Liver Physiol 2001;280:G58-67.
20. Ye H, Kelly TF, Samadani U, Lim L, Rubio S, Overdier DG, Roebuck KA, Costa RH. Hepatocyte nuclear factor 3/fork head homolog 11 is expressed in proliferating epithelial and mesenchymal cells of embryonic and adult tissues. Mol Cell Biol 1997;17:1626-41.
21. Hromas R, Costa R. The hepatocyte nuclear factor-3/forkhead transcription regulatory family in development, inflammation, and neoplasia. Crit Rev Oncol Hematol 1995;20:129-40.
22. Aslam F, Palumbo L, Augenlicht LH, Velcich A. The Sp family of transcription factors in the regulation of the human and mouse MUC2 gene promoters. Cancer Res 2001;61:570-6.
23. Van Seuningen I, Ostrowski J, Bustelo XR, Sleath PR, Bomsztyk K. The K protein domain that recruits the interleukin 1-responsive K protein kinase lies adjacent to a cluster of c-Src and Vav SH3-binding sites. Implications that K protein acts as a docking platform. J Biol Chem 1995;270:26976-26985.
24. Jonckheere N, Van Der Sluis M, Velghe A, Buisine MP, Sutmuller M, Ducourouble MP, Pigny P, Büller HA, Aubert JP, Einerhand AW, Van Seuningen I. Transcriptional activation of the murine Muc5ac mucin gene in epithelial cancer cells by TGF-beta/Smad4 signalling pathway is potentiated by Sp1. Biochem J 2004;377:797-808.
25. Perrais M, Pigny P, Copin MC, Aubert JP, Van Seuningen I. Induction of MUC2 and MUC5AC mucins by factors of the epidermal growth factor (EGF) family is mediated by EGF receptor/Ras/Raf/extracellular signal-regulated kinase cascade and Sp1. J Biol Chem 2002;277:32258-32267.
26. Quandt K, Frech K, Karas H, Wingender E, Werner T. MatInd and MatInspector: new fast and versatile tools for detection of consensus matches in nucleotide sequence data. Nucleic Acids Res 1995;23:4878-4884.
27. Besnard V, Wert SE, Hull WM, Whitsett JA. Immunohistochemical localization of Foxa1 and Foxa2 in mouse embryos and adult tissues. Gene Expr Patterns 2004;5:193-208.
28. DiPersio CM, Jackson DA, Zaret KS. The extracellular matrix coordinately modulates liver transcription factors and hepatocyte morphology. Mol Cell Biol 1991;11:4405-14.
29. Duncan SA, Navas MA, Dufort D, Rossant J, Stoffel M. Regulation of a transcription factor network required for differentiation and metabolism. Science 1998;281:692-5.
30. Krasinski SD, Van Wering HM, Tannemaat MR, Grand RJ. Differential activation of intestinal gene promoters: functional interactions between GATA-5 and HNF-1 alpha. Am J Physiol Gastrointest Liver Physiol 2001;281:G69-84.
31. Mitchelmore C, Troelsen JT, Spodsberg N, Sjostrom H, Noren O. Interaction between the homeodomain proteins Cdx2 and HNF1alpha mediates expression of the lactase-phlorizin hydrolase gene. Biochem J 2000;346 Pt 2:529-35.
32. Fang R, Olds LC, Sibley E. Spatio-temporal patterns of intestine-specific transcription factor expression during postnatal mouse gut development. Gene Expr Patterns 2006;6:426-32.

Chapter 9

Transcriptional Regulation of Mouse Mucin 5ac

Published as:
Nicolas Jonckheere, Maria van der Sluis, Amélie Velghe, Marie-Pierre Buisine, Marjolein Sutmuller, Marie-Paule Ducourouble, Pascal Pigny, Hans A. Büller, Jean-Pierre Aubert, Alexandra W.C. Einerhand and Isabelle van Seuningen. Tanscription activation of the murine Muc5ac mucin gene in epithelial cancer cells by TGF-β/Smad signaling pathway is potentiated by Sp1.

Biochemical Journal 1;377(Pt 3):797-808 Feb, 2004

Abstract

Changes in the expression of mucin genes in gastrointestinal cancers is thought to contribute to the development of the disease. In our laboratory we have previously shown that MUC5AC is aberrantly expressed in rectosigmoid villous adenomas. However, the regulatory mechanisms underlying that altered profile of expression is unknown. In order to study its regulation at the transcriptional level, we have isolated and characterized 5.5 kb of the 5'-flanking region of the mouse Muc5ac mucin gene. Results & Conclusions: The promoter is flanked by a TATA box and a transcriptional start site is located 22 bp downstream of the TATA box. Analysis of the sequence showed a high density of binding sites for Smad4, an essential factor in the signaling cascade activated by TGF-β, and Sp1, an important factor in the regulation of MUC5AC. This led us to study Muc5ac regulation by TGF-β. We show that exogenous addition of TGF-β to the cells induces Muc5ac endogenous expression, promoter activity and Smad4 binding to the promoter. By co-transfection studies we show that Smad4 is essential for Muc5ac promoter activation and that it does not synergize with Smad2 or Smad3. By gel-retardation and co-transfection assays, we identified Sp1 and Sp3 as important regulators of Muc5ac expression and showed that Smad4 and Sp1 act in a cooperative manner to transactivate Muc5ac promoter activity. Altogether these results bring new insights into the molecular mechanisms of TGF-β-mediated up-regulation of Muc5ac and enhance our understanding as to how Muc5ac is regulated in certain pathologies of the gastrointestinal tract.

Abbreviations used in this paper

aa, amino acid; EMSA, Electrophoretic Mobility Shift Assay; TBST, Tris-Buffered Saline-Tween 20; TGF-β, Transforming Growth Factor-β; SSC

Introduction

Mucins have been postulated to be important molecules in maintaining epithelial homeostasis in inflammatory diseases and cancer. Mucins are large O-glycoproteins expressed either at the cell surface as transmembrane proteins or as secreted oligomeric molecules to form a protective gel[1-4]. In the gastrointestinal tract, they play a cytoprotective role against acid and pepsin in the gastric juice and against deleterious effects of exogenous agents (pathogens, drugs) and against mechanical damage[5, 6]. MUC5AC belongs to the family of secreted mucins that participate in mucus formation and is encoded by a gene located on the p15 arm of chromosome 11 within a cluster of four mucin genes along with MUC2, MUC5B and MUC6[7, 8].

In normal adult, MUC5AC main territories of expression are the surface epithelium of the respiratory tract and stomach[9]. This expression is restricted to mucus-producing lung goblet cells and gastric pit cells. MUC5AC normal pattern of expression is altered in several epithelial diseases of the gastrointestinal tract. It is aberrantly expressed in Barrett's esophagus[10, 11], in gastric metaplasia in the duodenum[12], in colon adenoma and cancer[6, 13]. In rectosigmoid villous adenoma, MUC5AC expression was found very early during the carcinogenetic sequence, in low grade dysplasia, which makes it a valuable marker for recurrent patients[14]. Despite increasing amounts of data regarding its expression pattern in normal human tissues compared with that in disease[6, 15], the precise biological role of MUC5AC as a key gene during sequential steps of carcinogenesis or in inflammatory processes has yet to be proven. Moreover, the molecular mechanisms that govern MUC5AC expression in the gastrointestinal tract are still largely unknown, thus their identification is necessary if one wants to better understand the role of MUC5AC in the pathologies of the gastrointestinal epithelium.

Transforming growth factor-beta (TGF-β) is a member of the superfamily of cytokines that affect a variety of cell types and elicit a wide array of cell-type-specific biological effects such as differentiation, migration, cell cycle arrest, adhesion, extracellular matrix production, and apoptosis[16]. TGF-β is also an agent involved in gastritis and development of gastric cancer[17], two pathologies in which MUC5AC expression is altered. TGF-β-induced signaling occurs when the TGF-β ligand binds to the type II receptor (TGF-β RII), which heterodimerizes with the type I receptor (RI). RI then phosphorylates receptor-activated Smads (Smad2, Smad3). Once activated Smad2 and Smad3 bind to Smad4 and this complex translocates to the nucleus whereupon transcription activation of the target gene occurs[18].

Recent isolation of Muc1 and Muc2 murine mucin genes as well as their regulatory regions has helped a great deal in defining their biological roles in vivo and the molecular mechanisms responsible for their regulation. The studies performed on murine Muc1 mucin gene, which encodes a transmembrane mucin, and on Muc1$^{-/-}$ mice showed that it is overexpressed in most carcinomas, correlates with high metastatic potential and poor survival and participates to tumor progression[19]. More recently, the promoter region of murine Muc2, which belongs to the secreted mucins, was characterized[20]. The authors showed, as for its human counterpart and other mucin genes, that Sp1 is an important factor in Muc2 regulation[20]. Interestingly, the knock-out mice for Muc2 mucin gene allowed the authors to demonstrate for the first

time a direct link between Muc2 expression and tumor formation as Muc2$^{-/-}$ mice started to develop intestinal adenomas that progressed to invasive adenocarcinoma and colorectal tumors as they were getting older[21]. From this work, the authors concluded that Muc2 is involved in colon cancer and may be considered as a tumor suppressor gene[21].

Murine Muc5ac mucin gene is partially characterized and part of its tandem repeat region was published by Shekels *et al*[22]. Of interest, the authors showed that Muc5ac is located on murine chromosome 7 that is the syntenic chromosomal region corresponding to human chromosome 11. Thus, it appears from this work and recent data released from the human and mouse genome databases (NCBI, MGI) that murine Muc2, Muc5ac, Muc5b and Muc6 are clustered on murine chromosome 7, which means that this cluster of mucin genes is conserved throughout evolution[23].

Our aim is to better understand the transcriptional regulation of human and murine mucin genes in order to propose new therapeutic targets in epithelial diseases (inflammation and cancer) and better understand their role during embryonic development and differentiation of the gastrointestinal epithelium[8]. In this study, we have isolated, characterized and studied the regulation of the 5'-flanking region of murine Muc5ac mucin gene in order to obtain a base for future studies in animal models[6] and better understand MUC5AC biological role in the pathophysiology of the epithelium. We show for the first time that Muc5ac is regulated at the transcriptional level by TGF-β, an agent involved in gastritis and development of gastric cancer.

Material and methods

Cloning and characterization of murine Muc5ac 5'-flanking region

The 5'-flanking region of murine Muc5ac mucin gene was isolated and characterized after screening a murine OLA 129 genomic DNA library made in λGEM12 (kindly provided by Dr. A. Berns, Amsterdam, the Netherlands) with a probe spanning 750 basepairs (bp) of the human MUC5AC N-terminus (AF043909)[24]. Two positive plaques were identified and the corresponding DNA was isolated from the bacteriophages by using the Lambda DNA isolation kit (Qiagen, Courtaboeuf, France) according to the manufacturer's protocol. Southern blot analysis and restriction mapping of both inserts identified a 5.5 kilobases (kb) fragment that hybridized with 750 bp of the human MUC5AC. The positive 5.5 kb fragment was subsequently cloned into the SstI site of pBluescript II SK (+/-) (Stratagene, Amsterdam, the Netherlands), which resulted in clone pMS1. That fragment was then digested by ApaI and PstI to raise smaller fragments pMS2-pMS7. The clones pMS1-pMS7 were sequenced by Eurogentec (Seraing, Belgium) using T3 and T7 primers, and in the laboratory using the DYEnamic ET* Terminator Cycle Sequencing Kit, with fluorescent-labeled nucleotides (Amersham, GE Healthcare Bio-Sciences, Orsay, France), according to the manufacturer's protocol. Sequence reactions were analyzed on an ABI-PRISM 310 Genetic analyzer (Perkin Elmer-Applied Biosystems, Courtaboeuf, France). The obtained sequences were aligned with the BioEdit sequence alignment editor. The derived 5.5 kb nucleotide and amino acid sequences were compared to known sequences using NCBI-blast database. In addition, the sequence was analyzed with PC/Gene software (Intelligenetics, Inc., Mountain View, CA, USA), INFOBIOGEN

database and MatInspector V2.2 and Alibaba2 softwares based on the Genomatix database to determine the location of putative transcription factor binding sites[25]. The nucleotide sequence of pMS1 clone was submitted to Genbank under the accession number AF288076.

Determination of 5'-end of Muc5ac mRNA by RACE-PCR

The transcription start site was determined by 5'-RACE (rapid amplification of cDNA ends) using the 5'/3' RACE kit (Roche Molecular Biochemicals, Meylan, France) according to the manufacturer's instructions. RACE-PCR was conducted on mouse total gastric RNA (2 μg) using oligonucleotides 5'-CAGGGAAGTAGAAGACCTGTCC-3' as first primer and 5'-TGTGCATTGGCTGCAGGCCAG-3' as nested primer for reverse transcription and amplification. Resulting amplified PCR products were cloned directly into TA cloning vector (Invitrogen, Cergy Pontoise, France) and sequenced on an automatic LI-COR sequencer (ScienceTech, Bordeaux, France) with T7 and RM13 primers as described thereafter.

Animals

Adult specified pathogen free Balb/c mice, obtained from Harlan (Zoetermeer, the Netherlands), were sacrificed by cervical dislocation. Stomach was removed and fixed in 4% paraformaldehyde in PBS and subsequently processed for light microscopy as previously described[26]. The animal experiments were performed with the approval of the Animal Studies Ethics Committee of the Erasmus MC (Rotterdam, the Netherlands).

Histology

Five μm-thick sections of mouse stomach tissue were routinely stained with hematoxylin and eosin (HE) to study the morphology, or stained with Alcian Blue/ Periodic Acid Schiff (PAS) reagent to stain for acidic and neutral mucins, respectively. Immunolocalization of mouse Muc5ac was carried out as previously described[11] using 45M1 monoclonal antibody (Novocastra, Valkenswaard, the Netherlands).

Probe preparation for in situ hybridization

Total RNA was extracted from murine stomach using TRIzol (Life technologies, Breda, the Netherlands) following the manufacturer's protocol. RNA (1 μg) was transcribed at 42°C into cDNA using M-MLV Reverse transcriptase (Promega, Madison, WI, USA) in a total volume of 20 μl following the manufacturer's protocol. This was followed by a PCR reaction using 1 μl cDNA as template in 10 mM Tris-HCl buffer pH 8.4, containing 50 mM KCl, 2 mM $MgCl_2$, 0.01% gelatin, 1 U Taq polymerase (Eurogentec, Seraing, Belgium), 0.2 mM dNTPs, and 10 pmoles of each primer. The primers were (5'-CCAATTGGCTAGATGGCAGT-3') and (5'-AGATCAAACCCTCCTCTCG-3'), which corresponds to nucleotides 374-394 and 552-572 of murine Muc5ac, Genbank L42292[22]. The PCR sample (20 μl) was first denatured at 96°C for 5 min, followed by 30 cycles at 96°C for 1 min, 60°C for 1 min, and 72°C for 1 min and a final extension step at 72°C for 2 min. The resulting 199 bp PCR product was isolated using the Qiagen gel extraction kit and ligated into the EcoRI site of pBluescript SK vector and subsequently sequenced. The digoxigenin-

11-UTP-labeled sense and antisense Muc5ac RNA probes were prepared according to the manufacturer's protocol (Roche, Almere, the Netherlands).

In situ hybridization

Tissue sections were deparafinized with xylene and rehydrated through RNase free ethanol/water solutions. The non-radioactive *in situ* hybridization was essentially carried out as described previously[27]. Briefly, the riboprobes were diluted in hybridization solution (50% deionized formamide (v/v), 10% dextran sulfate (w/v), 2X SSC, 1X Denhardt's solution, 1 μg/ml tRNA, 250 μg/ml herring sperm DNA) to a concentration of 100 ng/ml, hybridized overnight at 55°C in a humid chamber. Post-hybridization washes were performed at 45°C using the following steps: 50% formamide (v/v) in 2X SSC, 50% formamide (v/v) in 1X SSC and 0.1X SSC. A 15 min incubation with RNase T1 (2 U/ml in 1 mM EDTA in 2X SSC) at 37 °C was followed by washes of 0.1X SSC at 45°C and 2X SSC at room temperature (RT). The digoxigenin-labeled hybrids were detected by incubation with anti-digoxigenin (Fab, 1:2000) conjugated to alkaline phosphatase for 2.5 h at RT. Thereafter, sections were washed in 0.025% (v/v) Tween in Tris-buffered saline pH 7.5. For staining, sections were layered with detection buffer (0.1M Tris-HCl, pH 9.5 containing 0.1M NaCl and 0.05M $MgCl_2$) containing 0.33 mg/ml 4-nitroblue tetrazolium chloride, 0.16 mg/ml 5-bromo-4-chloro-3-indolyl-phosphate, 8% (v/v) polyvinylalcohol (Mw 31000-50000 Aldrich Chemical, Milwaukee, WI, USA) and 1 mM levamisol (Sigma, St. Louis, MO, USA). Development of the reaction was performed overnight in the dark and was stopped when the desired intensity of the resulting blue precipitate was reached. Finally, sections were washed in distilled water and mounted with Aquamount improved (Gurr, Brunschwig, Amsterdam, the Netherlands).

Muc5ac-pGL3 deletion mutant constructions

The Muc5ac-pGL3 deletion mutants that cover 1.2 kb of the promoter were constructed into pGL3 Basic vector (Promega, Charbonnieres-les-Bains, France) using a PCR-based method as previously described[28, 29]. PCR reactions were carried out on pMS1 clone in order to subclone the promoter region of Muc5ac. PCR products were then subcloned into pCR2.1 vector (Invitrogen) before subcloning into SacI-MluI sites of the promoterless pGL3 Basic vector. Internal deletion mutants were generated by PCR using pairs of primers bearing specific restriction sites at their 5' and 3' ends (Table I). PCR products were digested, gel-purified (Qiaquick gel extraction kit, Qiagen) and subcloned into the pGL3 Basic vector that had been previously cut with the same restriction enzymes. All clones were sequenced on both strands on an automatic LI-COR sequencer using infra-red labeled RV3 and GL2 primers (Promega). Plasmids used for transfection studies were prepared using the Endofree plasmid Mega kit (Qiagen).

Cell culture

Murine rectal cancer cell line CMT-93 was a kind gift of Dr. D. Podolsky (Boston, USA). CMT-93 were cultured in DMEM medium containing 10% fetal bovine serum, 4 mM L-glutamine, penicillin (100 U/ml), and streptomycin (100 μg/ml). IEC-6 cells were purchased from ECACC (European collection of animal cell cultures). This cell

line was established from rat small intestine crypt cells and was cultured in DMEM medium containing 5% fetal bovine serum, 2 mM L-glutamine, 10 μg/ml insulin, 50 U/ml penicillin and 50 μg/ml streptomycin. HCT116-Smad4$^{+/+}$ and HCT116-Smad4$^{-/-}$ cells were a kind gift of Dr. A. Atfi (INSERM U482, Paris). Cells were cultured in DMEM supplemented with 2 mM glutamine and 10 % fetal calf serum. Human gastric cancer cell line KATO-III was cultured as previously described[30]. All cells were cultured at 37°C in a humidified 5% CO_2 water-jacketed incubator. To study TGF-β effect, cells were incubated for 24h with TGF-β (recombinant human TGF-β, 10 ng/ml). All reagents were from Sigma unless otherwise indicated.

Table I. Sequences of the pairs of oligonucleotides used in PCR to produce deletion mutants covering *Muc5ac* promoter.

Position in the promoter	Oligonucleotide sequences (5' → 3')	Orientation
-199/+3	5'-CGC ***GAG CTC*** TGG GGG AGC CTC AGG GAA -3'	S
	5'-CGC ***ACG CGT*** GAA AGA CTC TAG TCA CCA -3'	AS
-199/+132	5'-CGC ***GAG CTC*** TGG GGG AGC CTC AGG GAA -3'	S
	5'-CGC ***ACG CGT*** ACT TTG AGT CTT ACC TGT GCA-3'	AS
-376/+3	5'-CGC ***GAG CTC*** CTC CTC TCC AGG GAA ATG -3'	S
	5'-CGC ***ACG CGT*** GAA AGA CTC TAG TCA CCA -3'	AS
-376/+132	5'-CGC ***GAG CTC*** CTC CTC TCC AGG GAA ATG -3'	S
	5'-CGC ***ACG CGT*** ACT TTG AGT CTT ACC TGT GCA-3'	AS
-1021/+3	5'-CGC ***GAG CTC*** CTC TCT TTC ACA CAC ACA -3'	S
	5'-CGC ***ACG CGT*** GAA AGA CTC TAG TCA CCA -3'	AS
-1021/+132	5'-CGC ***GAG CTC*** CTC TCT TTC ACA CAC ACA -3'	S
	5'-CGC ***ACG CGT*** ACT TTG AGT CTT ACC TGT GCA-3'	AS
-1171/+3	5'-CGC ***GAG CTC*** CAC TCC TGT GAT GTG TGA -3'	S
	5'-CGC ***ACG CGT*** GAA AGA CTC TAG TCA CCA -3'	AS
-1171/+132	5'-CGC ***GAG CTC*** CAC TCC TGT GAT GTG TGA -3'	S
	5'-CGC ***ACG CGT*** ACT TTG AGT CTT ACC TGT GCA-3'	AS
-1021/-828	5'-CGC ***GAG CTC*** CTC TCT TTC ACA CAC ACA -3'	S
	5'-CGC ***ACG CGT*** AGA GAG GTC AAA GCT TAA -3'	AS
-1171/-828	5'-CGC ***GAG CTC*** CAC TCC TGT GAT GTG TGA -3'	S
	5'-CGC ***ACG CGT*** AGA GAG GTC AAA GCT TAA -3'	AS

NOTE *SacI* (GAGCTC) and *Mlu*I (ACGCGT) sites (bold and italicized) are added at the end of the primers to direct subcloning into pGL3 basic vector. S, sense; AS, antisense.

Reverse transcriptase PCR

Total RNAs from cultured cells and mouse tissues were prepared using the QIAamp RNA blood mini-kit and midi-kit (Qiagen), respectively. Total RNA (1.5 μg) was used to prepare first strand cDNA (Advantage™ RT-for-PCR kit, Clontech, Ozym, Saint Quentin Fallavier, France). PCR was performed on 2 μl of cDNA using specific pairs of primers as follows: Muc5ac (5'-GAGGGCCCAGTGAGCATCTCC-3', and 5'-TGGGACAGCAGCAGTATTCAGT-3'; accession number AJ010792); β-actin was used as an internal control (5'-GTGGGCCGCTCTAGGCACCA-3' and 5'-TGGCCTTAGGGTGCAGGGGG-3'; accession number M12481). Muc5ac and β-actin PCR product sizes are 361 and 241 bp, respectively. Mouse TGF-βRII (5'-CGTGTGGAGGAAGAACAACA-3' and 5'-TCTCAAACTGCTCTGAGGTG-3'; accession number S69114). PCR product is 560 bp long. Rat β-actin (5'-ATATCGCTGCGCTCGTCGTCGACAA-3' and 5'-AACACAGCCTGGATGGCTACGTACAT-3'; accession number V01217). PCR reactions were carried out in 50 μl final solutions as described in Mesquita *et al*[31]. Annealing temperature was 58°C. PCR products were analyzed on 1.5% ethidium bromide-agarose gels run in 1X Tris-borate-EDTA buffer. A 100 bp DNA ladder was purchased from Amersham Bioscience.

Transfections

Transfections and co-transfections experiments were performed using Effectene® reagent (Qiagen) as previously described using 1 μg of pGL3-Muc5ac deletion mutants[28]. Total cell extracts were prepared after a 48h incubation at 37°C using 1X Reagent Lysis Buffer (Promega) as described in the manufacturer's instruction manual. Luciferase activity (20 μl) was measured on a TD 20/20 luminometer (Turner Design, Promega). Total protein content in the extract (4 μl) was measured using the bicinchoninic acid method in 96-well plates as described in the manufacturer's instruction manual (Pierce, Bezons, France). In co-transfection experiments, 1 μg of the deletion mutant of interest was transfected with 0.25 μg of the expression plasmid encoding the transcription factor of interest. Results were expressed as fold activation of luciferase activity in samples co-transfected with the transcription factor of interest compared to the control co-transfected with the corresponding empty vector.

Nuclear extract preparation

Nuclear extracts from the different cells were prepared as described by Van Seuningen *et al*[32] and kept at -80°C until use. Protein content (2 μl of cell extracts) was measured using the bicinchoninic acid as described above.

Western-blotting

20 μg of nuclear proteins and 8 μl of prestained molecular weight markers (Life technologies, Cergy Pontoise, France) were loaded on a 10% SDS gel and electrophoresed for 1h15 min at 35 mA until bromophenol blue reached the bottom of the gel. The polyacrylamide gel was then electrotransferred on a 0.45 μm PVDF membrane (Millipore, Saint-Quentin-en-Yvelines, France) for 1h at 100V using a Bio-Rad transfer apparatus. Immunostaining was performed as follows: the PVDF

membrane was incubated with Tris-buffered saline-0.2% Tween20 (TBST) containing 20 % (w/v) non-fat dry milk for 2h at RT, then washed 3x5 min with TBST. Incubation with polyclonal anti-Sp1 PEP2 (sc-59) and anti-Sp3 (sc-644) antibodies (Santa Cruz laboratories, Tebu-Bio, Le Perray en Yvelines, France) at 1:1,275 dilution in TBST was carried out for 2h at RT under shaking. The membrane was then washed 3x5 min at RT with TBST before adding alkaline phosphatase conjugated-anti-rabbit IgGs (Promega) for 30 min at RT. The membrane was washed 1x5 min with TBST and 1x5 min with substrate buffer (0.1M Tris-HCl, pH 9.5 containing 0.1M NaCl and 0.05M $MgCl_2$). Staining was developed by incubating the membrane with 10 ml of substrate buffer containing 0.33 mg/ml 4-nitroblue tetrazolium chloride and 0.16 mg/ml 5-bromo-4-chloro-3-indolyl-phosphate. The enzymatic reaction was stopped by soaking the membrane in distilled water.

Oligonucleotides and DNA probes

The sequences of the oligonucleotides used for gel-shift assays are indicated in Table II. They were synthesized by MWG-Biotech (Ebersberg, Germany). Equimolar amounts of single-stranded oligonucleotides were annealed and radiolabeled using T4 polynucleotide kinase (Promega) and [γ^{32}P]-dATP. Radiolabeled probes were purified by chromatography on a Bio-Gel P-6 column (Bio-Rad, Ivry-sur-Seine, France).

Table II. Sequences and positions within the promoter of *Muc5ac* of the sense oligonucleotides used for EMSAs.

Probe	Position of putative binding site	Sequence (5' → 3')
-57/-34	Sp1 (-51/-42)	GTCACT*GGGGCTGGAG*CCAGCTCT
-83/-56	Sp1/CACCC (-76/-65)	AGACCTG*CTCCACCCACCC*ACGTGAAG
-113/-81	Sp1 (-100/-90)	GCCACTGTTTACC*TGGGTGAGGGG*AACCACAGA
-92/-71	Smad (-84/-80)	GGGAACCA*CAGAC*CTGCTCCAC
-467/-444	Smad (-458/-454)	CTCACTGGG*GTCTG*GGAACTTGAA
-552/-529	Smad (-538/-534)	TCTGTCCATCCCAG*CAGAC*ATGAA
-645/-622	Smad (-641/-637)	CCTG*GTCTG*GGCAAAGGTCCATGC
-1146/-1126	Smad (-1131/-1128)	TCTCTCTCTCTCCTC*TCTG*TC

NOTE Antisense oligonucleotides were also synthesized and annealed to the sense oligonucleotides to produce double-stranded DNA. Putative binding sites in the sequences are italicized and underlined.

Electrophoretic mobility shift assays (EMSA)

Incubation of nuclear proteins (8 μg) with radiolabeld probes, supershift analyses, and cold competitions were carried out as in Mesquita *et al*[31]. Anti-Sp1, anti-Sp3, anti-Smad2, anti-Smad4, and anti-NF-κB p65 antibodies and consensus Smad4 oligonucleotide were purchased from Santa-Cruz laboratories. Reactions were stopped by adding 2 μl of loading buffer. Samples were loaded onto a 4% non-denaturing polyacrylamide gel and electrophoresis conditions were as described previously[29]. Gels were vacuum-dried and autoradiographed overnight at -80°C.

Results

Cloning and characterization of murine Muc5ac mucin gene 5'-flanking region

In order to obtain the mouse Muc5ac 5'-flanking region, a mouse genomic library in λGEM12 was screened with a 750 bp DNA fragment encoding the N-terminal region of human MUC5AC[24]. The two positive plaques contained inserts of approximately 18 kb. After restriction mapping and Southern blot analysis, seven clones (pMS1-pMS7) were isolated and sequenced (see Materials and Methods section). Sequencing of the 5.5 kb pMS1 clone indicated that it contains the promoter region, the first three exons and the first three introns of the mouse Muc5ac mucin gene (Fig. 1A). Sequence analysis of the pMS1 clone and alignment to human and rat MUC5AC 5'-flanking regions revealed a translational start codon at position 3211 identical to rat Muc5ac first codon and 3 short exons encoding a total of 72 amino acids with 52% identity to human MUC5AC and 79% identity to rat Muc5ac (Fig.1B).

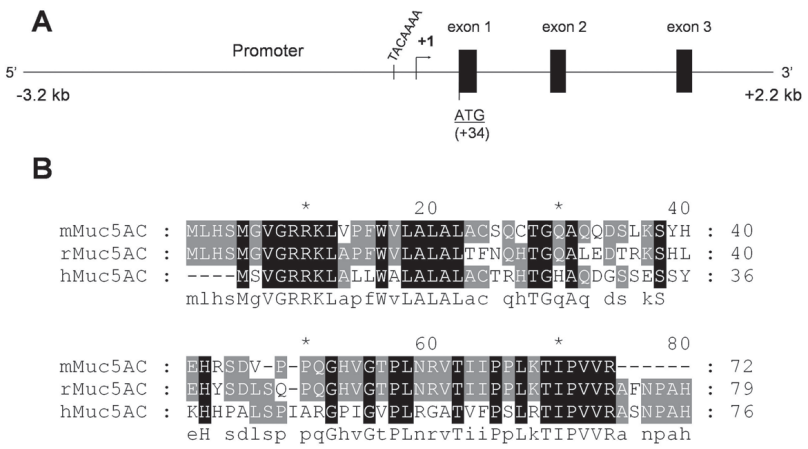

Figure 1. Isolation and characterization of a 5.5 kb genomic DNA fragment containing the 5'-flanking region of murine Muc5ac mucin gene. (A) Schematic representation of the organization of the 5'-flanking region of Muc5ac gene showing the promoter, the first three exons, ATG and transcription initiation site locations. (B) Alignment of deduced N-terminal amino acid sequences of mouse (mMuc5ac), rat (rMuc5ac) and human (hMuc5ac) MUC5AC peptides. Black boxes indicate conserved amino acid residues in the three species and gray boxes amino acid residues identical in two different species. The deduced consensus sequence is indicated at the bottom

Determination of the transcription start site of Muc5ac gene

To determine the transcription start site, 5'-RACE assays were performed on mouse gastric RNA using two nested antisense primers selected at about 300 bp and 70 bp downstream of the presumed start codon, respectively, based on comparison with the human MUC5AC gene[33]. The sequences showed 100% homology when aligned with the 5'-flanking sequence of mouse Muc5ac. The 5'-end of the longest product (117 bp) corresponded to a thymidine residue located 33 nucleotides upstream of the first ATG and 22 nucleotides downstream of the TATA box (Fig. 2). In conclusion, Muc5ac transcription start site is a T residue located 22 nucleotides downstream of the TATA box.

Characterization of the promoter sequence of Muc5ac

The sequence found upstream of the transcription initiation site is characterized by the presence of a TATA box (TACAAAA) at –28/-22 (Fig. 2). The first 150 nucleotides upstream of the TATA box are rich in GC and CACCC boxes and Sp1 binding sites. Putative binding sites for Smad factors are present throughout the promoter sequence. It is interesting to note that the Smad sites are always found in close vicinity or embedded within Sp1 binding sites and/or GC-rich sequences. More upstream (-944/-938) is found an AT-rich sequence that is a putative site representative of a TATA box. Note that this sequence may also bind the Cdx transcription factor. Two putative binding sites for GATA factors were found at -1001/-998 and -774/-771. Consensus binding sites for retinoid (ATF/RXR-α-837/-832) or thyroid hormone (T3R-α -634/-626) receptors were also found. In the 5'-UTR region, that is 33 nucleotides long, putative binding sites for AP-1 and Sp1 were found at +2/+10 and +14/+23, respectively. In the first exon, a putative binding site for YY1 transcription factor is found at +47/+56 adjoining an Sp1 binding site at +54/+63.

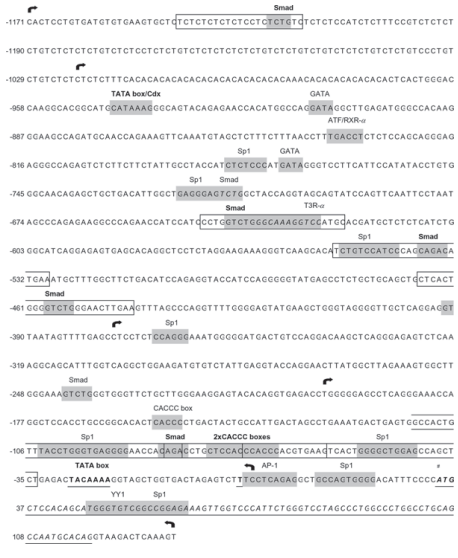

Figure 2. Sequence of the 5.5 kb genomic fragment containing Muc5ac promoter. The transcription start site +1 (bold and underlined) is located 22 nucleotides downstream of the TATA box (double underlined). The first ATG (+34) is bold, italicized and underlined. Nucleotides representing the first exon are italicized and underlined. Gray boxes indicate putative binding sites for transcription factors and boxed sequences indicate the sequences of oligonucleotides used in gel-shift assays. Broken arrows delimit the sequence of the deletion mutants used in this study.

Expression of Muc5ac in mouse tissues

Expression of Muc5ac mRNA in mouse tissues was studied by RT-PCR and *in situ* hybridization. By reverse transcriptase PCR, Muc5ac expression is only seen in stomach (Fig. 3A). No expression was found in submaxillary glands, parotid glands, trachea, thymus, gallbladder, liver, small intestine, colon or kidney. *In situ* hybridization was performed to localize Muc5ac expression in the stomach. Alcian blue-PAS staining of acidic mucins was found in mucus granules of surface epithelial cells (Fig. 3C). Labeling with Muc5ac anti-sense probe showed that Muc5ac mRNA is only expressed in the surface epithelium of the stomach (Fig. 3D). The specificity of the labeling was confirmed by the absence of signal when using a sense probe (Fig. 3E) and by absence of signal in colon when using the antisense probe (Fig. 3F). Immunohistochemical staining of a mouse gastric mucosa with 45M1 monoclonal anti-MUC5AC antibody confirmed the expression of Muc5ac mucin in surface gastric epithelial cells (Fig. 3G). In conclusion, Muc5ac expression in normal mice is restricted to the surface epithelium of the stomach.

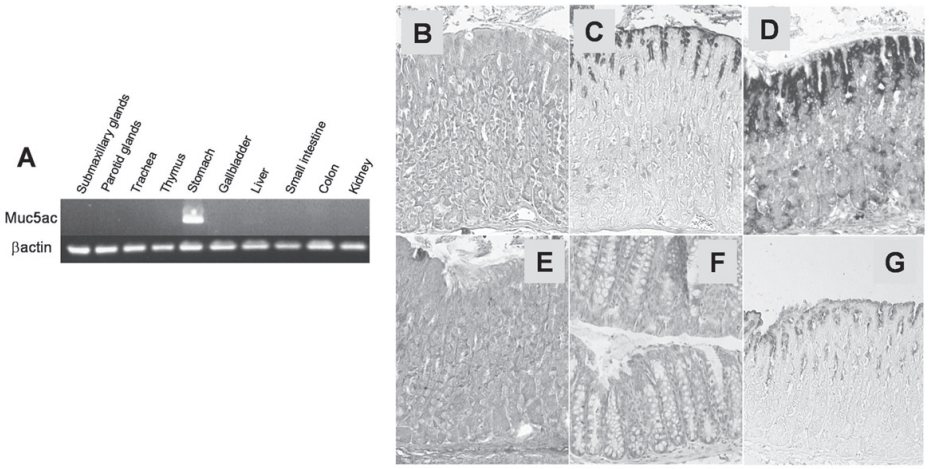

Figure 3. Expression of Muc5ac in mouse tissues by RT-PCR, in situ hybridization and immunohistochemistry. (A) Muc5ac (10 μl) and β–actin (2 μl) PCR products were separated on a 1.5% agarose gel. In situ hybridization (B-F) and immunohistochemistry (G) studies. (B) Hematoxylin and eosin staining of gastric mucosa, (C) Alcian blue and PAS staining of gastric mucosa, (D) Staining of gastric mucosa with Muc5ac digoxigenin-labeled antisense RNA probe, (E) Staining of gastric mucosa with Muc5ac digoxigenin-labeled sense probe, (F) Staining of colon mucosa with Muc5ac digoxigenin-labeled antisense probe, (G) Immunostaining of Muc5ac in gastric mucosa with monoclonal 45M1 antibody. Magnification x 200.

Characterization of Muc5ac promoter activity

To study Muc5ac promoter activity we used two Muc5ac-expressing (CMT-93, IEC-6) and one Muc5ac non-expressing (KATO-III) cell lines. Expression of Muc5ac in the murine rectal cancer cells (CMT-93, lane 3) and in the rat intestinal cell line (IEC-6, lane 6) is shown in Figure 4A. Absence of MUC5AC expression in KATO-III cells was previously published[8]. To define essential regions that drive transcription

of Muc5ac promoter, ten deletion mutants, that cover 1.2 kb of the promoter, were constructed in promoterless pGL3 basic vector (Fig. 4B). Numbering refers to the transcription start site designated as +1. Deletion mutants –1021/-828 and –1171/-828 were made in order to check the functional activity of the distal TATA box found at -944/-939.

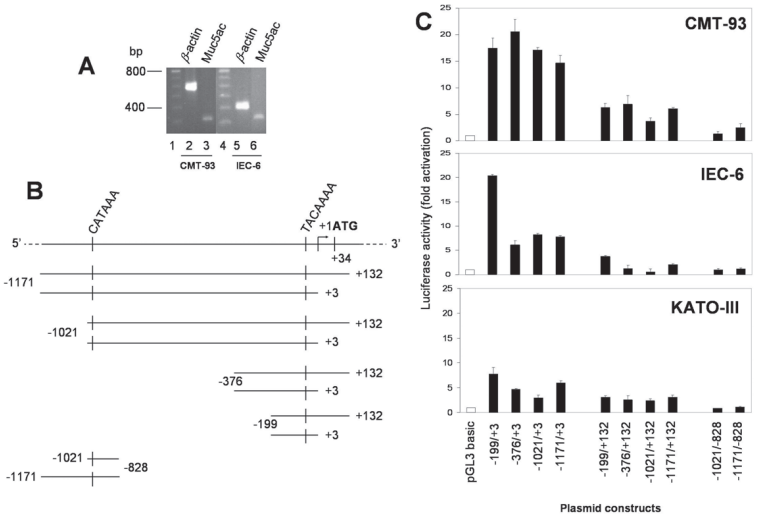

Figure 4. Characterization of Muc5ac promoter activity in CMT-93, IEC-6 and KATO-III cell lines by transient transfection. (A) Expression of Muc5ac mucin gene in CMT-93 (lane 3) and IEC-6 (lane 6) cells by RT-PCR. Mouse (lane 2) and rat (lane 5) β-actins (2 μl) were used as internal controls. A 100 bp DNA ladder (lanes 1 and 4). (B) Schematic representation of the different deletion mutants used to study Muc5ac promoter activity. Numbering refers to transcription initiation site designated as +1, (C) Luciferase activity diagrams showing Muc5ac promoter activity in murine rectal CMT-93, rat colon IEC-6 and human gastric KATO-III cells. Results are expressed as fold activation of luciferase activity of the deletion mutant of interest compared with the activity of empty pGL3 basic vector (white bar). Standard deviation represents the means of values obtained in triplicate in three separate experiments.

The luciferase diagrams obtained in the three cell lines indicate that Muc5ac promoter activity is the strongest in Muc5ac-expressing cell lines (Fig. 4C). In CMT-93 and IEC-6 cells, the highest luciferase activity was obtained with fragment –199/+3 (17-20 fold activation), which indicates that this region possesses essential positive regulatory elements that confer maximal activity to the promoter. In CMT-93 cells, the luciferase activity gradually decreases as the constructs include longer portion of the distal region of the promoter. In IEC-6 cells, a strong decrease in luciferase activity is seen with fragment –376/+3 (6 fold activation) and this decrease is maintained in fragments –1021/+3 and –1171/+3. This indicates that inhibitory elements, active in IEC-6 cells, are present within the –376/-200 region of the promoter. Interestingly, one can note that the fragments, in which the +3/+132 region was added, have a decreased luciferase activity of about 50% to 100%. The inhibitory activity was found in the three cell lines. That region includes the 5'-UTR and first exon in which a binding site for YY1 repressor (+47/+56) is clustered between two Sp1 binding sites

at +29/+38 and +54/+63, respectively. The –1021/+3 and –1171/+3 mutants that contain the distal TATA box located at -944/-939 are not active in the cell lines tested. In conclusion, essential regulatory elements for the basal activity of the promoter are found within the –199/+3 proximal region of Muc5ac promoter and negative elements are present within the 5'-UTR.

Regulation of Muc5ac promoter by TGF-β and Smads transcription factors

The high amount of putative binding sites for Smad transcription factors within Muc5ac promoter (Fig. 2) is in favor of a regulatory role for TGF-β on Muc5ac promoter activity. Smads are the main factors activated by TGF-β[18]. For this reason and because it was previously shown that MUC5AC mucin gene expression is altered in inflammatory pathologies of the epithelium in which TGF-β is implicated[34], we undertook to study the regulation of Muc5ac promoter by TGF-β and Smad factors. TGF-β sends intracellular signals after binding to TGF-βRII on the cell membrane. Thus, before studying TGF-β signaling pathway on Muc5ac expression in CMT-93 cells, we checked whether the cells expressed TGF-βRII. As shown in Figure 5A, TGF-βRII mRNAs are highly expressed in CMT-93 cells. Treatment of CMT-93 cells with TGF-β substantially induced the amount of Muc5ac mRNA in the cells (Fig. 5B). Identification of TGF-β responsive elements within Muc5ac promoter was then tested in transfection studies in which transfected cells were treated with TGF-β under the same conditions (Fig. 5C). The luciferase diagram indicates that exogenous TGF-β induces the activity of the fragments covering the -1021/+3 region (2.0, 2.7 and 1.8 fold, respectively). Induction was lost when the longest fragment (-1171/+3) was used. These results indicate that TGF-β responsive elements are present within the –1021/+3 region of the promoter of Muc5ac, which contains seven putative Smad binding sites (CAGAC).

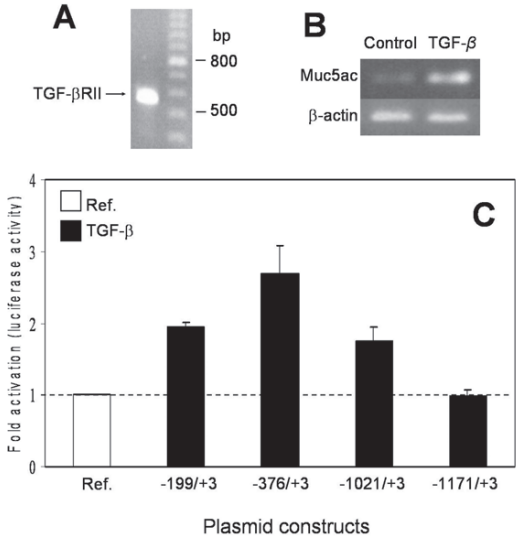

Figure 5. Regulation of Muc5ac mRNA expression and promoter activity by exogenous TGF-β in CMT-93 cells. (A) Expression of TGF-βRII in CMT-93 cells by RT-PCR. (B) Expression of Muc5ac mRNA by RT-PCR in untreated cells (control) and TGF-β-treated (TGF-β) cells. (C): Luciferase diagram showing effect of TGF-β on Muc5ac promoter activity. Results are expressed as fold activation of luciferase activity in samples treated with TGF-β (black bars) compared to the control (Ref., untreated cells, white bar).

In order to identify Smad binding sites, EMSA were performed with double-stranded oligonucleotides representative of the Smad binding sites found at -538/-534, -641/-637, -1131/-1128, -458/-454 and -84/-80, respectively (Table II). Incubation of the radiolabeled probes with CMT-93 nuclear extracts resulted in one shifted band characteristic of Smad DNA complexes (Fig. 6A, lanes 2, 7, 12) when compared with mobility of Smad4 consensus radiolabeled probe (lane 17). The specificity of the complexes were confirmed by total disappearance of the shifted bands when cold competition was performed (lanes 3, 8, 13, 18). Involvement of Smad4 in the DNA-protein shifted complex was then proven by inhibition of complex formation upon addition of Smad4 antibody (lanes 5, 10 and 14) whereas no effect was observed upon addition of Smad2 antibody (lanes 4, 9, and 15). The same result was obtained with -552/-529 and -92/-71 probes (not shown). Induction of Smad4 binding by TGF-β was then tested on nuclear extracts from TGF-β-treated cells. Increase of Smad4 binding to the Smad cis-elements was indeed observed with nuclear extracts from TGF-β-treated cells (lane 21) when compared with untreated cells (lane 20). These studies indicate that Smad4 binds to five cognate cis-elements at -84/-80, -458/-454, -538/-534, -641/-635 and -1131/-1128 within the TGF-β inducible region of Muc5ac promoter.

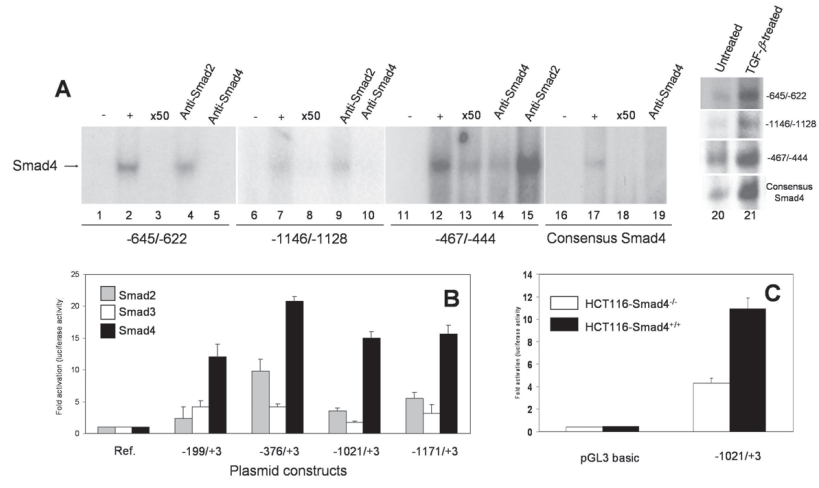

Figure 6. Identification of Smad4 binding sites within the promoter of Muc5ac by EMSA and regulation of the promoter by the Smads by transient transfection. (A) Nuclear extracts from CMT-93 cells were incubated with radiolabeled DNA probes, -645/-622 (lanes 1-5), -1146/-1126 (lanes 6-10), -467/-444 (lanes 11-15) and consensus Smad4 (lanes 16-19) probes. Radiolabeled probes alone (lanes 1, 6, 11, 16), nuclear extract incubated with radiolabeled probe (lanes 2, 7, 12, 17), cold competition with x50 excess of cold probe (lanes 3, 8, 13, 18), supershift analysis by preincubating nuclear extract with 1 μl of anti-Smad2 (lanes 4, 9, 15) or anti-Smad4 (lanes 5, 10, 14, 19) antibodies before adding the radiolabeled probe. The arrow on the left hand side of the gel indicates the position of the DNA-protein complex engaging Smad4. Smad4-DNA complex formation with nuclear extracts from untreated (lane 20) and TGF-β-treated (lane 21) cells. (B) Regulation of Muc5ac promoter by Smad2, Smad3 and Smad4 transcription factors in CMT-93 cells. Co-transfection experiments in the presence of pCMV-Smad2 (gray bars), pCMV-Smad3 (white bars) or pCMV-Smad4 (black bars) expression vectors. (C) Luciferase activity of Muc5ac promoter in HCT116-Smad4-/- (white bars) and in HCT116-Smad4+/+ (black bars) cells.

In order to show whether the TGF-β responsive region that binds Smad4 is indeed regulated by Smad factors, we then performed co-transfection experiments in which Muc5ac-pGL3 deletion mutants were co-transfected with Smad4 alone or in combination with expression vectors encoding Smad2 or Smad3, that are co-factors of Smad4. As shown in Figure 6B, Smad2 induces Muc5ac promoter activity with the strongest effect on fragment –376/+3 (10 fold, gray bar). Smad3 transactivation of Muc5ac promoter is confined to the –376/+3 region of the promoter and is not as strong (4-5 fold activation, white bars, fragments –199/+3 and –376/+3). The transactivating effect of Smad3 is lost when co-transfected with longer fragments of the promoter (-1021/+3, -1171/+3). Smad4, as expected, strongly transactivates Muc5ac promoter activity throughout the sequence (12-22 fold activation, black bars). Co-transfection experiments in the presence of Smad2 and Smad4 or Smad3 and Smad4 did not lead to synergistic activation of the promoter (not shown). The involvement of Smad4 in up-regulating Muc5ac transcription was then confirmed by comparing Muc5ac promoter activity in a cell line that either constitutively expresses active Smad4 (HCT116-Smad4$^{+/+}$) or is mutated for Smad4 (HCT116-Smad4$^{-/-}$) (Fig. 6C). The luciferase diagram shows that Muc5ac promoter activity (fragment –1021/+3) is three times more active in cells expressing Smad4 (black bar) compared with cells mutated for Smad4 (white bar). The same result was obtained with fragment –376/+3 (not shown).

From these studies, it can be concluded that Smad4 is an activator of Muc5ac transcription, that TGF-β responsive Smad4 binding sites are present throughout the promoter and that Smad2 and Smad3 factors do not act in synergy with Smad4 to induce Muc5ac transcription.

Role of Sp1 and Sp3 in the regulation of Muc5ac promoter

Since we showed that Smad2 and Smad3 are not the partners of Smad4 to activate Muc5ac transcription, we looked for other partners. Interestingly, when we looked at the location of the Smad4 binding sites in the promoter, we noticed that they were often either embedded in or neighboring Sp1 cis-elements and those transcription factors are known to synergize to activate transcription of many genes. Before testing the synergistic effect between Smad4 and Sp1, we studied the regulation of Muc5ac promoter by Sp1 and Sp3 since the proximal region is GC-rich and that Sp1/Sp3 are important regulators of mucin gene expression[8].

EMSAs studies were performed with nuclear extracts from CMT-93 cells in which we checked the presence of Sp1 (96 kDa) and Sp3 (two isoforms, 100 and 60 kDa) proteins by western-blotting (Fig. 7A). Three double-stranded radiolabeled probes (Table II), each containing a putative Sp1 binding site (-113/-81, -57/-34) and CACCC boxes (-83/-56), were tested. Incubation of the -113/-81 probe with CMT-93 nuclear proteins did not produce any shift. Incubation with -57/-34 probe produced a strong retarded band but that could not be supershifted in the presence of anti-Sp1 or anti-Sp3 antibodies (not shown). On the other hand incubation of -83/-56 probe (Fig. 7B), which contains CACCC box binding sites, with CMT-93 nuclear proteins produced three shifted complexes (lane 2, see arrows). Specificity of these complexes was confirmed by complete inhibition of complex formation when cold competition was performed with 50x excess of the cold probe (lane 3). Complex #1 was completely

supershifted upon addition of specific anti-Sp1 antibody in the reaction mixture (lane 4, SS Sp1) whereas complex #2 was specifically supershifted upon addition of anti-Sp3 antibody (lane 5, SS Sp3). No supershift was observed upon addition of irrelevant NF-κB p65 antibody (lane 6). In conclusion, Sp1 and Sp3 bind to the same cis-element located at –76/-65 within Muc5ac proximal promoter.

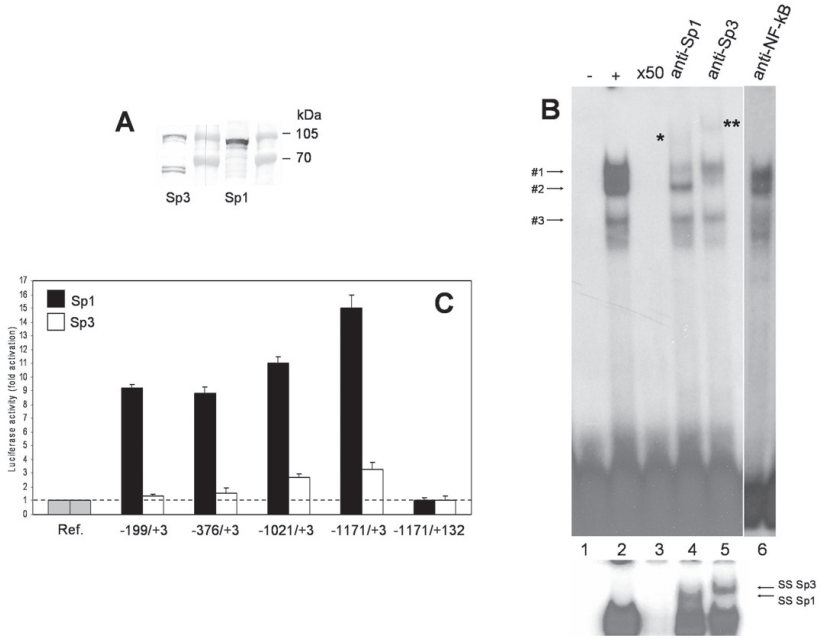

Figure 7. Regulation of Muc5ac promoter by Sp1 and Sp3 transcription factors in CMT-93 cells. Identification of an Sp1 cis-element in the promoter by EMSA. (A) Western-blotting of nuclear proteins prepared from CMT-93 cells. Prestained molecular weight markers (MWM). Immunostaining of the membrane with polyclonal PEP-2 anti-Sp1 (Sp1) and with polyclonal anti-Sp3 (Sp3) antibodies. (B) Identification of an Sp1 cis-element by EMSA. Nuclear extracts from CMT-93 cells were incubated with the -83/-56 radiolabeled DNA probe. Radiolabeled probe alone (lane 1). Incubation of -83/-56 probe with CMT-93 nuclear proteins (lane 2), cold competition with x50 excess of cold probe (lane 3), supershift analysis upon addition of anti-Sp1 (lane 4) or anti-Sp3 (lane 5) antibodies. Addition of irrelevant NF-κB p65 antibody (lane 6). DNA-protein complexes are indicated by an arrow on the left hand-side of the autoradiogram. Asterisks indicate the position of Sp1 (SS Sp1) and Sp3 (SS Sp3) supershifts. A longer exposure of the upper part of the same autoradiogram is shown at the bottom. (C) Co-transfection experiments in the presence of pCMV-Sp1 (black bars) or pCMV-Sp3 (white bars) expression vectors. Ref. refers to the normalized luciferase activity of the pGL3-deletion mutants of interest co-transfected with the empty expression vector pCMV4. Standard deviation represents the means of values obtained in triplicate in three separate experiments.

To study the role of Sp1 and Sp3 in regulating Muc5ac transcription, co-transfection experiments were carried out in CMT-93 cells in the presence of an expression vector encoding either Sp1 (pCMV4-Sp1, black bars) or Sp3 (pCMV4-Sp3, white bars) (Fig. 7C). Sp1 strongly transactivates both the proximal (fragments –199/+3 and –376/+3, 8-9 fold activation) and distal (fragments –1021/+3 and –1171/+3,

10-15 fold activation) regions of the promoter. Addition of the 5'-UTR to the promoter construct –1171/+3 (=construct –1171/+132) inhibited the transactivating effect of Sp1. Sp3 only has a mild transactivating effect on the distal part of the promoter (2-3 fold activation). Again, addition of the 5'-UTR inhibited that effect. Altogether, these studies indicate that Sp1 is a strong transactivator of Muc5ac promoter activity in CMT-93 cells.

Cooperation between Sp1 and Smad4 to activate Muc5ac promoter

Having shown that both Smad4 and Sp1 were strong activators of Muc5ac transcription in CMT-93 cells, we then undertook to look at their cooperative effect on the promoter. Co-transfection in the presence of Smad4 and Sp1 were performed on fragments –199/+3, -376/+3 and –1171/+3 (Fig. 8). No synergistic effect was seen on the shortest fragment –199/+3 (white bars). An additive effect was observed on the construct –376/+3 (black bars) whereas a synergistic transactivating effect was obtained on fragment –1171/+3 (gray bars). In conclusion, Sp1 appears to be the co-factor of Smad4 to activate Muc5ac transcription and essential elements that convey the synergistic effect are localized within the -1171/-377 region of the promoter.

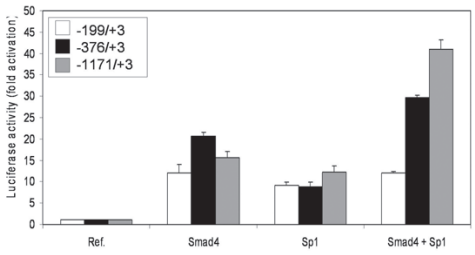

Figure 8. Cooperation between Smad4 and Sp1 to transactivate Muc5ac promoter. Co-transfection experiments were performed in CMT-93 cells in the presence of pCMV-Sp1, pCMV-Smad4 or both. Results are expressed as fold activation of the luciferase activity obtained in co-transfection with the expression vector encoding Smad4, Sp1 or both compared with cells transfected with corresponding empty vector (Ref.). Standard deviation represents the means of values obtained in triplicate in three separate experiments.

Discussion

Organization, evolution, and regulation of expression of the four 11p15 mucin genes, MUC2, MUC5AC, MUC5B and MUC6 have been extensively studied over the past few years[2, 7, 35]. *In situ* hybridization and promoter functional studies have led the investigators to the conclusion that these mucin genes are tightly regulated at the transcriptional level[8]. They often harbor an altered profile of expression in human tumors of the respiratory, gastrointestinal and urogenital tracts[2, 5, 6, 36] and such alterations (overexpression, repression, neoexpression) are usually characteristic of genes playing important roles in carcinogenesis. In order to study mucin gene regulation in animal models, isolation of the 5'-flanking regions including promoter of the murine counterparts are now mandatory.

In this paper, we have isolated and characterized the 5'-flanking region of the murine mucin gene Muc5ac including the promoter and first three exons/introns. Analysis and alignment of the first three exons with its human and rat counterparts

show a high degree of homology with rat Muc5ac (79%) whereas it is less with human MUC5AC (52%). First ATG is identical to rat Muc5ac (Oinuma, accession number AB042530), which adds four amino acid residues (MLHS) when compared to human MUC5AC N-terminal amino acid sequence[33]. The TATA box sequence (TACAAAA) is conserved throughout evolution since both mouse (this report) and human TATA boxes are identical[33]. The sequence of the TATA box in rat Muc5ac gene is not known. Overall, it can be stressed that the 5'-region of Muc5ac mucin gene is relatively well-conserved between human, mouse and rats and shows typical features of genes with cell-specific profile of expression. Indeed, in this report we found that expression of murine Muc5ac gene and protein was very specific and restricted to the surface epithelial cells of the gastric mucosa like what was previously described for rat Muc5ac[37]. No expression was found in trachea. This latter result is in contrast with expression territories in humans in which MUC5AC is expressed in the surface epithelium of stomach but also in goblet cells of the tracheobronchial tract[9]. This difference is most likely due to histological differences between rodents and humans, since the epithelium of their conducting airways mostly consist of ciliated cells (upper tract) and Clara cells (lower tract) whereas mucous cells remain rare[38].

Analysis of the promoter nucleotide sequence immediately upstream of the TATA box (over the first 199 nucleotides) shows that it is GC-rich and bears numerous putative consensus Sp1 binding sites or CACCC boxes also known to bind transcription factors of the Sp family[8]. Consistent with a role in cancer for factors of the Sp family is their ability to be oncogenic themselves or to interact with oncogenes or tumor suppressors[39]. The high GC content of proximal region of promoters is a common feature in mucin genes as it was also found in human MUC2, MUC5AC, MUC5B and murine Muc2 promoters[8, 20, 30, 40] and functional studies pointed out to an important role for the transcription factors of the Sp-family as mucin gene regulators. The fact that these cis-elements are conserved between mouse and human MUC5AC genes is also in favor of an important role for Sp1 in MUC5AC transcriptional regulation. Here, we confirmed that hypothesis by the means of co-transfection experiments in which we showed that Sp1 strongly transactivates the promoter of Muc5ac. Having previously shown that Sp3 interferes with Sp1-mediated regulation of human MUC5AC promoter[28], we studied its effect on murine Muc5ac promoter as well. Our results indicate that Sp3 is also a regulator of Muc5ac transcription but with a weaker effect. Since Sp1 and Sp3 are ubiquitously expressed in the cells and recognize the same DNA motif, it also implies that Sp1 and Sp3 will compete when they are both present in equimolar amounts in the cell.

Interestingly, Muc5ac promoter activity was repressed by 50% when pGL3 constructs contained the 5'-UTR (33 nucleotides long) and part of the first exon. Analysis of the sequence indicated that an AP-1 and Sp1 binding sites are present within the 5'-UTR. Those factors are generally considered as activators of the transcription and could not be responsible for the repression observed. In close vicinity of the Sp1 binding site, was found a second Sp1 cis-element overlapping a YY1 binding site. YY1 possesses dual activity (repressor or activator) depending on the molecular context and is known to interact with Sp1[41] As it was recently shown for hamster Muc1 mucin gene[42], YY1 may repress Muc5ac transcription via interactions with Sp1.

Muc5ac promoter contains binding sites for Smad4 transcription factor throughout its sequence. Alignment of human[33]and mouse sequences (this report) of the promoters indicates that Smad putative sites are present in both genes but not at the same location. The response of the two genes to TGF-β is different and seems to depend on the cellular situation as it was recently shown that human MUC5AC is negatively regulated when nontypeable Haemophilus influenzae-infected cells are treated with TGF-β[43]. Smad transcription factors are activated by growth factors of the TGF-β family in a sequential manner[18] and form either Smad2-Smad4 or Smad3-Smad4 complexes that are translocated into the nucleus where they bind to the promoter of the target gene to activate transcription. However, once bound to the promoter, Smad4 may interact with other factors to activate transcription. Our results indicate that Muc5ac is a target gene of TGF-β. However, they also suggest that the pathway induced by TGF-β does not imply complex formation between Smad4 and Smad2 or Smad4 and Smad3. Apart from activating Smad factors, TGF-β is also known to activate Sp1 site-dependent transcription of its target genes, Smad factors are known to activate transcription through Sp1 sites and Sp1 interact with Smad4 to induce transcription and this mechanism is TGF-β dependent[39, 44, 45]. The data presented in this manuscript are in favor of such a positive regulatory mechanism between Smad4 and Sp1 to explain the TGF-β-mediated upregulation of Muc5ac expression in cancer cells. Since TGF-β is a pleiotropic cytokine with diverse function during development, adult tissue homeostasis, carcinogenesis and inflammation[46, 47], it will be interesting in the future to study the correlation between TGF-β-mediated processes with that of Muc5ac expression and their consequences on epithelium homeostasis.

Acknowledgements
We are indebted to Danièle Petitprez, Brigitte Hémon and Dominique Demeyer for their excellent technical help. We thank Dr. J. M. Horowitz (Raleigh, NC, USA) for the kind gift of pCMV-Sp1 and pCMV-Sp3 expression vectors. We thank Dr. A. Atfi (INSERM U482, Paris, France) for pCMV-Smad2, pCMV-Smad3 and pCMV-Smad4 vectors and HCT116-Smad4-/- and HCT116-Smad4+/+ cell lines. This work was supported by grants from l'Association de Recherche sur le Cancer N° 5785 (IVS), Ligue Régionale du Pas de Calais Contre le Cancer (IVS), l'Association François Aupetit (IVS), Sophia Foundation for Medical Research (MvdS and AWCE) and from the European Regional Development Fund. N. Jonckheere is the recipient of a Conseil Régional Nord-Pas de Calais and the Centre Hospitalier & Universitaire de Lille PhD fellowship. M. Sutmuller received a fellowship from the Erasmus University of Rotterdam, the Netherlands.

References

1. Van Klinken BJ, Dekker J, Büller HA, Einerhand AW. Mucin gene structure and expression: protection vs. adhesion. Am J Physiol 1995;269:G613-27.
2. Porchet N, Buisine MP, Desseyn JL, Moniaux N, Nollet S, Degand P, Pigny P, Van Seuningen I, Laine A, Aubert JP. [MUC genes: a superfamily of genes? Towards a functional classification of human apomucins]. J Soc Biol 1999;193:85-99.
3. Dekker J, Rossen JW, Büller HA, Einerhand AW. The MUC family: an obituary. Trends Biochem Sci 2002;27:126-31.
4. Carraway KL, Ramsauer VP, Haq B, Carothers Carraway CA. Cell signaling through membrane mucins. Bioessays 2003;25:66-71.
5. Corfield AP, Myerscough N, Longman R, Sylvester P, Arul S, Pignatelli M. Mucins and mucosal protection in the gastrointestinal tract: new prospects for mucins in the pathology of gastrointestinal disease. Gut 2000;47:589-94.
6. Einerhand AW, Renes IB, Makkink MK, van der Sluis M, Büller HA, Dekker J. Role of mucins in inflammatory bowel disease: important lessons from experimental models. Eur J Gastroenterol Hepatol 2002;14:757-65.
7. Pigny P, Guyonnet-Duperat V, Hill AS, Pratt WS, Galiegue-Zouitina S, d'Hooge MC, Laine A, Van-Seuningen I, Degand P, Gum JR, Kim YS, Swallow DM, Aubert JP, Porchet N. Human mucin genes assigned to 11p15.5: identification and organization of a cluster of genes. Genomics 1996;38:340-52.
8. Van Seuningen I, Pigny P, Perrais M, Porchet N, Aubert JP. Transcriptional regulation of the 11p15 mucin genes. Towards new biological tools in human therapy, in inflammatory diseases and cancer? Front Biosci 2001;6:D1216-34.
9. Audie JP, Janin A, Porchet N, Copin MC, Gosselin B, Aubert JP. Expression of human mucin genes in respiratory, digestive, and reproductive tracts ascertained by *in situ* hybridization. J Histochem Cytochem 1993;41:1479-85.
10. Guillem P, Billeret V, Buisine MP, Flejou JF, Lecomte-Houcke M, Degand P, Aubert JP, Triboulet JP, Porchet N. Mucin gene expression and cell differentiation in human normal, premalignant and malignant esophagus. Int J Cancer 2000;88:856-61.
11. Warson C, Van De Bovenkamp JH, Korteland-Van Male AM, Büller HA, Einerhand AW, Ectors NL, Dekker J. Barrett's esophagus is characterized by expression of gastric-type mucins (MUC5AC, MUC6) and TFF peptides (TFF1 and TFF2), but the risk of carcinoma development may be indicated by the intestinal-type mucin, MUC2. Hum Pathol 2002;33:660-8.
12. Van De Bovenkamp JH, Korteland-Van Male AM, Warson C, Büller HA, Einerhand AW, Ectors NL, Dekker J. Gastric-type mucin and TFF-peptide expression in Barrett's oesophagus is disturbed during increased expression of MUC2. Histopathology 2003;42:555-65.
13. Bartman AE, Sanderson SJ, Ewing SL, Niehans GA, Wiehr CL, Evans MK, Ho SB. Aberrant expression of MUC5AC and MUC6 gastric mucin genes in colorectal polyps. Int J Cancer 1999;80:210-8.
14. Buisine MP, Janin A, Maunoury V, Audie JP, Delescaut MP, Copin MC, Colombel JF, Degand P, Aubert JP, Porchet N. Aberrant expression of a human mucin gene (MUC5AC) in rectosigmoid villous adenoma. Gastroenterology 1996;110:84-91.
15. Copin MC, Buisine MP, Devisme L, Leroy X, Escande F, Gosselin B, Aubert JP, Porchet N. Normal respiratory mucosa, precursor lesions and lung carcinomas: differential expression of human mucin genes. Front Biosci 2001;6:D1264-75.

16. Massague J. TGF-beta signal transduction. Annu Rev Biochem 1998;67:753-91.
17. Milani S, Calabro A. Role of growth factors and their receptors in gastric ulcer healing. Microsc Res Tech 2001;53:360-71.
18. Massague J, Wotton D. Transcriptional control by the TGF-beta/Smad signaling system. Embo J 2000;19:1745-54.
19. Gendler SJ. MUC1, the renaissance molecule. J Mammary Gland Biol Neoplasia 2001;6:339-53.
20. Aslam F, Palumbo L, Augenlicht LH, Velcich A. The Sp family of transcription factors in the regulation of the human and mouse MUC2 gene promoters. Cancer Res 2001;61:570-6.
21. Velcich A, Yang W, Heyer J, Fragale A, Nicholas C, Viani S, Kucherlapati R, Lipkin M, Yang K, Augenlicht L. Colorectal cancer in mice genetically deficient in the mucin Muc2. Science 2002;295:1726-9.
22. Shekels LL, Lyftogt C, Kieliszewski M, Filie JD, Kozak CA, Ho SB. Mouse gastric mucin: cloning and chromosomal localization. Biochem J 1995;311 (Pt 3):775-85.
23. Desseyn JL, Laine A. Characterization of mouse muc6 and evidence of conservation of the gel-forming mucin gene cluster between human and mouse. Genomics 2003;81:433-6.
24. van de Bovenkamp JH, Hau CM, Strous GJ, Büller HA, Dekker J, Einerhand AW. Molecular cloning of human gastric mucin MUC5AC reveals conserved cysteine-rich D-domains and a putative leucine zipper motif. Biochem Biophys Res Commun 1998;245:853-9.
25. Quandt K, Frech K, Karas H, Wingender E, Werner T. MatInd and MatInspector: new fast and versatile tools for detection of consensus matches in nucleotide sequence data. Nucleic Acids Res 1995;23:4878-84.
26. Renes IB, Boshuizen JA, Van Nispen DJ, Bulsing NP, Büller HA, Dekker J, Einerhand AW. Alterations in Muc2 biosynthesis and secretion during dextran sulfate sodium-induced colitis. Am J Physiol Gastrointest Liver Physiol 2002;282:G382-9.
27. Renes IB, Verburg M, Bulsing NP, Ferdinandusse S, Büller HA, Dekker J, Einerhand AW. Protection of the Peyer's patch-associated crypt and villus epithelium against methotrexate-induced damage is based on its distinct regulation of proliferation. J Pathol 2002;198:60-8.
28. Perrais M, Pigny P, Copin MC, Aubert JP, Van Seuningen I. Induction of MUC2 and MUC5AC mucins by factors of the epidermal growth factor (EGF) family is mediated by EGF receptor/Ras/Raf/extracellular signal-regulated kinase cascade and Sp1. J Biol Chem 2002;277:32258-67.
29. Van Seuningen I, Perrais M, Pigny P, Porchet N, Aubert JP. Sequence of the 5'-flanking region and promoter activity of the human mucin gene MUC5B in different phenotypes of colon cancer cells. Biochem J 2000;348 Pt 3:675-86.
30. Perrais M, Pigny P, Buisine MP, Porchet N, Aubert JP, Van Seuningen-Lempire I. Aberrant expression of human mucin gene MUC5B in gastric carcinoma and cancer cells. Identification and regulation of a distal promoter. J Biol Chem 2001;276:15386-96.
31. Mesquita P, Jonckheere N, Almeida R, Ducourouble MP, Serpa J, Silva E, Pigny P, Silva FS, Reis C, Silberg D, Van Seuningen I, David L. Human MUC2 mucin gene is transcriptionally regulated by Cdx homeodomain proteins in gastrointestinal carcinoma cell lines. J Biol Chem 2003;278:51549-56.
32. Van Seuningen I, Ostrowski J, Bustelo XR, Sleath PR, Bomsztyk K. The K protein domain that recruits the interleukin 1-responsive K protein kinase lies adjacent to a cluster of c-Src and Vav SH3-binding sites. Implications that K protein acts as a docking platform. J Biol Chem 1995;270:26976-85.
33. Li D, Gallup M, Fan N, Szymkowski DE, Basbaum CB. Cloning of the amino-terminal and 5'-flanking region of the human MUC5AC mucin gene and transcriptional up-regulation by

bacterial exoproducts. J Biol Chem 1998;273:6812-20.
34. Hanada T, Yoshimura A. Regulation of cytokine signaling and inflammation. Cytokine Growth Factor Rev 2002;13:413-21.
35. Desseyn JL, Aubert JP, Porchet N, Laine A. Evolution of the large secreted gel-forming mucins. Mol Biol Evol 2000;17:1175-84.
36. Lesuffleur T, Zweibaum A, Real FX. Mucins in normal and neoplastic human gastrointestinal tissues. Crit Rev Oncol Hematol 1994;17:153-80.
37. Inatomi T, Tisdale AS, Zhan Q, Spurr-Michaud S, Gipson IK. Cloning of rat Muc5AC mucin gene: comparison of its structure and tissue distribution to that of human and mouse homologues. Biochem Biophys Res Commun 1997;236:789-97.
38. Pack RJ, Al-Ugaily LH, Morris G. The cells of the tracheobronchial epithelium of the mouse: a quantitative light and electron microscope study. J Anat 1981;132:71-84.
39. Black AR, Black JD, Azizkhan-Clifford J. Sp1 and kruppel-like factor family of transcription factors in cell growth regulation and cancer. J Cell Physiol 2001;188:143-60.
40. Gum JR, Hicks JW, Kim YS. Identification and characterization of the MUC2 (human intestinal mucin) gene 5'-flanking region: promoter activity in cultured cells. Biochem J 1997;325 (Pt 1):259-67.
41. Thomas MJ, Seto E. Unlocking the mechanisms of transcription factor YY1: are chromatin modifying enzymes the key? Gene 1999;236:197-208.
42. Lee IJ, Hyun SW, Nandi A, Kim KC. Transcriptional regulation of the hamster Muc1 gene: identification of a putative negative regulatory element. Am J Physiol Lung Cell Mol Physiol 2003;284:L160-8.
43. Jono H, Xu H, Kai H, Lim DJ, Kim YS, Feng XH, Li JD. Transforming growth factor-beta-Smad signaling pathway negatively regulates nontypeable Haemophilus influenzae-induced MUC5AC mucin transcription via mitogen-activated protein kinase (MAPK) phosphatase-1-dependent inhibition of p38 MAPK. J Biol Chem 2003;278:27811-9.
44. Datta PK, Blake MC, Moses HL. Regulation of plasminogen activator inhibitor-1 expression by transforming growth factor-beta -induced physical and functional interactions between smads and Sp1. J Biol Chem 2000;275:40014-9.
45. Feng XH, Lin X, Derynck R. Smad2, Smad3 and Smad4 cooperate with Sp1 to induce p15(Ink4B) transcription in response to TGF-beta. Embo J 2000;19:5178-93.
46. Moustakas A, Pardali K, Gaal A, Heldin CH. Mechanisms of TGF-beta signaling in regulation of cell growth and differentiation. Immunol Lett 2002;82:85-91.
47. Dunker N, Krieglstein K. Targeted mutations of transforming growth factor-beta genes reveal important roles in mouse development and adult homeostasis. Eur J Biochem 2000;267:6982-8.

Part III

Epilogue

Chapter 10

Summary and General Discussion

Abbreviations used

IBD, inflammatory bowel disease; IL, interleukin; $IL10^{-/-}$, IL-10 deficient mice; MTX, methotrexate; Muc, Mucin; $Muc2^{-/-}$; Muc2 deficient mice; $Muc2/IL10^{DKO}$; Muc2/IL10 double knockout mice; NF-κB, nuclear factor kappa B; TLRs, Toll-like Receptors; TGF-β, Transforming Growth Factor-β; TNF-α, tumor necrosis factor alpha; WT, wild type

If we were to better understand function and regulation of mucin genes in the intestine, this could lead to the discovery of potential therapeutic targets in epithelial diseases. Therefore, the overall aims as investigated in this thesis were:

1. To investigate the influence of changes in mucus production, more specifically Mucin (Muc) 2, on the protective barrier function and elementary intestinal physiology.
2. To gain insight into the complex transcription regulatory mechanism of secretory mucins.

Role of mucins in the intestine

As described in **Chapter 1**, the mucin Muc2 is the predominant secretory large intestinal mucin in mammals[1-5]. Produced by goblet cells in the entire intestine, Muc2 is the most important compound of the mucus layer. As this layer is strategically positioned between the lumen and the epithelium, we hypothesized that it protects the intestinal cells against potential toxic and noxious agents present in the gut lumen. Further support for this hypothesis comes from studies showing decreased MUC2 synthesis in humans with inflammatory bowel disease (IBD)[6-8]. However, these clinical studies do not resolve the question whether these observed abnormalities in MUC2 synthesis are primary defects or whether they are secondary and induced by the inflammatory response. A major prerequisite for the development of colitis is the presence of bacteria in the colon. It has been convincingly shown that normal enteric bacteria can induce immune-mediated colitis in rodents with genetically engineered abnormalities in the immune system[9-14]. Muc2 provides a natural barrier between bacteria and the underlying colonic epithelium. Thus any change in quantity or structure of Muc2 could influence the effects of bacteria on the intestinal mucosa.

In **Chapter 2** we studied the effects of the introduction of specific pathogen-free, commensal bacteria on Muc2 synthesis and sulfation in germ-free, immuno-compromised, interleukin (IL)-10 deficient ($IL10^{-/-}$) mice. In germ-free state $IL10^{-/-}$ mice show no evidence of biochemical or histological inflammation[10]. We demonstrated that Muc2 synthesis was lower in the $IL10^{-/-}$ mice compared to wild type (WT) controls, even before bacterial colonization and the onset of inflammation. The inflammation in the $IL10^{-/-}$ mice after introduction of the enteric bacteria was characterized by thickening of the mucosa and a higher turnover of epithelial cells on account of increased proliferation in the crypts and apoptosis in the surface epithelium. In addition, as the colitis progressed from mild to severe in the $IL10^{-/-}$ mice, the colonic Muc2 sulfation decreased progressively. These quantitative and structural Muc2 aberrations in $IL10^{-/-}$ mice likely reduce the epithelium's ability to cope with (nonpathogenic) bacteria and therefore may contribute to colitis susceptibility. The role of Muc2 in epithelial protection was further assessed in **Chapter 3**. We first characterized the colon of Muc2 deficient ($Muc2^{-/-}$) mice and then challenged them luminally with dextran sulfate sodium, a colitis inducing agent. We showed that under specific pathogen-free conditions, loss of Muc2 in the intestine leads to mucosal thickening, increased proliferation, altered differentiation of epithelial cells and goblet cells, and superficial erosions in the colon. By challenging WT, Muc2 heterozygous and $Muc2^{-/-}$ mice with dextran sulfate sodium, we demonstrated that (partial) deficiency of Muc2 in the intestine predisposes to colonic

inflammation. These data provide evidence that changes in mucus composition, caused by Muc2 deficiency, leads to inflammation of the colon and that Muc2 can contribute to the onset and/or perpetuation of IBD. Considering that the severity of chronic intestinal inflammation is influenced by environmental, immunoregulatory, and epithelial factors, we investigated the protective capacities of Muc2 and IL10 in the intestine. To this aim we generated Muc2/IL10 double knockout (Muc2/IL10^{DKO}) mice and tested whether combinations of defects in immunoregulatory and epithelial factors could exacerbate the pathogenesis of inflammation. To obtain insight into the protective capacities of Muc2 and IL10 in the intestine, we characterized the Muc2/IL10^{DKO} mice and compared their clinical symptoms and intestinal pathology to Muc2$^{-/-}$ and IL10$^{-/-}$ mice of the same age (**Chapter 4)**. Microscopic analysis of the colon of Muc2$^{-/-}$ mice showed abnormal morphology marked by thickening of the mucosa, flattening and ulceration of epithelial cells, general loss of architecture, increase of inflammatory cells, an increase in proliferation, and reduced cell differentiation in the colon as described in chapter 3. These abnormalities were even more pronounced in Muc2/IL10^{DKO} mice of the same age. This indicates that absence of Muc2 in combination with changes in the immunological regulatory mechanisms, *e.g.* lack of IL10, leads to excessive uncontrollable inflammation of the colon, ultimately leading to the animal's death. The Muc2/IL10^{DKO} mouse clearly demonstrated that combined abnormalities in immunoregulatory and epithelial factors greatly accelerate and exacerbate the phenotype of colonic inflammation. Moreover, this study provided the evidence that the mucus layer in the intestine, more specifically the mucin Muc2, is pivotal in mucosal protection, suggesting that the mucus barrier is one of main factors for the genesis of colitis.

Another hypothesis involving Muc2 is the following: Muc2 also contributes to epithelial defense against other challenging factors, *i.e*. chemotherapy-induced damage. It is based on the finding that Muc2 protein expression was significantly increased during all phases of methotrexate (MTX)-induced damage in previous studies[15, 16]. To put this hypothesis to the test we challenged Muc2$^{-/-}$ mice with MTX. However, as described in **Chapter 5,** histological and biochemical analysis of the intestine of the Muc2$^{-/-}$ mice, showed that these mice were not more sensitive to MTX-treatment. As absence of Muc2, the structural component of the mucus layer, in Muc2$^{-/-}$ mice may lead to continuous exposure to luminal antigens (bacteria), this could unbalance cytokine production. The anti-inflammatory cytokine IL-10 has protective capacities in the intestine, and studies have shown that IL-10$^{-/-}$ mice are predisposed to develop chronic mucosal inflammation (chapter 2)[10, 17, 18]. IL-10 also protects the intestine from MTX-induced damage, seeing that IL10$^{-/-}$ mice develop more severe mucositis after MTX-treatment than their wild type littermates[19]. We confirmed that IL-10 was upregulated in these mice prior to MTX treatment, explaining why these mice did not show increased chemotherapy-induced mucositis.

The above-described studies confirm the importance of a healthy mucus layer. However, integrity of the mucus layer is also linked to availability of nutrients such as proteins, lipids, carbohydrates and essential amino acids within the intestine. For example, malnutrition and starvation alter the mucus layer by decreasing intestinal mucin synthesis[20, 21]. Further support for this hypothesis is that dietary restriction of threonine, one of the essential amino acids, has shown to impair intestinal mucin

synthesis[22]. We hypothesized that the gut's high demand for dietary threonine, as reported by Schaart *et al.*[23], is probably due to incorporation of the threonine into secretory mucins, mainly Muc2, which are rich in threonine residues. Therefore, as described in **Chapter 6,** we also investigated mucin involvement in the intestinal metabolism. We indeed demonstrated that a major fate of dietary threonine utilized by the intestine is its incorporation into Muc2. Furthermore, in the absence of Muc2, dietary threonine is mainly used for constitutive protein synthesis or becomes a substrate for oxidation.

In conclusion the first part of this thesis demonstrates a pivotal role for Muc2 in the intestine. Both quantitative and structural aberrations in Muc2 in the intestine lead to abnormal morphology marked by thickening of the gut mucosa, flattening and ulceration of epithelial cells, general loss of architecture, increase of inflammatory cells, intensified proliferation, and lessening of cell differentiation in the colon. The change in proliferation and differentiation, and resulting inflammation of the colon most likely result from altered interaction of the epithelium with nonpathogenic bacteria due to deficiency in Muc2.

Microbes in the intestine influence several aspects of epithelial differentiation. Altered differentiation in turn can influence nutrient absorption and processing by modulating expression of host genes in the intestine[24, 25]. Changes in mucus composition in the colon of the Muc2$^{-/-}$ and Muc2/IL10^{DKO} mice probably lead to altered, maybe even less, colonization and therefore to altered intestinal physiology/cell differentiation. The observed growth retardation in the Muc2$^{-/-}$, Muc2/IL10^{DKO} and, at a later age, IL10$^{-/-}$ mice could be attributed to the changes in colonization and thus altered intestinal physiology/cell differentiation. Multiple factors have been shown to affect growth in this situation, the most prominent of which are the presence and severity of inflammation and inadequate nutritional intake[26-28]. Not only intestinal damage, but also bacteria could affect nutritional uptake. Bacteria have been shown to be responsible for the conversion of many dietary substances into nutrients that can be absorbed and utilized by the host, as reviewed by Hooper *et al*[29]. Consequently, germ-free animals have less total body fat and need more caloric intake to maintain their body weight than conventionally raised animals[30, 31]. This can be explained by the fact that gut microbiota allow energy to be salvaged from otherwise indigestible dietary polysaccharides[32]. In addition, bacteria have shown to synthesize indispensable amino acids which are required and absorbed by the intestine[33, 34]. Furthermore, growth impairment was shown to be attributable to inflammation. Increased or altered bacterial exposure of the intestinal epithelium could also directly induce inflammatory cytokine production. Inflammatory cytokines in their turn are directly involved in mediating growth failure[26, 27]. The growth retardation seen in Muc2$^{-/-}$ and Muc2/IL10^{DKO} mice is most likely attributable to a difference in microflora and inflammation rather than to the intestinal damage or nutritional uptake. This hypothesis is supported by the fact that these mice show no distinct pathology of the small intestine under unchallenged conditions (chapter 5) and that the absorption capacity of free threonine (chapter 6) was not impaired or different in the Muc2$^{-/-}$ mice compared to WT mice. Interesting would be however, to assess when the inflammation in the Muc2$^{-/-}$ and Muc2/IL10^{DKO} mice is initiated. At 5 weeks of age both types of mice show inflammation of the colon, the severity dependent on

the mouse type. However, if the histology of these mice is already affected at birth, as Muc2 is expressed during embryonic development, or if the changes in histology are initiated during colonization, more specifically, sucking vs. weaning period of these mice remains to be investigated.

The increased proliferation and changes in both goblet cell and epithelial cell differentiation in the colon of the Muc2$^{-/-}$, Muc2/IL10^{DKO} and, at later age, IL10$^{-/-}$ mice might also stem from altered bacterial interaction with the epithelial cells of the intestine. This hypothesis is supported by a previous study showing that crypts in the colon of germ-free mice have a lower mitotic index and labeling index compared to conventional mice[35]. Bacteria and their products communicate with epithelial cells via pattern-recognition receptors, i.e. Toll-like Receptors (TLRs). These TLRs regulate gut immune responses to all kinds of bacterial interactions[36]. As reviewed by Cario[37], each TLR binds distinct features present on different classes of microorganisms. For example, type TLR2 recognizes bacterial lipopeptides and lipoteichoic acid found in the cell walls of Gram-positive bacteria; TLR4 is a receptor for lipopolysaccharide, a cell wall component of Gram-negative bacteria; and TLR9 is activated by unmethylated CpgDNA motifs which are common on certain bacterial and viral genomes[37]. TLR4 expression is increased in active human IBD and murine colitis[38-40]. Thus epithelial cells like goblet cells and enterocytes can detect (non)pathogenic bacteria and respond by altering gene expression. This may be the cause of the aberrant immune response seen in ulcerative and experimental colitis. Furthermore, a recent study has shown that IL10/MyD88 (a major adaptive protein essential for TLR-signaling) double knockout mice are resistant to spontaneous commensal induced colitis[41]. In this context, diminished Muc2 synthesis or absence of Muc2 may result in altered TLR signaling in epithelial cells, leading to changes in the different cell signaling pathways and thus possibly to increased proliferation and altered differentiation and immune responses.

Yet, this increase in proliferation and decrease in differentiation might also be direct responses to inflammation. De Koning *et al.* have suggested that during severe damage, the epithelium is preferentially involved with proliferation rather that differentiation, in order to restore intestinal barrier function[42]. This latter mechanism, however, does not explain why the expression of several intestinal specific markers is lower in the proximal colon of the Muc2/IL10^{DKO} mice compared to the distal colon, whereas the inflammation and cell damage are the most severe in the distal colon of these mice. However, enterocyte-specific protein expression was shown to be downregulated in the entire colon during dextran sodium induced damage[43]. Loss of differentiation of the goblet cells and epithelial cells as described in the different colitis models above was characterized by a distinct change in expression of Muc4 (chapter 4). Distinct changes in the mRNA expression levels of the mucins Muc1, -3 and -4 in the distal colon during dextran sodium sulfate induced damage and regeneration were also observed (data not shown). Especially downregulation of Muc4 seemed to be a common factor for colonic damage, as investigated in chapter 4. Although there is clear evidence that these mucins play a role in cell-signalling[44] related to growth, motility, differentiation and inflammation, the cause and consequence in change of expression and thus function of these mucins during colitis remains to be elucidated.

The protective capacities of Muc2 during MTX-induced damage and regeneration remain to be investigated. The Muc2$^{-/-}$ mouse did not turn out to be the appropriate model to investigate this hypothesis as its immune system was out of balance prior to MTX-induced damage. In addition to protecting against intestinal inflammatory processes as described in chapters 2 and 4, IL-10 is also strongly implicated as having protective capacities in MTX-induced mucositis[19]. These data to a certain extent imply that the pathogenesis of mucositis is quite similar to that of IBD. Novel experimental therapies for IBD patients such as the application of IL-10-producing *lactococci lactis* may therefore provide attractive means to prevent mucositis[45, 46]. Furthermore, these bacteria might also upregulate Muc2 as other probiotic strains have shown to do[47, 48]. Specifically upregulating Muc2 in WT mice before MTX-treatment might provide more evidence for a protective role of Muc2 against MTX-induced mucositis. Furthermore, supplementing the intestine with serine, proline, and cysteine, which also represent major components of mucins, in addition to threonine may also enhance mucin synthesis, more specifically that of Muc2. This hypothesis is supported by data showing that in piglets between 80-90% of dietary threonine is utilized by the intestine[23] and by chapter 6 of this thesis, which showed that threonine is incorporated into Muc2 and secreted in WT mice. A model that could elucidate the role of Muc2 in epithelial protection against MTX-induced damage in absence of IL-10, would be to treat IL10/Muc2^{DKO} mice with MTX. However, as described in chapter 4, these animals show significant growth retardation, even compared to Muc2$^{-/-}$ mice, and die before reaching maturity. Regrettably it is not feasible, therefore, to expose these mice to MTX treatment. Another interesting experiment would be to evaluate the expression of Muc1, -3 and -4 during MTX-induced mucositis so as to verify whether the changes in expression during colitis as described in chapter 4 of this thesis are common phenomena during intestinal damage.

Another point that needs to be addressed is the difference in phenotype displayed by the Muc2$^{-/-}$ mice in these studies compared to a previous described study[49]. Velcich *et al.* showed that Muc2$^{-/-}$ mice developed adenomas from six months of age, progressing to invasive adenocarcinoma in the small intestine as well as rectal tumors at later age, albeit with no histological nor clinical signs of colitis at younger ages. The mice described by Velcich *et al*. had a mixed genotypic background (C57/BL6-129SV), while in the current study, the knockout mice analyzed had a 129SV background only. Perhaps the phenotypic differences in the Muc2$^{-/-}$ mice can be attributed to differences in strain background and microbial environment as described for the IL10$^{-/-}$ mice[50]. However, the Muc2$^{-/-}$ 129SV mice might be at risk to develop cancer at an older age, in analogy to patients with IBD who are at increased risk of colorectal cancer[51], but this likelihood was not assessed in this thesis.

Regulation of mucin gene expression

Mucin gene expression is governed by complex regulatory mechanisms influenced by developmental and signal dependent transcription factors. The early expression of mucins before or during mucus cell, and more specifically goblet cell differentiation, indicates that they may be the targets of transcription factors responsible for those programs[52]. Muc2 is expressed early during embryonic

development of the intestine[53], which suggests that Muc2 transcription is under the influence of transcription factors responsible for intestinal development and cell differentiation. In line with this hypothesis the human MUC2 mucin gene was found to be regulated by Cdx1 and Cdx2 transcription factors[54], which are both involved in intestinal cell differentiation[55]. Having found binding sites for GATA and HNF factors in the promoter of Muc2, and seeing that Muc2 and these factors show spatio-temporal restricted patterns of expression along the crypt-villus axis in the intestine, we set out to study the regulation of the promoter of mouse Muc2 by GATA-4/-5/-6 and HNF-3α and -3β factors. As described in **Chapter 7**, GATA-4 was present in the nuclei of goblet cells in the small intestine. Furthermore, four GATA-4 *cis*-elements were identified in the promoter, and *Muc2* promoter was efficiently activated when GATA-4 was overexpressed in the cells, with loss of transactivation when the binding sites were mutated or when a mutated form of GATA-4 was used. Overexpression of GATA-5 and GATA-6 also induced activity of *Muc2* promoter. Altogether these results emphasize an important role for GATA factors as potent activators of Muc2 expression in the intestine. Subsequently in **Chapter 8**, we initiated to study the role of HNF-3α and -3β factors in Muc2 regulation. We first showed localization of HNF-3α and HNF-3β in Muc2-expressing goblet cells early in the developmental stages of the intestine (embryonic day 17.5). Furthermore, we demonstrated that both transcription factors regulate Muc2 transcription and bind to the Muc2 promoter *in vivo*. Altogether these results identify Muc2 as a new target of HNF-3α and HNF-3β and point at an important role for these transcription factors in Muc2 expression in the intestine during development and goblet cell differentiation. Furthermore, mucin gene transcription has been shown to be influenced by a broad range of cytokines. Analysis of the Muc5ac promoter showed a high density of binding sites for factors essential for Transforming Growth Factor-β (TGF-β) signaling. TGF-β is a member of the superfamily of cytokines that affect a variety of cell types and elicit a wide array of cell-type-specific biological effects such as differentiation, migration, cell cycle arrest, adhesion, extracellular matrix production, and apoptosis[56]. TGF-β is also involved in gastritis and development of gastric cancer[57], two pathologies that show altered MUC5AC expression. This knowledge led us to study Muc5ac regulation by TGF-β as described in **Chapter 9.** Our results indicate that Muc5ac is a target gene of TGF-β. However, they also suggest that the pathway induced by TGF-β does not only imply complex formation between Smad4 and Smad2 or Smad4 and Smad3. Apart from activating Smad factors, TGF-β is also known to activate Sp1 site-dependent transcription of its target genes; Smad factors are known to activate transcription through Sp1 sites; and Sp1 interacts with Smad4 to induce transcription, which mechanism is TGF-β dependent[58-60]. The data presented in chapter 9 are in favor of such a positive regulatory mechanism between Smad4 and Sp1 to explain the TGF-β-mediated upregulation of Muc5ac expression in cancer cells.

These studies give us insights into the regulation pathways of the mucin genes Muc2 and Muc5ac, however, these regulation pathways are not exclusive. For example, GATA-4 is expressed in the small intestine where Muc2 is also expressed. However, Muc2 is also highly expressed in the colon whereas GATA-4 is not. This shows that GATA-4 alone is not sufficient for the cell-specific transcriptional activation of Muc2. In addition, GATA-4 inducible knockout mice show increased Muc2

production. This can be accounted for, however, by a 50% increase of goblet cells[61]. Consistent with an expansion of secretory goblet cells, Math-1, a known activator of the secretory cell fate[62, 63], was induced in the jejunum of GATA-4 mutant mice. This suggests that GATA-4 does not only regulate Muc2 expression on a transcription level, but may also be involved in the choice of intestinal epithelial cell fate. The Notch pathway specifies cell fate through feedback amplification of relative differences in cellular levels of Notch and its ligand Delta[64]. Cells that produce large amounts of Notch induce expression of transcription factors, such as Hes-1[65]. Hes-1 is a transcriptional repressor, and therefore cells that express the Hes-1 gene remain precursor (enterocyte) cells. Math-1 is a downstream target of Hes-1, therefore controlling initial choice of cell fate. In cells in which Delta expression levels are high, Hes-1 expression is blocked, and Math-1 expression is induced. Expression of Math-1 allows precursor cells to choose whether to become goblet cells, Paneth cells or enteroendocrine cells. Nevertheless, the regulatory role of GATA-4 on the Math-1, Hes-1 transcription factors in this signaling pathway remains to be investigated.

Furthermore, it would be interesting to asses expressions of these different transcription factors during intestinal damage in order to gain insight into Muc2 regulation. A study described by de Koning *et al.*[42], showed diminished GATA-4, Cdx-2 and HNF-1 expression during most severe damage of the intestine after MTX-treatment and restoration of expression of these factors during regeneration. This suggests that the epithelium in the intestine is preferentially involved with proliferation rather than with differentiation during severe damage, but needs cell differentiation to restore intestinal barrier function during regeneration. Data by Verburg *et al*.[15] showed that there was indeed downregulation of Muc2 mRNA during MTX-induce intestinal damage, corresponding with the diminished expression of transcription factors as described above. However, they also showed that despite the low levels of Muc2 mRNA there was an increase in Muc2 protein levels, suggesting the involvement of post-transcriptional regulatory mechanisms that enhance Muc2 secretion in order to preserve Muc2 barrier function. There is no indication for a negative regulatory mechanism among the transcription factors studied. For an expression gradient along the small intestine has been identified in which GATA-4 expression decreases from proximal to distal, and HNF-1α and –β expression as well as Cdx-2 expression increase from proximal to distal small intestine[66]. This shows that downregulation of one factor does not automatically lead to downregulation of others.

General regulatory mechanisms may be involved, of through which developmental transcription factors target intestinal-specific genes expression. The four secretory mucins, Muc2, Muc5ac, Muc5B and Muc6 are clustered on chromosome 7. In addition, they are all expressed by tissues that derive from the primitive gut[53, 67] in which Cdx2, GATA and HNF also play an important role during the development (chapters 8 and 9 of this thesis and [68-71]). In line with this hypothesis, apart from the Muc2 promoter that appears to be activated by Cdx2[54], GATA-4,-5 and 6 (this thesis, chapter 7) as well as members of the HNF-3 family (this thesis, chapter 8), several other intestine-specific gene expressions, such as intestinal lactase-phlorizin hydrolase and sucrase isomaltase expression, have been shown to be controlled by Cdx-1/-2, HNF-1/-3 and GATA-4/-5/-6[72-77].

Interestingly, a recent publication showed that HNF-4 activity was downregulated

by tumor necrosis factor alpha (TNF-α) via a nuclear factor kappa B (NF-κB) dependent pathway[78]. As both TNF-α and NF-κB were found to be upregulated in ulcerative colitis patients[79-81], NF-κB might also affect other families of transcription factors, more specifically the HNF family, during inflammation. In line with this finding, another recent publication showed transdifferentation of cells (by upregulation of HNF-3α and -β) into distinct epithelial cell types to repair airway epithelium after injury[82]. These findings imply the workings of general mechanisms between endoderm tissues aimed at regeneration through upregulation of transcription factors involved in differentiation.

As described in chapter 9, TGF-β can induce Muc5ac transcription. Previous studies using epithelial cells showed that TGF-β can also mediate Muc2 transcription[83]. TGF-β is upregulated in patients with IBD[84], however its signaling was found to be impaired[85, 86]. In addition to decreased SMAD-3 phosphorylation, SMAD-7, an antagonist of the TGF-β pathway, appeared to be upregulated in the affected areas of the intestinal mucosa of these patients, thus blocking TGF-β signalling[85]. Interferon gamma, a proinflammatory cytokine, has proved an important mediator in enhancing SMAD-7 production[87] and may thus contribute to the uncontrolled inflammation seen in patients with IBD. Therefore, the physiological role of TGF-β signaling on Muc2 transcription in IBD patients remains to be investigated.

Muc2 may also be directly involved in proliferation and differentiation of epithelial cells. Studies, as described in chapters 8 and 9, show that Muc2 expression is under the control of transcription factors responsible for programs of cell differentiation in the intestine. This provides another argument in favor of Muc2 involvement in goblet cell differentiation along the crypt-villus axis. More evidence supporting this hypothesis comes from intensified proliferation in the small intestine of Muc2$^{-/-}$ mice as described by Velcich *et al.*[88], and in the Muc2$^{-/-}$129SV mice as the mice age (our unpublished observations). Thus, next to the fact that Muc2 is crucial for epithelial protection and as such is part of the innate defense mechanism in the intestine, this molecule might also be important in the regulation of epithelial homeostasis (*e.g.*, epithelial proliferation and differentiation).

General future perspectives

The findings from this thesis clearly point at a pivotal role for Muc2 in maintaining intestinal homeostasis. A next crucial step would be to unravel the mechanisms behind the development of inflammation in the absence of Muc2. Signaling profiling studies (*i.e.* TLRs) could be performed to identify molecules that i) initiate/perpetuate inflammation, ii) regulate epithelial proliferation, and iii) regulate epithelial differentiation. Furthermore, the fusion of germ-free and gnotobiotic technology, functional genomics and quantative PCR would make it possible to use the Muc2$^{-/-}$ and WT mouse models to quantify the impact of the microbial population on cell homeostasis, gene expression and subsequent barrier function of the gut. In addition, these models would enable evaluation of the roles of pre- and probiotics in intestinal protection, and more specifically mucin production. Cumulatively, these data would give more information about microbes, genes and signaling pathways involved in intestinal inflammation, possibly leading to identification of potential therapeutic targets.

References

1. Herrmann A, Davies JR, Lindell G, Martensson S, Packer NH, Swallow DM, Carlstedt I. Studies on the “insoluble” glycoprotein complex from human colon. Identification of reduction-insensitive MUC2 oligomers and C-terminal cleavage. J Biol Chem 1999;274:15828-36.
2. Karlsson NG, Herrmann A, Karlsson H, Johansson ME, Carlstedt I, Hansson GC. The glycosylation of rat intestinal Muc2 mucin varies between rat strains and the small and large intestine. A study of O-linked oligosaccharides by a mass spectrometric approach. J Biol Chem 1997;272:27025-34.
3. Tytgat KM, Büller HA, Opdam FJ, Kim YS, Einerhand AW, Dekker J. Biosynthesis of human colonic mucin: Muc2 is the prominent secretory mucin. Gastroenterology 1994;107:1352-63.
4. Tytgat KM, Bovelander FJ, Opdam FJ, Einerhand AW, Büller HA, Dekker J. Biosynthesis of rat MUC2 in colon and its analogy with human MUC2. Biochem J 1995;309:221-9.
5. Van Klinken BJ, Einerhand AW, Duits LA, Makkink MK, Tytgat KM, Renes IB, Verburg M, Büller HA, Dekker J. Gastrointestinal expression and partial cDNA cloning of murine Muc2. Am J Physiol 1999;276:G115-24.
6. Tytgat KM, van der Wal JW, Einerhand AW, Büller HA, Dekker J. Quantitative analysis of MUC2 synthesis in ulcerative colitis. Biochem Biophys Res Commun 1996;224:397-405.
7. Van Klinken BJ, Van der Wal JW, Einerhand AW, Büller HA, Dekker J. Sulphation and secretion of the predominant secretory human colonic mucin MUC2 in ulcerative colitis. Gut 1999;44:387-93.
8. Buisine MP, Desreumaux P, Leteurtre E, Copin MC, Colombel JF, Porchet N, Aubert JP. Mucin gene expression in intestinal epithelial cells in Crohn’s disease. Gut 2001;49:544-51.
9. Sartor RB. Microbial influences in inflammatory bowel disease. In: Sartor RB, Sandborn WJ, eds. Kirsner’s Inflammatory Bowel Diseases 6th ed. Amsterdam: Elsevier Publishers, 2004:138-162.
10. Sellon RK, Tonkonogy S, Schultz M, Dieleman LA, Grenther W, Balish E, Rennick DM, Sartor RB. Resident enteric bacteria are necessary for development of spontaneous colitis and immune system activation in interleukin-10-deficient mice. Infect Immun 1998;66:5224-31.
11. Dianda L, Hanby AM, Wright NA, Sebesteny A, Hayday AC, Owen MJ. T cell receptor-alpha beta-deficient mice fail to develop colitis in the absence of a microbial environment. Am J Pathol 1997;150:91-7.
12. Schultz M, Tonkonogy SL, Sellon RK, Veltkamp C, Godfrey VL, Kwon J, Grenther WB, Balish E, Horak I, Sartor RB. IL-2-deficient mice raised under germfree conditions develop delayed mild focal intestinal inflammation. Am J Physiol 1999;276:G1461-72.
13. Taurog JD, Richardson JA, Croft JT, Simmons WA, Zhou M, Fernandez-Sueiro JL, Balish E, Hammer RE. The germfree state prevents development of gut and joint inflammatory disease in HLA-B27 transgenic rats. J Exp Med 1994;180:2359-64.
14. Veltkamp C, Tonkonogy SL, De Jong YP, Albright C, Grenther WB, Balish E, Terhorst C, Sartor RB. Continuous stimulation by normal luminal bacteria is essential for the development and perpetuation of colitis in Tg(epsilon26) mice. Gastroenterology 2001;120:900-13.
15. Verburg M, Renes IB, Van Nispen DJ, Ferdinandusse S, Jorritsma M, Büller HA, Einerhand AW, Dekker J. Specific responses in rat small intestinal epithelial mRNA expression and protein levels during chemotherapeutic damage and regeneration. J Histochem Cytochem 2002;50:1525-36.
16. Verburg M, Renes IB, Meijer HP, Taminiau JA, Büller HA, Einerhand AW, Dekker J. Selective sparing of goblet cells and paneth cells in the intestine of methotrexate-treated rats. Am J Physiol Gastrointest Liver Physiol 2000;279:G1037-47.

17. Löhler J, Kühn R, Rennick D, Rajewsky K, Müller W. Interleukin-10-deficient mice: a model of chronic mucosal inflammation. In: Tytgat GNJ, Bartelsman MFWM, van Deventer SJH, eds. Inflammatory Bowel Diseases. Dordrecht: Kluwer Academic Publishers, 1995:410-417.
18. Kuhn R, Lohler J, Rennick D, Rajewsky K, Muller W. Interleukin-10-deficient mice develop chronic enterocolitis. Cell 1993;75:263-74.
19. de Koning BA, van Dieren JM, Lindenbergh-Kortleve DJ, van der Sluis M, Matsumoto T, Yamaguchi K, Einerhand AW, Samsom JN, Pieters R, Nieuwenhuis EE. Contributions of mucosal immune cells to methotrexate-induced mucositis. Int Immunol 2006;18:941-9.
20. Smirnov A, Sklan D, Uni Z. Mucin dynamics in the chick small intestine are altered by starvation. J Nutr 2004;134:736-42.
21. Sherman P, Forstner J, Roomi N, Khatri I, Forstner G. Mucin depletion in the intestine of malnourished rats. Am J Physiol 1985;248:G418-23.
22. Faure M, Moennoz D, Montigon F, Mettraux C, Breuille D, Ballevre O. Dietary threonine restriction specifically reduces intestinal mucin synthesis in rats. J Nutr 2005;135:486-91.
23. Schaart MW, Schierbeek H, van der Schoor SR, Stoll B, Burrin DG, Reeds PJ, van Goudoever JB. Threonine utilization is high in the intestine of piglets. J Nutr 2005;135:765-70.
24. Midtvedt T, Carlstedt-Duke B, Hoverstad T, Midtvedt AC, Norin KE, Saxerholt H. Establishment of a biochemically active intestinal ecosystem in ex-germfree rats. Appl Environ Microbiol 1987;53:2866-2871.
25. Hooper LV, Wong MH, Thelin A, Hansson L, Falk PG, Gordon JI. Molecular analysis of commensal host-microbial relationships in the intestine. Science 2001;291:881-884.
26. Levine A, Shamir R, Wine E, Weiss B, Karban A, Shaoul RR, Reif SS, Yakir B, Friedlander M, Kaniel Y, Leshinsky-Silver E. TNF promoter polymorphisms and modulation of growth retardation and disease severity in pediatric Crohn's disease. Am J Gastroenterol 2005;100:1598-604.
27. Sawczenko A, Azooz O, Paraszczuk J, Idestrom M, Croft NM, Savage MO, Ballinger AB, Sanderson IR. Intestinal inflammation-induced growth retardation acts through IL-6 in rats and depends on the -174 IL-6 G/C polymorphism in children. Proc Natl Acad Sci U S A 2005;102:13260-13265.
28. Motil KJ, Grand RJ. Growth failure in children and adolescents with inflammatory bowel disease. In: G.N.J. Tytgat MFWMB, S.J.H. van Deventer, ed. Inflammatory Bowel Diseases: Kluwer Academic Publishers, 1995:588-597.
29. Hooper LV, Midtvedt T, Gordon JI. How host-microbial interactions shape the nutrient environment of the mammalian intestine. Annu Rev Nutr 2002;22:283-307.
30. Yamanaka M, Nomura T, Kametaka M. Influence of intestinal microbes on heat production in germ-free, gnotobiotic and conventional mice. J Nutr Sci Vitaminol (Tokyo) 1977;23:221-6.
31. Wostmann BS. The germfree animal in nutritional studies. Annu Rev Nutr 1981;1:257-79.
32. Backhed F, Ding H, Wang T, Hooper LV, Koh GY, Nagy A, Semenkovich CF, Gordon JI. The gut microbiota as an environmental factor that regulates fat storage. Proc Natl Acad Sci U S A 2004;101:15718-23.
33. Metges CC. Contribution of microbial amino acids to amino acid homeostasis of the host. J Nutr 2000;130:1857S-64S.
34. Metges CC, Eberhard M, Petzke KJ. Synthesis and absorption of intestinal microbial lysine in humans and non-ruminant animals and impact on human estimated average requirement of dietary lysine. Curr Opin Clin Nutr Metab Care 2006;9:37-41.
35. Nowacki MR. Cell proliferation in colonic crypts of germ-free and conventional mice--preliminary report. Folia Histochem Cytobiol 1993;31:77-81.

36. Rakoff-Nahoum S, Paglino J, Eslami-Varzaneh F, Edberg S, Medzhitov R. Recognition of commensal microflora by toll-like receptors is required for intestinal homeostasis. Cell 2004;118:229-41.
37. Cario E. Bacterial interactions with cells of the intestinal mucosa: Toll-like receptors and NOD2. Gut 2005;54:1182-93.
38. Cario E, Podolsky DK. Differential alteration in intestinal epithelial cell expression of toll-like receptor 3 (TLR3) and TLR4 in inflammatory bowel disease. Infect Immun 2000;68:7010-7.
39. Ortega-Cava CF, Ishihara S, Rumi MA, Kawashima K, Ishimura N, Kazumori H, Udagawa J, Kadowaki Y, Kinoshita Y. Strategic compartmentalization of Toll-like receptor 4 in the mouse gut. J Immunol 2003;170:3977-85.
40. Singh JC, Cruickshank SM, Newton DJ, Wakenshaw L, Graham A, Lan J, Lodge JP, Felsburg PJ, Carding SR. Toll-like receptor-mediated responses of primary intestinal epithelial cells during the development of colitis. Am J Physiol Gastrointest Liver Physiol 2005;288:G514-24.
41. Rakoff-Nahoum S, Hao L, Medzhitov R. Role of Toll-like Receptors in Spontaneous Commensal-Dependent Colitis. Immunity 2006.
42. de Koning BA, Lindenbergh-Kortleve DJ, Pieters R, Rings EH, Büller HA, Renes IB, Einerhand AW. The effect of cytostatic drug treatment on intestine-specific transcription factors Cdx2, GATA-4 and HNF-1alpha in mice. Cancer Chemother Pharmacol 2006;57:801-10.
43. Renes IB, Verburg M, Van Nispen DJ, Büller HA, Dekker J, Einerhand AW. Distinct epithelial responses in experimental colitis: implications for ion uptake and mucosal protection. Am J Physiol Gastrointest Liver Physiol 2002;283:G169-179.
44. Hollingsworth MA, Swanson BJ. Mucins in cancer: protection and control of the cell surface. Nat Rev Cancer 2004;4:45-60.
45. Braat H, Rottiers P, Hommes DW, Huyghebaert N, Remaut E, Remon JP, van Deventer SJ, Neirynck S, Peppelenbosch MP, Steidler L. A phase I trial with transgenic bacteria expressing interleukin-10 in Crohn's disease. Clin Gastroenterol Hepatol 2006;4:754-9.
46. Steidler L, Hans W, Schotte L, Neirynck S, Obermeier F, Falk W, Fiers W, Remaut E. Treatment of murine colitis by Lactococcus lactis secreting interleukin-10. Science 2000;289:1352-5.
47. Mack DR, Michail S, Wei S, McDougall L, Hollingsworth MA. Probiotics inhibit enteropathogenic E. coli adherence in vitro by inducing intestinal mucin gene expression. Am J Physiol 1999;276: G941-50.
48. Mattar AF, Teitelbaum DH, Drongowski RA, Yongyi F, Harmon CM, Coran AG. Probiotics up-regulate MUC-2 mucin gene expression in a Caco-2 cell-culture model. Pediatr Surg Int 2002;18:586-90.
49. Velcich A, Yang W, Heyer J, Fragale A, Nicholas C, Viani S, Kucherlapati R, Lipkin M, Yang K, Augenlicht L. Colorectal cancer in mice genetically deficient in the mucin Muc2. Science 2002;295:1726-9.
50. Mahler M, Leiter EH. Genetic and environmental context determines the course of colitis developing in IL-10-deficient mice. Inflamm Bowel Dis 2002;8:347-55.
51. Itzkowitz SH, Yio X. Inflammation and cancer IV. Colorectal cancer in inflammatory bowel disease: the role of inflammation. Am J Physiol Gastrointest Liver Physiol 2004;287:G7-17.
52. Van Seuningen I, Pigny P, Perrais M, Porchet N, Aubert JP. Transcriptional regulation of the 11p15 mucin genes. Towards new biological tools in human therapy, in inflammatory diseases and cancer? Front Biosci 2001;6:D1216-1234.
53. Buisine MP, Devisme L, Savidge TC, Gespach C, Gosselin B, Porchet N, Aubert JP. Mucin gene expression in human embryonic and fetal intestine. Gut 1998;43:519-524.

54. Mesquita P, Jonckheere N, Almeida R, Ducourouble MP, Serpa J, Silva E, Pigny P, Silva FS, Reis C, Silberg D, Van Seuningen I, David L. Human MUC2 mucin gene is transcriptionally regulated by Cdx homeodomain proteins in gastrointestinal carcinoma cell lines. J Biol Chem 2003;278:51549-51556.
55. Silberg DG, Swain GP, Suh ER, Traber PG. Cdx1 and cdx2 expression during intestinal development. Gastroenterology 2000;119:961-971.
56. Massague J. TGF-beta signal transduction. Annu Rev Biochem 1998;67:753-91.
57. Milani S, Calabro A. Role of growth factors and their receptors in gastric ulcer healing. Microsc Res Tech 2001;53:360-71.
58. Black AR, Black JD, Azizkhan-Clifford J. Sp1 and kruppel-like factor family of transcription factors in cell growth regulation and cancer. J Cell Physiol 2001;188:143-60.
59. Datta PK, Blake MC, Moses HL. Regulation of plasminogen activator inhibitor-1 expression by transforming growth factor-beta -induced physical and functional interactions between smads and Sp1. J Biol Chem 2000;275:40014-9.
60. Feng XH, Lin X, Derynck R. Smad2, Smad3 and Smad4 cooperate with Sp1 to induce p15(Ink4B) transcription in response to TGF-beta. Embo J 2000;19:5178-93.
61. Bosse T, Piaseckyj CM, Burghard E, Fialkovich JJ, Rajagopal S, Pu WT, Krasinski SD. Gata4 Is Essential for the Maintenance of Jejunal-Ileal Identities in the Adult
Mouse Small Intestine. Supplement to Gastroenterology 2006;130:A-106.
62. Yang Q, Bermingham NA, Finegold MJ, Zoghbi HY. Requirement of Math1 for secretory cell lineage commitment in the mouse intestine. Science 2001;294:2155-8.
63. van Den Brink GR, de Santa Barbara P, Roberts DJ. Development. Epithelial cell differentiation--a Mather of choice. Science 2001;294:2115-6.
64. Lewis J. Notch signalling and the control of cell fate choices in vertebrates. Semin Cell Dev Biol 1998;9:583-9.
65. Kageyama R, Ohtsuka T, Tomita K. The bHLH gene Hes1 regulates differentiation of multiple cell types. Mol Cells 2000;10:1-7.
66. Fang R, Olds LC, Sibley E. Spatio-temporal patterns of intestine-specific transcription factor expression during postnatal mouse gut development. Gene Expr Patterns 2006;6:426-32.
67. Escande F, Porchet N, Bernigaud A, Petitprez D, Aubert JP, Buisine MP. The mouse secreted gel-forming mucin gene cluster. Biochim Biophys Acta 2004;1676:240-250.
68. Molkentin JD. The zinc finger-containing transcription factors GATA-4, -5, and -6. Ubiquitously expressed regulators of tissue-specific gene expression. J Biol Chem 2000;275:38949-52.
69. Sasaki H, Hogan BL. Differential expression of multiple fork head related genes during gastrulation and axial pattern formation in the mouse embryo. Development 1993;118:47-59.
70. Kaestner KH, Hiemisch H, Luckow B, Schutz G. The HNF-3 gene family of transcription factors in mice: gene structure, cDNA sequence, and mRNA distribution. Genomics 1994;20:377-85.
71. Silberg DG, Swain GP, Suh ER, Traber PG. Cdx1 and cdx2 expression during intestinal development. Gastroenterology 2000;119:961-71.
72. Gao X, Sedgwick T, Shi YB, Evans T. Distinct functions are implicated for the GATA-4, -5, and -6 transcription factors in the regulation of intestine epithelial cell differentiation. Mol Cell Biol 1998;18:2901-2911.
73. Van Wering HM, Bosse T, Musters A, De Jong E, De Jong N, Hogen Esch CE, Boudreau F, Swain GP, Dowling LN, Montgomery RK, Grand RJ, Krasinski SD. Complex regulation of the lactase-phlorizin hydrolase promoter by GATA-4. Am J Physiol Gastrointest Liver Physiol 2004;287:G899-G909.

74. Boudreau F, Rings EH, van Wering HM, Kim RK, Swain GP, Krasinski SD, Moffett J, Grand RJ, Suh ER, Traber PG. Hepatocyte nuclear factor-1 alpha, GATA-4, and caudal related homeodomain protein Cdx2 interact functionally to modulate intestinal gene transcription. Implication for the developmental regulation of the sucrase-isomaltase gene. J Biol Chem 2002;277:31909-31917.
75. Bosse T, van Wering HM, Gielen M, Dowling LN, Fialkovich JJ, Piaseckyj CM, Gonzalez FJ, Akiyama TE, Montgomery RK, Grand RJ, Krasinski SD. Hepatocyte nuclear factor-1{alpha} is required for expression but dispensable for histone acetylation of the lactase-phlorizin hydrolase gene in vivo. Am J Physiol Gastrointest Liver Physiol 2006;290:G1016-24.
76. Fang R, Olds LC, Santiago NA, Sibley E. GATA family transcription factors activate lactase gene promoter in intestinal Caco-2 cells. Am J Physiol Gastrointest Liver Physiol 2001;280: G58-67.
77. Krasinski SD, Van Wering HM, Tannemaat MR, Grand RJ. Differential activation of intestinal gene promoters: functional interactions between GATA-5 and HNF-1 alpha. Am J Physiol Gastrointest Liver Physiol 2001;281:G69-84.
78. Nikolaidou-Neokosmidou V, Zannis VI, Kardassis D. Inhibition of Hepatocyte Nuclear Factor 4 transcriptional activity by the Nuclear Factor kappaB pathway. Biochem J 2006.
79. Andresen L, Jorgensen VL, Perner A, Hansen A, Eugen-Olsen J, Rask-Madsen J. Activation of nuclear factor kappaB in colonic mucosa from patients with collagenous and ulcerative colitis. Gut 2005;54:503-9.
80. Fiocchi C. Inflammatory bowel disease: etiology and pathogenesis. Gastroenterology 1998;115:182-205.
81. Bouma G, Strober W. The immunological and genetic basis of inflammatory bowel disease. Nat Rev Immunol 2003;3:521-533.
82. Park KS, Wells JM, Zorn AM, Wert SE, Laubach VE, Fernandez LG, Whitsett JA. Transdifferentiation of ciliated cells during repair of the respiratory epithelium. Am J Respir Cell Mol Biol 2006;34:151-7.
83. Jono H, Shuto T, Xu H, Kai H, Lim DJ, Gum JR, Jr., Kim YS, Yamaoka S, Feng XH, Li JD. Transforming growth factor-beta -Smad signaling pathway cooperates with NF-kappa B to mediate nontypeable Haemophilus influenzae-induced MUC2 mucin transcription. J Biol Chem 2002;277:45547-57.
84. Babyatsky MW, Rossiter G, Podolsky DK. Expression of transforming growth factors alpha and beta in colonic mucosa in inflammatory bowel disease. Gastroenterology 1996;110:975-84.
85. Monteleone G, Kumberova A, Croft NM, McKenzie C, Steer HW, MacDonald TT. Blocking Smad7 restores TGF-beta1 signaling in chronic inflammatory bowel disease. J Clin Invest 2001;108:601-9.
86. Fiocchi C. TGF-beta/Smad signaling defects in inflammatory bowel disease: mechanisms and possible novel therapies for chronic inflammation. J Clin Invest 2001;108:523-6.
87. Ulloa L, Doody J, Massague J. Inhibition of transforming growth factor-beta/SMAD signalling by the interferon-gamma/STAT pathway. Nature 1999;397:710-3.
88. Velcich A, Yang W, Heyer J, Fragale A, Nicholas C, Viani S, Kucherlapati R, Lipkin M, Yang K, Augenlicht L. Colorectal cancer in mice genetically deficient in the mucin Muc2. Science 2002;295:1726-9.

Chapter 11

Dutch Summary
Curriculum Vitae & Publications
Acknowledgements - Dankwoord
Color Plates

Dutch Summary

Nederlandse Samenvatting voor Niet-ingewijden

De rol van mucines in de darm

Zoals beschreven in **Hoofdstuk 1** is het eiwit mucine 2 (Muc2) de meest voorkomende secretoire mucine in de dikke darm van zoogdieren. Muc2 wordt geproduceerd in slijmbeker-cellen – ook wel goblet-cellen genoemd – in de gehele darm, en is de belangrijkste component van de mucuslaag. Deze mucuslaag is strategisch gesitueerd tussen de darmholte en het epitheel (cellen die de darmoppervlakte bekleden). Onze hypothese is dat deze mucuslaag de darm(wand)cellen beschermt tegen mogelijk schadelijke stoffen in de darmholte. De resultaten van voorgaande studies ondersteunen deze hypothese; zo is aangetoond dat mensen met chronische ontstekingen aan de dikke darm (bijvoorbeeld Colitis Ulcerosa) een verlaagde productie van Muc2 hebben. Dit zijn echter klinische studies, die geen antwoord geven op de vraag of deze verlaagde Muc2 synthese een primair gebrek is, of indirect een gevolg is van een ontstekingsreactie. Een belangrijke oorzaak van colitis, een ontsteking van de dikke darm, is de aanwezigheid van bacteriën in de darm. Zo kunnen normale darmbacteriën bij knaagdieren met een genetische aanpassing in het afweersysteem colitis veroorzaken. Muc2 zorgt voor een natuurlijke barrière tussen bacteriën en de epitheelcellen. Veranderingen in de structuur van Muc2 of in de aangemaakte hoeveelheden zouden daarom de (schadelijke) uitwerking van bacteriën op het darmslijmvlies kunnen beïnvloeden.

Wanneer we beter zouden weten wat de functie van mucine-genen in de darm is en hoe deze gereguleerd worden, zouden we kunnen komen tot nieuwe behandelmethoden voor darmziektes. Met als doel om een beter begrip van deze materie te krijgen, richtte dit promotieonderzoek zich in grote lijnen op:

1. De invloed van een verlaagde productie van mucine, specifiek Muc2, op de barrièrefunctie en de fysiologie van de darm.
2. De mechanismen die het lichaam gebruikt om de hoeveelheid mucines te regelen.

In **Hoofdstuk 2** werd bij kiemvrije (steriele) interleukine-10 deficiënte muizen ($IL10^{-/-}$; deze muizen kunnen geen IL-10 maken) onderzocht wat de gevolgen zijn van het inbrengen van specifieke niet-schadelijke en natuurlijk voorkomende bacteriën op de aanmaak en structuur van Muc2. IL-10 is een eiwit dat het lichaam aanmaakt om ontstekingsreacties te dempen. $IL10^{-/-}$ muizen krijgen een ontsteking in de darm als ze aan (normale, niet-schadelijke) bacteriën worden blootgesteld. Deze $IL\text{-}10^{-/-}$ muizen vertoonden echter onder kiemvrije omstandigheden geen biochemische of histologische kenmerken van ontstekingsreacties in de darm. We zagen dat nog vóór het inbrengen van bacteriën en dus vóór het mogelijke ontstaan van een ontsteking, de hoeveelheid Muc2 die in de darm van de $IL10^{-/-}$ muizen werd aangemaakt lager was dan bij 'gewone' *wild-type* (WT) controlemuizen. De ontsteking bij de $IL10^{-/-}$ muizen na de introductie van darmbacteriën, kenmerkte zich door verdikking van het darmslijmvlies, een groter aantal zich delende cellen in de crypten en meer celdood bij de oppervlaktecellen van de darm. Met het verloop van de ontsteking van mild naar ernstig, was er ook een verandering in de structuur c.q. opbouw van Muc2 te zien. Door deze kwantitatieve en structurele veranderingen van Muc2 bij $IL10^{-/-}$

muizen waren de epitheelcellen van de darm minder goed in staat zich tegen (niet-schadelijke) bacteriën te beschermen. Het resultaat is een mogelijke verhoogde gevoeligheid voor colitis.

De rol van Muc2 bij de bescherming van de darm werd verder uitgediept in **Hoofdstuk 3**. Na karakterisering van de dikke darm van Muc2-deficiënte ($Muc2^{-/-}$) muizen (deze muizen maken geen Muc2 aan) kregen ze dextraan sulfaat sodium toegediend, een stof die colitis veroorzaakt . Dit werd ook gedaan bij Muc2 heterozygote muizen (deze hebben één gen van het Muc2 in plaats van twee) en WT muizen. Het tekort/gebrek aan Muc2 in de darm van deze muizen veroorzaakt, zelfs onder normale omstandigheden, verdikking van het darmslijmvlies, een groter aantal zich delende cellen, verandering in de differentiatie van epitheel- en goblet-cellen, en schade aan de epitheelcellen in de dikke darm. De proef met dextraan-sulfaat sodium toonde aan dat de $Muc2^{-/-}$ en de Muc2 heterozygote muizen, die een gebrek of een tekort hadden aan Muc2 in de darm, gevoeliger waren voor colitis dan de WT muizen. Deze proeven bewijzen dat veranderingen in de samenstelling van de mucuslaag als gevolg van minder of géén Muc2, leiden tot een ontsteking van de dikke darm. Ook lieten ze zien dat te weinig of géén Muc2 kan bijdragen tot inductie en verergering van een chronische vorm van ontsteking.

In de wetenschap dat de ernst van chronische ontstekingen van de dikke darm samenhangt met omgevingsfactoren (o.a. bacteriën), maar ook met eigenschappen van het epitheel (epitheliale factoren) en het afweersysteem, deden we onderzoek naar de beschermende capaciteiten van Muc2 en IL10 in de darm. Speciaal hiervoor werden Muc2/IL10 dubbel *knock-out* muizen ($Muc2/IL10^{DKO}$) gefokt. Bij deze muizen keken we of een combinatie van defecten in het afweersysteem en epitheliale factoren, het ziekteverloop van de ontsteking zou kunnen verergeren. Om inzicht te krijgen in de beschermende capaciteiten van Muc2 en IL10 in de darm, vergeleken we de klinische symptomen en darmpathologie van de $Muc2/IL10^{DKO}$ muis met die van $Muc2^{-/-}$ en $IL10^{-/-}$ muizen (**Hoofdstuk 4**). Microscopische analyse van de dikke darm van de $Muc2^{-/-}$ muis liet een abnormale vorm en structuur zien. We zagen een verdikking van het darmslijmvlies, afplatting en verzwering van epitheelcellen, algeheel verlies van structuur, een groter aantal cellen die betrokken zijn bij ontsteking, meer celdeling en minder celdifferentiatie, zoals beschreven in hoofdstuk 3. Deze afwijkingen waren nog sterker bij $Muc2IL10^{DKO}$ muizen van dezelfde leeftijd. Dit wijst er op dat afwezigheid van Muc2 in combinatie met veranderingen in het afweermechanismen, bijvoorbeeld gebrek aan IL10, leidt tot een buitensporige, oncontroleerbare ontsteking van de dikke darm, uiteindelijk leidend tot de dood van het dier. Deze studie geeft aan dat de mucuslaag in de darm, meer specifiek de mucine Muc2, een kernrol speelt in de bescherming van de darm, en dat de mucusbarrière waarschijnlijk één van de belangrijkste factoren is voor het ontstaan van colitis.

Een andere hypothese over Muc2 luidt als volgt: Muc2 draagt bij tot de bescherming van darmcellen tegen bijvoorbeeld de schadelijke gevolgen van chemotherapie (mucositis). Deze hypothese is gebaseerd op een eerdere studie die aantoonde dat methotrexaat (MTX) de Muc2 eiwitexpressie significant verhoogt. Om deze hypothese te kunnen bewijzen, werden $Muc2^{-/-}$ muizen behandeld met MTX. Zoals beschreven in **Hoofdstuk 5**, bleek uit histologische en biochemische

analyse van de dunne darm dat de Muc2$^{-/-}$ muizen niet gevoeliger waren voor behandeling met MTX. Afwezigheid van Muc2 kan bij Muc2$^{-/-}$ muizen kan leiden tot een continue blootstelling aan bacteriën in de darmholte, wat de productie van cytokines – boodschapperstoffen van het afweersysteem – uit balans kan brengen. De ontstekingsremmende cytokine IL-10 vertoont beschermende eigenschappen in de darm. Verschillende studies hebben aangetoond dat IL10$^{-/-}$ muizen gevoeliger zijn voor de ontwikkeling van chronische ontstekingen (hoofdstuk 2). De Koning *et al*., toonden ook aan dat IL10$^{-/-}$ muizen na behandeling met MTX een zwaardere vorm van mucositis ontwikkelen dan WT muizen. Dit bewijst dat IL-10 de darm tegen MTX-geïnduceerde schade beschermt. In Muc2$^{-/-}$ muizen was IL-10 verhoogd nog vóór behandeling met MTX. Dit geeft een verklaring waarom deze muizen geen verhoogde chemotherapie-geïnduceerde mucositis vertoonden.

De bovenstaand beschreven studies bevestigen het belang van een gezonde mucuslaag. Bovendien is een perfecte conditie van de mucuslaag ook afhankelijk van de beschikbaarheid van voedingsstoffen, zoals eiwitten, vetten, koolhydraten en essentiële aminozuren in de darm. Ondervoeding (zowel kwalitatief als kwantitatief) verlaagt de mucineproductie in de darm, en tast hiermee de mucuslaag aan. Verder is aangetoond dat te weinig threonine, een essentieel aminozuur, in de voeding de mucineproductie in de darm vermindert. Onze hypothese is dat de hoge vraag naar threonine van de darm uit de voeding, zoals beschreven in Schaart *et al*., waarschijnlijk te wijten is aan het feit dat threonine wordt gebruikt voor de opbouw van secretorische mucines, voornamelijk Muc2. Daarom werd in **Hoofdstuk 6** de betrokkenheid van mucines bij het metabolisme van de darm onderzocht. Er kon inderdaad aangetoond worden dat veel threonine uit de voeding in de darm in Muc2 wordt opgenomen. Als er geen Muc2 aanwezig is wordt het vooral gebruikt voor de onderhoudseiwitsynthese of als substraat voor oxidatie.

Samengevat laat het eerste deel van dit proefschrift zien dat kwantitatieve en structurele veranderingen in Muc2 in de darm uitwerking heeft op de celdeling en differentiatie, met als gevolg ontsteking. Dit bewijst dat Muc2 een kernrol speelt in de beschermende mucuslaag van de darm.

Regulatie van mucine-genexpressie

De aanmaak van alle eiwitten geschiedt d.m.v. transcriptie (dit gebeurt in de celkern: aanmaak van RNA complementair aan één van de DNA-strengen) en translatie (vertaling van RNA codes tot specifieke ketens aminozuren, de voorlopers van eiwitten). De promotor is dat deel van het gen dat de werking (expressie) van het gen reguleert. De transcriptie van mucine-genen wordt aangestuurd door complexe regelmechanismen, onder invloed van ontwikkelings- en signaalafhankelijke transcriptiefactoren. Deze factoren binden aan de promotor-regio van het gen. Muc2 wordt al vroeg tijdens de embryonale ontwikkeling van de darm tot expressie gebracht. Dit suggereert dat de Muc2-transcriptie beïnvloed wordt door bepaalde transcriptiefactoren die verantwoordelijk zijn voor de ontwikkeling en celdifferentiatie van de darm. In overeenstemming met deze hypothese werd in eerdere onderzoeken gevonden dat het Muc2 mucine–gen bij de mens wordt gereguleerd door Cdx1 en Cdx2 transcriptiefactoren. Deze Cdx-factoren zijn beide betrokken bij

de celdifferentiatie van de darm. Na mogelijke bindingsplaatsen voor GATA- en HNF-factoren op de Muc2-promotor te hebben gevonden en na gezien te hebben dat Muc2 en deze factoren slechts beperkt tot uiting komen in de crypte-villus as van de darm, onderzochten we de regulering van de Muc2 promotor door GATA-4/-5/-6, HNF-3α en HNF-3β transcriptiefactoren bij de muis. Zoals beschreven in **Hoofdstuk 7**, was GATA-4 aanwezig in de kernen van de goblet-cellen in de dunne darm. Bovendien werden er vier GATA-4 *cis*-elementen geïdentificeerd in de promotor. Een overexpressie van GATA-4 in cellijnen leidde tot activatie van de Muc2–promotor. Dit werd echter ongedaan gemaakt wanneer de bindingsplaatsen gemuteerd werden of wanneer een gemuteerde vorm van GATA-4 gebruikt werd. Ook kon overexpressie van GATA-5 en GATA-6 leiden tot activiteit van de Muc2-promotor. Deze resultaten tonen aan dat GATA-factoren belangrijke en krachtige activatoren zijn van de Muc2-expressie in de darm.

Vervolgens werd in **Hoofdstuk 8** de rol van HNF-3α en -3β factoren op de Muc2-regulatie bestudeerd. HNF-3α en 3β factoren werden gelokaliseerd in goblet-cellen, die Muc2 tot expressie brengen, vroeg in de ontwikkeling van de darm (embryonale dag 17.5). Bovendien werd aangetoond dat de beide transcriptiefactoren Muc2-transcriptie reguleren en zich kunnen binden aan de Muc2-promotor. Het blijkt dus dat Muc2 eveneens een doelwit is van HNF-3α en 3β, en dat deze transcriptiefactoren een belangrijke rol spelen bij de Muc2-expressie in de zich ontwikkelende darm tijdens goblet-cel differentiatie. Ook werd aangetoond dat de mucine-gentranscriptie onder invloed staat van een breed spectrum van cytokines. Analyse van de Muc5ac-promotor liet een hoge dichtheid van bindingplaatsen zien voor factoren die essentieel zijn voor de signalering van Transforming Growth Factor-β (TGF-β). TGF-β behoort tot een superfamilie van cytokines die diverse celtypes aangrijpt en een scala aan celspecifieke biologische effecten reguleert, zoals differentiatie, migratie, tijdelijk stopzetten van de celdeling, adhesie, extracellulaire-matrixproductie en celdood. Ook is TGF-β betrokken bij gastritis (ontsteking van het maagslijmvlies) en de ontwikkeling van maagkanker, twee ziektebeelden die ook een veranderde Muc5AC expressie laten zien. Deze bevindingen leidden tot een onderzoek naar de regulering van Muc5ac door TGF-β, zoals beschreven in **Hoofdstuk 9**. De resultaten toonden aan dat het Muc5ac-gen een doelwit is van TGF-β. Bovendien lijkt het aannemelijk dat de signaleringsroute, geïnduceerd door TGF-β, niet alleen een complexe formatie is van Smad4 en Smad2 of van Smad4 en Smad3. Los van het activeren van Smad-factoren, staat TGF-β ook bekend om het kunnen activeren van Sp1-afhankelijke transcriptie. De bevindingen in hoofdstuk 9 duiden op de werking een positief regelmechanisme tussen Smad4 en Sp1 dat de TGF-β-gemedieerde verhoging van Muc5ac expressie in kankercellen zou kunnen verklaren.

Samenvattend, we hebben aangetoond dat Muc2 gereguleerd wordt door transcriptiefactoren, in het bijzonder GATA en HNF3, die betrokken zijn bij de ontwikkeling en celdifferentiatie van de darm. Bovendien werd aangetoond dat TGF-β de transcriptie van het secretoire mucine-gen Muc5ac, kan verhogen in kankercellijnen. Dit suggereert dat de mucine-genexpressie hoogstwaarschijnlijk onder invloed staat van de homeostase-status van de darm. De onderzochte signaalroutes zijn echter niet exclusief en andere routes moeten in de toekomst nog verder uitgediept worden.

Algemene toekomstperspectieven

De bevindingen in dit proefschrift laten een duidelijke kernrol zien voor Muc2 bij de handhaving van de homeostase in de darm. Een volgende belangrijke stap zou het ontrafelen van het mechanisme achter de ontwikkeling van de ontsteking in de afwezigheid van Muc2 zijn. Signaal-profielstudies zouden kunnen dienen om moleculen te identificeren die i) ontstekingen initiëren en verergeren, ii) epitheliale proliferatie reguleren en iii) epitheliale differentiatie reguleren. Bovendien zouden er nieuwe onderzoekstechnieken ingezet kunnen worden. Te denken valt aan kiemvrije en gnotobiotische technologie, waarbij dieren gebruikt worden die specifiek gekoloniseerd zijn met, voor de onderzoeker bekende, één of meer bacteriestammen, functionele genomics en kwantitatieve PCR (*polymerase chain reaction*). Door deze gecombineerd toe te passen kunnen we $Muc2^{-/-}$ en WT muismodellen gebruiken om na te gaan wat de impact is van de microbiële populatie op de celhomeostase, de genexpressie en vervolgens de barrièrefunctie van de darm. Tevens kunnen we dan inzicht krijgen in de rol van pre- en probiotica bij de bescherming van de darm, en meer specifiek de productie van mucine. Al met al zou de informatie die dan beschikbaar komt over microben, genen en signaleringsroutes die betrokken zijn bij ontstekingen van de darm, kunnen leiden tot nieuwe behandelmethoden.

Curriculum Vitae & Publications

Curriculum Vitae

The author of this thesis was born on 6th January, 1978 in Terneuzen, Holland, of Dutch and English parents. She spent her childhood years traveling the world with her parents, was raised bilingually and formally taught in English by her mother. In the summer of 1989, they moved to 's- Heer Arendskerke to live in Holland permanently. Here, she attended the final year at the village primary school, "Schengenhof". From August 1990 till June 1996, she was a student at the "Stedelijke Scholengemeenschap Het Goese Lyceum" in Goes. In August 1996 she started to study at the Hogeschool Brabant, Faculty of Medicine in Etten-Leur, gaining a propaedeutic certificate in Medical Biology in 1997. She fulfilled her BSc research project at the department of Pharmacology (Dr. D.E. Elliott), TNO-PML in Rijswijk, after which she graduated as BSc in Biology in August 2000. In September 2000, she joined the Research Group of Pediatric Gastroenterology & Nutrition (Dr. A.W.C. Einerhand, Dr. J. Dekker, Prof. dr. H.A. Büller) at the laboratory of Pediatrics at the Erasmus MC and Sophia's Children's Hospital in Rotterdam. In January 2003, she started to work as a PhD student in collaboration with INSERM U560, "Groupe régulation transcriptionnelle et signalisation cellulaire" (Dr. I. van Seuningen) in Lille, France. In August 2004, Dr. A.W.C. Einerhand and Prof. dr. H.A. Büller left the group of Pediatric Gastroenterology & Nutrition and the project was continued and finalized in the Research Group of Neonatology (Dr. I.B. Renes and Prof. dr. J.B. van Goudoever) at the laboratory of Pediatrics at the Erasmus MC in Rotterdam. From January 2007, she will be employed as a Research Associate (post-doc) at the Laboratory of Pediatrics, Division of Neonatology (Dr. I.B. Renes, Prof. dr. J.B. van Goudoever), Erasmus MC and Sophia's Children's Hospital in Rotterdam, where she will study the interaction of bacteria with the epithelium of the intestine and their influence on epithelial homeostasis during intestinal development and differentiation and more specifically, mucin gene expression.

Publications

Maria van der Sluis#, Audrey Vincent#, Janneke Bouma, Anita Korteland-Van Male, Johannes B. van Goudoever, Ingrid B. Renes, and Isabelle Van Seuningen; *Hepatocyte Nuclear Factor 3alpha and -3beta are two important transcriptional regulators of the mucin Muc2 gene in intestinal goblet cells.*
# Both authors contributed equally to this study
Manuscript in preparation

Maria van der Sluis, Janneke Bouma, Anna Velcich, Hans A. Büller, Alexandra W.C. Einerhand, Johannes B. van Goudoever, Isabelle Van Seuningen and Ingrid. B. Renes; *Muc2-IL10 deficient mice: A lethal combination.*
Manuscript submitted for publication

Maaike W. Schaart#, **Maria van der Sluis#**, Barbara A.E. de Koning, Henk Schierbeek, Anna Velcich, Ingrid B. Renes and Johannes B. van Goudoever; *Dietary threonine metabolism in the intestine of wild type and mucin 2 deficient mice.*
# Both authors contributed equally to this study
Manuscript submitted for publication

Barbara A.E. de Koning#, **Maria van der Sluis#**, Dicky J. Lindenbergh-Kortleve, Anna Velcich, Rob Pieters, Hans A. Büller, Alexandra W.C. Einerhand and Ingrid B. Renes; *Methotrexate-induced mucositis in mucin 2 deficient mice.*
# Both authors contributed equally to this study
Journal Cellular Physiology, *in press*

Maria van der Sluis, Barbara A.E. de Koning, Adrianus C.J.M de Bruijn, Anna Velcich, Jules P. Meijerink, Johannes B. van Goudoever, Hans A. Büller, Jan Dekker, Isabelle Van Seuningen, Ingrid. B. Renes and Alexandra W.C. Einerhand; *Muc2-deficient mice spontaneously develop colitis, indicating that Muc2 is critical for colonic protection.*
Gastroenterology, 131(1);117-129, 2006

Barbara A.E. de Koning, Jolanda M. van Dieren, Dicky J. Lindenbergh-Kortleve, **Maria van der Sluis**, Tetsuya Matsumoto, Keizo Yamaguchi, Alexandra W.C. Einerhand, Janneke N. Samsom, Rob Pieters and Edward E.S. Nieuwenhuis; *Contributions of mucosa*l immune cells to methotrexate induced mucositis.
International Immunology, 18(6):941-9, 2006

Maria van der Sluis, Monique H.M. Melis, Nicolas Jonckheere, Marie-Paule Ducourouble, Hans A. Büller, Ingrid Renes, Alexandra W.C. Einerhand and Isabelle Van Seuningen; *The murine Muc2 mucin gene is transcriptionally regulated by the zinc-finger GATA-4 transcription factor in intestinal cells.*
Biochemical & Biophysical Research Communications, Vol 325(3);952-960, 2004

Nicole M.J. Schwerbrock, Mireille K. Makkink, **Maria van der Sluis**, Alexandra W.C. Einerhand, Hans A. Büller, Balfour R. Sartor and Jan Dekker; *Interleukin 10 deficient mice are defective in colonic Muc2 synthesis, both before and after induction of colitis by commensal bacteria.*
Inflammatory Bowel Diseases 10(6): 811-823, 2004

Nicolas Jonckheere, **Maria van der Sluis**, Amélie Velghe, Marie-Pierre Buisine, Marjolein Sutmuller, Marie-Paule Ducourouble, Pascal Pigny, Hans A. Büller, Jean-Pierre Aubert, Alexandra W.C. Einerhand and Isabelle van Seuningen; *Tanscription activation of the murine Muc5ac mucin gene in epithelial cancer cells by TGF-β/Smad signaling pathway is potentiated by Sp.*
Biochemical Journal 1;377(Pt 3):797-808 Feb, 2004

Alexandra W.C. Einerhand, Ingrid B. Renes, Mireille K. Makkink, **Maria van der Sluis**, Hans A. Büller and Jan Dekker; *Role of mucins in inflammatory bowel diseases: important lessons from experimental models.*
European Journal of Gastroenterology & Hepatology, Vol 14 (6); 1-8, 2002.

Acknowledgements - Dankwoord

Samenwerken is een kernwoord van onderzoek. Het onderzoek, zoals beschreven in dit proefschrift, is een goed voorbeeld hiervan: ik heb dit zeker niet alleen gedaan!

Dit vind ik ook het moeilijkste stukje om te … Ik begin maar gewoon en waar anders kom ik dan uit dan bij het lab KGK. Ik wil de hele groep (natuurlijk ook alle ex-KGers!) bedanken voor de gezellige en goede werksfeer. Zonder jullie was het nooit gelukt en was ik er waarschijnlijk ook nooit aan begonnen!
Ik zou het natuurlijk hierbij kunnen laten (het risico van iemand over het hoofd zien heb ik dan niet meer), maar toch wil ik ook nog enkelen in het bijzonder noemen.

Allereerst mijn co-promotoren, Dr. A.C.W. Einerhand en Dr. I.B. Renes. Beste Sandra, ik ben echt zo gelukkig met het vertrouwen dat je in mij had toen je me deze kans hebt aangeboden. Bedankt voor je enthousiasme, het becommentariëren van alle manuscripten en dat niet alles even serieus hoefde te zijn (ik zeg nog zo.... geen bommetje!). Het was voor mij even schrikken (understatement!) toen je halverwege mijn promotie besloot een andere draai aan je carrière te geven. Ik wens je veel succes, gezondheid en alle geluk in de toekomst! Beste Ingrid, toen Sandra vertrok heb jij mij onder je hoede genomen. Bedankt voor je begeleiding, inzet, scherpe blik, enthousiasme…….eigenlijk voor alles. Op naar het vervolg; Ik heb er zin in!

Mijn promotoren, Prof. dr. H.A. Büller en Prof. dr. J.B. van Goudoever. Professor Büller, beste Hans, in 2002 vroeg je me, samen met Sandra, voor dit onderzoek. Ik ben blij dat ik jullie aanbod heb geaccepteerd. Als promotor volgde je het onderzoek op afstand, altijd belangstellend (niet alleen in de resultaten) en zeer attent, wat een vertrouwd gevoel gaf. Professor van Goudoever, beste Hans, bedankt dat je mij op wilde vangen en dit proefschrift met me wilde afmaken. Ik vind het geweldig hoe je je hebt ingezet voor onderzoek waar je in het begin weinig raakvlakken mee had. Bedankt voor je begeleiding, nuchterheid, discussies en vertrouwen. Op naar de toekomst!

Dr. J. Dekker, beste Jan, je hebt een keer tegen me gezegd dat iedereen kan schrijven, als je maar durft te strepen. Die opmerking heb ik altijd onthouden en het gaf me moed. Bedankt hiervoor, maar ook voor het bediscussiëren van resultaten en voor het zeer snel en kritisch na lezen van de manuscripten. Geweldig dat je je op afstand toch zo hebt ingezet!

And of course the *L'équipe lilloise!* Dr. I. van Seuningen. Dear Isabelle, you were the one, stable factor during my whole thesis, letting me know straight away when Sandra left, that our collaboration and your support were there. This was a real comfort. Your enthusiasm and preciseness how to perform research was a great example. Thank you very much for the opportunity to learn from you and I am looking forward to collaborating with you in the future! Dear Nicolas, thank you for your many translations, teaching sessions and patience during my stay in Lille. Remember driving to Tournai to take me to a cinema where there would be an English version movie? Dear Marie-Paule, *THE RNA-isolation-queen*. We communicated in a mixture of French, English and German. Other people did not understand us, but you managed to teach me your secrets. Thank you for this! Dear Audrey, thank you for all your hard work on the promoter study. I am sure that you will complete a wonderful thesis yourself! Brigitte, Christophe, Pascal and Valérie; thank you for putting up with the *Dutchy* who could not speak any French and good luck with all your studies!

Dr. A. Velcich, dear Anna, a big part of my thesis is based on the opportunity you provided us by collaborating and sharing your Muc2 deficient mouse. Thank you! And many thanks for the thorough revisions and always critical questions of the manuscripts we worked on. I hope we will meet in person some day.

J. Hagoort, L.W. Goedegebure. Beste Ko en Leo, ook voor jullie ook een special woordje, want zonder jullie zou dit boekje er niet zo fraai uitzien. Ko, bij vele van de teksten heb jij (altijd zeer snel!) de puntjes op de i gezet en heb je ook nog eens de zeer toepasselijke titel bedacht. Leo, jij hebt heel creatief alle lappen tekst en figuren omgezet tot een mooi geheel. Bedankt voor jullie inzet!

Alle "oud" AIO's van KG&V; Ingrid, Jeroen, Melissa, Jos en Barbara. Allemaal gingen jullie mij voor en gaven voorbeeld. Ingrid, in de tussentijd heb je een eigen groep en nu ben je mijn co-promotor. Het kan snel gaan! Jeroen, onze cliniclown, door jou heb ik de noodzaak van back-ups maken geleerd (wash and gone?!) en daar ben ik je (achteraf!) vaak dankbaar voor geweest. Bedankt voor al je gekkigheid en welkom weer terug in de mucine wereld! Lieve Barbara; ik heb echt bewondering voor jou. Hoe positief jij door het leven gaat, daar kunnen veel mensen van leren. Vond het heerlijk om met je samen te werken (en te lachen). Bedankt ook voor alle nachtjes "logeren". Veel succes met het afronden van je opleiding tot kinderarts. Je wordt en geweldige kinderdokter! En wie weet kunnen we in de toekomst eens een onderzoekje opzetten.

Het "Neo" labgroepje: Ad, André, Henk, Janneke, Maaike, Monique, Nanda en Patrycja. We krijgen een steeds grotere gezellige groep! Beste Ad, onvermoeibaar heb jij blotjes voor mij gedraaid en had je geduld met mij, zelfs toen ik op het laatst een beetje hectisch was. Bedankt hiervoor! Henk, zonder jou zou het hele artikel over threonine metabolisme er niet zijn! Bedankt voor alle massaspectrometrie metingen die je hebt uitgevoerd. Lieve Janneke, bedankt voor je toewijding en inzet, al je harde werk en de waarschuwingen wanneer het tijd was voor een lekkere cappuccino. Ik vind het echt super hoe je me op allerlei manieren steunt en helpt, inclusief op de grote dag zelf! Ik zie uit naar de vervolgprojecten! Lieve Maaike, promotiegenoot, het was geweldig om met je samen te werken aan het "science" onderzoek en iemand te hebben die op eenzelfde schema lag als ik. Heel veel succes op je weg naar kinderarts, ik weet zeker dat je ook dat helemaal goed gaat doen! Ik ga je zeker missen, maar we houden contact (lang leve de MSN).

(Ex-) Kamergenootjes van Ee 15-12. Voor jullie ook een speciaal woordje: Ons kamertje is een voorbeeld van een geslaagde "integratie" van de verschillende groepen. Bedankt voor adviezen, praatjes (serieus of minder serieus), snoep, schaatslessen (!) enz enz.

Ook zonder de hulp van studenten zou dit project niet zo geslaagd zijn. Monique, Irene, Wai Yee en Marcel, bedankt voor jullie inzet. Het was erg leuk (en voor mij ook leerzaam) om jullie te mogen begeleiden. Toch nog een speciaal woordje voor jou Monique. Jij was de eerste student die ik mocht begeleiden. Super enthousiast kwam jij mij versterken toen ik echt hard hulp nodig had. Ik ben met jou met mijn neus in de boter gevallen (zoals menigeen mij dat ook heeft verteld). Super bedankt en heel veel succes met al je eigen ondernemingen en onderzoeken!

De steunpilaren van het hele lab kindergeneeskunde: Anita, Dicky, Ingrid, Rolien, Marcel en Theo. Jullie zijn onmisbaar in alle opzichten.

Een paar ex-KGers: Anita, Danielle, Maartje en Nathalie. Jullie Brabantse gezelligheid heb ik gemist. Bedankt voor alle gezelligheid (vooral de gesprekjes tijdens de lunch). De “Nijmegen gang”: een nieuwe uitdaging voor jullie en een groot gemis voor ons! En in het bijzonder Christa, mijn mede-zeeuw. Zonder jou had ik, op het laatst, het reizen misschien niet zo makkelijk vol kunnen houden. Je bent een uniek persoon. Bedankt voor alles en we houden contact daar met Nijmegen!

En dan kom ik uit op het persoonlijke front. Monique en Annemiek, jullie vormen eigenlijk letterlijk en figuurlijk de overgang. Treinmaatjes van het lab op weg naar huis. Alles hebben we ongeveer besproken; we zijn boos geweest, hebben gelachen en geslapen op de trap. Ook al reizen we ondertussen niet meer samen, we hebben nog wel contact. Annemiek, jij reist alle congressen af om je prijzen als “young investigator” op te halen. Tussen de bedrijven door ook nog een prachtig dochtertje kregen; jij komt er wel! Lieve Monique, ik heb grote bewondering voor hoe jij je drukke leven (Martijn/dansen/onderzoek) in de baan houdt en toch zoveel energie overhoudt. En nu ook nog een heerlijk dochtertje om jullie gezinnetje aan te vullen. Succes met de laatste loodjes van je promotie!

Lieve Wim, Mirella, Sam, Peter, Chandra, Mik, Jens, Robert, Charlotte, Mark, Esther en Sil. “Grote” en “kleine” vrienden. Samen korfbal kijken, borrelen, naar de sauna gaan, lachen, 25^{+}, spelletjes spelen, feesten, Patricks broodjes, telefoontjes, verhaaltjes lezen, shoppen, reizen, BBQ-en etc. etc…..Bedankt voor alle afleiding en gezelligheid!

Lieve Marjan. Wij kennen elkaar sinds de brugklas van de middelbare school. Na ons jaar samen in Den Haag zijn we uiteindelijk ieder een eigen weg ingegaan. Toch is de vriendschap er niet op minder geworden. Bedankt voor alles! Ik ben er trots op dat je naast me staat als paranimf (die ook echt iedere hoofdstuk van dit proefschrift gelezen heeft!).

Mijn geweldige schoonouders, Jan en Nel. Door jullie interesse en vertrouwen voel ik me echt één van de (grote) familie. Zonder jullie hulp (“hand- en spandiensten”) was ik niet zover gekomen; denk alleen al aan alle ritjes naar Lille in jouw autootje Nel!

Lieve Orion, broertje, wat zou ik zonder mijn eigen computer helpdesk moeten doen? Soms, als ik je dan “zomaar” even belde vroeg je gelijk; wat heb je nu weer gedaan? En je haalde opgelucht adem als ik zei dat er met de computer niets aan de hand was. Veel succes met al je eigen ondernemingen en veel geluk samen met Christel.

Lieve Pa en Ma. Bedankt voor jullie blind vertrouwen, steun..... eigenlijk voor alles! Onze band is heel speciaal en dat zal altijd wel zo blijven. Lieve Mam, jij hebt letterlijk de beginselen voor dit alles gelegd: je hoeft nooit meer te twijfelen of je het wel goed genoeg hebt gedaan!

Ik had me nog zo voorgenomen om het kort en krachtig te houden, maar ik had kunnen weten dat dat niet zou lukken. Voordat ik ermee stop, ga ik nog één persoon in het bijzonder noemen; lieve Gerben, jij zag het in me en hebt geholpen om het de rest ook te laten zien. Bedankt voor al je steun, geduld, duwtjes in de rug als ik het niet meer zag zitten en alle keren dat je me hebt moeten missen zonder te klagen! Op naar de volgende uitdaging….

Maria

Color Plates

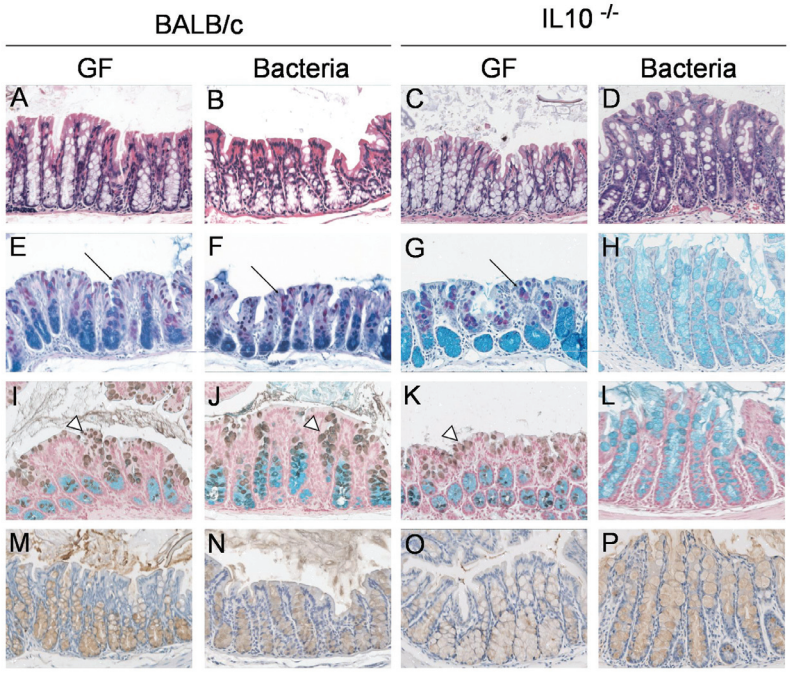

Chapter 2 Figure 3. Histochemistry of BALB/c and IL10$^{-/-}$ proximal colon. Tissue sections were prepared from the proximal colon of BALB/c and IL10$^{-/-}$ mice in germ-free (GF) conditions and at 7 days after the introduction of SPF normal enteric bacteria (Bacteria). The tissue sections were stained histochemically with hematoxylin and eosin (Panels A-D), AB/PAS (Panels E-H), or HID/AB (Panels I-L). The arrows in Panels E-G indicate PAS-positive goblet cells in the upper half of the crypts. The arrowheads in Panels I-K indicate HID-positive goblet cells in the upper half of the crypts. Sections were stained immunohistochemically for the presence of Muc2 protein, using a polyclonal anti-murine Muc2 antiserum (Panels M-P). All micrographs were recorded at the identical magnification of 200x.

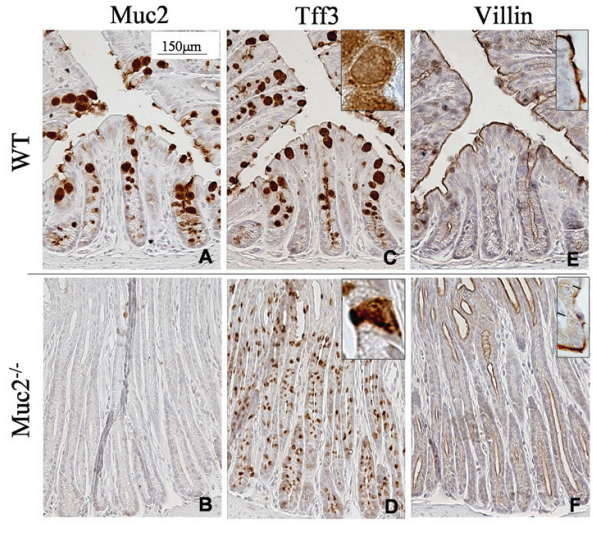

Chapter 3 Figure 4. Protein expression in the distal colon. Goblet cells were stained for (A and B) Muc2 and (C and D) Tff3. As an enterocyte marker villin was used (E and F). A, C, and E, are sections representing tissue from the distal colon of WT animals and B, D, and F, represent tissue from the distal colon of Muc2$^{-/-}$ animals, respectively. Inserts in C and D show a close-up of a goblet cell in WT and Muc2$^{-/-}$ mice, respectively. Insert in E shows a close-up of normal villin expression by WT enterocytes. F shows loss and redistribution (*arrow heads*) of villin expression by the epithelial cells of Muc2$^{-/-}$ mice.

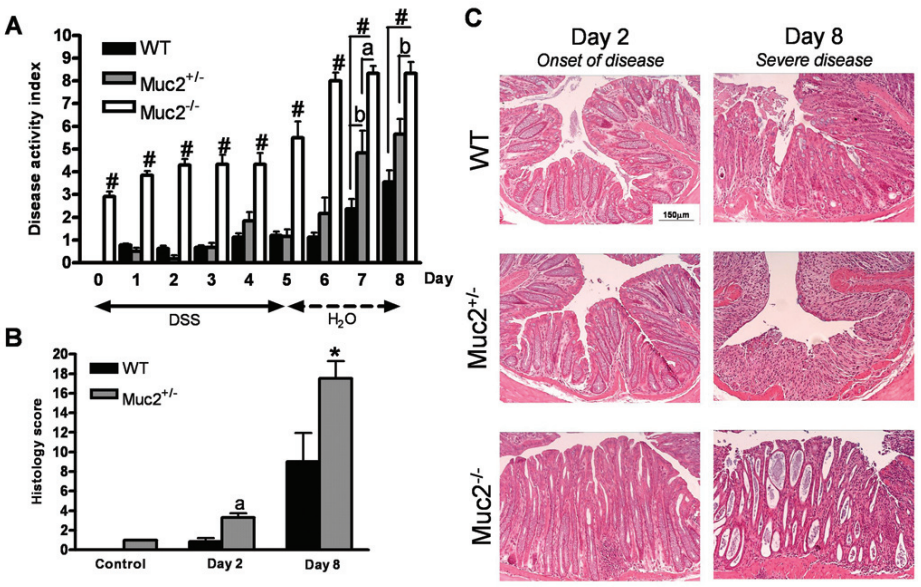

Chapter 3 Figure 7. Effects of DSS treatment on disease activity score (DAI) and histology. (A) Relative changes in the DAI of WT (black bars), Muc2$^{+/-}$ (stippled bars) and Muc2$^{-/-}$ (white bars) DSS-treated mice. To be able to calculate percentage weight loss, WT, Muc2$^{+/-}$ and Muc2$^{-/-}$ animals were compared to their individual body weight prior to the DSS-administration. Error bars reflect the SEM of the changes of the DAI score on each day. Days of DSS/water treatment are indicated as *arrows* under the x-axis. (DAI Muc2$^{-/-}$ vs. WT $^{\#}$P<.001 all time points; DAI Muc2$^{-/-}$ vs. Muc2$^{+/-}$ P<.001 up to day 6, ^{a}P<.01 day 7 and ^{b}P<.05 day 8; DAI WT vs. Muc 2$^{+/-}$ day 7 and 8 P<.05) (B) Histology scores as determined according to Rath *el al* [21] determined for WT vs. Muc2$^{+/-}$ mice (^{a}P<.001, *P<.05). Error bars reflect the SEM. (C) Representative sections of the distal colon on day 2 and day 8 after the start of the DSS-administration of WT, Muc2$^{+/-}$ and Muc2$^{-/-}$ mice.

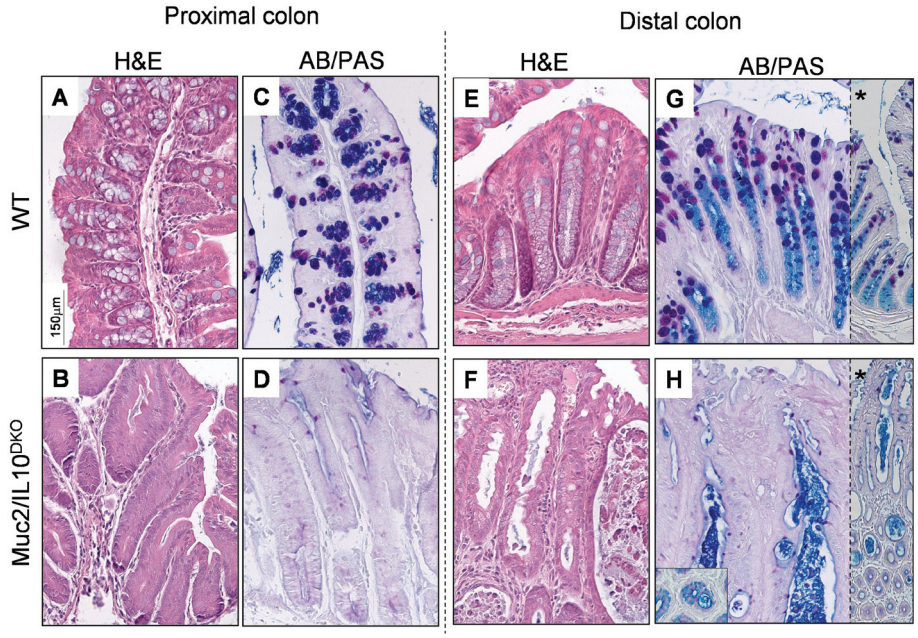

Chapter 4 Figure 2. Colonic morphology the WT and Muc2/IL10^{DKO} mice. Representative sections of the colon are depicted at 5 weeks of age (A-C; proximal colon, D-H; distal colon). A-B; E-F represent H&E stainings whereas C-D; G-H represent AB-PAS stainings. A and C, and E and G represent proximal colon and distal colon, respectively of the WT mice. B and D, and F and H represent proximal colon and distal colon, respectively of the WT mice. The insert in H shows a close-up of goblet cells in the crypts of Muc2/IL10^{DKO} mice. The a*sterisks* represents a lower magnification of the distal colon.

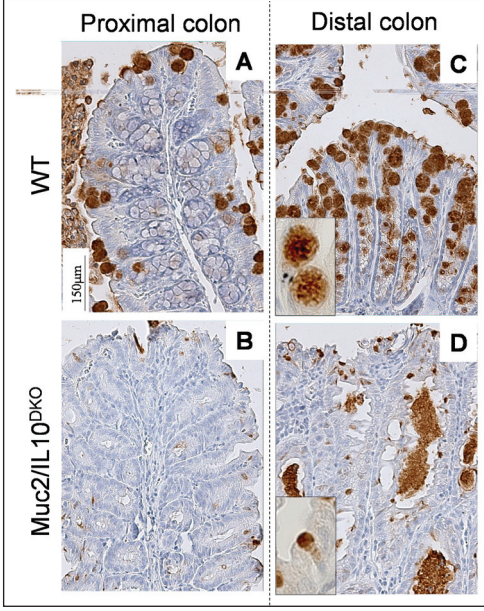

Chapter 4 Figure 4. Tff3 expression in colon. Tff3 was expressed by goblet cells in the proximal colon of **(A)** WT mice, but was virtually absent in the proximal colon of **(B)** Muc2/IL10^{DKO} mice. In the distal colon, Tff3 was present in the goblet cells of **(C)** WT mice**,** but in larger numbers compared to the goblet cells of the **(D)** Muc2/IL10^{DKO} mice.

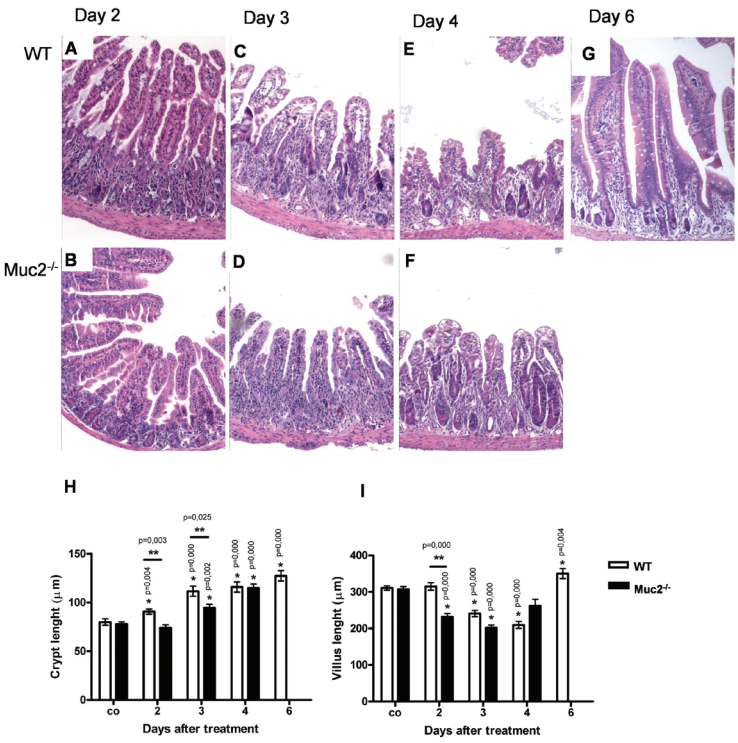

Chapter 5 Figure 4. MTX-induced changes in the small intestine in WT and Muc2$^{-/-}$ mice. Morphology of the jejunum of WT (**A,C,E,G**) and Muc2$^{-/-}$ (**B,D,F**) mice on days 2 (**A-B**), 3 (C-D), 4 (E-F) and 6 (G) after MTX-treatment. On day 2, morphology of WT and Muc2$^{-/-}$ mice was mildly affected and characterized by mild crypt loss and epithelial flattening. On days 3 and 4, intestinal damage was more severe, showing increased crypt loss on day 3 and epithelial flattening and villus atrophy on days 3 and 4. Crypt regeneration was seen on day 4, but was more pronounced in the Muc2$^{-/-}$ mice compared to WT mice. On day 6, the intestinal morphology of the WT mice had started to regenerate as evidenced by higher numbers of well-formed crypts and villi. (**H**)Crypt and (**I**) villus lengths of WT and Muc2$^{-/-}$ littermates before and after MTX-treatment. Both groups showed significant villus atrophy and crypt elongation after MTX-treatment. Significant differences were seen on day 2; Muc2$^{-/-}$ mice showed more villus atrophy, but less elongation of crypt length compared to WT mice. On day 3, villus atrophy was comparable in both groups, but still minimal differences were seen in crypt length. In the regenerative phase, day 6, WT mice showed an increase in villus and crypt length compared to control littermates. Bars are expressed in Mean ± SEM.

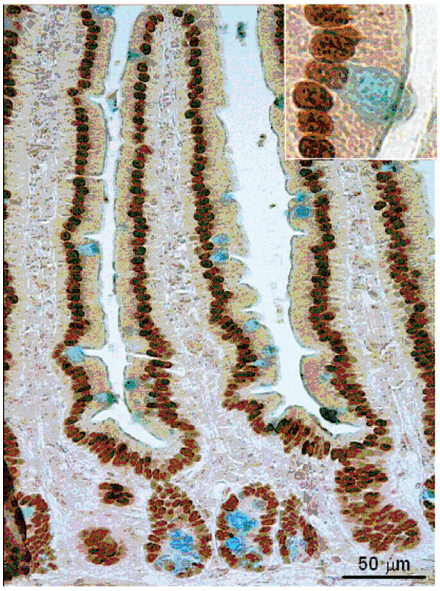

Chapter 7 Figure 1. Expression of GATA-4 transcription factor in mouse small intestine by immuno-histochemistry. Alcian blue staining was performed as described in the material and methods section. GATA-4 immunostaining was carried out on the same section of mid jejunum of an adult mice using a specific antibody for GATA-4. Sections were counterstained with haematoxylin. Inset : close-up of one GATA-4 expressing goblet cell.

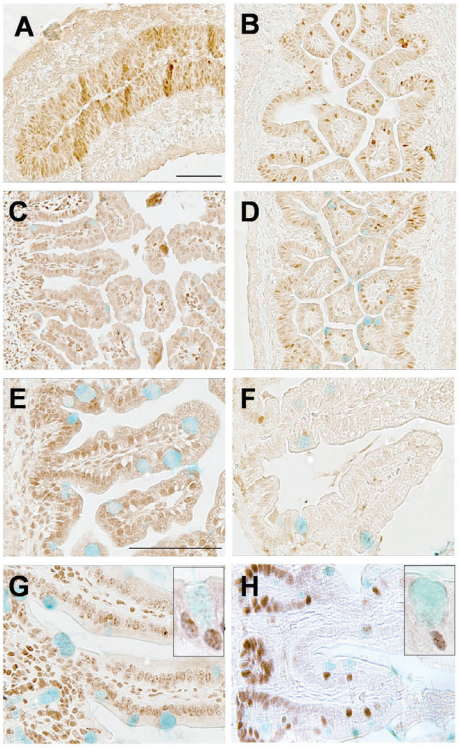

Chapter 8 Figure 1. Spatio-temporal expression of HNF-3α and HNF-3β in the mouse small intestine. HNF-3β expression was observed in (A) the pseudostratified epithelium at E15.5, and in the intervillus cells and goblet cells along the villi at (B) E17.5. HNF-3α and -3β staining, respectively of (C-D) E18.5 (E-F) P1.5 and (G-H) adult small intestine. Inserts of G and H show a close-up of a goblet cell stained with HNF-3α and -3β, respectively and counterstained with Alcian Blue. Magnification in A-D and E-H are equal, respectively, bar representing 75µm.